University of California
Santa Barbara

The Development of Robust and Sustainable Methods Toward Greener Syntheses of Pharmaceuticals and Agrochemicals

A dissertation submitted in partial satisfaction
of the requirements for the degree

Doctor of Philosophy
in
Chemistry

by

Chandler Blaine Nelson

Committee in charge:

Professor Bruce H. Lipshutz, Chair

Professor Liming Zhang

Professor Armen Zakarian

Professor Christopher Bates

June 2026

The Dissertation of Chandler Blaine Nelson is approved.

Professor Liming Zhang

Professor Armen Zakarian

Professor Christopher Bates

Professor Bruce H. Lipshutz, Chair

May 2026

Dedicated to the memory of my father, Wayne P. Nelson.

Acknowledgements

The endeavor of a PhD in organic chemistry, and what it exactly entails, is esoteric to the average layperson. What is common knowledge, however, is how arduous and challenging it is for one to obtain this degree. Over the past five years, I found, first-hand, that it indeed lives up to this reputation. My journey in the program involved countless early mornings, late nights, and long weekends in the lab. Troubleshooting challenging experiments, teaching undergraduates and grading their homework, mentoring new graduate students, fixing equipment I had never really encountered before, and much more were all par for the course. Additionally, beyond the science, I had to learn to navigate interpersonal relationships in the lab, I had to figure out how to survive in Santa Barbara on a graduate student salary, and I had to navigate department and university bureaucracy. Throughout all of this, I found that this was also largely a solo endeavor. In fact, this is, at least in part, by design. A key takeaway from a doctoral degree in the physical and life sciences is becoming an independent researcher. However, while I indeed found myself standing on my own two feet in this regard, I would be remiss not to acknowledge the support and community that made my dissertation possible. My appreciation extends to so many individuals that it would not be feasible to list them all here. However, not being specifically named does not diminish the appreciation I have for them. Nonetheless, there are certain people that are especially due my sincerest gratitude.

I must first thank my advisor, Professor Bruce H. Lipshutz. His advisement and mentorship forged me into the chemist that I am today. Over the past five years, he has generously provided the funding and resources needed to explore my research interests. I would especially like to

express my gratitude for his understanding during challenging periods of health-related issues and his amenability to me conducting an internship in the summer following my fourth year.

I would also like to acknowledge and thank my committee members, Professor Liming Zhang, Professor Armen Zakarian, and Professor Christopher Bates. They took time out of their very busy schedules to serve on my committee and provide invaluable feedback during my PhD studies.

A very special thanks must be given to the Pasadena Community Foundation (PCF) for selecting me to be a recipient of the Josephine de Karmann fellowship in my fifth year. During these disturbing times when American science and scientific funding are under attack, private nonprofit fellowships like this are a saving grace and, frankly, a crucial part of scientific funding infrastructure. The selfless donors to this fellowship, and the incredibly gracious administrators at the PCF, provided the aid I needed to finish my thesis work and continue my contributions to the field of organic chemistry. For this, they have my eternal thanks.

I must also acknowledge and express my gratitude for Dr. Hongjun Zhou, the NMR manager at the UCSB chemistry department. Beyond being a kind face and a true friend, Hongjun was a powerful resource. His knowledge and expertise on NMR far exceeded that of anyone I had met before, and this ended up helping immensely during my research. During the borylations project (Chapter 2), I found a method to isolate our boron NMR signal from the background noise produced by the borosilicate glass present in the NMR probe. However, I had no idea how to implement it on our instruments. After a short email, Hongjun, in a matter

of minutes, implemented the method on the NMR for myself and my collaborators. This is just one example of the above and beyond help that he provided over the years.

In the first year of graduate school, students are assigned a senior graduate student mentor. For myself, I had the privilege of working with Dr. Vani Singhania. When I was struggling to get my bearings as a new student, Vani got me on track and helped me grow into a place where I was able to independently pursue my own research projects. Her patience and mentorship set me on the right course in graduate school, and for this, I am deeply grateful.

Chris Dominey and Adrian Shelor are the Shipping and Receiving Managers, as well as the Chemistry Storeroom Keepers for the UCSB Chemistry Dept. Their diligent work and helpfulness kept the lab stocked with the supplies we needed and made sure our chemicals were arriving on time. My research would not have been possible without them, and I thank them for all of their hard work and assistance over the course of my degree.

Deserving of my utmost gratitude is my former partner, Maya. A dedicated partner to a PhD student in the physical sciences truly takes a special individual. Her immense patience allowed me to dedicate the hefty amounts of time and energy needed to put into this program. During particularly dark and challenging times when I was left wondering if it was all worth it, she was there to gently push me to keep going. Maya helped me to remember to get out of my own head and to remember to live life every now and again. It is with certainty that I say that this dissertation work would not at all have been possible without her and her love and support.

I would also like to truly thank Kathy and Junji Uemura. Throughout my graduate studies, they were so profoundly supportive and generous that I am forever in their debt. They took me

in like a member of their family and afforded me opportunities that I never would have had on my own. They made the past five years a lot more bearable and enjoyable, and for that, I am forever grateful.

My mother, Victoria, and my sister, Savanah, were also key to my success as a graduate student. They checked in with me regularly to show their support, provided me with financial help when I needed it, and were understanding with the amount of time and effort I was dedicating to my studies.

As mentioned above, it would be impossible to list every person that I am grateful for in obtaining my PhD. Fellow group members, collaborators, family, friends, etc., all come to mind when I consider those who helped make this possible. Science seldomly occurs in isolation, and this thesis is patently an example of that.

Curriculum Vitæ

Chandler Blaine Nelson

Education

University of California, Santa Barbara — **Santa Barbara, CA**
Doctor of Philosophy in Organic Chemistry (GPA:4.000) — *Jun 2026 (expected)*

University of California, Los Angeles — **Westwood, CA**
Bachelor of Science in Chemistry (GPA:3.882) — *Jun 2021*

Research and Professional Experience

University of California, Santa Barbara — **Santa Barbara, CA**

- ▷ Graduate Student Researcher — *Aug 2021 - present*
- ▷ Graduate Teaching Assistant — *Sep 2021 - Jun 2023*
  General and Organic Chemistry Lab Courses

Arcus Biosciences — **Hayward, CA**

- ▷ Graduate Student Intern: Process Chemistry — *Jun 2025 - Sept 2025*

University of California, Los Angeles — **Westwood, CA**

- ▷ Undergraduate Student Researcher — *Oct 2020 - Jun 2021*

Publications

1. **Nelson, C.B.**; Yirak, J.R.; Baumann, M.E.; Freiberg, K. M.; Lipshutz, B. H.; A Green Chemistry Approach to the Synthesis of an Emerging Celiac Drug; *Green Chem.* 2026, 28, 938-944

2. **Nelson, C. B.**; L'Heureux, S. J.; Wong, M. J.; Lipshutz, B. H.; Environmentally Friendly near-neat Miyaura Borylations allowing for green, one-pot borylation-Suzuki-Miyaura couplings; *Green Chem.* 2024, 26, 10115 - 10122.

3. Singhania, V.; **Nelson, C. B.**; Reamey, M.; Morin, E.; Kavthe, R. D.; and Lipshutz, B. H.; A Streamlined, Green, and Sustainable Synthesis of the Anticancer Agent Erdafitinib; *Org. Lett.* 2023, 25 (23), 4308-4312.

4. Iyer, K. S.; **Nelson, C. B.**; and Lipshutz, B. H.; Facile, green, and functional group-tolerant reductions of carboxylic acids…in, or with, water; *Green Chem.*, 2023, 25, 2663-2671.

Conferences and Presentations

Graduate Research Symposium **San Diego, CA**

Poster: Sustainable Borylations and 1-Pot Suzuki Couplings *Jul 2026*

Awards and Honors

- ▷ Josephine DeKarman Fellow 2025-26
- ▷ Phi Lambda Upsilon Award – UCSB Dept. of Chemistry 2022
- ▷ ACS Award for Outstanding Senior in Organic Chemistry 2021
- ▷ Departmental Honors – UCLA Dept. of Chemistry 2021

Abstract

The Development of Robust and Sustainable Methods Toward Greener Syntheses of Pharmaceuticals and Agrochemicals

by

Chandler Blaine Nelson

I. The Suzuki-Miyaura coupling reaction is a cornerstone of modern organic chemistry and, in the decades since its first disclosure, significant strides have been made to enhance its efficiency and environmental sustainability. However, the directly preceding reaction, the Miyaura borylation, routinely involves the use of toxic and wasteful solvents, harsh reaction conditions, and high loadings of transition metal catalysts. Reported is a new 'near-neat' method for synthesizing *ethyl*pinacol boronic esters (BEpins) that generates these stable boron reagents in concentrated EtOAc, with moderate reaction temperatures, and with highly efficient palladium catalyst loadings. Additionally, despite their enhanced stability, the BEpins are also shown to be effectively implemented in a sustainable 1-pot, on-water borylation/Suzuki-Miyaura coupling protocol to generate a diverse library of bi(hetero)aryl substrates, including several notable pharmacologically relevant examples.

II. A new, sustainable synthesis is presented for *ZED1227*, a first of its kind therapeutic for the treatment of celiac disease. Through implementation of an aqueous carbonyl iron powder (CIP) nitro reduction, a 1-pot 2-pyridyl thioesterification/amide coupling in recoverable EtOAc, and an *N*-Boc deprotection in isopropyl alcohol, the route generates the drug in a manner that minimizes waste generating processes. In comparison to the existing published route for medicinal chemistry studies, this synthesis makes marked improvements in terms of E factor and yield, utilizing significantly more benign coupling reagents and reaction conditions.

III. Running reactions under inert atmospheres is an imperative for much of organic chemistry. From a life-cycle perspective, this requirement serves to impart significant external costs for these transformations. Currently, huge amounts of energy are expended to cool gas mixtures to cryogenic temperatures so that they can be fractionally distilled into their individual components. Shipping and usage of these inert gases is also hazardous and wasteful. Explored is the implementation of an oxidase/catalase dual enzyme system for ex-situ deoxygenation of reaction vessels. Limitations encountered are articulated, and potential solutions are proposed.

Contents

Acknowledgements **iv**

Curriculum Vitæ **viii**

Abstract **x**

1 General Background and Introduction **1**

2 Development of a Sustainable 1-Pot Borylation/Suzuki-Miyaura Coupling **8**

2.1 Background and Introduction 8

2.2 Results and Discussion 13

2.2.1 Sustainable Borylation Method 13

2.2.2 Green 1-Pot Miyaura Borylation/Suzuki-Miyaura Coupling Method . . 23

2.2.3 Application of this Methodology to a Precursor of Anidulafungin . . . 29

2.2.4 Sequence Toward a Key Agrochemical 30

2.3 Conclusion 31

2.3.1 Closing Remarks 34

2.3.2 Acknowledgements and Noted Contributions 34

2.4 Experimental Data and Information. 35

2.4.1 General Information 35

2.4.2 General Procedures 37

2.4.3 Optimization Data 45

2.4.4 E-Factor[77] Calculations 50

2.4.5 Analytical Data 52

2.4.6 ICPMS Data 81

2.4.7 NMR Spectra 82

3 A Green Chemistry Approach to the Synthesis of a Novel Celiac Therapeutic **135**

3.1 Introduction 135

3.2 Results and Discussion 138

3.2.1 Reduction of Nitro Group on Dihydropyridinylacetamide 139

3.2.2 Use of 2-pyridyl Thioester Intermediate to Form First Amide Bond . . 141

3.2.3 Installing *ZED1227*'s Unsaturated Methyl Ester 143

3.2.4 Cleavage of *N*-Boc and 2nd Amidation 145

3.2.5 Scale Up and Sequence . . . 148
3.3 Conclusion . . . 151
3.3.1 Closing remarks . . . 153
3.3.2 Acknowledgements and Noted Contributions . . . 154
3.4 Experimental Data and Information. . . . 155
3.4.1 General Information . . . 155
3.4.2 Synthetic Scheme . . . 158
3.4.3 General Procedures: . . . 160
3.4.4 Optimization Data . . . 161
3.4.5 Sequence and Scale Up . . . 174
3.4.6 Calculation for Final Overall Yield of Compound **3.7** (*ZED1227*) . . . 178
3.4.7 E-Factor[77] Calculations from Preparation of *ZED1227* . . . 179
3.4.8 Analytical Data . . . 183
3.4.9 HPLC Traces . . . 189
3.4.10 ICPMS Data . . . 194
3.4.11 NMR Spectra . . . 195

4 Investigations Into Reactor Degassing via Ex-Situ Enzymatic Oxygen Fixation 203
4.1 Introduction . . . 203
4.2 Results and Discussion . . . 206
4.3 Conclusion . . . 212
4.3.1 Closing Remarks . . . 214
4.3.2 Acknowledgements and Noted Contributions . . . 214
4.4 Experimental Data and Information. . . . 216
4.4.1 General Information . . . 216
4.4.2 General Procedures and Results . . . 218

References 218

Chapter 1:

General Background and Introduction

Organic chemistry, though a relatively young science relative to other modern scientific disciplines, has had a profound impact on our modern world. The ever-evolving study of carbon-based molecules and their reactivity has allowed chemists to advance technology to such a broad extent that this impact, in and of itself, could constitute a thesis. Organic synthesis has enabled the creation of pharmaceuticals that have extended the average human lifespan by decades.[46,83] It has enabled the creation of new vaccines[71] that prevent disease and end pandemics. Chemists have synthesized crop protectants[8,83,88] to ensure we can sustain a global population of 8 billion people.[†] Novel polymers and materials allow for a vast array of new consumer goods, ranging from personal hygiene products,[67] to new electronics.[21,34] In this fashion, organic chemistry has, often in a literal sense, constructed much of the world as we know it today. Over recent decades, however, this field has faced increasing challenges borne of the modern era's urgent need to reduce greenhouse gas emissions, to attenuate our production

[†]United Nations Population Report (accessed 11/08/2025). https://www.un.org/en/global-issues/population

of toxic pollutants, and to reduce our reliance on expensive and non-sustainable resources. These demands stand as an affront to the very nature of this subdiscipline of chemistry, which is inherently comprised of wasteful, dangerous, and energy intensive processes. This is, arguably, most exemplified by the synthesis of pharmaceuticals.

Standing in stark contrast to the profound benefits described above, for every kilogram of Active Pharmaceutical Ingredient (API) produced, anywhere between 25 and 100 kilograms of waste is generated.[76] The vast majority of this waste consists of hazardous solvents that are combusted to emit CO_2, a potent greenhouse gas,[25,26] along with other toxic environmental pollutants.* For the waste that can't be burned, procedures involve sealing it in barrels and burying it in the ground, creating a serious risk for accidental exposure to the environment and, ultimately, leaving this waste to be dealt with by future generations.[30] While pharmaceutical manufacturing is the main offender in this regard, it does not stand alone (e.g. for every kilogram of fine chemicals produced, anywhere between 5 and 50 kilograms of waste are produced[77]). It is clear from these waste metrics and the existential consequences of this problem, including a significant contribution to climate change, that a paradigm shift has been a pressing need for organic chemistry.

Inherently, organic synthesis relies on petroleum feedstocks for both chemical reagents and for the solvents in which these reactions take place. These carbon-based solvents provide solubilization of these carbon-based compounds, provide for efficient thermal heat transfer, and often have high vapor pressures that allow for facile distillation and drying processes. How-

*See https://cen.acs.org/environment/green-chemistry/organic-chemists-cut-waste-switching-water/101/i23.

ever, as was briefly mentioned above, these solvents present several major detriments that are challenging to reconcile. Beyond high flammability and presenting fire and explosion risks, organic solvents are toxic: frequently being acutely poisonous, carcinogenic, neurotoxic, and combinations thereof.[66] While sometimes recyclable to an extent, much of these solvents stand as waste and pose serious problems to human and environmental health. Nonetheless, over recent decades, academia and the chemical industries have recognized these issues and have been addressing them in several ways.

The first step was to readily quantify and characterize the efficiency of various chemical processes, as well as define a core set of principles for chemists to try and adhere to in order to mitigate unnecessary waste, hazards, and costs. The first was accomplished in a succinct and effective way by Dr. Roger Sheldon in 1992. In what he coined as the "E-Factor",[75,77] any chemical process' efficiency can be assigned a value simply resulting from the dividing the kilograms of waste generated by the kilograms of the product obtained. In this fashion, the synthesis of any product, from fine chemical to pharmaceutical, can be compared to another and, thus, gives chemists a benchmark or reference to assess and improve upon production efficiency. Naturally, there is nuance that this quotient doesn't convey, such as the nature of the waste generated. If one process has a higher E-Factor, but the waste generated is fairly benign, that process would be preferred to one that has a smaller E-Factor, but yields particularly egregious by-products. Notwithstanding, though different interpretations of the E-Factor, as well as new formulas entirely, have been developed, Sheldon's E-Factor remains a useful fundamental metric at the time of writing this thesis, and is utilized across each topic discussed herein.

Table 1.1: E-Factor[a] for the Main Chemical Industries.[76]

Industry Section	Volume/ton per annum[b]	E-Factor
Bulk Chemicals	10^4–10^6	<1–5
Fine Chemicals	10^2–10^4	5–>50
Pharmaceuticals	10–10^3	25–>100

[a]This table is an adaptation of one provided in the associated reference.[76] [b]Annual production of the product worldwide or at a single site.

The latter, the set of principles for chemists to adhere to in order to mitigate costs, hazards, and impact to the environment and human health, was disclosed by Drs. Paul Anastas and John Warner. In their 1998 watershed work, "Green Chemistry: Theory and Practice," they accomplished this by defining The 12 Principles of Green Chemistry (Table 1.2).[3] Since its inception, the 12 Principles have served as a "north star" in the development of new technologies, reactivities, and synthetic routes toward the goal of making chemistry a more sustainable enterprise. The works discussed in this thesis are examples of such advancements. While the research in this area is broad and applicable to many different subtopics, this work is particularly focused on transition metal catalysis and micellar catalysis as a means of developing greener methods toward small molecule therapeutics and agrochemicals.

Micellar catalysis has been one of the most significant advancements in the area of green chemistry in the past 20 years, and has been a significant step toward challenging the paradigm of running chemical reactions in toxic organic solvents. Specifically, it enables chemistry to be conducted in water, which is inherently non-toxic, non-flammable, and readily abundant. Normally, water is a poor choice of reaction medium, as organic reagents and substrates are

Table 1.2: The 12 Principles of Green Chemistry.[3]

◆ Prevention	◆ Atom Economy
◆ Less Hazardous Chemical Syntheses	◆ Designing Safer Chemicals
◆ Safer Solvents and Auxiliaries	◆ Design for Energy Efficiency
◆ Use of Renewable Feedstocks	◆ Reduce Derivatives
◆ Catalysis	◆ Design for Degradation
◆ Real Time Analysis for Pollution Prevention	◆ Inherently Safer Chemistry for Accident Prevention

generally insoluble. Micellar catalysis addresses this issue by allowing them to go into aqueous solution with very little, or even no organic solvent present. Specifically, the introduction of designer surfactants to water results in their aggregation to form small vesicles known as micelles (Table 1.1). The core of these formed micelles is a lipophilic pocket that, in serving as the reaction "solvent", can uptake substrates and, thus, allows for solubilization. Remarkably, because the micellar pocket has a high local concentration, reactions experience enhanced kinetics. This has significant implications: reactions have been shown to proceed at lower temperatures and with lower catalysts loadings. In this manner, micellar catalysis not only enables water as a benign medium, but also yields less energy intensive, and more catalytically efficient processes. It is, therefore, obvious the significant contributions that this technology has made for green chemistry.

Of course, there is a high degree of nuance to transitioning organic synthesis to water in an attempt to improve environmental sustainability. Hypothetically, if the reagents of a reaction are soluble in ethyl acetate* and the product crashes out of solution, then this affords chemists

*Ethyl acetate is considered a fairly benign organic solvent due to its low toxicity.[2]

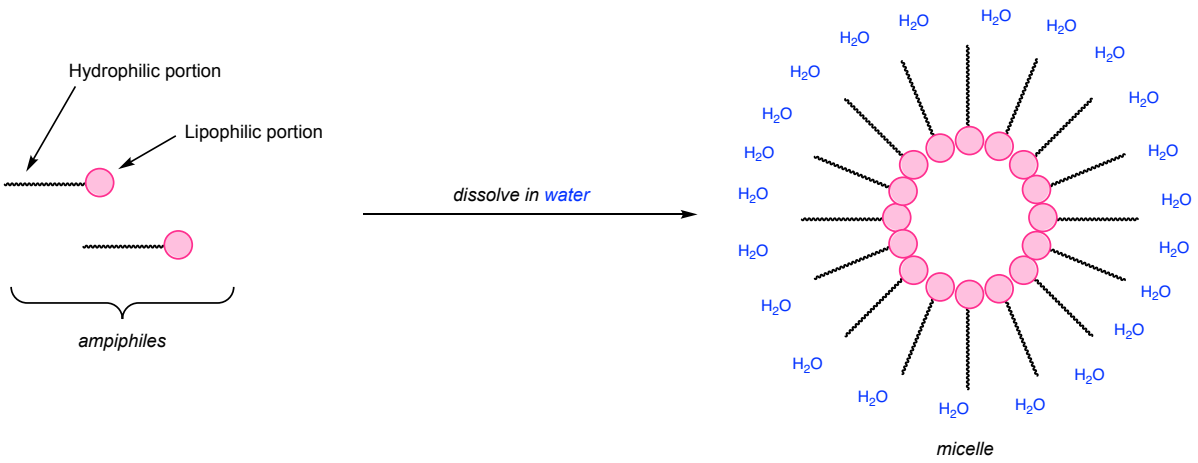


Figure 1.1: Micelle Formation in Water

the ability to collect the product via simple filtration. Conversely, if the reaction can be run under micellar conditions, it would be necessary to extract with organic solvent, thus, not effectively obfuscating the use of solvent, and ultimately generating more waste overall.* Beyond this, some moieties are simply too water-sensitive to be compatible. Moreover, if a reaction requires a large excess of acid or base under aqueous conditions, then it would be impractical due to the need for an intensive quench procedure. Notwithstanding these limitations, micellar catalysis stands as powerful technology, and knowing these limits enables chemists to find the avenues in which it is most effective. Much of this thesis work has sought to expand the scope of micellar catalysis, and to articulate such limitations encountered.

The contents of this thesis involve two main categories of contributions to sustainable organic chemistry: methods development, and sustainable syntheses of important API's. For methodology development, outlined in Chapter 2 is a robust, near-neat, and sustainable Miyaura

*Though requiring an energy input, this solvent is recoverable. If, in the same scenario the product crashes out in DCM (a carcinogenic solvent),[72] then it would be preferable to just run the reaction in micellar media, and then extract using ethyl acetate.

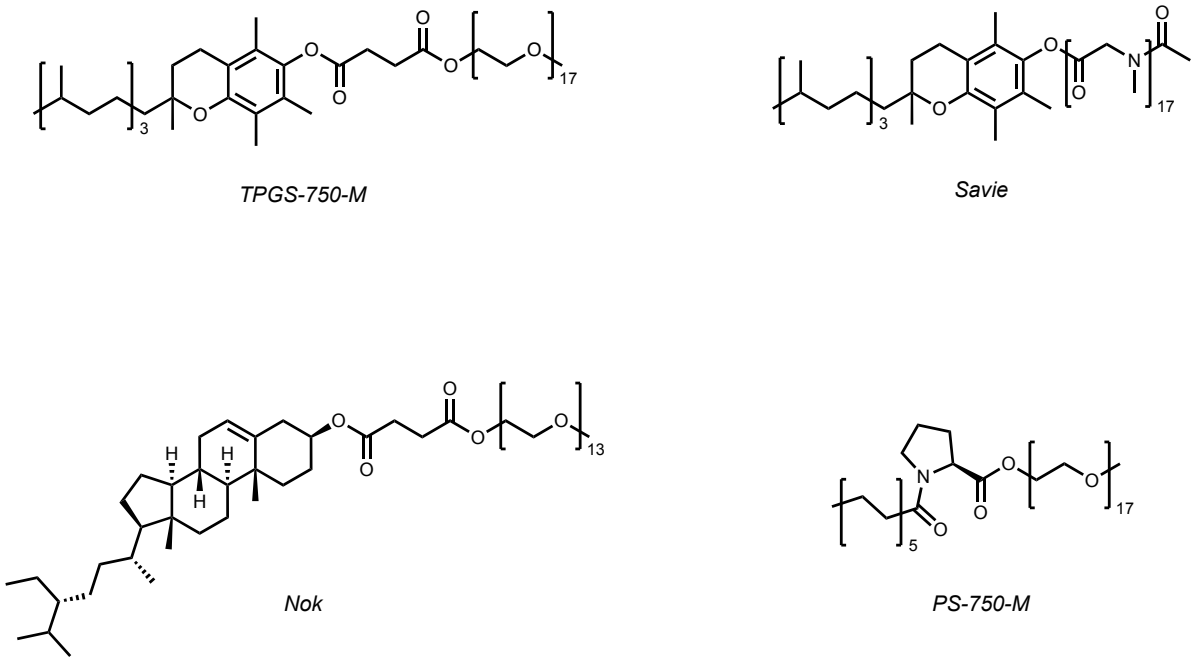


Figure 1.2: Select Examples of Designer Surfactants Developed by the Lipshutz Group.[40,41,49]

borylation, with applications to green 1-pot borylation-Suzuki-Miyaura couplings.[61] For the green total synthesis of API's, two main bodies of work are described. First, is the green synthesis of the important anticancer agent, Erdafitinib, with the first report* of such a synthesis utilizing a 1-pot protocol in biodegradeable aqueous surfactant.[40] The second synthesis is that of *ZED1227*, a world first treatment for the treatment of celiac disease.[10] The synthesis makes marked improvements to the preparation of this drug, with a ten fold reduction in E-Factor when compared to the original synthesis performed for medicinal chemistry studies.[10]

*This is to the best understanding of the author at the time of writing this thesis.

Chapter 2:

Environmentally friendly Miyaura borylations allowing for green, 1-pot borylation/ SuzukiMiyaura couplings

The contents of Chapter 2 have been reproduced with permission from:

Nelson, C. B.; L'Heureux, S. J.; Wong, M. J.; Kuhn, S. L.; Ghiglietti, E.; Lipshutz, B. H. *Green Chem.* **2024**, *26*, 10115–10122.

Green Chem. is © The Royal Society of Chemistry 2024.

2.1 Background and Introduction

To date, an innumerable number of transformations in organic chemistry have been reported in the literature. Each is an entry into the tool set for chemists to utilize in constructing molecules. However, of all these contributions, one of the most consequential subsets for the

chemistry of carbon, are, naturally, reactions that yield a carbon-carbon bond. Of the library of transformations to this end, the most robust and functional group tolerant of those is the Suzuki-Miyaura coupling.[57] The power and ubiquity of this reaction* is most exemplified by the fact that more than three decades after this Nobel Prize winning work[57] was first disclosed, it was found to be the second most employed by the pharmaceutical industry.[9] Such omnipresence is seen across the other chemical industries as well (*e.g.*, agrochemicals and materials).[8,23,83] Giving its widespread use, there has been considerable work toward improving the efficiency and environmental responsibility of this transformation. Notable contributions include ligand design and micellar catalysis. New phosphine ligands have allowed for extremely efficient catalyst loadings,[65] and aqueous micellar media† has also greatly furthered this, along with allowing for this coupling to be run in water at fairly benign temperatures.[40,48] In spite of such advancements, however, there is a stark dichotomy presented when comparing this progress to the more traditional and wasteful means by which the key starting materials for this reaction are produced.

Toward the conclusion of the project where Dr. Vani Singhania and I developed a sustainable synthesis of erdafitinib,[80] I was curious as to the origin of the boronic ester we were utilizing for the Suzuki coupling step. As a thought experiment, I wondered what an additional step to the green synthesis, specifically in producing this coupling partner, would look like. What was available for general, sustainable borylations? Remarkably, the options available in

*This coupling is specifically for binding two sp^2 hybridized carbons; however, recent work has expanded the reaction to sp^2–sp^3 C–C bonds as well.[85,86,90]

†More extensive discussion on micellar catalysis is provided in Chapter 1.

the literature were limited. Borylations, traditionally, involve cryogenic lithium halogen exchange,[54] and this method still sees frequent use in modern organic synthesis.[63] Beyond this, the go-to method for making such carbon–boron bonds was developed by Norio Miyaura in 1995.[35] Utilizing very similar chemistry to that of the Suzuki-Miyaura coupling, catalytic palladium was demonstrated to enable the cross-coupling of an aryl halide with a *bis*-boronic ester. This resulting protocol was significantly more benign than the aforementioned lithium halogen exchange method, and was made especially attractive by the fact that, in using the same palladium-catalyzed cross-coupling platform, it was readily amenable to 1-pot applications of borylation/Suzuki-Miyaura (SM)* couplings. Nonetheless, while Miyaura's method has rightfully gained widespread use over the decades since its initial disclosure, it routinely runs into much the same issues initially presented by the SM coupling. Frequently throughout the literature, one can see excessively elevated reaction temperatures,[6,11,13,89] high palladium† mol percentages,[6,13,20,35], and the use of wasteful, and toxic organic solvents. To add insult to injury, the resulting borylated products frequently experience limited shelf stabilities, and can be fairly difficult to purify.[1,6,38,42,64] The natural questions that sprung to mind from observing a gap in the literature with regard to sustainable borylation were as follows: why is this the case? What progress has been made to make this reaction green? And what can be done to make more robust, environmentally-friendly borylations?

*For the sake of brevity and readability, I will often abbreviate the Suzuki Miyaura coupling as SM

†Palladium is an endangered precious metal with a higher rarity than gold in the earth's crust.[70] The cost of palladium at the time of writing is $1,503.20/oz (price obtained from apmex.com on 12/03/2025).

A very interesting and novel approach to "greening-up" this reaction has been C–H activation. In this method, largely put forth and advanced by John Hartwig, an iridium catalyst is used to activate an aryl C–H bond, and then cross couple with a *bis*-boronic ester.[31,43] This is particularly attractive as it obviates the need for halogenated starting materials. However, there are several notable drawbacks. Naturally, selectivity for the desired C-H bond can be challenging, and so specific directing groups are necessary.[43] This limits the scope of this methodology, and can often yield a mixture of products. Frequently, as well, relatively high temperatures are needed.[43,45] Moreover, and arguably worst of all, these reactions[31,43,45] require fairly high loadings of iridium,* a precious metal that is more rare and far more costly than is palladium.[69] The applications of this chemistry are apparent, but, given these detriments, C–H borylations need significantly more development to become widely applicable. As I began to ponder what contributions could be made to sustainable borylations, the large limiting factors for C–H activation turned me toward maintaining my focus on the palladium-catalyzed Miyaura borylations given its existing precedent as being more robust and general.

For sustainable Miyaura borylations, the state of the art up until the time of engaging in this project had been the use of *bis*-boronic acid (BBA) as the boron source.[59,60] In addition to being more atom economical. Green aspects of using BBA are also seen with its application to methods utilizing relatively modest equivalents of palladium (*i.e.*, 0.5 mol %), moderate reaction temperatures (*i.e.*, rt–80°C), and fairly responsible solvents (*i.e.*, 2-MeTHF, EtOH).[58–60] While these metrics are absolutely a step in the right direction, the drawbacks of using BBA are

*The price of irridium the time of writing is reported to be $4,534.51/oz (price obtained from strategicmetalsinvest.com on 12/03/2025).

challenging to reconcile. First, the scopes of these methods remain relatively simplistic. Subsequently, these simple boronic acids then see limited applicability and/or efficiency in their respective 1-pot Suzuki coupling protocols.[59,60] Here, total palladium loadings exceed 1 mol %,[59,60] and the complexity of resulting biaryls are lacking.[58] Lastly, the use of BBA itself is not perhaps as green as it initially seems. In these reports discussed, the atom economy of BBA is attenuated by the need to use a decent excess (1.5 equiv). BBA has also been seen to readily decompose in the presence of moisture, oxygen, heat, and palladium (II) complexes.[17,29] The usability of this reagent is even further diminished by the fact that the by-product of such decomposition is hydrogen gas[17,29,55] (a serious fire and explosion risk at scale). It is also worth noting that such instability and decomposition into hydrogen gas is seen, though to a lesser extent, with the more classical B_2pin_2 reagent* as well.[55]

It became evident at this point in my investigations into the literature that the lag in progress in developing greener Miyaura borylations is due, at least in part, to the inherent sensitivities of *bis*-boron reagents and the resulting borylated products. Based on this observation, I had a rough outline for how a greener method could be envisioned. First, I needed to find or develop a boronic ester that was more nonreactive toward water, base, heat, etc. Secondly, and fairly contradictory to the first point, the resulting aryl boronic ester still needed to be reactive enough to effectively participate in the SM coupling. Lastly, I needed the borylation for this to be as congruent as possible with existing green SM coupling methods such that one-pot procedures would be facile.

*Recent research has shown that the shelf stability of B2pin2 is not as long as previously assumed.[32]

2.2 Results and Discussion

2.2.1 Sustainable Borylation Method

Not long before the time of completing the synthesis of erdafitinib,[80] Takashi Ikawa and colleagues from the University of Osaka published a study showing the nonintuitive and unique properties of *ethyl*pinacol boronic esters.[64] First, and rather remarkably, their nonreactivity with silica is demonstrated. This was a complete about-face* from the typical behavior of boronic esters (and especially boronic acids) on silica gel, which are known to streak, or decompose entirely, when running TLC† or column chromatography. This unusual observation is then carried forth in a stability study where 3-pyridyl boronic acid, pinacol ester, and ethyl pinacol ester are subjected to conditions emulating a SM coupling. Specifically, these three reagents were dissolved, respectively, in toluene/H_2O (10:1) and K_3PO_4 (1.3 equiv.) is added to each solution; these solutions are then heated to 100 °C with stirring.[64] Over the course of 24 h, the solutions were monitored for decomposition. The boronic acid was completely decomposed by hour 12. At the end of the 24 h, less than 85% of the pinacol boronic remained. And for the fate of the ethyl pinacol boronic acid? Unscathed. Beyond a surprising point to read, this sprung to mind two additional questions. Why was this the case? What did their Suzuki coupling reactivity look like if they were so stable in basic aqueous media?

*Though this is a substrate dependent phenomenon, it tends to be a strong trend for these reagents.
†Thin Layer Chromatography (TLC).

A relatively obvious factor is that these BEpin boronic esters have more steric hindrance around the reactive boron atom. However, intuition wouldn't suggest that this effect would impart such dramatic resistance to hydrolysis, especially under basic conditions at elevated temperatures. Ikawa and coworkers rationalize this by stating that the hydrogens on the terminal carbons of the ethyl "arms" of the diol preferentially occupy the empty p-orbital of the boron atom (Figure 2.1).[64] This equilibrium is resulting, I surmised, from the stabilizing effect of these terminal hydrogens donating some electron density to the p-orbital. As such, a much lower percentage of the boronic ester molecules populate the more reactive "open" conformation. An interesting supporting piece of data could be that of DFT analysis. It was not initially considered at the time of engaging in this project, but, hopefully, this can be performed in the future to more definitively characterize this phenomenon.

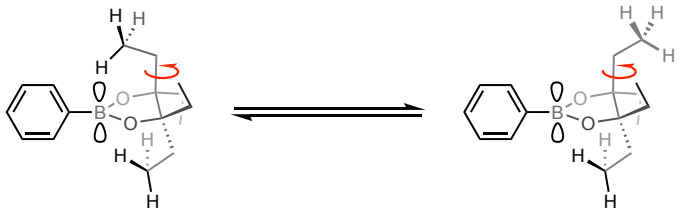


Figure 2.1: Rationale for BEpin stability (figure adapted from work published by Ishikawa *et al.*[64]).

The boron being more shielded in this way would, intuitively, make BEpins poor Suzuki coupling partners as it would largely prevent the formation of the borate species, and thus would prevent transmetallation. However, in another set of remarkable results from Ishikawa and colleagues, these BEpins tended to outperform their pinacol boronic ester and boronic acid counterparts in this regard. Not much was provided in the way of discussion from their paper with regard to why this was the case. My rationale is as follows: first, for boronic acids, the

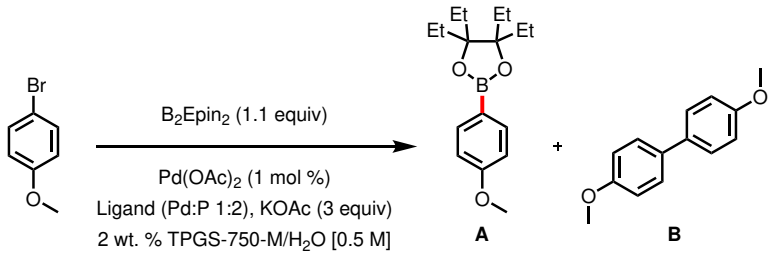
active borate is quite prone to deboronation (as is seen by the Ishikawa paper, and in other literature[19]). Second, pinacol boronic esters are fairly readily hydrolyzed* to the corresponding boronic acid where, as just discussed, they then undergo protodeboronation. Given these two facts, and given BEpin's strong divergence from this trend, it can be reasonably postulated that BEpins are never hydrolyzed to the boronic acid. The enhanced stabilization of the ethyl pinacol diol leads to it not being cleaved from the activated borate intermediate. Herein lies why these BEpins likely perform better for the Suzuki coupling. For the boronic acid turned borate (or boronic ester turned boronic acid turned borate), the two available forward processes are decomposition (*i.e.*, protodeboronation) or transmetallation. Inherently, you'll get a mix of the two depending on the substrate and reaction conditions, which in turn would impact the yield, and the distribution of products. For the BEpin borate, the only available forward process would be that of transmetallation (*it is important to note that work done by Prof. Scott Denmark's group at the University of Illinois, Urbana-Champaign has shown that transmetallation of boronic esters can occur without hydrolysis to the corresponding boronic acid*[82]). This inherently provides higher selectivity for the desired biaryl as unwanted decomposition or byproducts (protodeboronation) are avoided. Hence, the BEpin boronic esters yield more effective Suzuki couplings.

The combined stability factors as well as efficacy in SM couplings all were found to be highly encouraging toward developing a green borylation method, and, furthermore, a sustainable 1-pot borylation/SM coupling. First, the hydrolytic stability of BEpins pointed to a

*There are interesting cases where protodeboronation of boronic esters can occur without hydrolysis to the corresponding acid,[33] but these are beyond the scope of the discussion provided in this thesis.

potential water compatible borylation protocol. Beyond the fact that water is a benign and abundant solvent, borylations in water were simply underexplored in the literature. In certain instances, they had been accomplished to very limited success: reported examples are simplistic, yields are modest, and those that perform tend to be simple electron rich substrates.[15,50] In reading this, I saw BEpins as a means of expanding borylations to water, not only for water's sake, but also as a demonstration of a much more robust borylation protocol. Further beyond this, and arguably the most significant aspect, is that water is already an imperative component of the following SM coupling. In this fashion, having the borylation in water makes it further congruent with the next step. Chemists would, thus, see less need for any modification, or manipulation, of the reaction mixture when utilizing it directly in the second step, all done in the same pot.

Table 2.1: Ligand Optimization[61]



Entry[a]	Ligand	Yield (A%)[b]	Yield (B%)[b]
1	QPhos	46	9
2	**[*t*-Bu$_3$PH]BF$_4$**	**80**	**trace**
3	DPPF	38	trace
4	XPhos	25	trace
5	*t*-BuXPhos	13	trace
6	SPhos	26	trace
7	RuPhos	36	trace

Continued on next page

Entry[a]	Ligand	Yield (A%)[b]	Yield (B%)[b]
8	*t*-BuXantPhos	trace	NR
9	DPPP	trace	trace
10	*t*-BuBrettPhos	11	trace
11	N_2Phos	trace	trace
12	EvanPhos	trace	trace
13	**AmPhos**	**82**	**trace**
14	DavePhos	42	trace
15	JohnPhos	8	NR
16	BINAP (racemic)	17	trace
17	2-(*t*-Bu_2P)-1-Ph-1H-pyrrole	14	10

[a] Reactions run on a 0.25 mmol scale. [b] Yield determined via qNMR using 1,3,5-trimethoxybenzene as an internal standard.

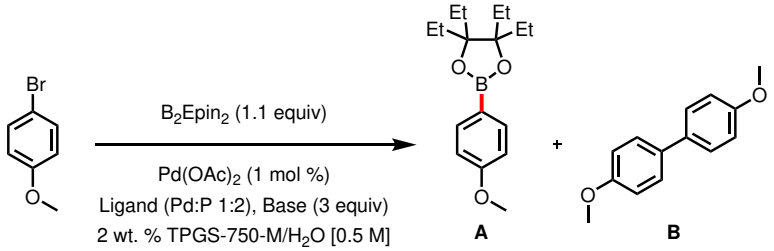
I first sought to test my hypothesis that the Miyaura borylation to generate aryl BEpins would succeed in water. I started with my group's work-horse aqueous surfactant solution, 2 wt % TPGS-750-M/H_2O.* Naturally, I employed B_2Epin_2 as the *bis*-boronic ester, and I utilized KOAc as the base, giving its long-standing precedence as the base of choice for this transformation.[35] Under these conditions I screened a series of ligands, as seen in **Table 2.1**.

Two relatively simple monodentate ligands showed promise from this screen: [*t*-Bu_3PH]BF_4 and AmPhos. From here, I prioritized [*t*-Bu_3PH]BF_4 given its superior bench stability and ease of use (Table 2.2). However, in a resulting base screen, the yield never was seen to break the initial hit of 80% (by qNMR). A find in the literature then prompted the use of 2-ethylhexanoate (2-KEH) as a means of improving the reaction yield. These sterically bulky carboxylate bases had recently been shown to decrease the temperature and palladium loading for borylations by preventing over-complexation of the base with the palladium (II) transmetallation complex.

*Discussion on surfactants and how they enable chemistry in water is provided in Chapter 1.

This, unfortunately, was not found to be efficacious with [*t*-$Bu_3PH]BF_4$. Nonetheless, from here, I took the top performing bases from this screen and applied them to the other top performing ligand, AmPhos.

Table 2.2: Base & Ligand Optimization Scheme[61]



Entry[a]	Ligand	Base	Yield (A%)[b]	Yield (B%)[b]
1	[*t*-$Bu_3PH]BF_4$	KOAc	80	trace
2	[*t*-$Bu_3PH]BF_4$	NaOAc	77	trace
3	[*t*-$Bu_3PH]BF_4$	K_2CO_3	40	10
4	[*t*-$Bu_3PH]BF_4$	KF	34	trace
5	[*t*-$Bu_3PH]BF_4$	K_2HPO_4	78	trace
6	[*t*-$Bu_3PH]BF_4$	K_3PO_4	trace[c]	sig.[c]
7	[*t*-$Bu_3PH]BF_4$	NaOPh	trace[c]	sig.
8	[*t*-$Bu_3PH]BF_4$	2-KEH[d]	60	trace
9	[*t*-$Bu_3PH]BF_4$	KH_2PO_4	11	trace
10	[*t*-$Bu_3PH]BF_4$	tBuOK	19	33
11	[*t*-$Bu_3PH]BF_4$	TEA	27	25
12	[*t*-$Bu_3PH]BF_4$	DIPEA	25	10
13	[*t*-$Bu_3PH]BF_4$	Pyridine	trace	NR
14	[*t*-$Bu_3PH]BF_4$	KOTMS	trace[c]	sig.[c]
15	AmPhos	NaOAc	trace[c]	trace[c]
16	AmPhos	K_2HPO_4	73	8
17	**AmPhos**	**2-KEH[d]**	**87**	**trace**

[a] Reactions run on a 0.25 mmol scale. [b] Yield determined via qNMR using 1,3,5-trimethoxybenzene as an internal standard. [c] Qualitative assessment based off TLC of crude reaction mixture ("sig." = significant). [d] Potassium 2-ethylhexanoate.

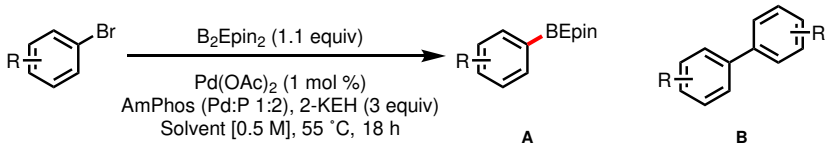
Gratifyingly, 2-KEH improved the reaction when used with AmPhos, showing good efficacy for the borylation protocol in water. This, however, is where an interesting observation changed the course of the project. Though optimization was proceeding smoothly, it was observed that when the 2-KEH base and B_2Epin_2were added to the same vial, coalescense of the two solids into a viscous slurry was observed. This immediately hearkened back to my first project assisting Dr. Karthik Iyer in developing a benign set of conditions for reducing carboxylic acids via the corresponding 2-pyridyl thioester intermediate.[36] In order to form the thioester intermediate, the carboxylic acids were stirred neat at temperature with dipyridyldithiocarbonate (DPDTC), which forms a readily stirred slurry in the range of 55-65 °C.* While the drive to use greener solvents is always important, the least wasteful process is, naturally, one that doesn't use solvent at all. Thus, the similar appearance of the 2-KEH/B_2Epin_2slurry to that of aryl carboxylic acid/DPDTC slurries begged the question: does this borylation protocol require solvent at all?

This observation and question were quickly followed by another observation and question. Shortly after observing coalescence, the older 2-KEH bottle in use was depleted, and a newer bottle was procured. When this newer batch of base was added to a vial with $B_2Epin_2$for further experimentation, the previous coalescence was no longer observed. Why was this the case? It was then realized that the older bottle of 2-KEH was bringing in moisture due to the highly hygroscopic nature of this solid. The newer aliquot, naturally, did not yet retain such moisture and so didn't see such coalescence. This finding made clear that a small amount of

*The melting point of $B_2Epin_2$is similarly around 55°C.

solvent would be necessary for adequate stirring. To ensure generality in this regard, we added 2-bromomethylindole as a solid model substrate*, and screened various solvents (Table 2.3; Entries 1-6 were run prior to considering a potential near-neat protocol).

Table 2.3: Surfactant/Solvent Screen[61]



Entry[a]	Substrate	Solvent	Yield (A%)[b]	Yield (B%)[b]
1	SM_1[f]	H_2O	80	trace
2[e]	SM_1	2 wt % TPGS-750-M / H_2O	78	trace
3[e]	SM_1	2 wt % Savie / H_2O	76	trace
4[e]	SM_1	2 wt % MC-1 / H_2O	70	trace
5[e]	SM_1	2 wt % Coolade / H_2O	88	trace
6[e]	SM_1	2 wt % Brij / H_2O	69	trace
7	SM_2	H_2O	91	trace
8	**SM_2**	**EtOAc**	**95**	**trace**
9	SM_2	EtOH	trace[c]	trace[c]
10	SM_2	toluene	trace[d]	n.d.
11	SM_2	2-MeTHF	89	trace
12	SM_2	none	trace[c]	trace[c]

[a] Reactions run on a 0.25 mmol scale. [b] Yield determined via qNMR using 1,3,5-trimethoxybenzene as an internal standard[c] Qualitative assessment based off TLC of crude reaction mixture ("sig." = significant). [d] Poor stirring of reaction mixture. [e] 10 v/v % THF included as a cosolvent.[f] SM_1 = 4–bromoanisole; SM_2 = 5–Bromo–1–methylindole.

This assay of various solvents (specifically entries 7-12) led to three effective options that performed within error of one another: EtOAc, H_2O, and 2-MeTHF. Though bio-derived, 2-MeTHF was ruled out as the least green of the these options.† For differentiating the other two:

*Naturally, it is less than ideal to switch/add model substrates during optimization, but shifting to a near-neat method prompted the use of a solid substrate in order to more accurately land on a more general protocol.

†With ethereal solvents, peroxide formation is always a hazard, and mitigating against their formation entails additional costs and energy.

EtOAc simply proved to be more general (see entry 1 in Table 2.3).* It is important to note that though ethyl acetate was an effective general choice, water alone was still effective for several highly functionalized substrates (see Figure 2.3). As such, chemists looking to employ this method would have the option of using either of the two solvents depending on the substrate and the requirements for the process.†

Nonetheless, further optimization in ethyl acetate allowed for the concentration to be brought up to 2.5 M, the base loading down to 1.5 equivalents, and further trials led to a very efficient general palladium loading of just 0.25 mol %. The generality of this sustainable method is displayed by the variety of substrates presented in Figure 2.2. Each product was isolable on silica gel columns, notably including several heteroaromatic compounds. There isn't any obvious trend in terms of substrate success, such as the substrate being electron-rich/poor. However, the ineffective substrates shown can be rationalized as follows. Compound **2.13** is particularly electron poor, and **2.14** has an adjacent coordinating nitrogen heteroatom that likely interferes with catalysis. Furthermore, due to the bulky nature of the *ethyl*pinacol boronic ester, sterically hindered aryl halides were shown to do poorly (Compound **2.15**).

The ultimate goal and motivation for almost every environmentally friendly project is to develop a green method that demonstrates robustness and promiscuity‡ and, thus, promotes application to organic synthesis beyond just an academic research lab setting. In this fashion, I moved forward with applying this near-neat protocol to API's,§ API precursors, and other

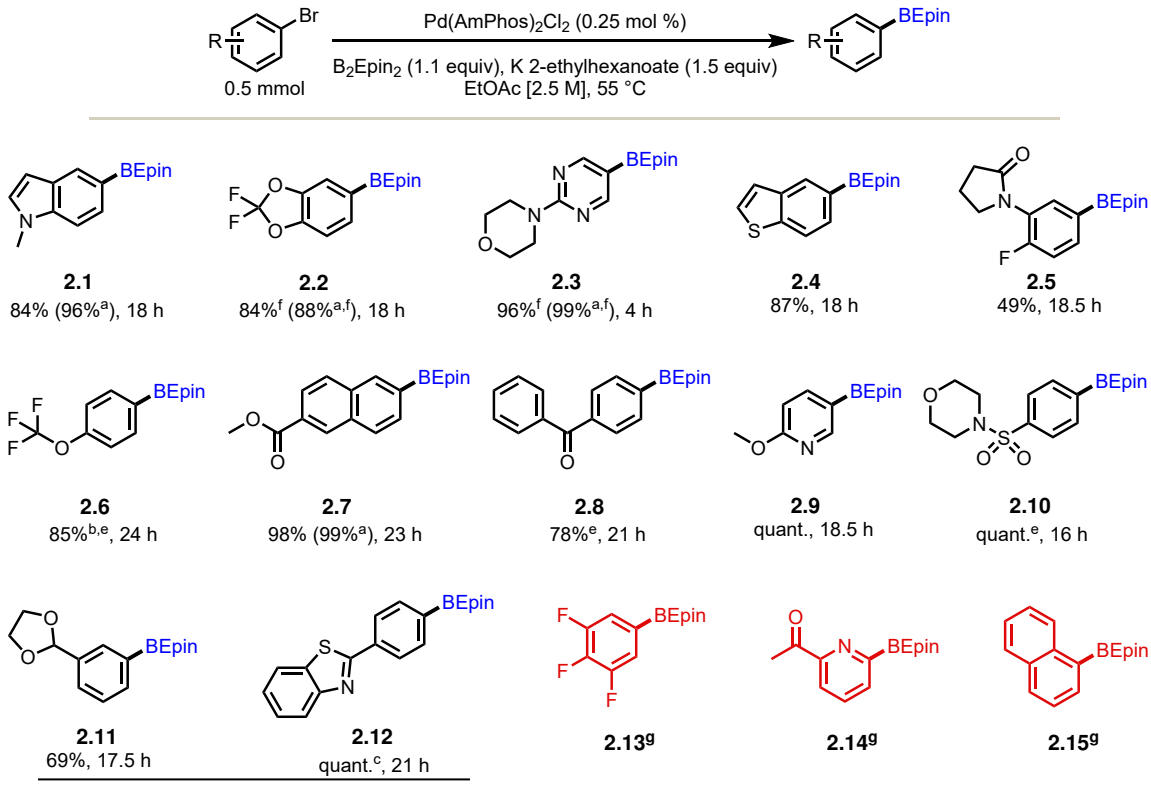
*Simple TLC and HNMR conversion for the borylation of 4-bromoanisole showed it to be a better option than any of the aqueous based solutions.

†Noted is that scale may also impact this choice.

‡Generally applicable to many different substrates.

§Active Pharmaceutical Ingredient (API).

Figure 2.2: Scope of Aryl BEpin Products.[62]



[a] Yield determined via qNMR using 1,3,5-trimethoxybenzene as an internal standard. [b] Utilized 0.5 mol% of Pd. cat. (Pd:P 1:4). EtOAc conc. of [1.25 M]. [c] Dilution to [1.67 M] EtOAc. [d] 2 mmol scale. [e] 0.3 mmol scale. [f] 0.25 mmol scale. [g] Unsuccessful substrate.

highly functionalized compounds. Of course, such compounds tend to be more polar than the substrates presented in Figure 2.2, and tend to have higher molecular weights. As such, some alterations to the general conditions were anticipated and then implemented on an as-needed basis. This included minor dilutions of EtOAc, moderate increases in palladium loading (up to 0.5 mol %), somewhat longer reaction times, and/or higher temperatures (*e.g.*, 70°C). For aryl chlorides, the literature has reported the use of XPhos to be more efficacious,[6] and several substrates in Figure 2.3 stand in support of those findings. Notwithstanding such minor adjustments, these remarkably green conditions afforded moderate to excellent yields for highly

functionalized substrates, including indomethacin, loratidine, fenofibrate, and Merck Informer Compound X3. Notable as well is that the antipsychotic, perphenazine, was fairly effectively borylated in a concentrated aqueous medium.* Later, though timing didn't permit it to be included in the manuscript, it was found that loratadine proceeded equally well in water as in organic solvent. Though our general method relies on a small addition of EtOAc, these results provided strong support for our initial hypothesis that B_2Epin_2(and the newly formed, stable aryl BEpins) would provide enough hydrolytic stability to be effective in water. Nonetheless, these examples highlight the strong efficacy of our conditions, and they represent a significant, long-overdue improvement to the environmental responsibility associated with Miyaura borylations.

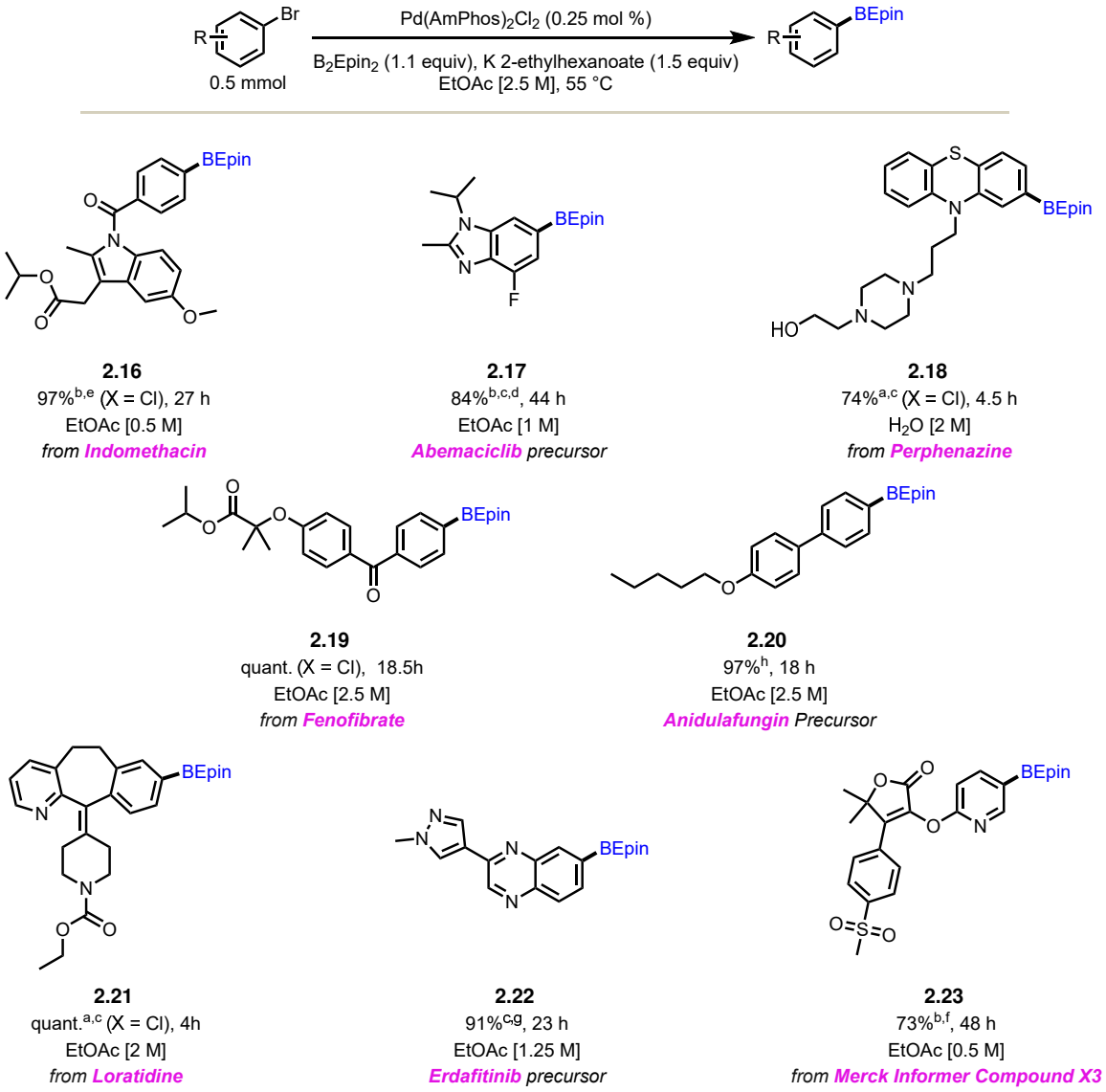
2.2.2 Green 1-Pot Miyaura Borylation/Suzuki-Miyaura Coupling Method

Ultimately, the carbon-boron bond is largely a synthetic handle chemists generate *en route* to other desired functional groups or products. While there's a range of such reactions, the most overwhelmingly prolific of those, as discussed, has been the Nobel Prize winning Suzuki-Miyaura (SM) coupling.[57] While our borylation conditions had been successfully developed, I then sought to fully complete our method and further highlight its efficacy for the broader scientific community by carrying it forward to the targeted biaryl products. I anticipated this to be a fairly straightforward endeavor: my research group had already developed technology

*The substrate was not effectively borylated in water with B_2pin_2 (determined via TLC and crude NMR).

for sustainable SM couplings in water.[48] These presumptions ended up, however, proving erroneous.

Figure 2.3: Scope of Highly Functionalized Aryl BEpin Products.[62]



[a] XPhos utilized. [b] Utilized 0.5 mol % of Pd. cat. [c] (Pd:P 1:4). [d] 70 °C. [e] 0.25 mmol scale. [f] 0.2 mmol scale. [g] 0.125 mmol scale. [h] 2 mmol scale.

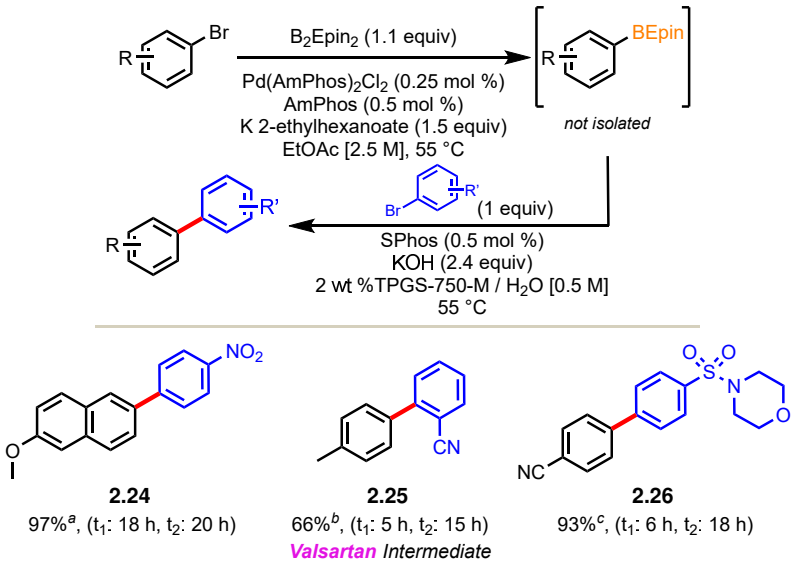
"Suffering from one's own success" is a succinct way of describing the difficulties encountered trying to implement aqueous micellar conditions in this final step. What was observed via GC-MS,* was that, due to it's enhanced hydrolytic stability, residual B_2Epin_2 from the first step persisted through to the crude reaction mixture going into the second step. This allowed for borylation of the aryl halide included in that step. In turn, this also allowed for homocoupling of this second halide. Thus, the final crude mixture was seen to contain the first borylated material, the second halide, the borylated second halide, the homocoupled second halide, as well as the desired biaryl.† Beyond greatly complicating isolation of the desired product, such side reactions served to diminish the overall yield greatly. It was in this manner that, having initially developed a successful borylation method in aqueous surfactant, we could not then effectively implement such surfactant conditions in a 1-pot borylation/SM coupling protocol. Nonetheless, though not as general as initially hoped, we were able to generate three biaryl compounds under these conditions (Figure 2.4). It was presumed that the 2nd halide for these cases was a poor borylation substrate under micellar conditions and, thus, didn't produce the side products just discussed. Further testing of this hypothesis is needed, but could provide a rationale for when chemists might be able to implement this protocol and, hence, would only need to use 0.25 mol % of the palladium catalyst for the entire 1-pot process.

Focus was then turned to other green avenues for the Suzuki-Miyaura coupling step. Namely, I sought a known "on-water" method shown previously to be efficacious.[4] The implementation

*Gas Chromatography-Mass Spectrometry

†Naturally, lower loadings of B_2Epin_2 were assayed to help mitigate this issue, but such conditions only served to diminish the initial borylation yield. Also attempted was an inversion in stoichiometry, which also proved to be ineffective in this case.

Figure 2.4: 1-pot Suzuki Scope in Aqueous Media.[62]



[a] Run on a 0.5 mmol scale with 0.8 equiv. of bromide in the SM coupling. [b] Run on 0.3 mmol scale; conc. of [0.25 M] and 3 equiv. of K_3PO_4 in SM coupling. [c] Run on a 0.25 mmol scale.

of water and TBAB as a phase transfer catalyst (first reported in the associated reference[4]) proved to be more effective when applied to the same substrates attempted under micellar conditions. Still observed was some minor borylation and homocoupling of the second halide, but, unlike with the surfactant conditions, an inversion of stoichiometry* prevented these side reactions from diminishing the yield for the desired biaryl product. Unfortunately, attempts at maintaining the initial catalyst loading throughout the entire 1-pot process wasn't possible. Some poisoning of the initial catalyst loading was presumed. Additions of extra equivalents of ligand to prevent such poisoning showed some improvement, but was overall ineffectual. A second charge of 0.25 mol % palladium going into the second step was, ultimately, found to push the reaction to completion. Even with this second addition, it is noted that the overall

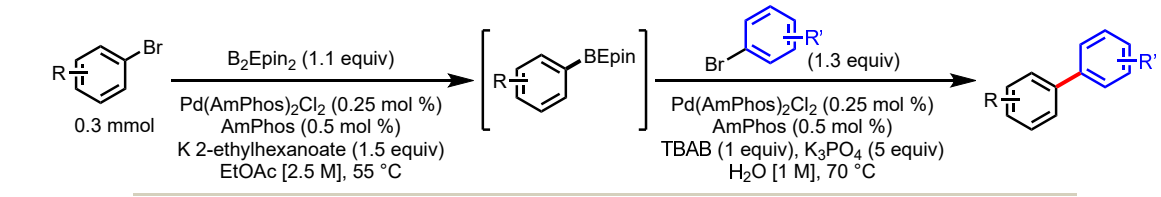
*Second halide in excess.

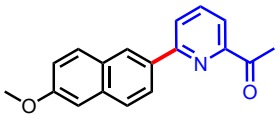
loading for the palladium for the entire process is still a very efficient 0.5 mol %, and stands as a significant improvement relative to other 1-pot protocols.[59,60] It is worth pointing out, as well, that charging the entire loading of 0.5 mol % palladium at the beginning borylation step also leads to lower levels of conversion to the final biaryl, further supporting the presumption that some catalyst poisoning occurs during/immediately after the first transformation.*

Discussed above is that a green process is not only measured by its sustainability metrics, but, perhaps with more significance, it is measured by the efficacy of its application to relevant, real-world synthesis of functionalized compounds. The scope of the developed method reported herein for the 1-pot borylation/SM coupling demonstrates cases that represent just that (Figure 2.5). In moderate-to-excellent yields are many heteroaromatic compounds, and present are API/API-like coupling partners (*i.e.*, loratidine and Merck Informer Library Compound, X3). Nonetheless, some functionality lacking is that of particularly base-sensitive substrates. While optimizing the Suzuki step, a semi-excess of K_3PO_4 (5 equivalents) was needed to drive the reaction to completion (likely due in part to the added stability of the BEpins). As such, some bas-sensitive esters were not tolerated and, thus, not pursued further. Notwithstanding this limitation, the scope of substrates conveys generality and strong applicability to many functionalized coupling partners.

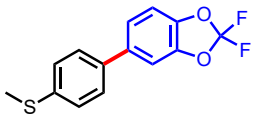
*Great care was taken to ensure oxygen was not the culprit in this regard.

Figure 2.5: General Sustainable 1-pot Barylation/Suzuki Scope.[62]

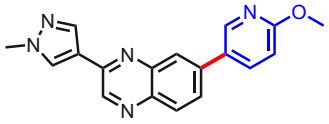




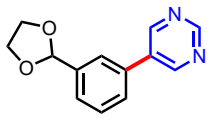
2.27
93%, (t_1: 18 h, t_2: 5.5 h)



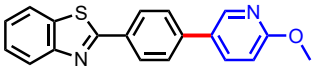
2.28
quant.[b], (t_1: 17 h, t_2: 23.5 h)



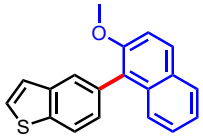
2.29
88%, (t_1: 24 h, t_2: 16 h)



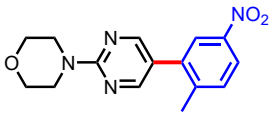
2.30
88%, (t_1: 15.5 h, t_2: 9 h)



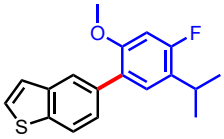
2.31
81%, (t_1: 21 h, t_2: 17 h)



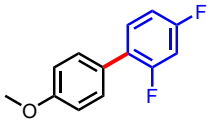
2.32
73%[a], (t_1: 23 h, t_2: 18 h)



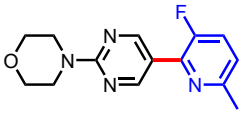
2.33
65%[f], (t_1 20.5 h, t_2: 19 h)



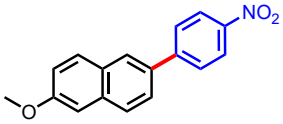
2.34
48%[b], (t_1: 23 h, t_2: 24 h)



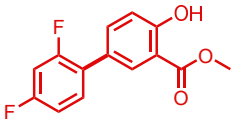
2.35
81%[b], (t_1: 15 h, t_2: 24 h)
***Diflusinal** Precursor*



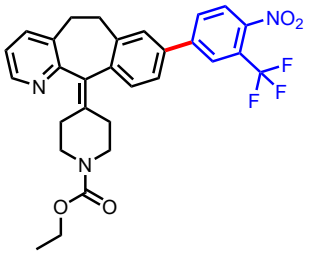
2.36
69%[f], (t_1: 20.5 h, t_2: 19 h)



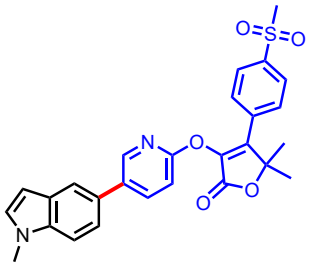
2.37
quant., (t_1: 18 h, t_2: 24 h)



2.38[c,e]



2.39
quant.[d], (t_1: 4 h, t_2: 22 h), X_1 = Cl
*from **Loratidine***



2.40
quant.[g], (t_1: 18h, t_2: 36h)
*from **Merck Informer Compound X3***

7.9 ppm residual palladium

[a] 1 equiv. of bromide used in the SM coupling. [b] 1.5 equiv. of bromide used in the SM coupling. [c] 0.5 mol% of Pd at 70 °C utilized in the borylation step. [d] XPhos (Pd:P 1:4) utilized in the borylation step. [e] Unsuccessful coupling (first step conversion confirmed via GC). [f] Run on a 0.5 mmol scale. [g] Run on a 0.125 mmol scale.

2.2.3 Application of this Methodology to a Precursor of Anidulafungin

To further substantiate this methodology as a sustainable cross-coupling tool in the tool-kit of industrial chemists, we performed a gram scale synthesis of a pharmaceutical intermediate. To this end, we carried out our 1-pot protocol on a 3 mmol scale for the preparation of a key anidulafungin precursor. With the only modification being the inclusion of a small amount of 2-MeTHF in the Suzuki step, the preparation of this terphenyl proved remarkably efficient, with the product being collected in 99% yield via simple filtration. Moreover, an E-Factor of only 10.9 calculated for this scale up accentuates the remarkable sustainability of this work.

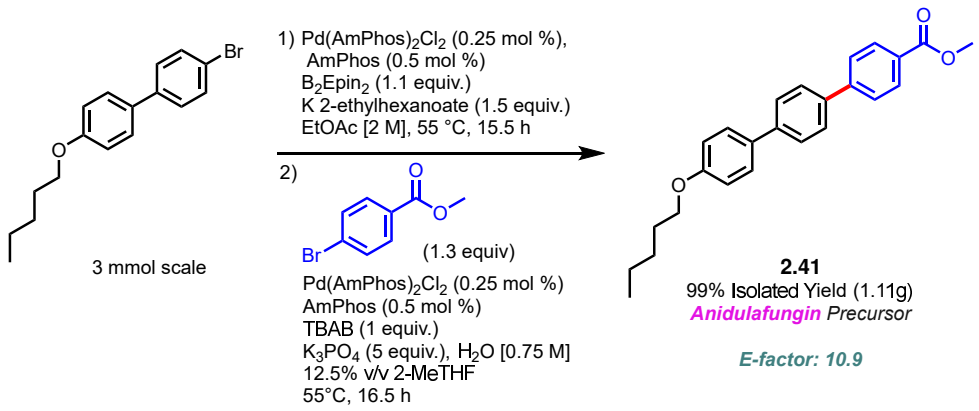


Figure 2.6: Sustainable 1-pot Borylation/Suzuki Scale Up.[62]

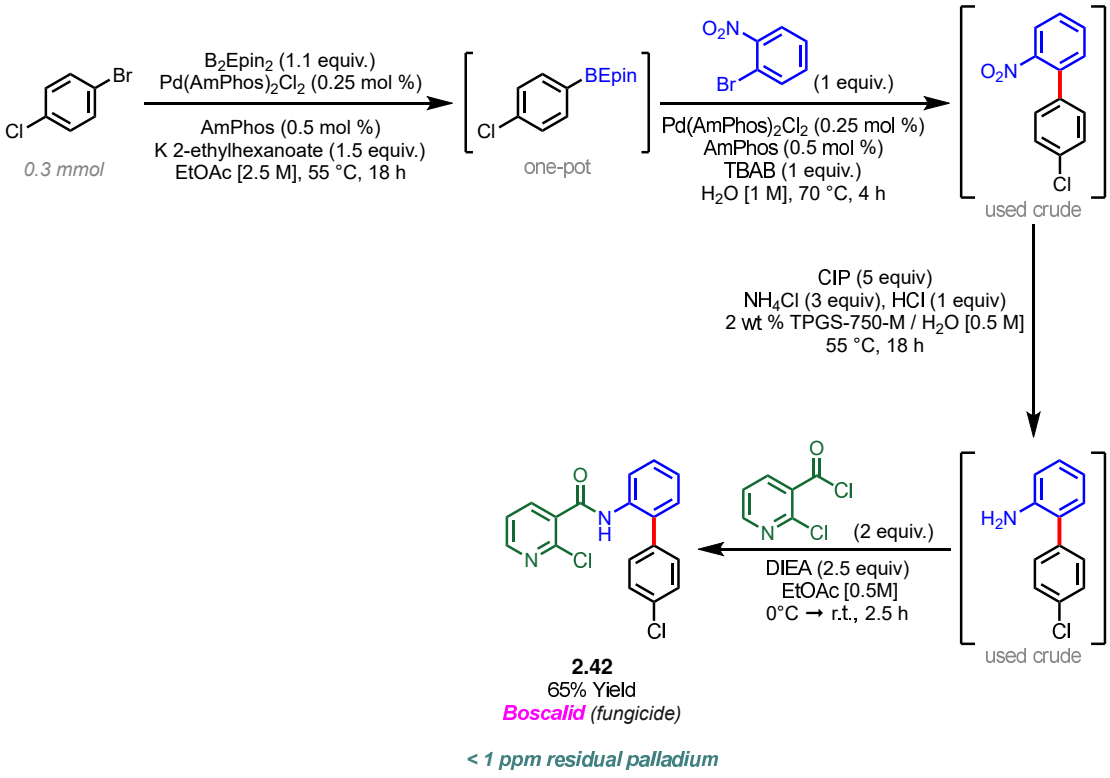
A final important note for this 1-pot method is that compound **2.39**, upon subjection to ICPMS analysis, was found to only contain 7.9 ppm of residual palladium, which is less than the 20 ppm/dose/day limit allowed by the FDA.[24] This demonstrates that, for this method, low residual metal contents can be anticipated from standard isolation procedures, without any further scavenging efforts.

2.2.4 Sequence Toward a Key Agrochemical

With similar motivation to the scale up process, we then sought to demonstrate the application of the method to an overall sequence *en route* to the widely used fungicide, boscalid. Each fragment following the application of our 1-pot would see to the application of other green methods developed in our research group. When applying our borylation conditions to 1-bromo-4-chloroanisole, GC-MS analysis of the crude reaction mixture displayed full conversion and complete chemoselectivity for the bromide over the chloride. From here, the newly developed Suzuki-Miyaura coupling conditions were implemented, in the same pot, with the addition of 1-bromo-2-nitrobenzene. For this step, however, a 1:1 stoichiometry was utilized as I surmised that this second halide retains enough steric bulk to hinder any undesired borylation of this halide. Gratifyingly, the desired biaryl was obtained in full conversion in four hours with no discernable side products (GC-MS and proton NMR). Via simple extraction and then concentration *in vacuo*, the crude biaryl was subjected to my group's green CIP nitro reduction protocol[44] under micellar conditions to obtain the penultimate amine. Again, via simple extraction and concentration in vacuo, the crude product was carried forward to the final step. For this amide bond formation, I attempted using our group's DPDTC enabled amidation methodology. These coupling partners, unfortunately, proved ineffectual under these conditions. Notwithstanding, the amide coupling was accomplished using 2-chloronicotinoyl chloride in green EtOAc. With the first two transformations being done in 1-pot, and each subsequent one using the prior's crude product, boscalid was reached in 65% overall yield in

just four steps. This sequence, again, shows the application of the developed 1-pot cross electrophile coupling to sustainably generate valuable biaryls. Additionally, the final product was found to contain an insignificant amount palladium, highlighting that minimal metal contamination is to be expected from this 1-pot protocol.*

Figure 2.7: Application of 1-Pot Method *en route* to Boscalid.[62]



2.3 Conclusion

As discussed at the beginning of this Chapter, it was in considering a green synthesis of a new anticancer agent that it became evident that, though the second most utilized reaction in the

*It is important to note that subsequent steps and workup procedures can serve to remove metal content, but the initial low loading of palladium ensures the issue of metal contamination will be low.

pharmaceutical industry had been immensely optimized for efficiency and sustainability, the reaction that immediately precedes it, lagged far behind. This was in spite of using an essentially identical catalytic system. What I gleaned from the literature is that the inherent robustness of the Suzuki-Miyaura coupling enabled such advancements. By contrast, the inherent sensitivities of Miyaura borylations have precluded chemists from employing similar techniques (*i.e.*, micellar catalysis). This is not to say that some strides have been made. Nonetheless, in many ways, many of these reports represent a step in the wrong direction. For example, the extreme sensitivity of BBA and the sensitivities of the resulting boronic acids force one to abandon the notion of atom-economy. Moreover, the risk of generating hydrogen gas poses serious safety concerns at scale. Furthermore, the limited 1-pot applicability hinders the primary use of such borylations: to enable subsequent carbon-carbon bond formation.

These findings forced me towards looking at a more stable, but still sufficiently reactive, *bis*-boron species. I envisioned that improving the inherent robustness of the reaction would open it up to similar advancements in the Suzuki coupling. As discussed, ethyl pinacol boronic esters had recently been found to not only be remarkably stable, but also more efficacious in Suzuki coupling when compared to their boronic acid, and pinacol boronic acid counterparts. Through optimization, my hypothesis proved largely correct, leading to good efficacy for the Miyaura borylation in aqueous media containing a surfactant. However, as is often the case in research, observation during experimental setup led to another opportunity to significantly improve the sustainability of the reaction. This resulted in a highly efficient "near-neat" method that relies on small dilutions with green solvent (EtOAc) and very efficient palladium loadings.

Though this was perhaps not the initial motivation of using micellar catalysis to "green-up" the borylation, the final method was found to be highly efficient with low catalytic loadings, and was seen to be applicable to highly functionalized substrates. It is noted, nonetheless, that several API's were still seen to borylate well in water. Beyond confirming initial hypotheses, this accentuates the robustness of the developed method for producing these ethyl pinacol boronic esters. It also displays the adaptability of the technology to meet the needs of the chemist employing it.

Ultimately, this method addresses the major inherent sensitivity issues of the Miyaura borylation, and this enhanced stability is leveraged to greatly improve the sustainability of this cornerstone transformation. This, however, I only saw as a launching point. As has been reinforced throughout this Chapter, process chemists prefer not having to isolate intermediate borylated materials. Doing so only serves to greatly add to the time, cost, and waste of a synthetic route. The standard for efficiency and sustainability is simply to add the next aryl/alkenyl halide to the same reactor to then get the desired C-C bond formation. This is accomplished in several instances in the production of API's;[37,53] however, I had yet to see an actual general method of doing so, especially one that relies on green conditions for both steps. Though a challenge to find the right conditions initially, we landed upon a general 1-pot method that relies on a very efficient overall palladium loading of just 0.5 mol %, and performs the Suzuki coupling on-water to provide a broad, functionalized scope of biaryls in good to excellent yield. Furthermore, though less general than initially hoped, we were able to accomplish the Suzuki step in surfactant with an even more efficient palladium loading of just 0.25 mol %.

The applicability and real-world utility of the green 1-pot method were additionally underscored with its use in a scale up toward a key precursor to anidulafungin and its use in a green multistep sequence in the preparation of the widely used fungicide, boscalid. Also highlighted is that such efficient metal loadings are apt to yield residual palladium levels that lie below the mandated FDA limit for drugs. Noted as well are impressive E-Factors,[77] like that seen for scale up.

2.3.1 Closing Remarks

In all, this was found to be a very challenging, yet rewarding project. First witnessed was a gap in the literature, from there I leveraged my chemical intuition and synthetic knowledge to hypothesize on how to fill this gap. Then, through perseverance, tenacity, and creativity in the lab, my work saw to significant confirmation of my hypotheses, and ultimately yielded a substantially improved method compared to any recent 1-pot borylation/Suzuki-Miyaura coupling methodologies.

2.3.2 Acknowledgements and Noted Contributions

Assistance by Scott L'Heureux in optimization, in obtaining substrate scope examples, and in the scale up. is acknowledged with thanks. Assistance in obtaining substrate scope examples and in obtaining analytical data by Dr. Madison Wong is recognized and appreciated.

2.4 Experimental Data and Information.

2.4.1 General Information

NMR

^{1}H, ^{13}C, ^{11}B, and ^{19}F NMR were recorded at 25 °C on either a Bruker Avance III HD 400 MHz, a Bruker Advance NEO 500 MHz, or on a Varian Unity Inova 500 MHz in $CDCl_3$ with residual $CHCl_3$ (^{1}H = 7.26 ppm, ^{13}C = 77.26 ppm). Chemical shifts are reported in parts per million (ppm) and coupling constants (J values) are reported in Hz. Peak splitting is reported in the following fashion: singlet (s), broad singlet (bs), doublet (d), triplet (t), quartet (q), pentet (p), and multiplet (m).

Note on obtaining ^{11}B NMR

Boron NMR suffers from significant background noise due to the borosilicate glass that comprises not only standard NMR tubes, but also the probe of the NMR instrument itself. For obtaining the ^{11}B NMR spectra (see Section 2.4.5: NMR spectra), the background noise was mitigated in two main ways. Firstly, boron NMRs were taken in 5 mm Thin Wall Precision Quartz NMR Sample Tube 7" from Wilmad-LabGlass. Secondly, a ^{11}Bzgbsig pulse sequence was utilized and served to suppress background noise and, thus, significantly improve the quality of the obtained ^{11}B NMR spectra. This pulse sequence is available in Bruker's pulse program library. For information on the development and implementation of this NMR technique, please see the associated reference.[52]

Reagents

Unless mentioned otherwise, all chemical reagents were utilized directly from vendors without any further purification. EtOAc, hexanes, Et_2O, methylene chloride, and methanol were obtained from Fischer Scientific and no special considerations were taken to ensure these solvents were anhydrous. When needed, EtOAc and water were degassed by sparging the solvent with a stream of argon gas. Deuterated chloroform was purchased from Cambridge Isotope Laboratories and kept over activated 4 Å molecular sieves in order to maintain dryness. AmPhos and $Pd(AmPhos)_2Cl_2$ were purchased from Combi Blocks Int. and Ambeed Inc. respectively. $Pd(OAc)_2$ was purchased from Johnson Matthey. *Tetrakis*(dimethylamino)diboron and 3,4-diethylhexane-3,4-diol were purchased from Ambeed Inc. Potassium 2-ethylhexanoate (2-KEH) was purchased from Ambeed Inc and was kept and handled in a glovebox under an atmosphere of argon. Potassium phosphate tribasic was purchased from Sigma Aldrich. TPGS-750-M[49] was obtained PHT International (TPGS-750-M is also available from Sigma-Aldrich catalog #733857). All other chemical reagents, including aryl/heteroaryl halides and organic and inorganic bases were purchased from Combi Blocks Int., Ambeed Inc., Fischer Scientific, Enamine, PHT International, Fluorochem, Alfa Aesar, Acros Organics, and Chem Scene. Thin Layer Chromatography (TLC) was performed using Silica Gel 60 F254 (Merck, 0.25mm thickness) and developed plates were visualized under a UV lamp (254 nm). Further analysis was performed via Cerium Molybdate Stain or Potassium Permanganate Stain, and subsequently developed using a heat gun. Manual flash chromatography was performed utilizing Silicycle Silicaflash® P60 unbonded grade silica. Automatic flash chromatography was performed utilizing a Telydene Combi Flash and Silica Gel P60 (Teledyne). Gas Chromatography (GC) Spectrums were obtianed on an Agilent. High Resolution

Mass Spectrums (HRMS) were obtained on a Waters GCT Premier GC TOF, Agilent 6230 TOF LC/MS System, or Xevo G2-XS UPLC-QTOF.

Generating a Solution of 2 wt % TPGS-750-M / H_2O

To a clean 100 mL round bottom flask charged with a PTFE coated stirbar was added 2 g of TPGS-750-M.[49] The flask was then fitted with a septum and attached to a vacuum/argon manifold via a needle through the septum. The flask was then subjected to three cycles of vacuum and then backfilling with argon. Under an atmosphere of argon, to the flask was then added 98 mL of degassed HPLC grade water. Still attached to the manifold and under an atmosphere of argon, the flask was fitted to a stir plate and vigorously stirred for 12 h. The flask was kept under a constant atmosphere of argon.

2.4.2 General Procedures

Unless stated otherwise, all reactions were carried out in a fume hood in order to ensure proper ventilation.

General Procedure: Preparation of *bis*(1,1,2,2-tetraethylethylene glycoato)diboron.

To a flame dried 50 mL round bottom flask charged with PTFE coated stir bar, was added 3,4-diethylhexane-3,4-diol (70.6 mmol, 12.3 g) and *tetrakis*(dimethylamino)diboron (37.1 mmol, 0.525 equiv, 7.34 g). The flask was then sealed with a rubber septum and was set in an oil bath at 80 °C with stirring set to 500 rpm. A line of positive argon pressure was pierced through the septum. A drying tube filled with calcium chloride was also pierced through the septum to allow for the release of developing dimethylamine gas. The reaction was allowed to proceed until completion at 4 h (confirmed via TLC).

The reaction was allowed to cool under the same argon flow. The crude reaction mixture was then purified directly via silica plug (R_f = 0.37; 5% ether/hexanes) to afford a crystalline white solid (11.25g, 87%). Purity was confirmed via ^{1}H NMR, ^{13}C NMR, ^{11}B NMR, HRMS (see Section 2.4.5), and Mp (58-62 °C). The white solid can be kept and weighed out on the bench top.

General Procedure: Preparation of Palladium Stock Solutions

General Procedure 2a: Preparation of Palladium Stock Solution from pre-ligated Palladium: To a 1-dram microwave vial was added a PTFE coated magnetic stir bar. The vial was taken into the glove box and *bis*(di-*t*Bu(4-dimethylaminophenyl)phosphine)- dichloropalladium(II) (0.0075 mmol, 5.3 mg) is added. If additional ligand was added, this was also added in the glovebox to the desired loading. The vial was then sealed with a septum, brought out of the glove box, and the septum was secured with Teflon® tape. The vial is attached to a vacuum/argon manifold and, under an atmosphere of argon, 0.5 mL of degassed DCM is syringed into the vial to achieve a concentration of [0.015 M]. The vial was allowed to stir and homogenize at rt on the stir plate for 5 min. From this stock solution, 50 µL could be taken up and added to the desired reaction vial to achieve a 0.25 mol % loading of the palladium catalyst. The catalyst stock solution was used within 1 h.

General Procedure 2b: Preparation of Pd Stock Solutions from Palladium Acetate and Ligand. To two separate 1-dram microwave vials were added PTFE coated magnetic stir bars. The vials were taken into the glove box and, to one vial, palladium(II) acetate (0.075 mmol, 16.8 mg) is added. To the other vial is added the desired ligand (Pd:P 10:2). Both vials were then sealed with a septum, brought out of the glove box, and the septa were secured with Teflon tape. The vials were attached to a vacuum/argon manifold and, under an atmosphere of argon, 1 mL of degassed DCM is syringed into the vial containing

palladium(II) acetate. Under an atmosphere of argon, 400 µL of degassed DCM is syringed into the vial containing the ligand of choice.* Both vials were stirred for 5 min. and allowed to homogenize at rt. From the vial containing palladium(II) acetate was taken up 100 µL, which was then added to the vial containing the Ligand in order to establish a catalyst stock solution (Pd:P 1:2) with a concentration of [0.015 M]. This vial, with combined palladium acetate and ligand, was stirred at rt for 15 min. to allow for ligation. From this stock solution, 50 µL could be taken up and added to the desired reaction vial to achieve a 0.25 mol % loading of the palladium catalyst. The catalyst stock solution was used within 1 h.

General Procedure: Preparation of Aryl and Heteroaryl BEpins.

Representative case: preparation of (6-(methoxycarbonyl)naphthalen-2-yl)boronic acid diethyl pinacol ester. To 1-dram microwave vial is added a PTFE coated magnetic stir bar, methyl 6-bromo-2-naphthoate (1 equiv, 0.5 mmol, 184.1 mg), and B_2Epin_2 (1.1 equiv, 0.55 mmol, 201.38 mg). Subsequently, the vial was brought into a glove box under an atmosphere of argon. To the vial was added potassium 2-ethylhexanoate (2-KEH) (1.5 equiv, 0.75 mmol, 136.7 mg). The vial was resealed with the rubber septum and brought out of the glove box. An argon line was pierced through the septum, and 50 µL of [0.025 M] $Pd(AmPhos)_2Cl_2$ in DCM was added via micro syringe through the septum (see general procedure's Section 2.4.5 for generating the catalyst solution). The DCM was removed *in vacuo* and the vial was then backfilled with argon. To the vial was added via syringe 120 µL of degassed EtOAc (4 equiv). Moving rapidly, the septum was removed and capped as the cap served to limit the loss of EtOAc at higher temperatures. Alternatively, the vial can be capped in a glove box with an argon atmosphere

*When using [*t*-$Bu_3PH]BF_4$, 1 equiv of TEA (relative to the ligand) was added to deprotonate the phosphonium and, thus, promote ligation when stirred with palladium(II) acetate

in order to further limit oxygen exposure. The vial was further sealed by tightly wrapping the cap-vial partition with Teflon® tape. From here, the reaction was heated to achieve an internal temperature of 55 °C. Once the reaction mixture had reached temperature, stirring was set to 500 rpm. Upon completion of the reaction at 23 h (determined by TLC and GC), the vial was allowed to cool to rt. To the vial was then added 1 mL of saturated sodium bicarbonate solution and was extracted with 1 mL x 5 of EtOAc. The extracts were combined, passed through Celite, and then dried with anhydrous $MgSO_4$. The crude mixture was filtered, concentrated *in vacuo*, and purified via column chromatography (R_f = 0.47; 10% EtOAc/hexanes) to afford **6** (181.4 mg, 99 %) as a clear, viscous oil. Purity was confirmed via ^{1}H NMR, ^{13}C NMR, ^{11}B NMR, and HRMS (see Section 2.4.5; NMR Data).

General Procedure: Protocol for 1-Pot Borylation/Suzuki-Miyaura Reaction in TPGS

Representative case: preparation of 4'-(morpholinosulfonyl)-[1,1'-biphenyl]-4-carbonitrile. (4-Cyanophenyl)boronic acid ethyl pinacol ester was prepared on 0.25 mmol scale according to the general procedure Section 2.4.2 (TPGS 1-pot protocol). The reaction vial was allowed to cool to rt once the reaction was judged complete at 18 h (determined by TLC and GC). Moving rapidly in order to mitigate against oxygen exposure, the vial was decapped, fitted with a septum, and then fitted via needle to a vacuum/argon manifold. The vial was subjected to three cycles of exposure to vacuum and then backfilled with argon. The EtOAc from the first step was removed *in vacuo* with gentle heating (40 ^{o}C). The vial was then taken into a glovebox under an inert atmosphere of argon. To the reaction vial was added potassium hydroxide (2.4 equiv, 0.6 mmol, 33.7 mg) and 4-((4-bromophenyl)sulfonyl)morpholine (1 equiv, 0.25 mmol, 76.5 mg). The vial was fitted with a septum, brought out of the glove box, and attached via needle to a vacuum/argon manifold. To the reaction vial was then added 25 μL of degassed [0.025 M] stock solution of SPhos in DCM. The DCM was removed *in vacuo* and the vial was then backfilled with

argon. To the vial via syringe was added 0.5 mL of 2 wt % TPGS-750-M to achieve a concentration of [0.5 M]. The vial was then disconnected from the manifold and set in a vial adapter on a heated stir plate. The reaction mixture allowed to reach an internal temperature of 55 ^{o}C and stirring was set to 1000 rpm. The reaction was monitored by TLC and judged complete at 20 h. The vial was allowed to cool to rt and 1 mL of saturated sodium bicarbonate solution was added. The reaction was extracted with 1 mL x 5 of EtOAc and the extracts were combined, passed through Celite, and then dried with anhydrous $MgSO_4$. The crude mixture was then filtered, concentrated *in vacuo*, and purified via column chromatography (R_f = 0.18; 30% EtOAc/hexanes) to afford **26** (76.4 mg, 93%) as a white solid. Purity was confirmed via ^{1}H NMR, ^{13}C NMR, and HRMS (see Section 2.4.5; NMR Data).

General Procedure: Protocol for 1-Pot Borylation/Suzuki-Miyaura Reaction using TBAB

Representative case: preparation of 2,2-difluoro-5-(4-(methylthio)phenyl)benzo[d][1,3]dioxole. 4-Thioanisole boronic acid ethyl pinacol ester was prepared on 0.3 mmol scale according to the general procedure provided in 2.4.2 (TBAB 1-pot protocol) with a 1:4 ratio of palladium to AmPhos ligand. The reaction vial was allowed to cool to rt once it was judged complete at 18 h (determined by TLC and GC). Moving rapidly in order to mitigate against oxygen exposure, the vial was decapped, fitted with a septum, and then fitted via needle to a vacuum/argon manifold. The vial was subjected to three cycles of exposure to vacuum and then backfilling with argon. The EtOAc from the first step was removed *in vacuo* with gentle heating (40 °C). The vial was then taken into a glovebox under an inert atmosphere of argon. To the reaction vial was added K_3PO_4 (5 equiv, 1.5 mmol, 318.4 mg) and tetrabutylammonium bromide (1 equiv, 0.3 mmol, 96.7 mg).* The vial was fitted with a septum, brought out of the glove box, and attached via needle to a vacuum/argon manifold. To the reaction vial was then

*If the second bromide added was a solid, it was added at this point in the glove box.

added 50 μL of [1.5 mM] catalyst stock solution (see the general procedure's Section 2.4.2) in order to achieve 0.25 mol % of $Pd(AmPhos)_2Cl_2$ and 0.5 mol % AmPhos. The DCM was removed *in vacuo* and the vial was then backfilled with argon. Subsequently, via syringe through the septum, 5-bromo-2,2-difluorobenzo[d][1,3]dioxole (1.5 equiv,* 0.39 mmol, 92.43 mg (53 μL)) was added and 300 μL of sparged DI water also added. The vial was disconnected from the manifold and set in a vial adapter on a heated stir plate. The reaction mixture allowed to reach an internal temperature of 70 ^{o}C and stirring was set to 1000 rpm. The reaction was monitored by TLC and judged complete at 24 h. The vial was allowed to cool to rt and 1 mL of saturated sodium bicarbonate solution was added. The reaction was extracted with 1 mL x 5 of EtOAc and the extracts were combined, passed through Celite, and then dried with anhydrous $MgSO_4$. The crude mixture was then filtered, concentrated *in vacuo*, and purified via column chromatography (R_f = 0.19; hexanes) to afford **28** as a white solid (83.8 mg, quant.). Purity was confirmed via ^{1}H NMR, ^{13}C NMR, ^{19}F NMR, and HRMS (see Section 2.4.5).

Gram Scale Synthesis of Anidulafungin Precursor (Compound 2.41)

To a 50 mL round bottom flask was added a PTFE coated magnetic stir bar, 4-bromo-4'-(pentyloxy)-1,1'-biphenyl (1 equiv, 3 mmol, 957.72 mg), and B_2Epin_2 (1.1 equiv, 3.3 mmol, 1.21 g). Subsequently, the flask was brought into a glove box under an atmosphere of argon. To the flask was added potassium 2-ethylhexanoate (2-KEH) (1.5 equiv, 4.5 mmol, 820.8 mg), $Pd(AmPhos)_2Cl_2$ (0.25 mol %, 0.0075 mmol, 5.30 mg) and AmPhos (0.50 mol %, 0.015 mmol, 4.0 mg). The flask was resealed with the rubber septum and brought out of the glove box. To the flask was added via syringe 1.5 mL of degassed EtOAc to achieve a concentration of [2.5 M]. Moving rapidly, the septum was removed and a reflux

*Generally, 1.3 equivalents of the second bromide was sufficient for our method. However, 5-bromo-2,2-difluorobenzo[d][1,3]dioxole is vaporous and thus presented concerns of loss through the septum at temperature. Thus, 1.5 equivalents was utilized for this example.

condenser connected to an argon line was fitted to the round bottom flask. From here, the round bottom was set in an oil bath and the reaction was heated to achieve an internal temperature of 55 °C. Once the reaction mixture had reached this temperature, stirring was set to 500 rpm. Upon completion of the reaction (determined by TLC and/or GC, 15.5 h), the flask was allowed to cool to rt and the residual EtOAc was removed *in vacuo* for at least 1 h with mild heating (40 °C). Subsequently, the reaction flask was allowed to cool to rt and then brought into the glove box under an inert atmosphere of argon. To the flask was added methyl 4-bromobenzoate (1.3 equiv, 3.9 mmol, 839 mg), K_3PO_4 (5 equiv, 15 mmol, 3.18 g), tetrabutyl-ammonium bromide (TBAB) (1 equiv, 3 mmol, 967 mg), $Pd(AmPhos)_2Cl_2$ (0.25 mol %, 0.0075 mmol, 5.30 mg) and AmPhos (0.50 mol %, 0.015 mmol, 4.0 mg). The flask was fitted with a rubber septum, brought out of the glove box, and the septum was secured to the flask with Teflon® tape. The flask was hooked up to a vacuum/argon manifold and, under an atmosphere of argon, was then added 4 mL of degassed DI H_2O in order to obtain a concentration of [0.75 M]. The reaction flask was added to an oil bath and heated to achieve an internal temperature of 70 °C. The stirring was set to 1000 rpm. After 1.5 h, 0.5 mL (12.5 % v/v) of degassed 2-MeTHF was added to the flask as a cosolvent. Upon completion of the reaction (as determined by TLC, 16.5 h), the reaction was allowed to cool to rt, then 10 mL of 1 M HCl was added. The reaction mixture was then cooled to 0 °C, and the solid precipitate was collected in a Buchner funnel. This solid was then rinsed with 20 mL aliquots of cold H_2O, cold EtOAc, and 200 mL of Et_2O. The filter cake was allowed to dry under vacuum, then was transferred to a flask and left under high-vac overnight to afford **40** as a white solid (99%, 1.12 g; R_f = 0.34, 10% EtOAc / hexanes).* Mp (decomp. 300°C). Purity was confirmed via ^{1}H NMR, ^{13}C NMR, and HRMS (see Section 2.4.5).

*For the E-Factor calculation associated with this procedure, please see Section 2.4.4.

Multistep sequence: boscalid (Compound 2.42)

In a 1-dram vial, 4'-chloro-2-nitro-1,1'-biphenyl is prepared according to the general procedure reported in Section 2.4.2 (protocol utilizing TBAB) on a 0.3 mmol scale with borylation step running for 18 h, and the Suzuki-Miyaura coupling running for 4 h.* Once the reaction vial was allowed to cool to rt, 1 mL of cold saturated sodium bicarbonate solution was added to the reaction vial. The reaction vial was then extracted with 1 mL x 5 of EtOAc. The extracts were combined, passed through a pad of Celite, and the crude mixture concentrated *in vacuo* in a 2-dram vial. To the 2-dram vial was then added a PTFE coated stir bar, carbonyl iron powder (CIP) (1.5 mmol, 5 equiv, 83.8 mg), and ammonium chloride (0.9 mmol, 3 equiv, 48.1 mg).† The vial was fitted with a rubber septum that was secured with Teflon®. The vial was attached to a vacuum/argon manifold via a needle through the septum. The vial was then subjected to three cycles of exposure to vacuum and then backfilling with argon. To the vial was then added via syringe sparged 5M HCl (0.3 mmol, 1 equiv, 60 μL), and 0.6 mL of degassed 2 wt % TPGS-750-M / H_2O to establish a reaction concentration of [0.5 M]. The vial was removed from the manifold, set in a stirplate vial adapter, heated to an internal temperature of 55 °C, and set to stir at 300 rpm. The reaction was allowed to proceed for 18 h,* and then removed from the stirplate and allowed to cool to rt. To the 2-dram vial was added 1 mL of cold 1M NaOH, and the reaction vial extracted with 5 x 1 mL of EtOAc. The extracts were combined, passed through a pad of Celite, and the crude mixture concentrated *in vacuo* in a 2-dram vial. For the final step, the 2-dram vial containing crude 4'-chloro-[1,1'-biphenyl]-2-amine was charged with a PTFE coated stir bar and fitted with a rubber septum. The vial was attached to a vacuum/argon manifold via a needle through the septum. The vial was then subjected to three cycles of exposure to vacuum and then backfilling with argon. Next was

*Each step was judged complete via TLC and GC.

†For more information on this nitro-reduction protocol, please see the associated reference.[44]

added degassed, anhydrous DIEA (0.75 mmol, 2.5 equiv, 131 μL), and 0.6 mL of degassed, anhydrous EtOAc to establish of concentration of [0.5 M]. The vial was set in an ice bath at 0 °C and stirred for 5 min. Moving rapidly to avoid exposure to moisture, the septum was removed, 2-chloronicotinoyl chloride (0.6 mmol, 2 equiv, 105.6 mg) was added, and the septum refitted. The vial was set back in the ice bath and stirred for 15 min at 600 rpm. Subsequently, the reaction was removed from the ice bath, set on a room temperature stir plate at 600 rpm, and allowed to proceed for 1 h and 45 min.* The reaction was then quenched with 1 mL of cold saturated sodium bicarbonate solution and removed from stirring. This was then extracted with 5 x 1 mL of EtOAc and the crude extracts combined. Due to difficulty in separating the product from residual 3,4-diethylhexane-3,4-diol, following work up, the crude reaction mixture was stirred at 80 °C with 2 equiv of 2-iodoxybenzoic acid (IBX) in wet EtOAc [0.5 M] under an inert atmosphere of argon for 4 h.[28] The reaction mixture was then cooled to rt, passed through a pad of Celite, concentrated *in vacuo*, and then further purified via column chromatography (R_f = 0.33, 40% EtOAc/hexanes) to afford boscalid (**41**) as a white solid (66.9 mg, 65 %). Purity was confirmed via ^{1}H NMR, ^{13}C NMR, HRMS (see Section xx), and Mp (139-142 °C).

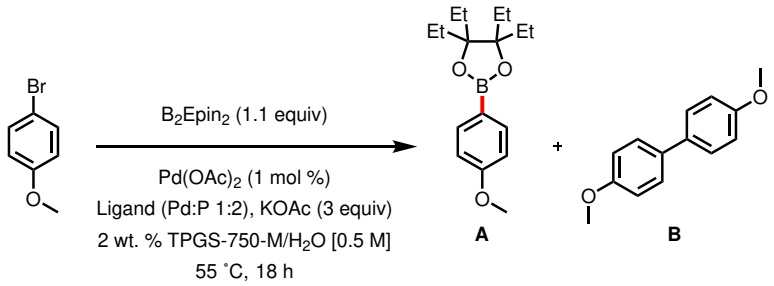
2.4.3 Optimization Data

Reaction set up and conditions: a 1-dram glass vial was charged with a PTFE coated magnetic stir bar. To the vial was added 4-bromoanisole (0.25 mmol, 1 equiv, 46.8 mg) and B_2Epin_2 (0.275 mmol, 1.1 equiv, 100.7 mg). The vial was taken into the glove box and to the vial was added KOAc (0.75 mmol, 3 equiv, 73.6 mg). The vial was fitted with a septum secured with Teflon tape, and, subsequently, taken out of the glove box and attached to a vacuum/argon manifold. The catalyst (see Section 2.4.2) was generated utilizing the desired ligand and was added to the reaction vial under argon. Residual solvent

*Each step was judged complete via TLC and GC.

from the catalyst stock solution was removed *in vacuo*, and the vial was then backfilled with argon. To the vial was then added 0.5 mL of 2 wt % TPGS-750-M / H_2O and 10 % v/v THF. The reaction vial was allowed to come to a temperature of 55 °C and set to a stirring rate of 1000 rpm. Upon completion (as determined by TLC), the reaction was allowed to cool and subsequently extracted with 5 x 1 mL of EtOAc. The extracts were combined, passed through Celite, and then dried with anhydrous $MgSO_4$. The crude mixture was filtered and then concentrated *in vacuo*. The crude reaction material was dissolved in 2 mL of $CDCl_3$, 1,3,5-trimethoxybenzene (0.5 or 1 equiv) was added, and the qNMR yield was subsequently determined via ^{1}H NMR.

Table 2.4: Ligand Optimization[61]



Entry[a]	Ligand	Yield (A%)[b]	Yield (B%)[b]
1	QPhos	46	9
2	**[*t*-Bu$_3$PH]BF$_4$**	**80**	**trace**
3	DPPF	38	trace
4	XPhos	25	trace
5	*t*-BuXPhos	13	trace
6	SPhos	26	trace
7	RuPhos	36	trace
8	*t*-BuXantPhos	trace	NR
9	DPPP	trace	trace
10	*t*-BuBrettPhos	11	trace
11	N_2Phos	trace	trace
12	EvanPhos	trace	trace
13	**AmPhos**	**82**	**trace**
14	DavePhos	42	trace
15	JohnPhos	8	NR

Continued on next page

Entry[a]	Ligand	Yield (A%)[b]	Yield (B%)[b]
16	BINAP (racemic)	17	trace
17	2-(*t*-Bu_2P)-1-Ph-1H-pyrrole	14	10

[a] Reactions run on a 0.25 mmol scale. [b] Yield determined via qNMR using 1,3,5-trimethoxybenzene as an internal standard.

Figure 2.8: Structures of Ligands Screened.

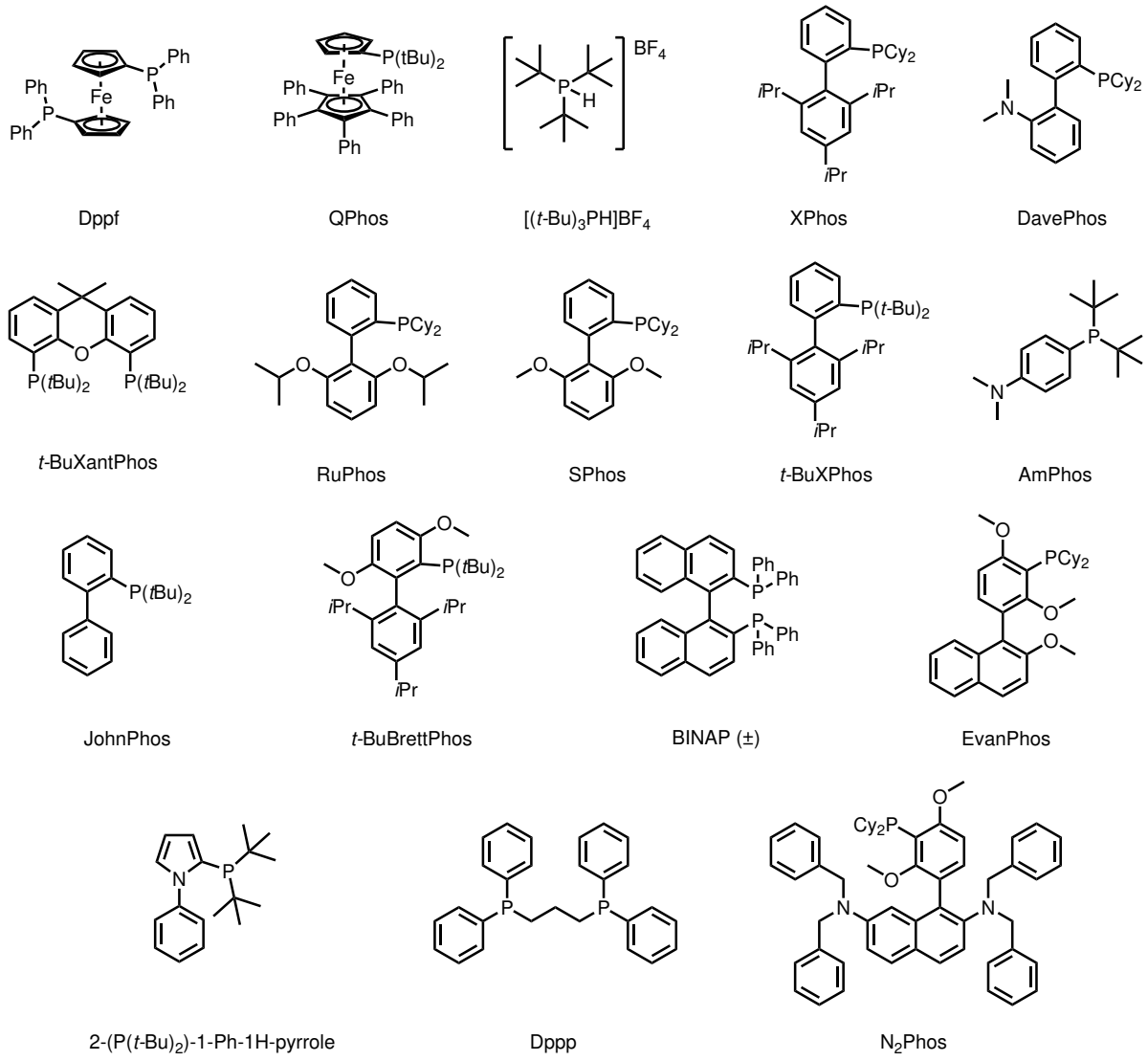
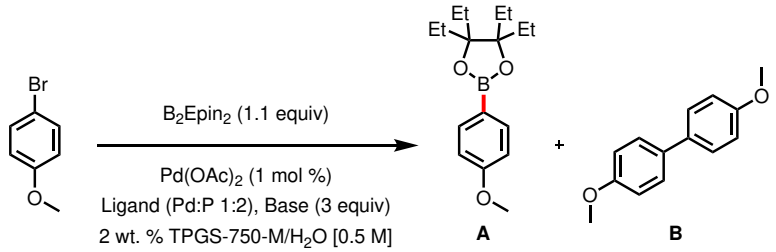


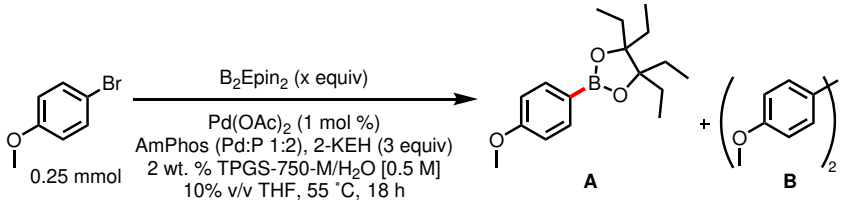
Table 2.5: Base & Ligand Optimization[61]



Entry[a]	Ligand	Base	Yield (A%)[b]	Yield (B%)[b]
1	[*t*-Bu_3PH]BF_4	KOAc	80	trace
2	[*t*-Bu_3PH]BF_4	NaOAc	77	trace
3	[*t*-Bu_3PH]BF_4	K_2CO_3	40	10
4	[*t*-Bu_3PH]BF_4	KF	34	trace
5	[*t*-Bu_3PH]BF_4	K_2HPO_4	78	trace
6	[*t*-Bu_3PH]BF_4	K_3PO_4	trace[c]	sig.[c]
7	[*t*-Bu_3PH]BF_4	NaOPh	trace[c]	sig.
8	[*t*-Bu_3PH]BF_4	2-KEH[d]	60	trace
9	[*t*-Bu_3PH]BF_4	KH_2PO_4	11	trace
10	[*t*-Bu_3PH]BF_4	tBuOK	19	33
11	[*t*-Bu_3PH]BF_4	TEA	27	25
12	[*t*-Bu_3PH]BF_4	DIPEA	25	10
13	[*t*-Bu_3PH]BF_4	Pyridine	trace	NR
14	[*t*-Bu_3PH]BF_4	KOTMS	trace[c]	sig.[c]
15	AmPhos	NaOAc	trace[c]	trace[c]
16	AmPhos	K_2HPO_4	73	8
17	**AmPhos**	**2-KEH[d]**	**87**	**trace**

[a] Reactions run on a 0.25 mmol scale. [b] Yield determined via qNMR using 1,3,5-trimethoxybenzene as an internal standard. [c] Qualitative assessment based off TLC of crude reaction mixture ("sig." = significant). [d] Potassium 2-ethylhexanoate.

Table 2.6: *bis*-BEpin Loading Optimization[61]



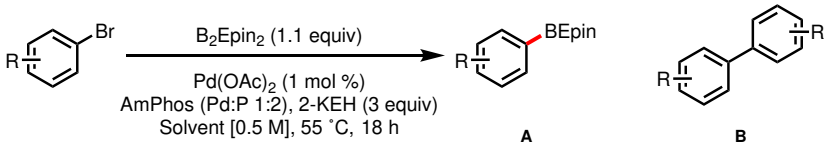
Entry[a]	B_2Epin_2 (x equiv)	Yield (A%)[b]	Yield (B%)[b]
1	**1.1**	**88**	**trace**
2	1.2	88	trace
3	1.3	38	trace

Continued on next page

Entry[a]	B_2Epin_2 (x equiv)	Yield (A%)[b]	Yield (B%)[b]
4	1.4	25	trace
5	1.5	13	trace

[a] Reactions run on a 0.25 mmol scale. [b] Yield determined via qNMR using 1,3,5-trimethoxybenzene as an internal standard.

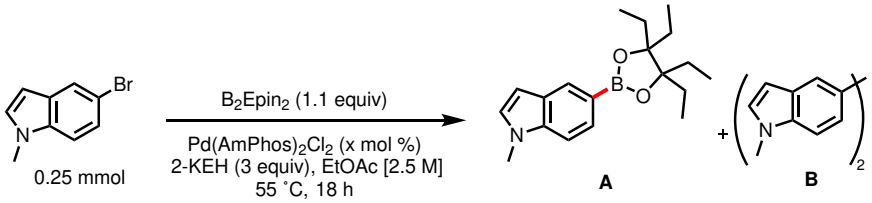
Table 2.7: Surfactant/Solvent Optimization[61]



Entry[a]	Substrate	Solvent	Yield (A%)[b]	Yield (B%)[b]
1	SM_1[f]	H_2O	80	trace
2[e]	SM_1	2 wt % TPGS-750-M / H_2O	78	trace
3[e]	SM_1	2 wt % Savie / H_2O	76	trace
4[e]	SM_1	2 wt % MC-1 / H_2O	70	trace
5[e]	SM_1	2 wt % Coolade / H_2O	88	trace
6[e]	SM_1	2 wt % Brij / H_2O	69	trace
7	SM_2	H_2O	91	trace
8	**SM_2**	**EtOAc**	**95**	**trace**
9	SM_2	EtOH	trace[c]	trace[c]
10	SM_2	toluene	trace[d]	n.d.
11	SM_2	2-MeTHF	89	trace
12	SM_2	none	trace[c]	trace[c]

[a] Reactions run on a 0.25 mmol scale. [b] Yield determined via qNMR using 1,3,5-trimethoxybenzene as an internal standard. [c] Qualitative assessment based off TLC of crude reaction mixture ("sig." = significant). [d] Poor stirring of reaction mixture. [e] 10 v/v % THF included as a cosolvent. [f] SM_1 = 4–bromoanisole; SM_2 = 5–Bromo–1–methylindole.

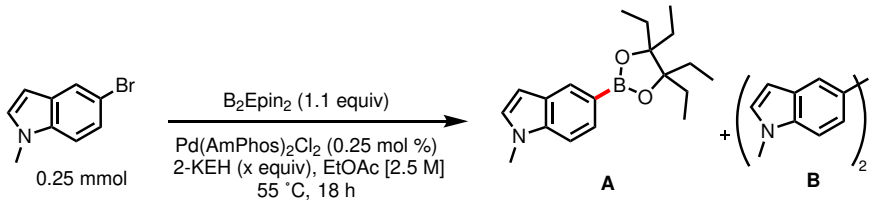
Table 2.8: Palladium Loading Optimization[61]



Entry[a]	Pd cat. (x mol %)	Yield (A%)[b]	Yield (B%)[b]
1	0.05	trace[c]	trace[c]
2	0.1	84	trace
3	0.15	90	trace
4	**0.25**	**96**	**trace**

[a] Reactions run on a 0.25 mmol scale. [b] Yield determined via qNMR using 1,3,5-trimethoxybenzene as an internal standard.

Table 2.9: Base Loading Optimization[61]



Entry[a]	2-KEH[b] (x equiv)	Yield (A%)[c]	Yield (B%)[c]
1	1.1	79	trace
2	**1.5**	**96**	**trace**
3	2	87	trace
4	2.5	87	trace
5	3	95	trace

[a] Reactions run on a 0.25 mmol scale. [b] Yield determined via qNMR using 1,3,5-trimethoxybenzene as an internal standard.

2.4.4 E-Factor[77] Calculations

The procedure for the gram scale preparation of the Anidulafungin Precursor (**2.41**) *is provided in general procedures Section 2.4.2* *

$$\text{E-Factor} = \frac{\text{mass of waste generated}^{**}}{\text{mass of product}} \tag{2.1}$$

Source	Mass of Waste
B_2Epin_2	1.21 g
2-KEH	0.8208 g
$Pd(AmPhos)_2Cl_2$	0.0106 g
AmPhos	0.008 g
EtOAc	1.353 g
K_3PO_4	3.18 g
TBAB	0.967 g
Water	4 g
2-MeTHF	0.4285 g
Unreacted SM	0.0048 g
Excess 2nd Bromide	+ 0.194 g

Continued on next page

*For E-factor calculations, the work-up solvents of H_2O, Et_2O, and EtOAc are recyclable via distillation and other purification techniques and are, thus, not considered for the E-factor calculation. Furthermore, it is noted that the relative volume of workup solvent is highly dependent on the scale utilized. For recent literature with representative E-factor calculations, please refer to the associated references.[27,87]

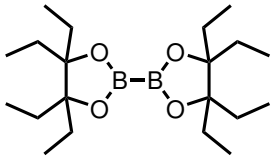
TOTAL:	**12.175 g**

$$\text{E-Factor} = \frac{\text{mass of waste generated}^*}{\text{mass of product}} = \frac{12.175\ \text{g}}{1.12\ \text{g}} = \mathbf{10.9} \tag{2.2}$$

2.4.5 Analytical Data

Product Descriptions: Ar-BEpin Products

(1,1,2,2-Tetraethylethylene glycoato)diboron



Synthesized according to general procedure reported in Section 2.4.2.

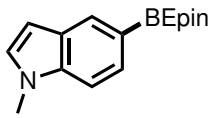
^{1}H NMR (500 MHz, $CDCl_3$): δ 1.74 – 1.57 (m, 16H), 0.90 (t, J = 7.5 Hz, 24H).

^{13}C NMR (101 MHz, $CDCl_3$): δ 88.42, 26.52, 9.08.

^{11}B NMR (128 MHz, $CDCl_3$): δ 29.96.

HRMS (ESI^+): Calcd for $C_{20}H_{40}B_2O_4Na$, $[M+Na]^+$ 389.3011; found 389.3025.

(1-Methyl-5-(4,4,5,5-tetraethyl-1,3,2-dioxaborolan-2-yl)-1H-indole (2.1)



Product **2.1** was synthesized according to general procedure reported in Section 2.4.2 using 5-bromo-1-methyl-1H-indole on a 0.5 mmol scale for 18 h. Due to difficulty in separating the product from remaining B_2Epin_2 and residual 3,4-diethylhexane-3,4-diol, following work up, the crude reaction mixture was stirred at 80 °C with 2 equiv of 2-iodoxybenzoic acid (IBX) in wet EtOAc [0.5 M] under an inert atmosphere of argon.[28] The reaction mixture was then cooled to rt, passed through a pad of Celite, concentrated *in vacuo*, and then further purified via column chromatography using silica gel (R_f: 0.45; gradient of 0-5% EtOAc/hexanes). Yield: 84%, 131.1 mg; crystalline white solid. Mp* (60 - 63 °C).

^{1}H NMR (500 MHz, $CDCl_3$): δ 8.18 (s, 1H), 7.70 (dd, J = 8.2, 1.1 Hz, 1H), 7.32 (d, J = 8.3 Hz, 1H),

*Melting point is stated for novel solids that haven't yet been reported prior to this publication.

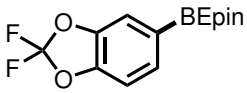
7.04 (d, *J* = 3.1 Hz, 1H), 6.52 (d, *J* = 3.0 Hz, 1H), 3.79 (s, 3H), 1.80 (m, *J* = 33.3, 14.2, 7.2 Hz, 8H), 1.01 (t, *J* = 7.4 Hz, 12H).

^{13}C NMR (126 MHz, $CDCl_3$): δ 138.71, 128.96, 128.92, 128.34, 127.85, 108.65, 101.75, 88.46, 32.93, 26.65, 9.06. The boron-bound carbon was not detected likely due to quadrupolar relaxation.[28]

^{11}B NMR (128 MHz, $CDCl_3$): δ 30.76.

HRMS (ESI^+): Calcd for $C_{19}H_{29}BNO_2$, $[M+H]^+$ 314.2291; found 314.2301.

2-(2,2-Difluorobenzo[d][1,3]dioxol-5-yl)-4,4,5,5-tetraethyl-1,3,2-dioxaborolane (2.2)



Product **2.2** was synthesized according to general procedure reported in Section 2.4.2 using 2-difluoro-5-bromo-benzodioxole on a 0.25 mmol scale for 18 h. The reaction mixture was then cooled to rt, passed through a pad of Celite, and then further purified via column chromatography using silica gel (R_f: 0.50; hexanes). Yield: 84%, 72.0 mg; clear oil.

^{1}H NMR (500 MHz, $CDCl_3$): δ 7.58 (dd, *J* = 7.9, 1.1 Hz, 1H), 7.48 (s, 1H), 7.05 (d, *J* = 8.0 Hz, 1H), 1.84 – 1.66 (m, 8H), 0.96 (t, *J* = 7.5 Hz, 12H).

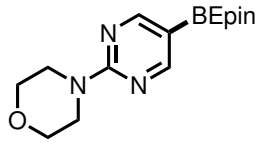
^{13}C NMR (126 MHz, $CDCl_3$): δ 146.06, 143.71, 131.58 (t, *J* = 254.6 Hz), 131.10, 115.16, 109.18, 89.33, 26.60, 8.95. The boron-bound carbon was not detected likely due to quadrupolar relaxation.

^{11}B NMR (128 MHz, $CDCl_3$): δ 29.66.

^{19}F NMR (371 MHz, $CDCl_3$): δ -50.21.

HRMS ($GC\text{-}EI^+$): Calcd for $C_{17}H_{23}BF_2O_4$, $[M]^+$ 340.1661; found 340.1668.

4-(5-(4,4,5,5-Tetraethyl-1,3,2-dioxaborolan-2-yl)pyrimidin-2-yl)morpholine (2.3)



Product **2.3** was synthesized according to general procedure reported in Section 2.4.2 using 5-bromo-2-morpholinopyrimidine on a 0.25 mmol scale for 4 h. The reaction mixture was then cooled to rt, passed through a pad of Celite, and then further purified via column chromatography using silica gel (R_f: 0.20; 10% EtOAc/hexanes). Yield: 96%, 83.4 mg; light orange oil.

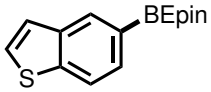
^{1}H NMR (500 MHz, $CDCl_3$): δ 8.61 (s, 2H), 3.86 (dd, J = 5.7, 4.1 Hz, 4H), 3.74 (dd, J = 5.7, 4.0 Hz, 4H), 1.72 (dtt, J = 21.8, 14.6, 7.5 Hz, 8H), 0.94 (t, J = 7.5 Hz, 12H).

^{13}C NMR (126 MHz, $CDCl_3$): δ 164.23, 162.56, 88.84, 66.99, 44.20, 26.54, 8.93. The boron-bound carbon was not detected likely due to quadrupolar relaxation.

^{11}B NMR (128 MHz, $CDCl_3$): δ 29.90.

HRMS (ESI^+): Calcd for $C_{18}H_{31}BN_3O_3$, $[M+H]^+$ 348.2458; found 348.2447.

2-(Benzo[b]thiophen-5-yl)-4,4,5,5-tetraethyl-1,3,2-dioxaborolane (2.4)



Product **2.4** was synthesized according to general procedure reported in Section 2.4.2 using 5-bromobenzothiophene on a 0.5 mmol scale for 18 h. The reaction mixture was then cooled to rt, passed through a pad of Celite, and then further purified via column chromatography using silica gel (R_f: 0.55; gradient of 0-5% Et_2O/hexanes). Yield: 87%, 136.8 mg; white solid. Mp (73-76 °C).

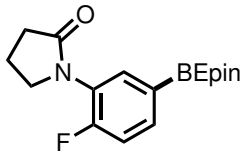
^{1}H NMR (400 MHz, $CDCl_3$): δ 8.33 (t, *J* = 0.9 Hz, 1H), 7.89 (dt, *J* = 8.1, 0.8 Hz, 1H), 7.78 (dd, *J* = 8.1, 1.1 Hz, 1H), 7.42 (d, *J* = 5.4 Hz, 1H), 7.37 (dd, *J* = 5.4, 0.8 Hz, 1H), 1.90 – 1.70 (m, 8H), 1.00 (t, *J* = 7.5 Hz, 12H).

^{13}C NMR (126 MHz, $CDCl_3$): δ 142.71, 139.32, 130.86, 129.99, 126.06, 124.27, 121.92, 88.95, 26.66, 9.04. The boron-bound carbon was not detected likely due to quadrupolar relaxation.

^{11}B NMR (128 MHz, $CDCl_3$): δ 30.46.

HRMS (ESI^+): Calcd for $C_{18}H_{25}BO_2S$, $[M]^+$ 316.1668; found 316.1667.

1-(2-Fluoro-5-(4,4,5,5-tetraethyl-1,3,2-dioxaborolan-2-yl)phenyl)pyrrolidin-2-one (2.5)



Product **2.5** was synthesized according to general procedure reported in Section 2.4.2 using 1-(5-bromo-2-fluorophenyl)pyrrolidin-2-one on a 0.5 mmol scale for 18.5 h. The reaction mixture was then cooled to rt, passed through a pad of Celite, and then further purified via column chromatography using silica gel (R_f: 0.31; 30% hexanes/Et_2O). The product streaks on silica. Yield: 49%, 88.3 mg; white solid. Mp (89-92 °C).

^{1}H NMR (400 MHz, $CDCl_3$): δ 7.78 (dd, J = 8.1, 1.6 Hz, 1H), 7.72 (ddd, J = 8.3, 5.4, 1.6 Hz, 1H), 7.13 (dd, J = 10.8, 8.2 Hz, 1H), 3.81 (t, J = 7.0 Hz, 2H), 2.57 (t, J = 8.1 Hz, 2H), 2.28 – 2.15 (m, 2H), 1.83 – 1.65 (m, 8H), 0.95 (t, J = 7.5 Hz, 12H).

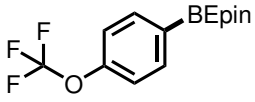
^{13}C NMR (126 MHz, $CDCl_3$): δ 174.88, 159.63 (d, J = 254.7 Hz), 135.59 (d, J = 8.2 Hz), 134.77 (d, J = 2.3 Hz), 126.02 (d, J = 11.8 Hz), 116.29 (d, J = 19.3 Hz), 89.23, 50.23 (d, J = 2.9 Hz), 31.18, 26.53, 19.19, 8.97. The boron-bound carbon was not detected likely due to quadrupolar relaxation.

^{11}B NMR (128 MHz, $CDCl_3$): δ 29.63.

^{19}F NMR (376 MHz, $CDCl_3$): δ -116.11.

HRMS (ESI^+): Calcd for $C_{20}H_{29}BFNO_3Na$, $[M+Na]^+$ 384.2123; found 384.2142.

4,4,5,5-Tetraethyl-2-(4-(trifluoromethoxy)phenyl)-1,3,2-dioxaborolane (2.6)



Product **2.6** was synthesized according to general procedure reported in Section 2.4.2 using 4-bromo-trifluoromethoxybenzene on a 0.3 mmol scale for 24 h with 0.50 mol % Pd at a 1:4 ratio of Pd to AmPhos and at a concentration of 1.25M EtOAc. The reaction mixture was then cooled to rt, passed through a pad of Celite, and then further purified via column chromatography using silica gel (R_f: 0.21; hexanes). Yield: 85%, 87.6 mg; clear, viscous oil.

^{1}H NMR (500 MHz, $CDCl_3$): δ 7.85 (d, *J* = 8.6 Hz, 2H), 7.20 (d, *J* = 8.0 Hz, 2H), 1.76 (ddt, *J* = 24.3, 14.4, 7.2 Hz, 9H), 0.97 (t, *J* = 7.5 Hz, 12H).

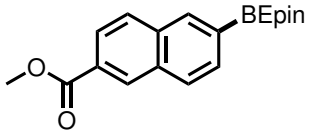
^{13}C NMR (126 MHz, $CDCl_3$): δ 151.70 (d, *J* = 1.5 Hz), 136.67, 120.59 (q, *J* = 257.5 Hz), 120.03, 89.22, 26.59, 8.97. The boron-bound carbon was not detected likely due to quadrupolar relaxation.

^{11}B NMR (160 MHz, $CDCl_3$): δ 29.91.

^{19}F NMR (471 MHz, $CDCl_3$): δ -57.57.

HRMS (GC-EI$^+$): Calcd for $C_{17}H_{24}BF_3O_3$, $[M]^+$ 344.1771; found 344.1763.

Methyl 6-(4,4,5,5-tetraethyl-1,3,2-dioxaborolan-2-yl)-2-naphthoate (2.7)



Product **2.7** was synthesized according to general procedure reported in Section 2.4.2 using methyl 6-bromo-2-naphthoate on a 0.5 mmol scale for 23 h. The reaction mixture was then cooled to rt, passed through a pad of Celite, and then further purified via column chromatography using silica gel (R_f: 0.47; 10% EtOAc/hexanes). Yield: 98%, 181.4 mg; clear, viscous oil.

^{1}H NMR (400 MHz, $CDCl_3$): δ 8.60 (dt, *J* = 1.7, 0.7 Hz, 1H), 8.40 (d, *J* = 1.1 Hz, 1H), 8.05 (dd, *J* =

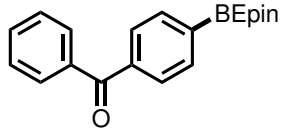
8.6, 1.7 Hz, 1H), 7.96 – 7.91 (m, 3H), 3.98 (s, 3H), 1.81 (dtt, *J* = 21.7, 14.5, 7.5 Hz, 8H), 1.01 (t, *J* = 7.5 Hz, 12H).

^{13}C NMR (126 MHz, $CDCl_3$): δ 167.41, 135.91, 134.98, 134.13, 131.50, 130.98, 129.00, 128.45, 128.32, 125.27, 89.29, 52.40, 26.66, 9.03. The boron-bound carbon was not detected likely due to quadrupolar relaxation.

^{11}B NMR (128 MHz, $CDCl_3$): δ 30.14.

HRMS (GC-EI$^+$): Calcd for $C_{22}H_{29}BO_4$, $[M]^+$ 368.2159; found 368.2166.

Phenyl(4-(4,4,5,5-tetraethyl-1,3,2-dioxaborolan-2-yl)phenyl)methanone (2.8)



Product **2.8** was synthesized according to general procedure reported in Section 2.4.2 using (4-bromophenyl)(phenyl)methanone on a 0.3 mmol scale for 21 h. The reaction mixture was then cooled to rt, passed through a pad of Celite, and then further purified via column chromatography using silica gel (R_f: 0.22; gradient of 0-5% Et_2O/hexanes). Yield: 78%, 142.1 mg; clear, viscous oil.

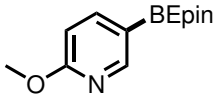
^{1}H NMR (400 MHz, $CDCl_3$): δ 7.97 – 7.91 (m, 2H), 7.83 – 7.74 (m, 4H), 7.62 – 7.56 (m, 1H), 7.51 – 7.45 (m, 2H), 1.79 (ddp, *J* = 21.7, 14.6, 7.5 Hz, 8H), 0.99 (t, *J* = 7.5 Hz, 12H).

^{13}C NMR (126 MHz, $CDCl_3$): δ 197.05, 139.77, 137.65, 134.71, 132.62, 130.25, 129.12, 128.39, 89.32, 26.60, 8.97. The boron-bound carbon was not detected likely due to quadrupolar relaxation.

^{11}B NMR (128 MHz, $CDCl_3$): δ 30.26.

HRMS (ESI$^+$): Calcd for $C_{23}H_{30}BO_3$, $[M+H]^+$ 365.2288; found 365.2306.

2-Methoxy-5-(4,4,5,5-tetraethyl-1,3,2-dioxaborolan-2-yl)pyridine (2.9)



Product **2.9** was synthesized according to general procedure reported in Section 2.4.2 using 5-bromo-2-methoxypyridine on a 0.5 mmol scale for 18.5 h. The reaction mixture was then cooled to rt, passed through a pad of Celite, and then further purified via column chromatography using silica gel (R_f: 0.38; gradient of 0-10% Et_2O/hexanes). Yield: quant., 147.0 mg; clear, viscous oil.

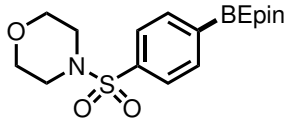
^{1}H NMR (400 MHz, $CDCl_3$): δ 8.56 (dd, J = 2.0, 0.9 Hz, 1H), 7.92 (dd, J = 8.3, 2.0 Hz, 1H), 6.71 (dd, J = 8.3, 0.9 Hz, 1H), 3.95 (s, 3H), 1.84 – 1.65 (m, 8H), 0.96 (t, J = 7.5 Hz, 12H).

^{13}C NMR (126 MHz, $CDCl_3$): δ 166.18, 154.33, 144.63, 110.37, 88.95, 53.55, 26.55, 8.95. The boron-bound carbon was not detected likely due to quadrupolar relaxation.

^{11}B NMR (128 MHz, $CDCl_3$): δ 30.09.

HRMS (ESI^+): Calcd for $C_{16}H_{27}BNO_3$, $[M+H]^+$ 292.2084; found 292.2093.

4-((4-(4,4,5,5-Tetraethyl-1,3,2-dioxaborolan-2-yl)phenyl)sulfonyl)morpholine (2.10)



Product **2.10** was synthesized according to general procedure reported in Section 2.4.2 using 4-((4-bromophenyl)sulfonyl)morpholine on a 0.3 mmol scale for 16 h. The reaction mixture was then cooled to rt, passed through a pad of Celite, and then further purified via column chromatography using silica gel (R_f: 0.30; 40% Et_2O/hexanes). Yield: quant., 122.3 mg; clear, viscous oil.

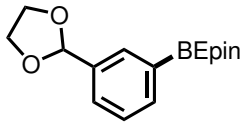
^{1}H NMR (500 MHz, $CDCl_3$): δ 7.98 (d, J = 7.9 Hz, 2H), 7.72 (d, J = 8.0 Hz, 2H), 3.76 – 3.69 (m, 4H), 2.99 (dd, J = 5.9, 3.6 Hz, 4H), 1.77 (dhept, J = 21.8, 7.4 Hz, 8H), 0.97 (t, J = 7.5 Hz, 12H).

^{13}C NMR (126 MHz, $CDCl_3$): δ 137.21, 135.48, 126.92, 89.66, 66.24, 46.12, 26.58, 8.96.

^{11}B NMR (128 MHz, $CDCl_3$): δ 29.89.

HRMS (ESI^+): Calcd for $C_{20}H_{32}BNO_5SNa$, $[M+Na]^+$ 432.1992; found 432.2003.

2-(3-(1,3-Dioxolan-2-yl)phenyl)-4,4,5,5-tetraethyl-1,3,2-dioxaborolane (2.11)



Product **2.11** was synthesized according to general procedure reported in Section 2.4.2 using 2-(3-bromophenyl)-1,3-dioxolane on a 0.5 mmol scale for 17.5 h. The reaction mixture was then cooled to rt, passed through a pad of Celite, and then further purified via column chromatography using silica gel (R_f: 0.21; 10% Et_2O/hexanes). Yield: 69%, 114.8 mg; clear, viscous oil.

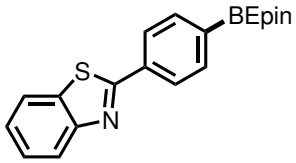
^{1}H NMR (400 MHz, $CDCl_3$): δ 7.92 (ddt, J = 1.9, 1.2, 0.6 Hz, 1H), 7.83 (dt, J = 7.3, 1.3 Hz, 1H), 7.61 – 7.54 (m, 1H), 7.43 – 7.34 (m, 1H), 5.83 (s, 1H), 4.19 – 3.99 (m, 4H), 1.75 (qq, J = 14.6, 7.0 Hz, 8H), 0.97 (t, J = 7.5 Hz, 12H).

^{13}C NMR (126 MHz, $CDCl_3$): δ 137.17, 135.90, 133.06, 129.19, 127.88, 104.03, 88.96, 65.46, 26.60, 9.01. The boron-bound carbon was not detected likely due to quadrupolar relaxation.

^{11}B NMR (128 MHz, $CDCl_3$): δ 30.18.

HRMS (ESI^+): Calcd for $C_{19}H_{30}BO_4$, $[M+H]^+$ 333.2237; found 333.2247.

2-(4-(4,4,5,5-Tetraethyl-1,3,2-dioxaborolan-2-yl)phenyl)benzo[d]thiazole (2.12)



Product **2.12** was synthesized according to general procedure reported in Section 2.4.2 using (4-bromophenyl)benzo[d]thiazole on a 0.5 mmol scale for 21 h in a dilution of [1.67 M] EtOAc. The reaction mixture was then cooled to rt, passed through a pad of Celite, and then further purified via column

chromatography using silica gel (R_f: 0.30; 5% Et_2O/hexanes). Yield: quant., 200.3 mg; White solid. Mp (64-66 °C).

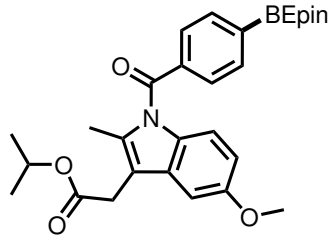
^{1}H NMR (400 MHz, $CDCl_3$): δ 8.09 (dd, J = 8.1, 1.3 Hz, 3H), 8.00 – 7.86 (m, 3H), 7.50 (ddd, J = 8.3, 7.2, 1.2 Hz, 1H), 7.39 (ddd, J = 8.3, 7.2, 1.2 Hz, 1H), 1.79 (qq, J = 14.5, 7.4 Hz, 8H), 0.99 (t, J = 7.5 Hz, 12H).

^{13}C NMR (126 MHz, $CDCl_3$): δ 168.23, 154.32, 135.85, 135.55, 135.29, 126.82, 126.50, 125.44, 123.48, 121.78, 89.25, 26.62, 9.01. The boron-bound carbon was not detected likely due to quadrupolar relaxation.

^{11}B NMR (128 MHz, $CDCl_3$): δ 30.17.

HRMS (ESI^+): Calcd for $C_{23}H_{29}BNO_2S$, $[M+H]^+$ 394.2012; found 394.2029.

Isopropyl 2-(5-methoxy-2-methyl-1-(4-(4,4,5,5-tetraethyl-1,3,2-dioxaborolan-2-yl)benzoyl)-1H-indol-3-yl)acetate (2.16)



Product **2.16** was synthesized according to general procedure reported in Section 2.4.2 using isopropyl 2-(1-(4-chlorobenzoyl)-5-methoxy-2-methyl-1H-indol-3-yl)acetate on a 0.25 mmol scale for 27 h with a catalyst loading of 0.5 mol % and a concentration of 0.5M EtOAc. The reaction mixture was then cooled to rt, passed through a pad of Celite, and then further purified via column chromatography using silica gel (R_f: 0.43; 20% EtOAc/hexanes). Yield: 97%, 133.0 mg; yellow oil.

^{1}H NMR (400 MHz, $CDCl_3$): δ 7.92 (d, J = 7.7 Hz, 2H), 7.68 (d, J = 7.7 Hz, 2H), 6.97 (d, J = 2.6 Hz, 1H), 6.94 (d, J = 9.0 Hz, 1H), 6.65 (dd, J = 9.0, 2.6 Hz, 1H), 5.02 (p, J = 6.2 Hz, 1H), 3.83 (s, 3H), 3.62

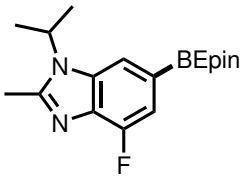
(s, 2H), 2.36 (s, 3H), 1.79 (th, J = 14.5, 7.4 Hz, 8H), 1.24 (d, J = 6.3 Hz, 6H), 0.99 (t, J = 7.4 Hz, 12H).

^{13}C NMR (126 MHz, $CDCl_3$): δ 170.57, 169.63, 156.02, 137.93, 135.98, 135.04, 131.05, 130.74, 128.69, 115.25, 112.80, 111.70, 101.26, 89.41, 68.51, 55.73, 30.87, 26.51, 21.92, 13.58, 8.93. The boron-bound carbon was not detected likely due to quadrupolar relaxation.

^{11}B NMR (128 MHz, $CDCl_3$): δ 29.75.

HRMS (ESI^+): Calcd for $C_{32}H_{42}BNO_6Na$, $[M+Na]^+$ 570.3003; found 570.3016.

4-Fluoro-1-isopropyl-2-methyl-6-(4,4,5,5-tetraethyl-1,3,2-dioxaborolan-2-yl)-1H-benzo[d]imidazole (2.17)



Product **2.17** was synthesized according to general procedure reported in Section 2.4.2 using 6-bromo-4-fluoro-1-isopropyl-2-methyl-1H-benzo[d]imidazole on a 0.3 mmol scale for 44 h, at 70 ^{o}C, with a Pd:AmPhos ratio of 1:4, a Pd loading of 0.5 mol %, and at a concentration of 1.0M EtOAc. The reaction mixture was then cooled to rt, passed through a pad of Celite, and then further purified via column chromatography using silica gel (R_f: 0.29; 40% hexanes/EtOAc). Yield: 84%, 94.5 mg; white solid. Mp (80-85 °C).

^{1}H NMR (500 MHz, $CDCl_3$): δ δ 7.68 (s, 1H), 7.34 (d, J = 10.6 Hz, 1H), 4.69 (p, J = 7.0 Hz, 1H), 2.64 (s, 3H), 1.85 – 1.69 (m, 8H), 1.64 (d, J = 6.9 Hz, 6H), 0.98 (t, J = 7.5 Hz, 12H).

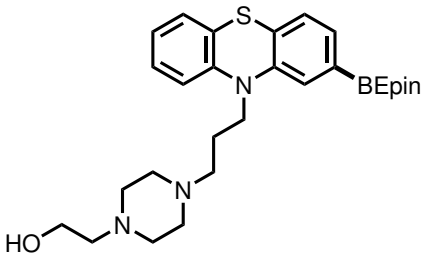
^{13}C NMR (126 MHz, $CDCl_3$): δ δ 153.42 (d, J = 252.2 Hz), 152.28, 136.83 (d, J = 8.2 Hz), 134.26 (d, J = 17.0 Hz), 113.58 (d, J = 3.5 Hz), 112.60 (d, J = 15.4 Hz), 89.07, 48.43, 26.57, 21.64, 15.33, 9.00. The boron-bound carbon was not detected likely due to quadrupolar relaxation.

^{11}B NMR (160 MHz, $CDCl_3$): δ 30.26.

^{19}F NMR (471 MHz, $CDCl_3$): δ -130.57 (d, J = 10.6 Hz).

HRMS (ESI^+): Calcd for $C_{21}H_{33}BFN_2O_2$, $[M+H]^+$ 375.2619; found 375.2630.

2-(4-(3-(2-(4,4,5,5-Tetraethyl-1,3,2-dioxaborolan-2-yl)-10H-phenothiazin-10-yl)propyl)piperazin-1-yl)ethan-1-ol (2.18)



Product **2.18** was synthesized according to general procedure reported in Section 2.4.2 using perphenazine on a 0.3 mmol scale for 4.5 h with a Pd:XPhos ratio of 1:4 and at a concentration of 2.0M H_2O. The reaction mixture was then cooled to rt, passed through a pad of Celite, and then further purified via column chromatography using silica gel (R_f: 0.32; gradient of 0-5% MeOH/DCM). Yield: 74%, 123.0 mg; clear, yellow-green, waxy solid.

^{1}H NMR (500 MHz, $CDCl_3$): δ 7.36 (d, J = 7.5, 1.0 Hz, 1H), 7.27 (s, 1H), 7.16 – 7.08 (m, 3H), 6.92 – 6.85 (m, 2H), 3.97 (t, J = 6.8 Hz, 2H), 3.60 (t, 2H), 2.96 – 2.41 (m, 12H), 1.97 (p, J = 7.2 Hz, 2H), 1.82 – 1.67 (m, 8H), 0.96 (t, J = 7.4 Hz, 12H).

^{13}C NMR (126 MHz, $CDCl_3$): δ 145.26, 144.76, 129.17, 129.15, 127.52, 127.37, 126.98, 124.98, 122.45, 121.22, 115.73, 88.95, 59.33, 57.74, 55.76, 53.22, 52.91, 45.35, 26.60, 24.38, 9.02. The boron-bound carbon was not detected likely due to quadrupolar relaxation.

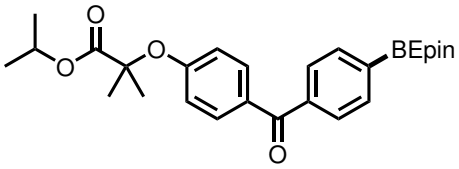
^{11}B NMR (160 MHz, $CDCl_3$): δ 30.43.

HRMS (ESI^+): Calcd for $C_{31}H_{47}BN_3O_3S$, $[M+H]^+$ 552.3431; found 552.3438.

Isopropyl

2-methyl-2-(4-(4-(4,4,5,5-tetraethyl-1,3,2-dioxaborolan-2-yl)benzoyl)phenoxy)propanoate

(2.19)



Product **2.19** synthesized according to general procedure reported in Section 2.4.2 using fenofibrate on a 0.3 mmol scale for 18.5 h. The reaction mixture was then cooled to rt, passed through a pad of Celite, and then further purified via column chromatography using silica gel (R_f: 0.40; 10% EtOAc/hexanes). Yield: quant., 154 mg; clear, viscous oil.

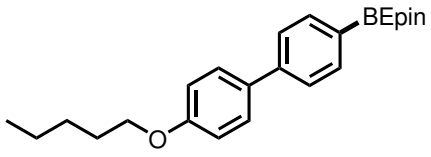
^{1}H NMR (400 MHz, $CDCl_3$): δ 7.95 – 7.88 (m, 2H), 7.79 – 7.73 (m, 2H), 7.73 – 7.67 (m, 2H), 6.88 – 6.81 (m, 2H), 5.08 (hept, J = 6.3 Hz, 1H), 1.78 (ddp, J = 21.7, 14.5, 7.4 Hz, 8H), 1.66 (s, 6H), 1.20 (d, J = 6.2 Hz, 6H), 0.98 (t, J = 7.5 Hz, 12H).

^{13}C NMR (126 MHz, $CDCl_3$): δ 195.85, 173.29, 159.74, 140.39, 134.65, 132.23, 130.69, 128.82, 117.25, 89.28, 79.49, 69.45, 26.60, 25.51, 21.64, 8.98. The boron-bound carbon was not detected likely due to quadrupolar relaxation.

^{11}B NMR (128 MHz, $CDCl_3$): δ 30.35.

HRMS (ESI^+): Calcd for $C_{30}H_{41}BO_6Na$, $[M+Na]^+$ 531.2894; found 531.2919.

4,4,5,5-Tetraethyl-2-(4'-(pentyloxy)-[1,1'-biphenyl]-4-yl)-1,3,2-dioxaborolane (2.20)



Product **2.20** was synthesized according to general procedure reported in Section 2.4.2 using 4-bromo-4'-(pentyloxy)-1,1'-biphenyl on a 2.0 mmol scale for 18 h. The reaction mixture was then cooled to rt,

passed through a pad of Celite, and then further purified via column chromatography using silica gel (R_f: 0.45; 5% Et_2O/hexanes). Yield: 97%, 816.7 mg; clear, crystalline solid. Mp (38-40 °C).

^{1}H NMR (400 MHz, $CDCl_3$): δ 7.90 – 7.84 (m, 2H), 7.60 – 7.51 (m, 4H), 7.00 – 6.94 (m, 2H), 4.00 (t, J = 6.6 Hz, 2H), 1.87 – 1.69 (m, 10H), 1.51 – 1.35 (m, 4H), 0.96 (m, 15H).

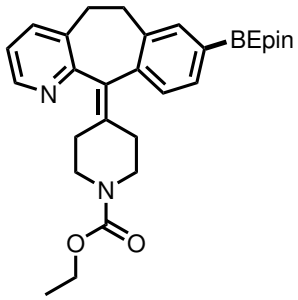
^{13}C NMR (126 MHz, $CDCl_3$): δ 159.10, 143.55, 135.43, 133.52, 128.35, 126.09, 114.93, 88.87, 68.23, 29.14, 28.37, 26.62, 22.62, 14.18, 9.02. The boron-bound carbon was not detected likely due to quadrupolar relaxation.

^{11}B NMR (128 MHz, $CDCl_3$): δ 30.60.

HRMS (GC-EI$^+$): Calcd for $C_{27}H_{39}BO_3$, $[M]^+$ 422.2992; found 422.2992.

ethyl

4-(8-(4,4,5,5-Tetraethyl-1,3,2-dioxaborolan-2-yl)-5,6-dihydro-11H-benzo[5,6]cyclohepta[1,2-b]pyridin-11-ylidene)piperidine-1-carboxylate (2.21)



Product **2.21** was synthesized according to general procedure reported in Section 2.4.2 using loratidine on a 0.3 mmol scale for 4 h using Pd:XPhos in a 1:4 ratio and at a concentration of 2.0M EtOAc. The reaction mixture was then cooled to rt, passed through a pad of Celite, and then further purified via column chromatography using silica gel (R_f: 0.32; 50% EtOAc/hexanes). Yield: quant., 160.4 mg; white solid. Mp (68-78 °C).

^{1}H NMR (400 MHz, $CDCl_3$): δ 8.38 (dd, J = 4.8, 1.7 Hz, 1H), 7.66 – 7.61 (m, 2H), 7.41 (dd, J = 7.7,

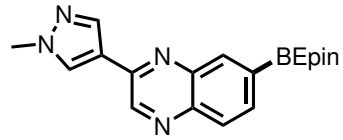
1.7 Hz, 1H), 7.21 (d, *J* = 7.8 Hz, 1H), 7.06 (dd, *J* = 7.7, 4.8 Hz, 1H), 4.13 (q, *J* = 7.1 Hz, 2H), 3.80 (s, 2H), 3.49 – 3.28 (m, 2H), 3.18 – 3.07 (m, 2H), 2.91 – 2.79 (m, 2H), 2.49 (ddd, *J* = 14.1, 9.5, 4.6 Hz, 1H), 2.33 (dp, *J* = 18.2, 4.7 Hz, 3H), 1.84 – 1.63 (m, 8H), 1.24 (t, *J* = 7.1 Hz, 3H), 0.95 (t, *J* = 7.4 Hz, 12H).

^{13}C NMR (126 MHz, $CDCl_3$): δ 157.21, 155.66, 146.65, 142.45, 137.71, 137.09, 136.97, 135.57, 135.46, 133.84, 132.76, 128.72, 122.24, 88.88, 61.42, 45.02, 44.99, 32.01, 31.71, 30.91, 30.66, 26.57 (d, *J* = 5.0 Hz), 14.83, 8.99 (d, *J* = 4.6 Hz). The boron-bound carbon was not detected likely due to quadrupolar relaxation.

^{11}B NMR (128 MHz, $CDCl_3$): δ 31.02.

HRMS (ESI^+): Calcd for $C_{32}H_{44}BN_2O_4$, $[M+H]^+$ 531.3394; found 531.3411.

2-(1-Methyl-1H-pyrazol-4-yl)-7-(4,4,5,5-tetraethyl-1,3,2-dioxaborolan-2-yl)quinoxaline (2.22)



Product **2.22** was synthesized according to general procedure reported in Section 2.4.2 using 7-bromo-2-(1-methyl-1H-pyrazol-4-yl)quinoxaline on a 0.125 mmol scale for 23 h with a Pd:AmPhos ratio of 1:4 and at a concentration of 1.25M EtOAc. The reaction mixture was then cooled to rt, passed through a pad of Celite, and then further purified via column chromatography using silica gel (R_f: 0.24; 50% EtOAc/hexanes). Yield: 91%, 44.6 mg; clear, pale yellow waxy solid.

^{1}H NMR (600 MHz, $CDCl_3$): δ 9.04 (s, 1H), 8.53 (d, *J* = 1.2 Hz, 1H), 8.18 (s, 1H), 8.13 (s, 1H), 8.04 (d, *J* = 8.3, 1.3 Hz, 1H), 8.01 (d, *J* = 8.2 Hz, 1H), 4.01 (s, 3H), 1.87 – 1.73 (m, 8H), 1.00 (t, *J* = 7.5 Hz, 12H).

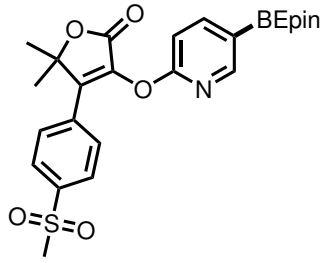
^{13}C NMR (126 MHz, $CDCl_3$): δ 147.11, 143.76, 142.65, 141.97, 138.34, 136.82, 133.79, 129.89,

128.30, 121.29, 89.43, 39.49, 26.62, 8.98. The boron-bound carbon was not detected likely due to quadrupolar relaxation.

^{11}B NMR (160 MHz, $CDCl_3$): δ 30.45.

HRMS (ESI^+): Calcd for $C_{22}H_{30}BN_4O_2$, $[M+H]^+$ 393.2462; found 393.2474.

5,5-Dimethyl-4-(4-(methylsulfonyl)phenyl)-3-((5-(4,4,5,5-tetraethyl-1,3,2-dioxaborolan-2-yl)pyridin-2-yl)oxy)furan-2(5H)-one (2.23)



Product **2.23** was synthesized according to general procedure reported in Section 2.4.2 using Merck Informer Compound X3 on a 0.2 mmol scale for 48 h using 0.5 mol % $PdAmPhos_2Cl_2$ and at a concentration of 0.5M EtOAc. The reaction mixture was then cooled to rt, passed through a pad of Celite, and then further purified via column chromatography using silica gel (R_f: 0.33; 45% EtOAc/hexanes). Yield: 73%, 79.2 mg; white solid. Mp (72-82 °C).

^{1}H NMR (500 MHz, $CDCl_3$): δ 8.51 (d, J = 1.7 Hz, 1H), 8.06 (dd, J = 8.3, 1.9 Hz, 1H), 7.97 (d, J = 8.2 Hz, 2H), 7.72 (d, J = 8.2 Hz, 2H), 6.96 (d, J = 8.1 Hz, 1H), 3.05 (s, 3H), 1.81 – 1.65 (m, 15H), 0.94 (t, J = 7.5 Hz, 12H).

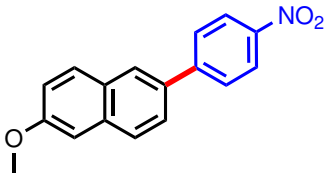
^{13}C NMR (126 MHz, $CDCl_3$): δ 165.90, 163.28, 154.39, 148.84, 146.11, 141.42, 137.85, 135.04, 129.02, 127.99, 110.36, 89.23, 84.47, 44.45, 26.49, 26.41, 8.88. The boron-bound carbon was not detected likely due to quadrupolar relaxation.

^{11}B NMR (160 MHz, $CDCl_3$): δ 30.17.

HRMS (ESI^+): Calcd for $C_{28}H_{37}BNO_7S$, $[M+H]^+$ 542.2384; found 542.2396.

Product Descriptions: Suzuki Couplings and Sequence

2-Methoxy-6-(4-nitrophenyl)naphthalene (2.24)



Product **2.24** was first synthesized according to general procedure reported in Section 2.4.2 (TPGS protocol) using 2-bromo-6-methoxynaphthalene first to make the boronic ester on a 0.5 mmol scale and then adding 0.8 equiv of 4-bromo-nitrobenzene as the coupling partner, step 1 for 18 h and step 2 for 20 h. Yield: 97%, 108.9 mg; yellow solid. Mp (136-140 °C).

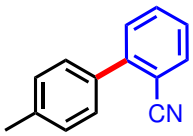
Product **2.24** was then synthesized according to the general procedure reported in Section 2.4.2 (protocol utilizing TBAB) using 2-bromo-6-methoxynaphthalene first to make the boronic ester on a 0.3 mmol scale and then adding 1.3 equiv of 4-bromo-nitrobenzene as the coupling partner, step 1 for 18 h and step 2 for 24 h. The reaction mixture was then cooled to rt, passed through a pad of Celite, and then further purified via column chromatography using silica gel (R_f: 0.34; 15% EtOAc/hexanes). Yield: quant., 84.6; yellow solid.

^{1}H NMR (500 MHz, $CDCl_3$): δ 8.35 – 8.29 (m, 2H), 8.03 (d, J = 1.9 Hz, 1H), 7.84 (dt, J = 9.6, 7.6 Hz, 4H), 7.71 (dd, J = 8.5, 1.9 Hz, 1H), 7.22 (dd, J = 8.9, 2.6 Hz, 1H), 7.18 (d, J = 2.5 Hz, 1H), 3.96 (s, 3H).

^{13}C NMR (126 MHz, $CDCl_3$): δ 158.66, 147.80, 146.98, 134.77, 133.87, 130.13, 129.10, 127.93, 127.82, 126.75, 125.50, 124.32, 119.90, 105.75, 55.54.

HRMS (GC-EI$^+$): Calcd for $C_{17}H_{13}NO_3$, $[M]^+$ 279.0895; found 279.0900.

2-Cyano-4'-methylbiphenyl (2.25)



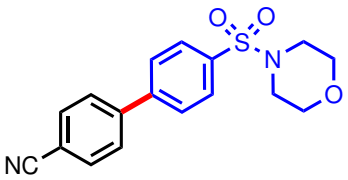
Product **2.25** was synthesized according to general procedure reported in Section 2.4.2 (TPGS protocol) using 4-bromotoluene first to make the boronic ester on a 0.3 mmol scale, and then adding 1 equiv of 2-bromobenzonitrile as the coupling partner, step 1 for 5 h and step 2 for 15 h. The reaction mixture was then cooled to rt, passed through a pad of Celite, and then further purified via column chromatography using silica gel (R_f: 0.43; gradient of 5-13% Et_2O/hexanes). Yield: 66%, 38.3 mg; white solid. Mp (48-56 °C).

^{1}H NMR (500 MHz, $CDCl_3$): δ 7.75 (dd, J = 7.8, 1.4 Hz, 1H), 7.63 (td, J = 7.7, 1.4 Hz, 1H), 7.53 – 7.49 (m, 1H), 7.47 (d, J = 8.0 Hz, 2H), 7.42 (td, J = 7.6, 1.2 Hz, 1H), 7.31 (d, J = 7.8 Hz, 2H), 2.43 (s, 3H).

^{13}C NMR (126 MHz, $CDCl_3$): δ 145.61, 138.78, 135.36, 133.80, 132.86, 130.07, 129.54, 128.70, 127.37, 118.97, 111.27, 21.34.

HRMS (GC-EI$^+$): Calcd for $C_{14}H_{11}N$, $[M]^+$ 193.0891; found 193.0894.

4'-(Morpholinosulfonyl)-[1,1'-biphenyl]-4-carbonitrile (2.26)



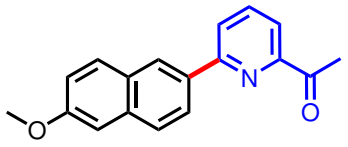
Product **2.26** was synthesized according to general procedure reported in Section 2.4.2 (TPGS protocol) using 4-bromobenzonitrile first to make the boronic ester on a 0.25 mmol scale and then adding 1 equiv of 4-bromophenylsulfonylmorpholine as the coupling partner, step 1 for 6 h and step 2 for 18 h. The reaction mixture was then cooled to rt, passed through a pad of Celite, and then further purified via column chromatography using silica gel (R_f: 0.18; 30% EtOAc/hexanes). Yield: 93%, 76.4 mg; white solid. Mp (190-192 °C).

^{1}H NMR (400 MHz, $CDCl_3$): δ 7.90 – 7.83 (m, 2H), 7.82 – 7.73 (m, 4H), 7.73 – 7.68 (m, 2H), 3.80 – 3.73 (m, 4H), 3.05 (dd, J = 5.7, 3.8 Hz, 4H).

^{13}C NMR (126 MHz, $CDCl_3$): δ 143.96, 143.67, 135.34, 133.01, 128.77, 128.18, 128.11, 118.58, 112.50, 66.22, 46.11.

HRMS (GC-EI$^+$): Calcd for $C_{17}H_{16}N_2O_3S$, $[M]^+$ 328.0882; found 328.0887.

1-(6-(6-Methoxynaphthalen-2-yl)pyridin-2-yl)ethan-1-one (2.27)



Product **27** was synthesized according to the general procedure reported in Section 2.4.2 (protocol utilizing TBAB) using 2-bromo-6-methoxynaphthalene first to make the boronic ester on a 0.3 mmol scale and then adding 1.3 equiv of 1-(6-bromopyridin-2-yl)ethan-1-one as the coupling partner, step 1 for 18 h and step 2 for 5.5 h. The reaction mixture was then cooled to rt, passed through a pad of Celite, and then further purified via column chromatography using silica gel (R_f: 0.29; 15% EtOAc/hexanes). Yield:

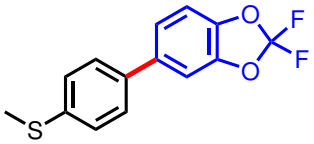
93%, 77.0 mg; white solid. Mp (114-115 °C).

^{1}H NMR (500 MHz, $CDCl_3$): δ 8.48 (d, *J* = 1.4 Hz, 1H), 8.24 (dd, *J* = 8.6, 1.8 Hz, 1H), 8.04 (dd, *J* = 7.8, 1.1 Hz, 1H), 7.98 (dd, *J* = 7.7, 1.1 Hz, 1H), 7.94 – 7.84 (m, 3H), 7.23 – 7.17 (m, 2H), 3.96 (s, 3H), 2.88 (s, 3H).

^{13}C NMR (126 MHz, $CDCl_3$): δ 200.81, 158.57, 156.60, 153.52, 137.70, 135.33, 133.73, 130.38, 128.99, 127.52, 126.33, 125.01, 123.47, 119.62, 119.48, 105.79, 55.47, 25.98.

HRMS (ESI$^+$): Calcd for $C_{18}H_{16}NO_2$, $[M+H]^+$ 278.1181; found 278.1181.

2,2-Difluoro-5-(4-(methylthio)phenyl)benzo[d][1,3]dioxole (2.28)



Product **2.28** was synthesized according to the general procedure reported in Section 2.4.2 (protocol utilizing TBAB) using 4-bromothioanisole first to make the boronic ester on a 0.3 mmol scale and then adding 1.5 equivalents of 2,2-difluorobenzodioxole as the coupling partner, step 1 for 17 h and step 2 for 23.5 h. The reaction mixture was then cooled to rt, passed through a pad of Celite, and then further purified via column chromatography using silica gel (R_f: 0.19; hexanes). Yield: quant., 83.8 mg; white solid. Mp (82-85 °C).

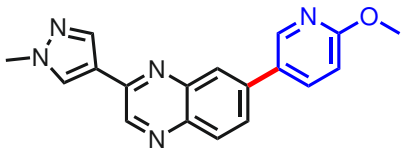
^{1}H NMR (500 MHz, $CDCl_3$): δ 7.43 (d, *J* = 8.4 Hz, 2H), 7.32 (d, *J* = 8.5 Hz, 2H), 7.24 (d, *J* = 1.9 Hz, 2H), 7.10 (d, *J* = 8.8 Hz, 1H), 2.52 (s, 3H).

^{13}C NMR (126 MHz, $CDCl_3$): δ 144.45, 143.22, 138.45, 137.31, 136.83, 131.84 (t, *J* = 255.3 Hz), 127.53, 127.05, 122.29, 109.73, 108.32, 15.90.

^{19}F NMR (471 MHz, $CDCl_3$): δ -49.99.

HRMS (GC-EI$^+$): Calcd for $C_{14}H_{10}F_2O_2S$, $[M]^+$ 280.0370; found 280.0369.

7-(6-Methoxypyridin-3-yl)-2-(1-methyl-1H-pyrazol-4-yl)quinoxaline (2.29)



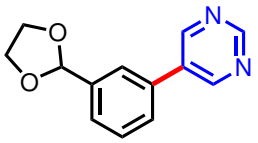
Product **2.29** was synthesized according to the general procedure reported in Section 2.4.2 (protocol utilizing TBAB) using 7-bromo-2-(1-methyl-1H-pyrazol-4-yl)quinoxaline first to make the boronic ester on a 0.3 mmol scale and then adding 1.3 equiv of 5-bromo-2-methoxypyridine as the coupling partner, step 1 for 24 h and step 2 for 16 h. The reaction mixture was then cooled to rt, passed through a pad of Celite, and then further purified via column chromatography using silica gel (R_f: 0.24; gradient of 1-2% MeOH/DCM). Yield: 88%, 83.6 mg; pale yellow solid. Mp (200 °C).

^{1}H NMR (500 MHz, $CDCl_3$): δ 9.03 (s, 1H), 8.57 (d, *J* = 2.5 Hz, 1H), 8.18 (d, *J* = 21.3 Hz, 2H), 8.15 (d, *J* = 2.1 Hz, 1H), 8.11 (d, *J* = 8.6 Hz, 1H), 7.96 (dd, *J* = 8.7, 2.6 Hz, 1H), 7.87 (dd, *J* = 8.7, 2.1 Hz, 1H), 6.89 (d, *J* = 8.6 Hz, 1H), 4.03 (s, 3H), 4.02 (s, 3H).

^{13}C NMR (126 MHz, $CDCl_3$): δ 164.32, 147.68, 145.70, 143.12, 142.90, 140.54, 139.92, 138.45, 137.74, 130.03, 129.96, 128.92, 127.87, 125.84, 121.21, 111.36, 53.85, 39.56.

HRMS (ESI$^+$): Calcd for $C_{18}H_{16}N_5O$, $[M+H]^+$ 318.1355; found 318.1354.

5-(3-(1,3-Dioxolan-2-yl)phenyl)pyrimidine (2.30)



Product **2.30** was synthesized according to the general procedure reported in Section 2.4.2 (protocol utilizing TBAB) using 2-(3-bromophenyl)-1,3-dioxolane first to make the boronic ester on a 0.3 mmol scale and then adding 1.3 equiv of 5-bromo-pyrimidine as the coupling partner, step 1 for 15.5 h and step 2 for 9 h. The reaction mixture was then cooled to rt, passed through a pad of Celite, and then further

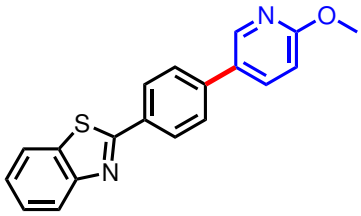
purified via column chromatography using silica gel (R_f: 0.39; 25% hexanes/EtOAc). Yield: 88%, 60.6 mg; yellow oil.

^{1}H NMR (500 MHz, $CDCl_3$): δ 9.21 (s, 1H), 8.96 (s, 2H), 7.71 (t, J = 1.8 Hz, 1H), 7.59 (dd, J = 6.5, 1.9 Hz, 2H), 7.57 – 7.52 (m, 1H), 5.89 (s, 1H), 4.20 – 4.05 (m, 4H).

^{13}C NMR (126 MHz, $CDCl_3$): δ 157.77, 155.12, 139.54, 134.65, 134.26, 129.68, 127.92, 127.37, 125.18, 103.37, 65.59.

HRMS (ESI^+): Calcd for $C_{13}H_{13}N_2O_2$, $[M+H]^+$ 229.0977; found 229.0980.

2-(4-(6-Methoxypyridin-3-yl)phenyl)benzo[d]thiazole (2.31)



Product **2.31** was synthesized according to the general procedure reported in Section 2.4.2 (protocol utilizing TBAB) using 2-(4-bromophenyl)benzo[d]thiazole first to make the boronic ester on a 0.3 mmol scale and then adding 1.3 equiv of 5-bromo-2-methoxypyridine as the coupling partner, step 1 for 21 h and step 2 for 17 h. The reaction mixture was then cooled to rt, and 1 mL of 1.0M HCl was added to the vial, and was set to stir for 10 min. Then the reaction mixture was cooled to 0 °C and collected on a buchner funnel and washed with 5 mL of cold water, 5 mL of cold EtOAc and 5 mL of cold Et_2O. The resulting solid was concentrated in vacuo. (R_f: 0.11; 10% Et_2O/hexanes). The product streaks on silica. Yield: 81%, 77.6 mg; white solid. Mp (196-198 °C).

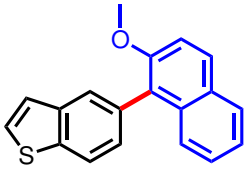
^{1}H NMR (400 MHz, $CDCl_3$): δ 8.47 (dd, J = 2.6, 0.7 Hz, 1H), 8.24 – 8.13 (m, 2H), 8.09 (dt, J = 8.2, 1.0 Hz, 1H), 7.92 (ddd, J = 8.0, 1.3, 0.6 Hz, 1H), 7.89 – 7.76 (m, 1H), 7.70 – 7.62 (m, 2H), 7.51

(ddd, *J* = 8.3, 7.2, 1.3 Hz, 1H), 7.40 (ddd, *J* = 8.2, 7.2, 1.2 Hz, 1H), 6.86 (dd, *J* = 8.6, 0.7 Hz, 1H), 4.00 (s, 3H).

^{13}C NMR (126 MHz, $CDCl_3$): δ 167.63, 164.18, 154.37, 145.30, 140.59, 137.45, 135.22, 132.72, 129.16, 128.34, 127.22, 126.55, 125.41, 123.39, 121.79, 111.20, 53.80.

HRMS (ESI$^+$): Calcd for $C_{19}H_{15}N_2OS$, $[M+H]^+$ 319.0905; found 319.0918.

5-(2-Methoxynaphthalen-1-yl)benzo[b]thiophene (2.32)



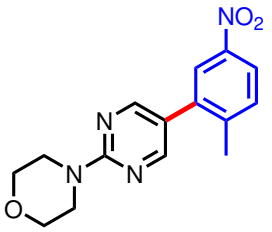
Product **2.32** was synthesized according to the general procedure reported in Section 2.4.2 (protocol utilizing TBAB) using 5-bromo-benzothiophene first to make the boronic ester on a 0.3 mmol scale and then adding 1 equiv of 1-bromo-2-methoxy-naphthalene as the coupling partner, step 1 for 23 h and step 2 for 18 h. The reaction mixture was then cooled to rt, passed through a pad of Celite, and then further purified via column chromatography using silica gel (R_f: 0.40; gradient of 0-3% Et_2O/hexanes). Yield: 73%, 63.8 mg; white solid. Mp (79-82 °C).

^{1}H NMR (500 MHz, $CDCl_3$): δ 8.02 (d, *J* = 8.2 Hz, 1H), 7.92 (d, *J* = 9.0 Hz, 1H), 7.89 – 7.82 (m, 2H), 7.56 – 7.46 (m, 2H), 7.45 – 7.29 (m, 5H), 3.86 (s, 3H).

^{13}C NMR (126 MHz, $CDCl_3$): δ 154.08, 139.93, 138.76, 134.01, 132.59, 129.28, 129.17, 127.99, 127.62, 126.66, 126.47, 125.99, 125.48, 125.36, 124.21, 123.67, 122.32, 113.91, 56.91.

HRMS (GC-EI$^+$): Calcd for $C_{19}H_{14}OS$, $[M]^+$ 290.0765; found 290.0774.

4-(5-(2-Methyl-5-nitrophenyl)pyrimidin-2-yl)morpholine (2.33)



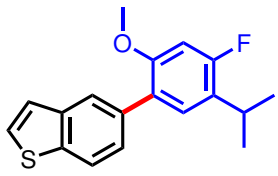
Product **2.33** was synthesized according to the general procedure reported in Section 2.4.2 (protocol utilizing TBAB) using 4-(5-bromo-pyrimidin-2-yl)morpholine first to make the boronic ester on a 0.5 mmol scale and then adding 1.3 equiv of 1-bromo-2-methyl-4-nitrobenzene as the coupling partner, step 1 for 20.5 h and step 2 for 19 h. The reaction mixture was then cooled to rt, and 1 mL of 1.0M HCl was added to the vial, and was set to stir for 10 min. Then the reaction mixture was cooled to 0 ^{o}C and collected on a buchner funnel and washed with 5 mL of cold water, 5 mL of cold EtOAc and 5 mL of cold Et_2O. The resulting solid was concentrated in vacuo. (R_f: 0.31; 33% EtOAc/hexanes). The product streaks on silica. Yield: 65%, 97.0 mg; yellow, powder solid. Mp (188-192 °C).

^{1}H NMR (500 MHz, $CDCl_3$): δ 8.34 (s, 2H), 8.12 (dd, J = 8.4, 2.5 Hz, 1H), 8.06 (d, J = 2.4 Hz, 1H), 7.45 (d, J = 8.4 Hz, 1H), 3.92 – 3.85 (m, 4H), 3.83 – 3.78 (m, 4H), 2.41 (s, 3H).

^{13}C NMR (126 MHz, $CDCl_3$): δ 161.09, 157.56, 146.69, 144.05, 137.15, 131.66, 124.68, 122.70, 121.87, 66.94, 44.42, 20.97.

HRMS (ESI^+): Calcd for $C_{15}H_{17}N_4O_3$, $[M+H]^+$ 301.1300; found 301.1311.

5-(4-Fluoro-5-isopropyl-2-methoxyphenyl)benzo[b]thiophene (2.34)



Product **2.34** was synthesized according to the general procedure reported in Section 2.4.2 (protocol

utilizing TBAB) using 5-bromobenzothiophene first to make the boronic ester on a 0.3 mmol scale and then adding 1.5 equivalents of 1-bromo-4-fluoro-5-isopropyl-2-methoxybenzene as the coupling partner, step 1 for 23 h and step 2 for 24 h. The reaction mixture was then cooled to rt, passed through a pad of Celite, and then further purified via column chromatography using silica gel (R_f: 0.39; gradient of 45% EtOAc/hexanes). Yield: 48%, 43.4 mg; white solid. Mp (146-149 °C).

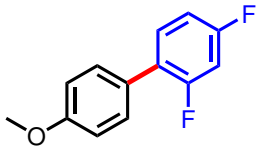
^{1}H NMR (500 MHz, $CDCl_3$): δ 7.96 – 7.89 (m, 2H), 7.51 (dd, J = 8.3, 1.8 Hz, 1H), 7.47 (d, J = 5.5 Hz, 1H), 7.38 (d, J = 5.4 Hz, 1H), 7.24 (d, J = 8.7 Hz, 1H), 6.72 (d, J = 12.2 Hz, 1H), 3.80 (s, 3H), 3.24 (h, J = 6.9 Hz, 1H), 1.31 (d, J = 7.0 Hz, 6H).

^{13}C NMR (101 MHz, $CDCl_3$): δ 160.43 (d, J = 245.1 Hz), 155.49 (d, J = 9.9 Hz), 139.86, 138.57, 134.51, 129.55 (d, J = 7.1 Hz), 127.05 (d, J = 15.0 Hz), 126.75, 126.54 (d, J = 3.6 Hz), 126.34, 124.42, 124.15, 122.01, 99.61 (d, J = 27.4 Hz), 56.02, 26.90 (d, J = 1.7 Hz), 23.03.

^{19}F NMR (376 MHz, $CDCl_3$): δ -117.97 (dd, J = 12.2, 8.8 Hz).

HRMS (GC-EI$^+$): Calcd for $C_{18}H_{17}FOS$, $[M]^+$ 300.0984; found 300.0998.

2,4-Difluoro-4'-methoxy-1,1'-biphenyl (2.35)



Product **2.35** was synthesized according to the general procedure reported in Section 2.4.2 (protocol utilizing TBAB) using 4-bromoanisole first to make the boronic ester on a 0.3 mmol scale and then adding 1.5 equivalents of 2,2-difluorobenzodioxole as the coupling partner, step 1 for 15 h and step 2 for 24 h. The reaction mixture was then cooled to rt, passed through a pad of Celite, and then further purified via column chromatography using silica gel (R_f: 0.14; hexanes). Yield: 81%, 53.4 mg; white solid.

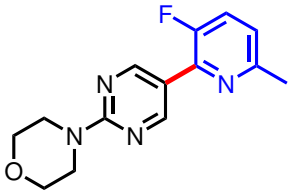
^{1}H NMR (500 MHz, $CDCl_3$): δ 7.46 – 7.41 (m, 2H), 7.37 (td, J = 8.7, 6.5 Hz, 1H), 7.00 – 6.96 (m, 2H), 6.96 – 6.87 (m, 2H), 3.86 (s, 3H).

^{13}C NMR (126 MHz, $CDCl_3$): δ 162.16 (dd, J = 226.6, 11.8 Hz), 159.69 (dd, J = 228.1, 11.8 Hz), 159.41, 131.27 (dd, J = 9.3, 5.0 Hz), 130.16 (d, J = 3.0 Hz), 127.49 (d, J = 1.4 Hz), 125.14 (dd, J = 13.7, 3.9 Hz), 114.14, 111.58 (dd, J = 21.0, 3.8 Hz), 104.43 (dd, J = 26.9, 25.2 Hz), 55.46.

^{19}F NMR (376 MHz, $CDCl_3$): δ -112.37 (d, J = 7.3 Hz), -113.81 (d, J = 7.4 Hz).

HRMS (GC-EI$^+$): Calcd for $C_{13}H_{10}F_2O$, $[M]^+$ 220.0700; found 220.0701.

4-(5-(3-Fluoro-6-methylpyridin-2-yl)pyrimidin-2-yl)morpholine (2.36)



Product **2.36** was synthesized according to the general procedure reported in Section 2.4.2 (protocol utilizing TBAB) using 4-(5-bromo-pyrimidin-2-yl)morpholine first to make the boronic ester on a 0.5 mmol scale and then adding 1.3 equiv of 2-bromo-3-fluoro-5-methylpyridine as the coupling partner, step 1 for 20.5 h and step 2 for 19 h. The reaction mixture was then cooled to rt, and 1 mL of 1.0M HCl was added to the vial, and was set to stir for 10 min. Then the reaction mixture was cooled to 0 °C and collected on a buchner funnel and washed with 5 mL of cold water, 5 mL of cold EtOAc and 5 mL of cold Et_2O. The resulting solid was concentrated in vacuo. (R_f: 0.33; 33% EtOAc/hexanes). The product streaks on silica. Yield: 69%, 95.1 mg; white, powder solid. Mp (149 °C).

^{1}H NMR (500 MHz, $CDCl_3$): δ 8.97 (d, J = 1.2 Hz, 2H), 7.33 (dd, J = 10.9, 8.4 Hz, 1H), 7.04 (dd, J = 8.4, 3.4 Hz, 1H), 3.94 – 3.87 (m, 4H), 3.81 – 3.75 (m, 4H), 2.56 (d, J = 1.0 Hz, 3H).

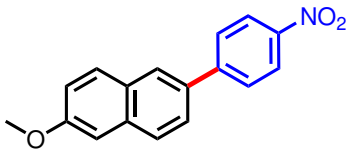
^{13}C NMR (126 MHz, $CDCl_3$): δ 161.29, 157.91 (d, J = 7.8 Hz), 155.71 (d, J = 256.2 Hz), 154.41 (d,

J = 4.7 Hz), 140.81 (d, *J* = 11.5 Hz), 124.25 (d, *J* = 20.2 Hz), 122.60 (d, *J* = 3.7 Hz), 118.65 (d, *J* = 6.3 Hz), 66.99, 44.48, 24.01 (d, *J* = 1.8 Hz).

^{19}F NMR (376 MHz, $CDCl_3$): δ -129.30.

HRMS (ESI$^+$): Calcd for $C_{14}H_{16}FN_4O$, $[M+H]^+$ 275.1308; found 275.1318.

2-Methoxy-6-(4-nitrophenyl)naphthalene (2.37)



Product **2.37** was first synthesized according to general procedure reported in Section 2.4.2 (TPGS protocol) using 2-bromo-6-methoxynaphthalene first to make the boronic ester on a 0.5 mmol scale and then adding 0.8 equiv of 4-bromo-nitrobenzene as the coupling partner, step 1 for 18 h and step 2 for 20 h. Yield: 97%, 108.9 mg; yellow solid. Mp (136-140 °C).

Product **2.37** was then synthesized according to the general procedure reported in Section 2.4.2 (protocol utilizing TBAB) using 2-bromo-6-methoxynaphthalene first to make the boronic ester on a 0.3 mmol scale and then adding 1.3 equiv of 4-bromo-nitrobenzene as the coupling partner, step 1 for 18 h and step 2 for 24 h. The reaction mixture was then cooled to rt, passed through a pad of Celite, and then further purified via column chromatography using silica gel (R_f: 0.34; 15% EtOAc/hexanes). Yield: quant., 84.6; yellow solid.

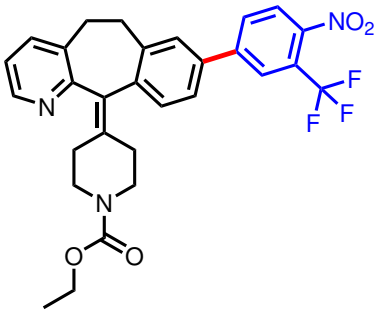
^{1}H NMR (500 MHz, $CDCl_3$): δ 8.35 – 8.29 (m, 2H), 8.03 (d, *J* = 1.9 Hz, 1H), 7.84 (dt, *J* = 9.6, 7.6 Hz, 4H), 7.71 (dd, *J* = 8.5, 1.9 Hz, 1H), 7.22 (dd, *J* = 8.9, 2.6 Hz, 1H), 7.18 (d, *J* = 2.5 Hz, 1H), 3.96 (s, 3H).

^{13}C NMR (126 MHz, $CDCl_3$): δ 158.66, 147.80, 146.98, 134.77, 133.87, 130.13, 129.10, 127.93,

127.82, 126.75, 125.50, 124.32, 119.90, 105.75, 55.54.

HRMS (GC-EI$^+$): Calcd for $C_{17}H_{13}NO_3$, $[M]^+$ 279.0895; found 279.0900.

Ethyl 4-(8-(4-Nitro-3-(trifluoromethyl)phenyl)-5,6-dihydro-11H-benzo[5,6]cyclohepta[1,2-b]pyridin-11-ylidene)piperidine-1-carboxylate (2.38)



Product **2.38** was synthesized according to the general procedure reported in Section 2.4.2 (protocol utilizing TBAB) using loratadine first to make the boronic ester on a 0.3 mmol scale using 0.25 mol % Pd:XPhos (1:4 ratio) and then adding 1.3 equivalents of 4-bromo-1-nitro-2-(trifluoromethyl)benzene as the coupling partner, step 1 for 4 h and step 2 for 22 h. The reaction mixture was then cooled to rt, passed through a pad of Celite, and then further purified via column chromatography using silica gel (R_f: 0.31; 30% hexanes/EtOAc). Yield: quant., 165.7 mg; yellow solid. Mp (84-92 °C).

^{1}H NMR (500 MHz, $CDCl_3$): δ 8.42 (dd, J = 4.9, 1.6 Hz, 1H), 8.00 – 7.95 (m, 2H), 7.86 (dd, J = 8.4, 1.9 Hz, 1H), 7.48 (dd, J = 7.8, 1.6 Hz, 1H), 7.45 – 7.40 (m, 2H), 7.35 (d, J = 8.4 Hz, 1H), 7.12 (dd, J = 7.7, 4.7 Hz, 1H), 4.14 (q, J = 7.0 Hz, 2H), 3.84 (s, 2H), 3.52 (ddd, J = 15.8, 9.9, 4.6 Hz, 1H), 3.42 (ddd, J = 15.7, 8.4, 4.6 Hz, 1H), 3.22 – 3.12 (m, 2H), 2.93 (dddd, J = 20.3, 15.8, 8.6, 4.7 Hz, 2H), 2.51 (ddd, J = 14.1, 9.4, 4.6 Hz, 1H), 2.47 – 2.30 (m, 3H), 1.25 (t, J = 7.1 Hz, 3H).

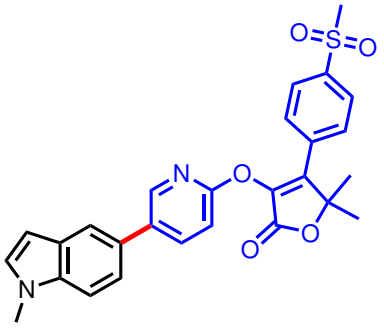
^{13}C NMR (126 MHz, $CDCl_3$): δ 157.13, 155.64, 146.93, 146.79, 145.88, 140.78, 139.12, 137.92, 137.69, 136.65, 134.52, 133.56, 130.93, 130.53, 128.21, 126.45 (q, J = 5.4 Hz), 126.03, 125.16, 124.50 (q, J = 33.9 Hz), 122.52, 122.12 (q, J = 273.7 Hz), 61.49, 44.97, 44.92, 32.12, 31.71, 30.98, 30.71,

14.81.

^{19}F NMR (471 MHz, $CDCl_3$): δ -59.90.

HRMS (ESI$^+$): Calcd for $C_{29}H_{27}F_3N_3O_4$, $[M+H]^+$ 538.1953; found 538.1958.

5,5-Dimethyl-3-((5-(1-methyl-1H-indol-5-yl)pyridin-2-yl)oxy)-4-(4-(methylsulfonyl)phenyl)-furan-2(5H)-one (2.40)



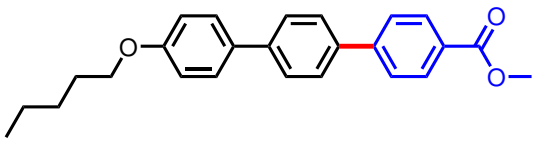
Product **2.40** was synthesized according to the general procedure reported in Section 2.4.2 (protocol utilizing TBAB) using 5-bromo-1-methyl-1H-indole first to make the boronic ester on a 0.125 mmol scale and then adding 1.3 equivalents of Merck Informer Compound X3 as the coupling partner, step 1 for 18 h and step 2 for 36 h. The reaction mixture was then cooled to rt, passed through a pad of Celite, and then further purified via column chromatography using silica gel (R_f: 0.21; 50% EtOAc/hexanes). Yield: quant., 62.9 mg; off-white solid.

^{1}H NMR (500 MHz, $CDCl_3$): δ 8.38 (d, J = 2.6 Hz, 1H), 8.00 (d, J = 8.1 Hz, 2H), 7.95 (dd, J = 8.6, 2.5 Hz, 1H), 7.80 (d, J = 8.1 Hz, 2H), 7.74 (s, 1H), 7.38 (q, J = 8.5 Hz, 2H), 7.10 (d, J = 3.2 Hz, 1H), 7.07 (d, J = 8.5 Hz, 1H), 6.53 (d, J = 3.2 Hz, 1H), 3.82 (s, 3H), 3.05 (s, 3H), 1.78 (s, 6H).

^{13}C NMR (126 MHz, $CDCl_3$): δ 166.08, 160.10, 148.37, 145.68, 141.40, 138.93, 138.13, 136.51, 135.14, 134.85, 129.95, 129.11, 128.66, 128.01, 121.01, 119.42, 110.87, 109.94, 101.46, 84.47, 77.41, 77.16, 76.91, 44.47, 33.07, 29.81, 26.54.

HRMS (ESI$^+$): Calcd for $C_{27}H_{24}N_2O_5SNa$, $[M+Na]^+$ 511.1304; found 511.1305.

1-Carbomethoxy-4”-(pentyloxy)terphenyl (2.41)



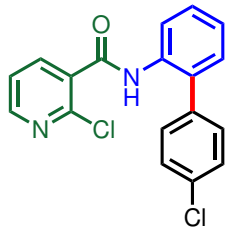
Product **2.41** was synthesized according to the gram scale general procedure reported in Section 2.4.2.

^{1}H NMR (400 MHz, $CDCl_3$): δ 8.14 – 8.09 (m, 2H), 7.73 – 7.63 (m, 6H), 7.60 – 7.54 (m, 2H), 7.02 – 6.96 (m, 2H), 4.01 (t, J = 6.6 Hz, 2H), 3.95 (s, 3H), 1.87 – 1.78 (m, 2H), 1.52 – 1.35 (m, 4H), 0.95 (t, J = 7.1 Hz, 3H).

^{13}C NMR (126 MHz, $CDCl_3$): δ 167.17, 159.14, 145.35, 140.88, 138.25, 132.81, 130.29, 128.95, 128.19, 127.74, 127.29, 126.97, 115.03, 68.27, 52.28, 29.14, 28.37, 22.63, 14.19.

HRMS (GC-EI$^+$): Calcd for $C_{25}H_{26}O_3$, $[M]^+$ 374.1882; found 374.1880.

2-Chloro-N-(4’-chlorobiphenyl-2-yl)nicotinamide (boscalid) (2.42)



Product **2.42** was synthesized according to the gram scale general procedure reported in Section 2.4.2.

^{1}H NMR (400 MHz, $CDCl_3$): δ 8.37 (dd, J = 4.8, 2.0 Hz, 1H), 8.34 (d, J = 8.2 Hz, 1H), 8.11 – 8.03 (m, 2H), 7.41 – 7.34 (m, 2H), 7.27 (m, 3H), 7.22 – 7.16 (m, 2H).

^{13}C NMR (126 MHz, $CDCl_3$): δ 162.61, 151.47, 146.83, 140.31, 136.39, 134.59, 134.47, 132.37, 131.20, 130.93, 130.37, 129.45, 129.03, 125.46, 123.05, 122.23.

HRMS (ESI$^+$): Calcd for $C_{18}H_{12}Cl_2N_2ONa$, $[M+Na]^+$ 365.0225; found 365.0229.

2.4.6 ICPMS Data

Compounds listed in Table 2.11 were analyzed via Inductively Coupled Plasma Mass Spectrometry (ICPMS) by the Nano and Pico Characterization Lab at the California NanoSystems Institute at UCLA, Dr. Chong Hyun "Paul" Chang, P.h.D.

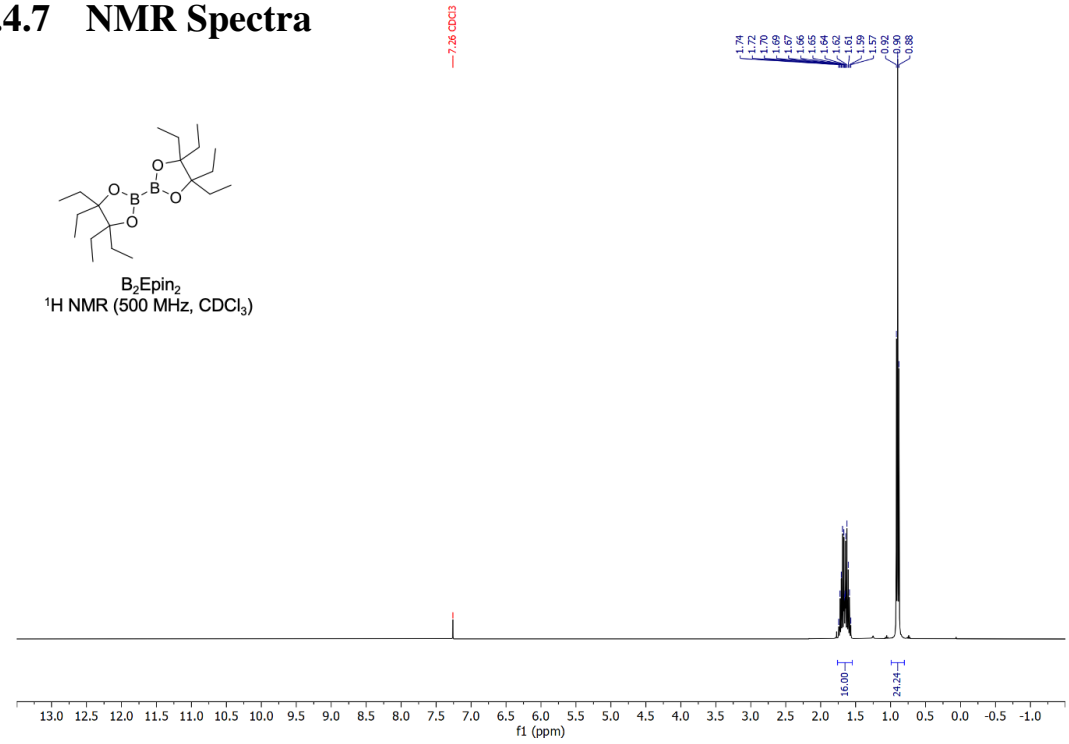
Table 2.10: ICPMS Analysis Data[61]

		Palladium [µg/g]	
Sample:	**Sample weight in analysis [mg]:**	**Average**[a]	σ[b]
Product **42**	4.70	0.696	0.013
Product **38**	6.60	7.857	0.039

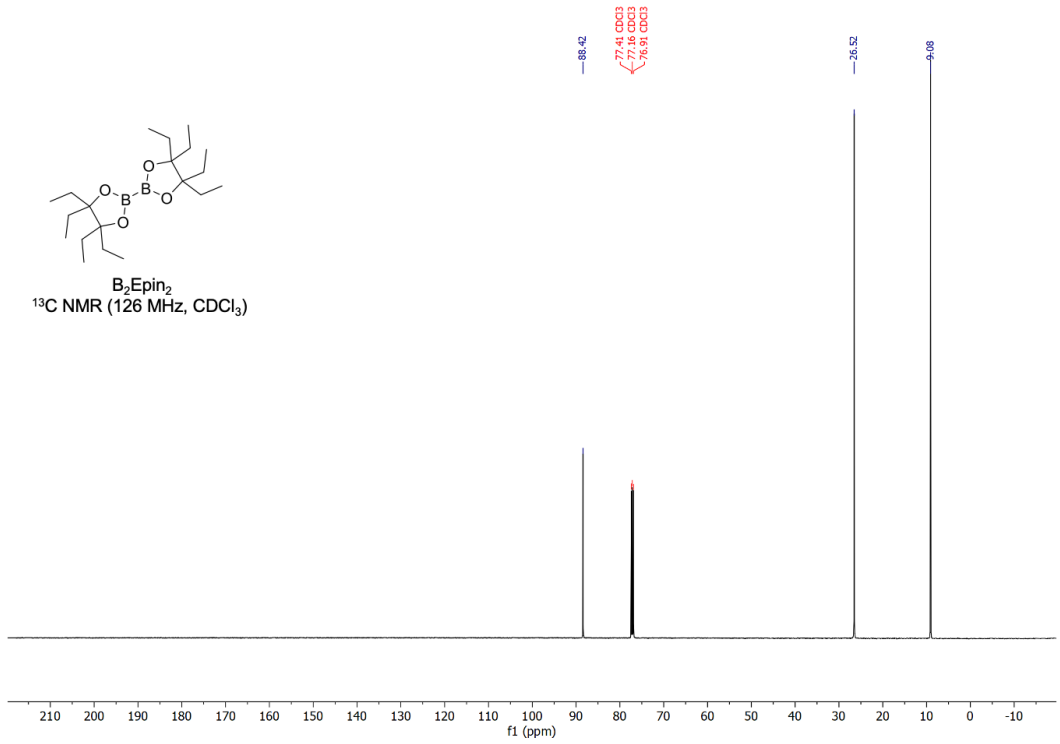
[a] Each sample was done in triplicated measurements with background correction. [b] Standard deviation.

Note for the following subsection: *The compound number presented on each of the spectra is with respect to the chapter in which it presented. For example,* **7** *refers to Compound* **2.7** *presented above.*

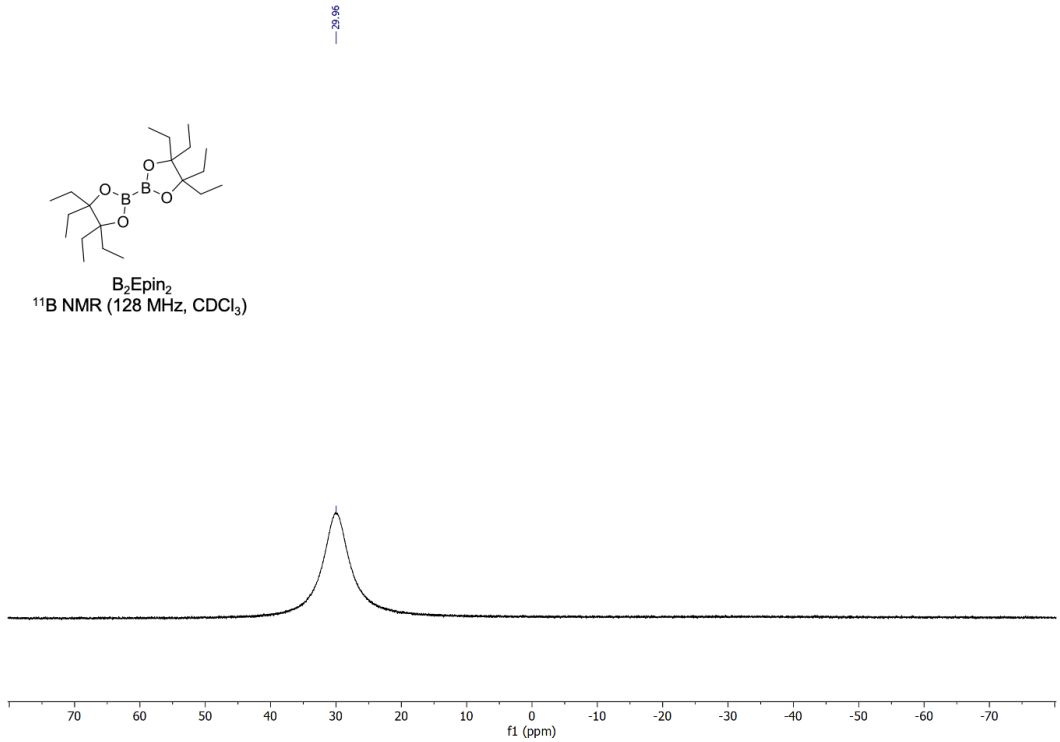
2.4.7 NMR Spectra



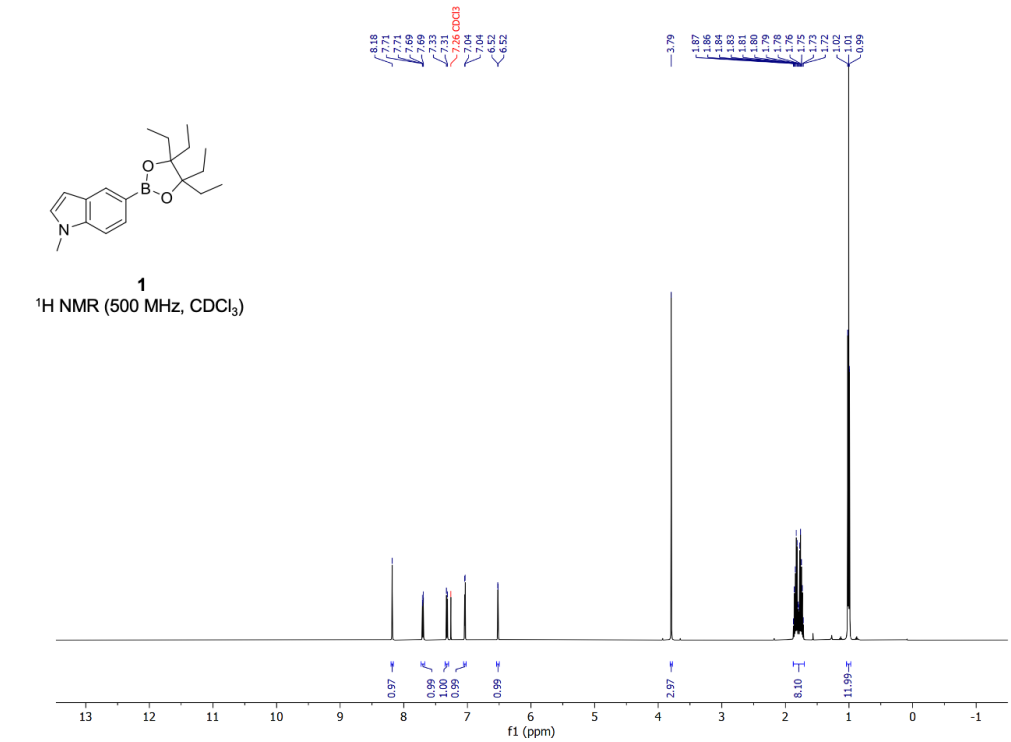
B_2Epin_2
^1H NMR (500 MHz, $CDCl_3$)



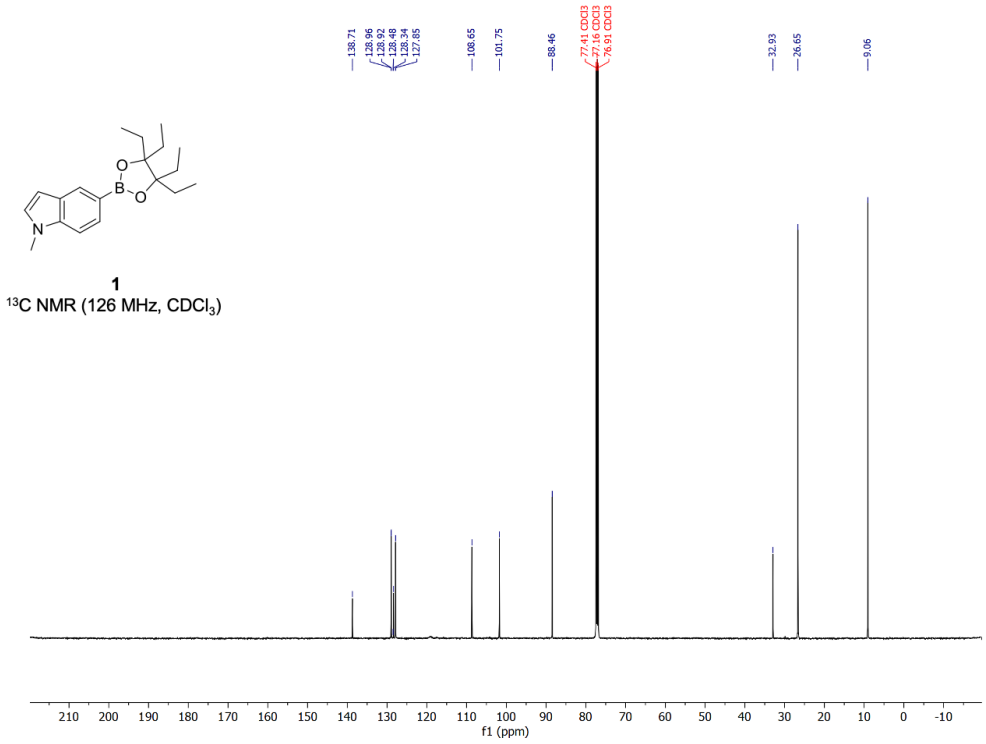
B_2Epin_2
^{13}C NMR (126 MHz, $CDCl_3$)



B_2Epin_2
^{11}B NMR (128 MHz, $CDCl_3$)

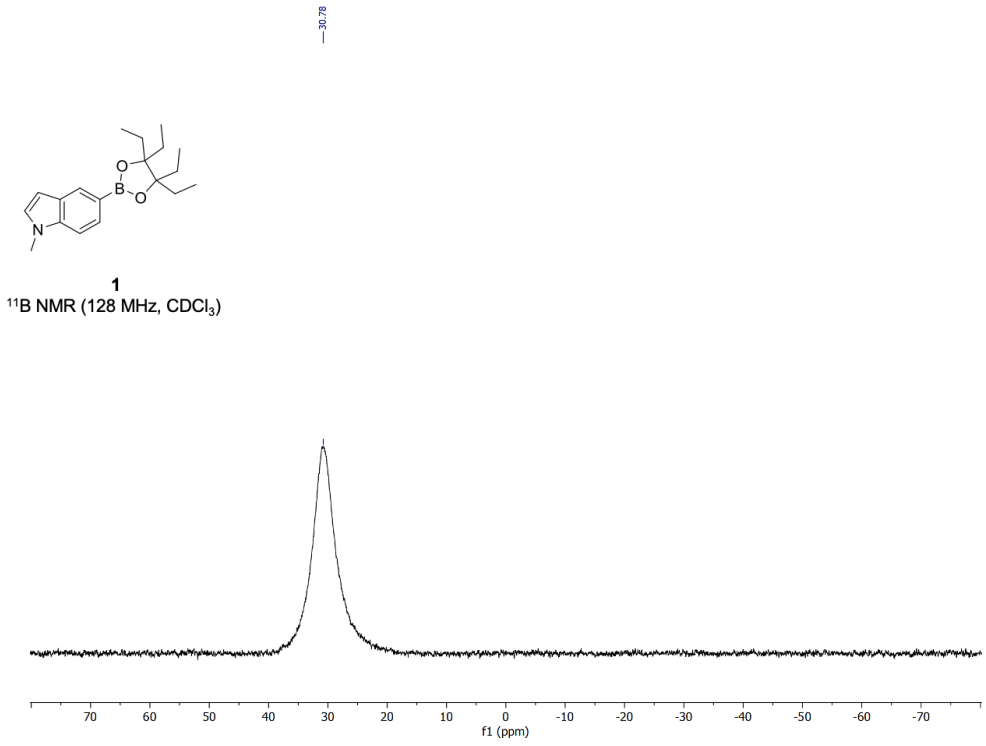


1
^{1}H NMR (500 MHz, $CDCl_3$)



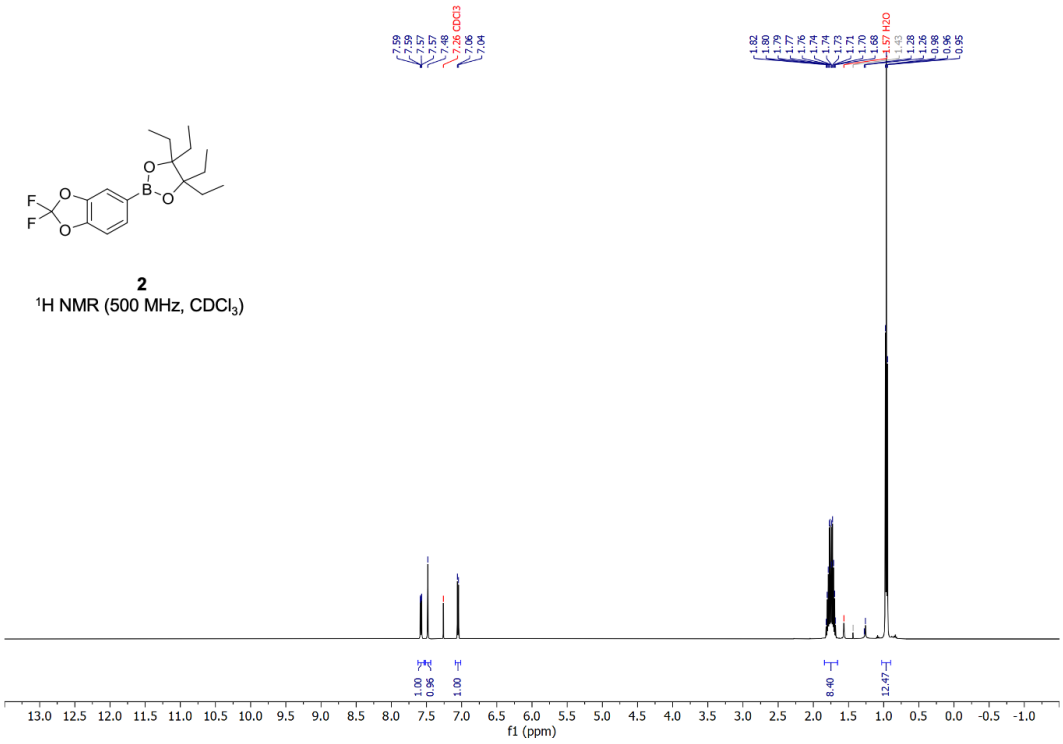
1

^{13}C NMR (126 MHz, $CDCl_3$)

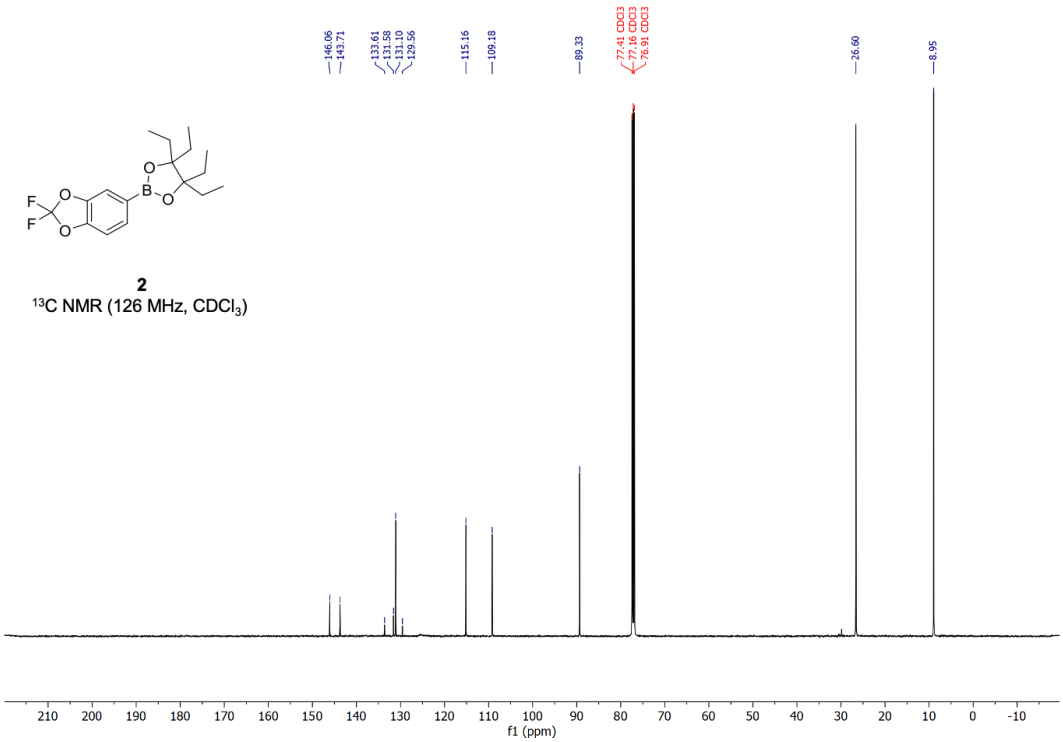


1

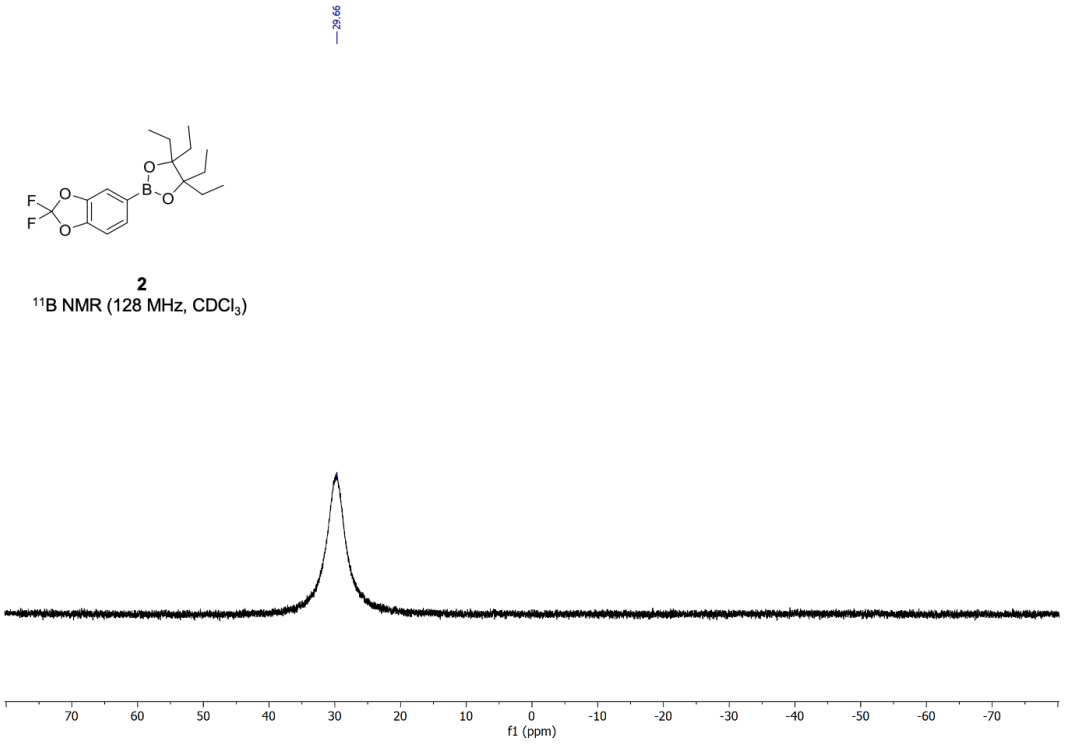
^{11}B NMR (128 MHz, $CDCl_3$)



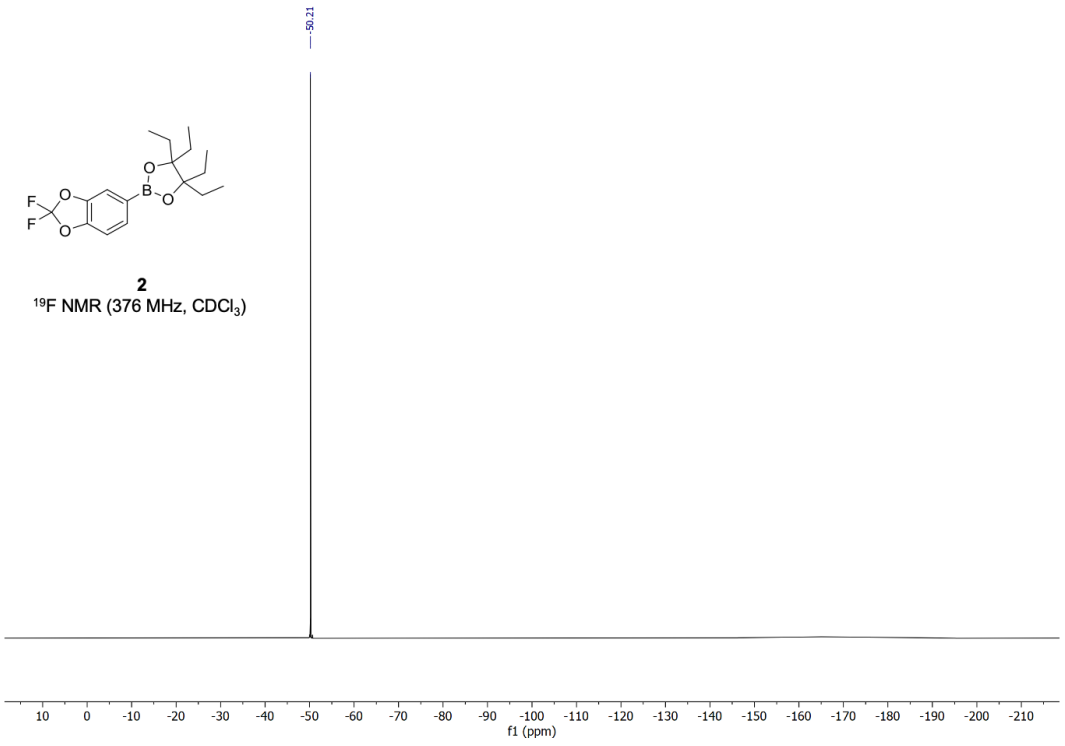
2
^{1}H NMR (500 MHz, $CDCl_3$)



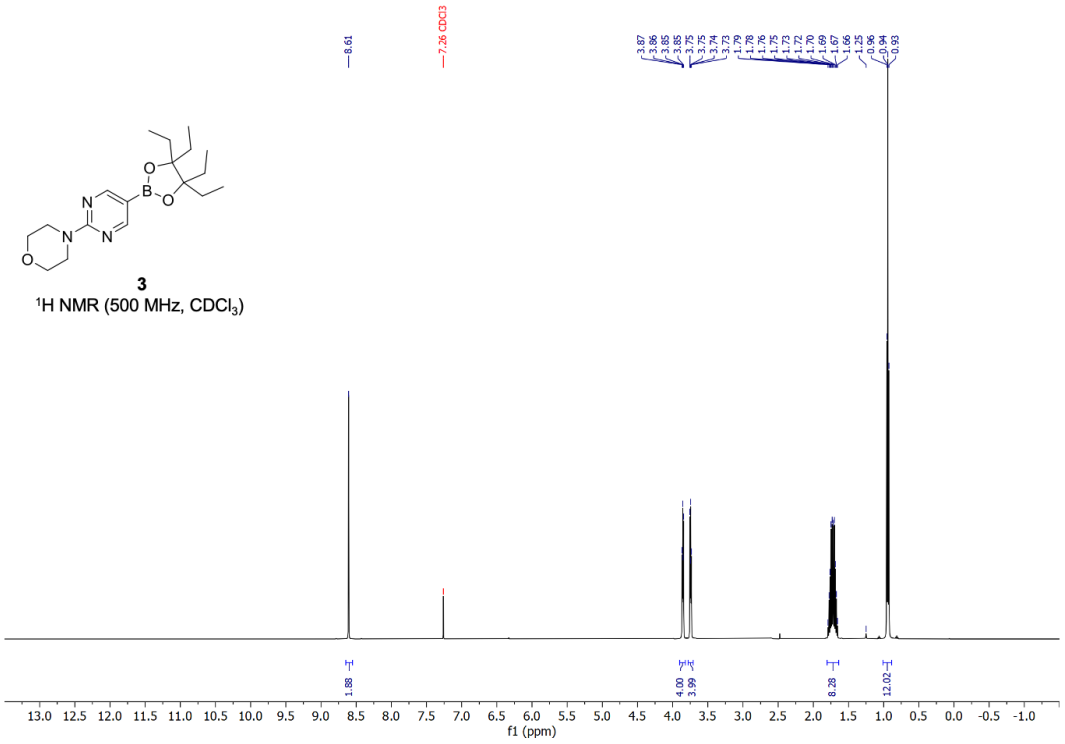
2
^{13}C NMR (126 MHz, $CDCl_3$)



2
^{11}B NMR (128 MHz, $CDCl_3$)

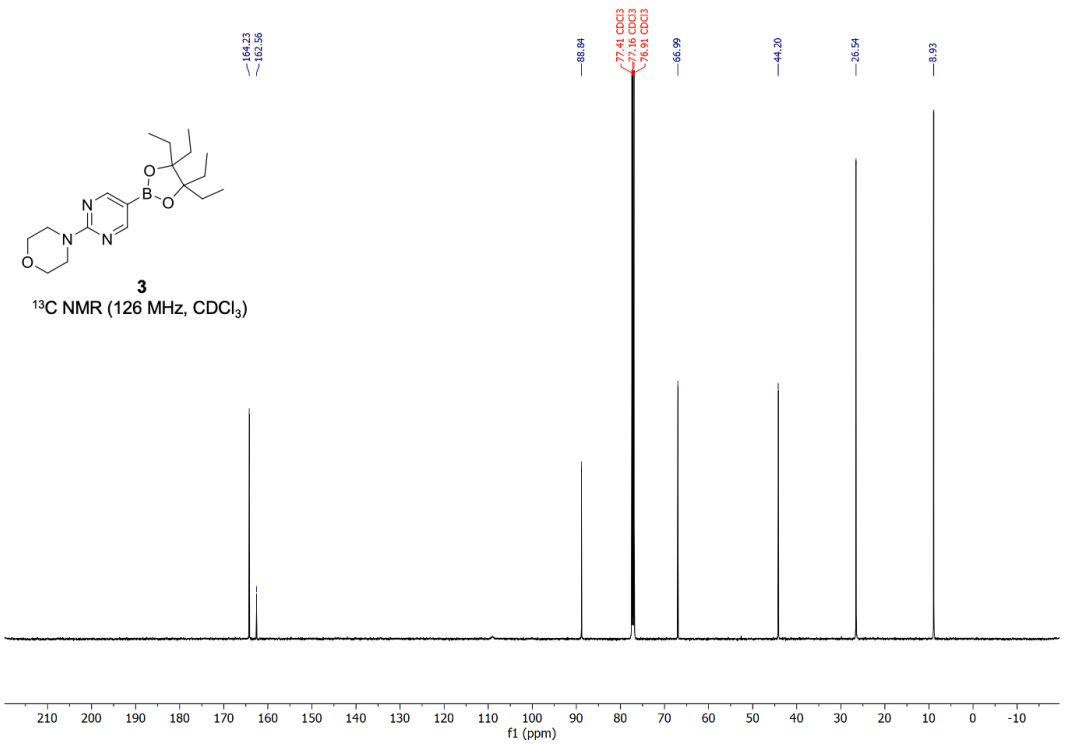


2
^{19}F NMR (376 MHz, $CDCl_3$)



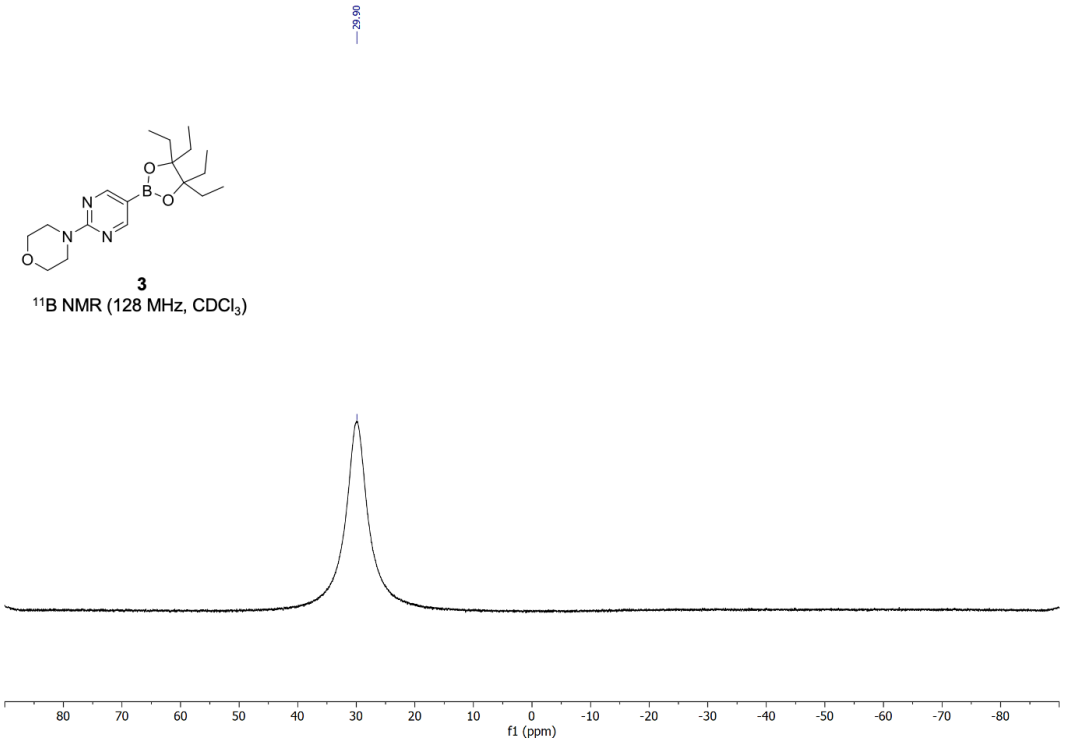
3

^{1}H NMR (500 MHz, $CDCl_3$)

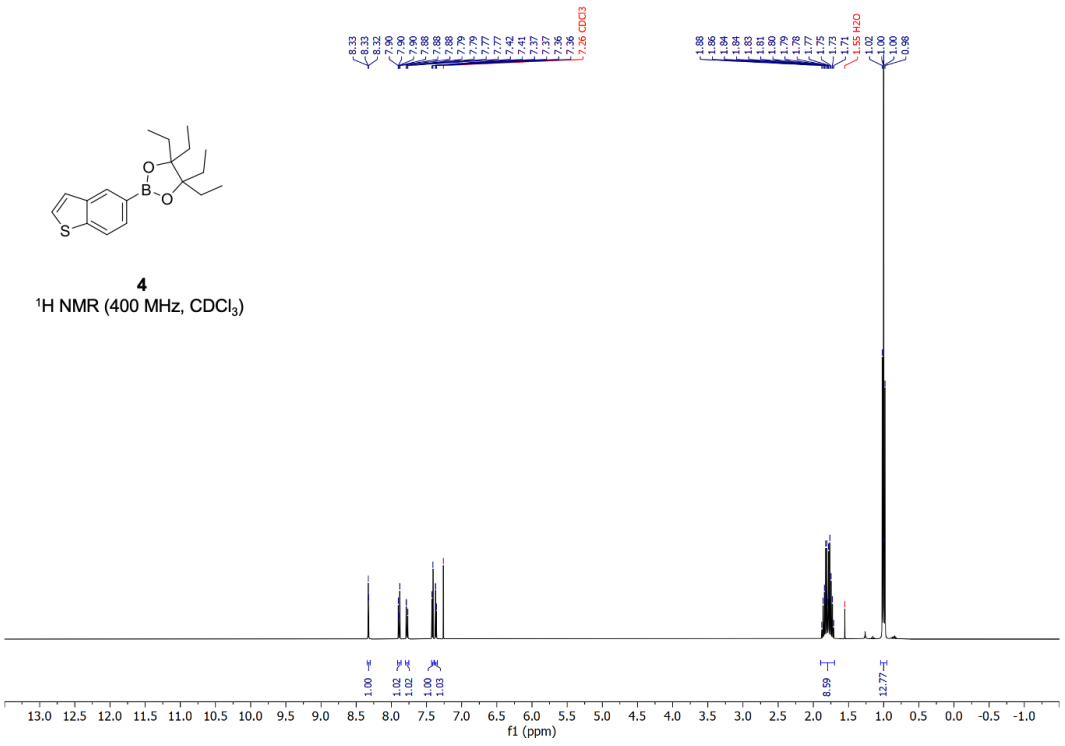


3

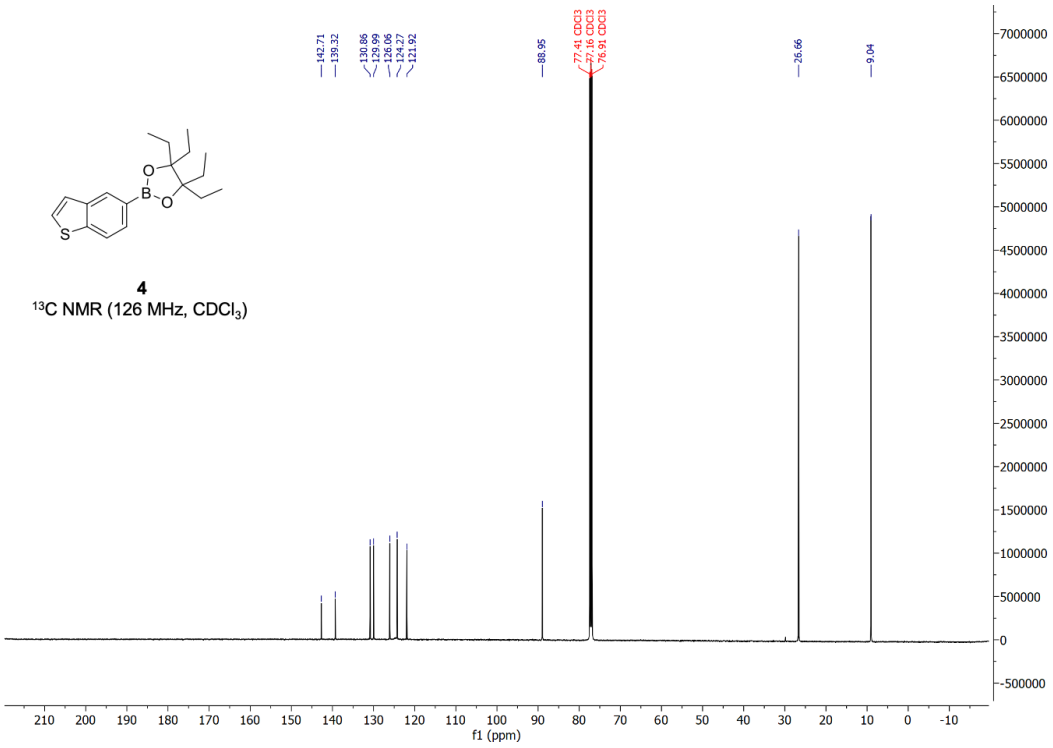
^{13}C NMR (126 MHz, $CDCl_3$)



3
^{11}B NMR (128 MHz, $CDCl_3$)

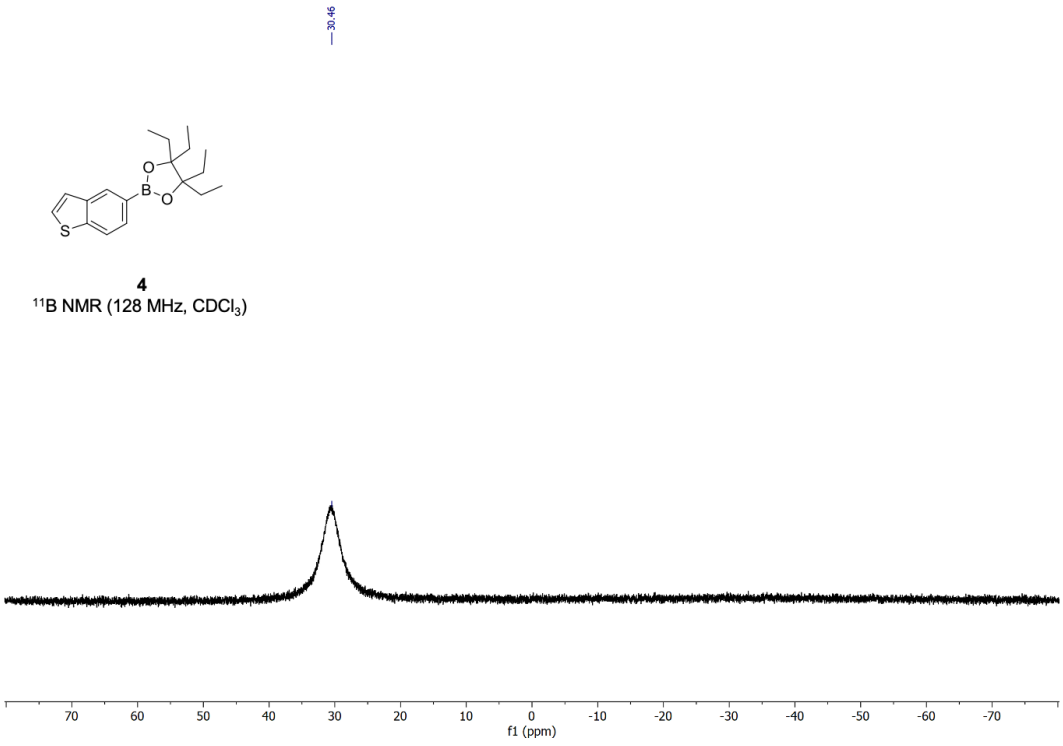


4
^{1}H NMR (400 MHz, $CDCl_3$)



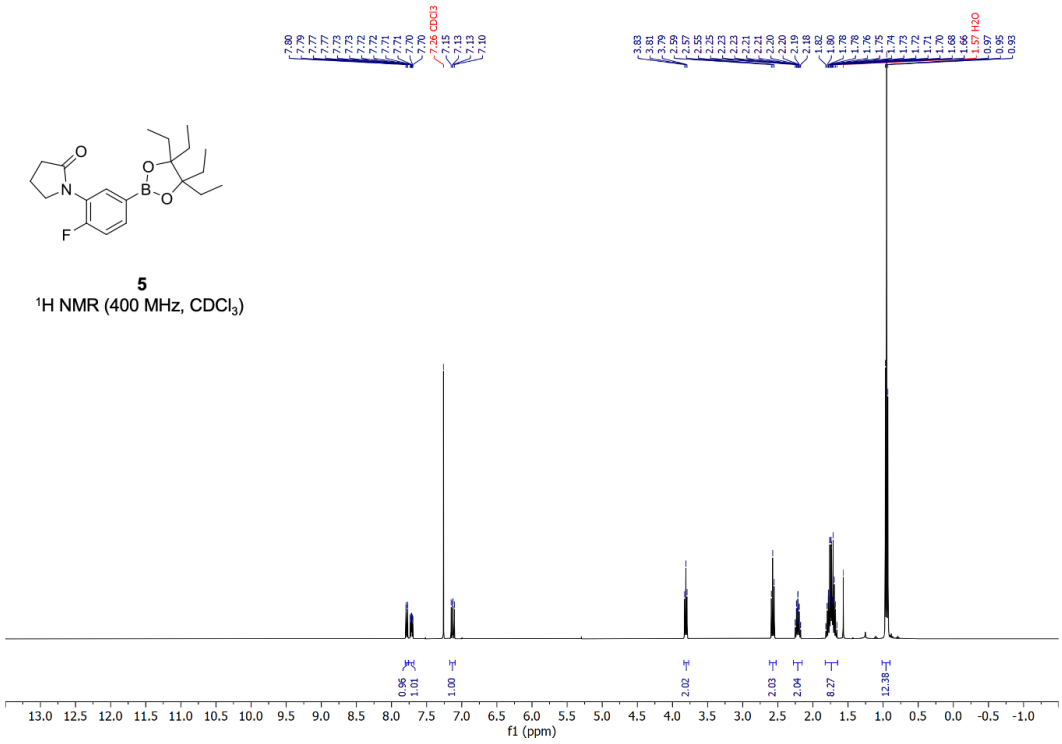
4

^{13}C NMR (126 MHz, $CDCl_3$)

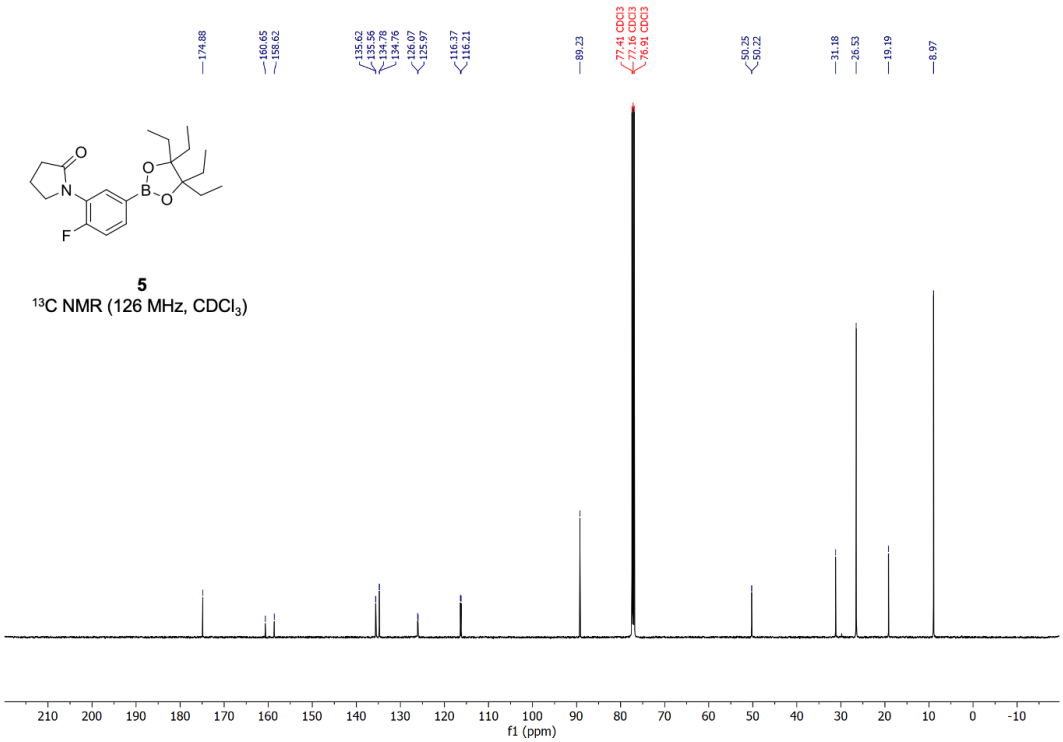


4

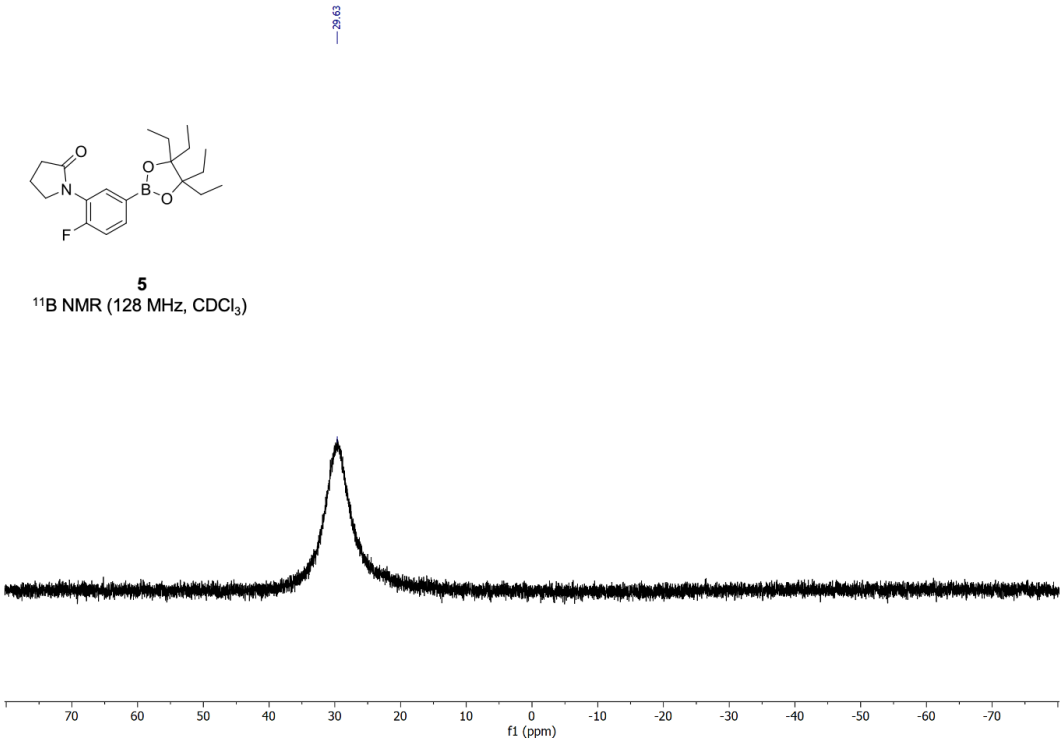
^{11}B NMR (128 MHz, $CDCl_3$)



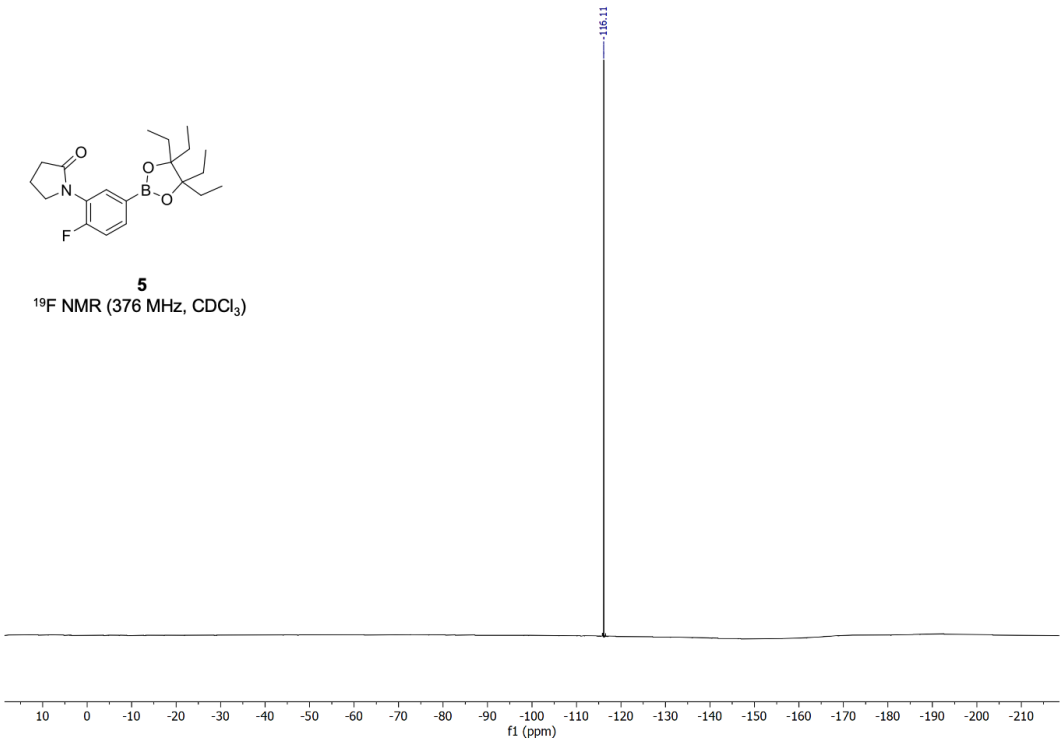
5
^{1}H NMR (400 MHz, $CDCl_3$)



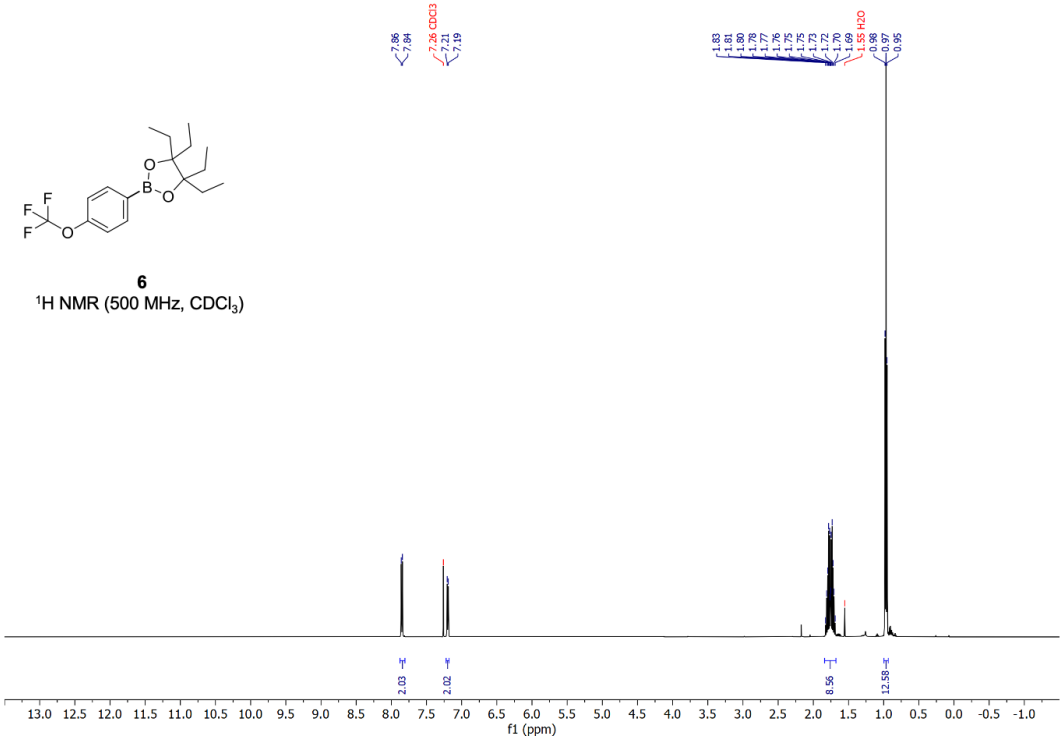
5
^{13}C NMR (126 MHz, $CDCl_3$)



5
^{11}B NMR (128 MHz, $CDCl_3$)

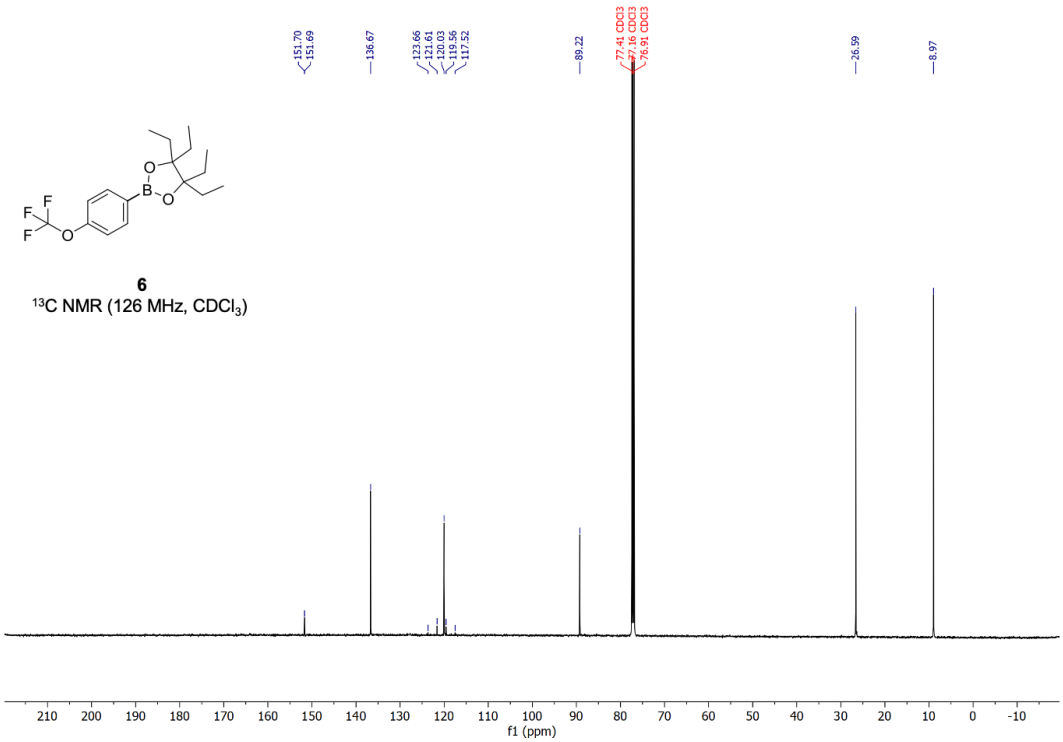


5
^{19}F NMR (376 MHz, $CDCl_3$)



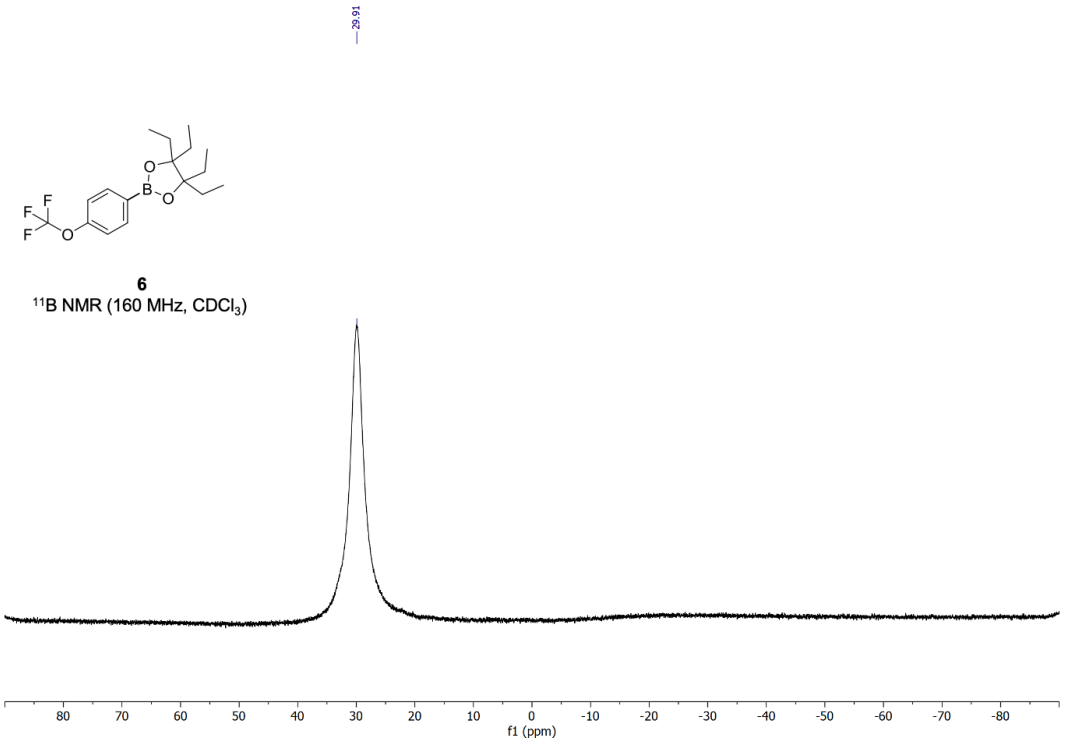
6

^{1}H NMR (500 MHz, $CDCl_3$)

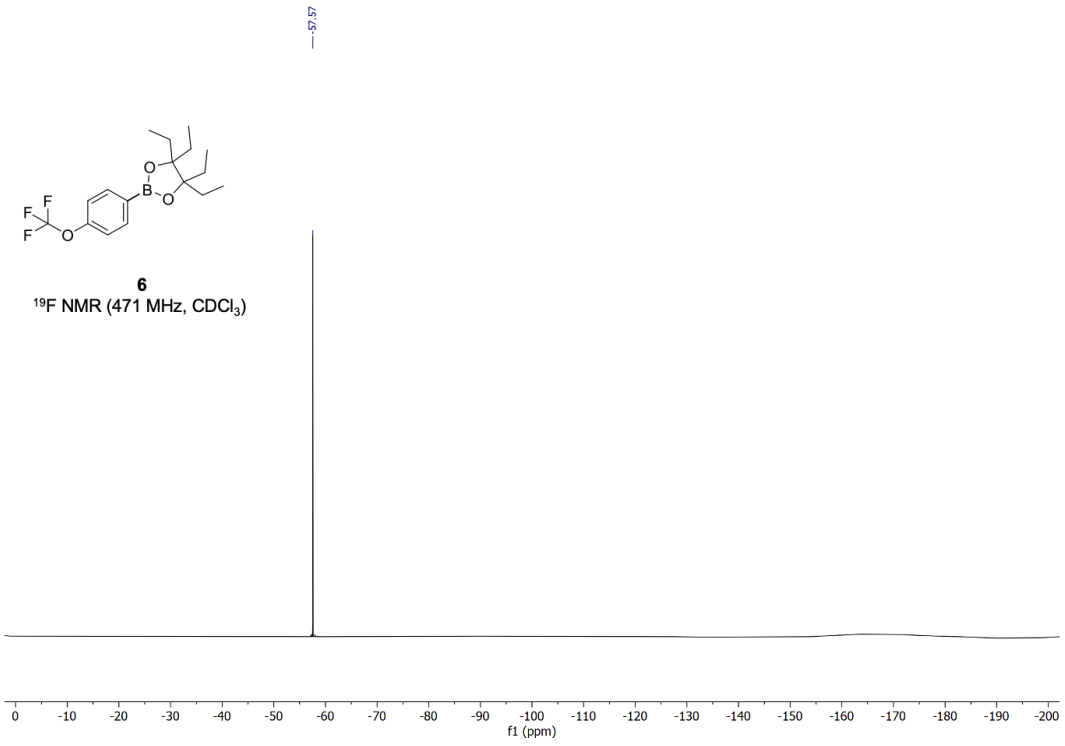


6

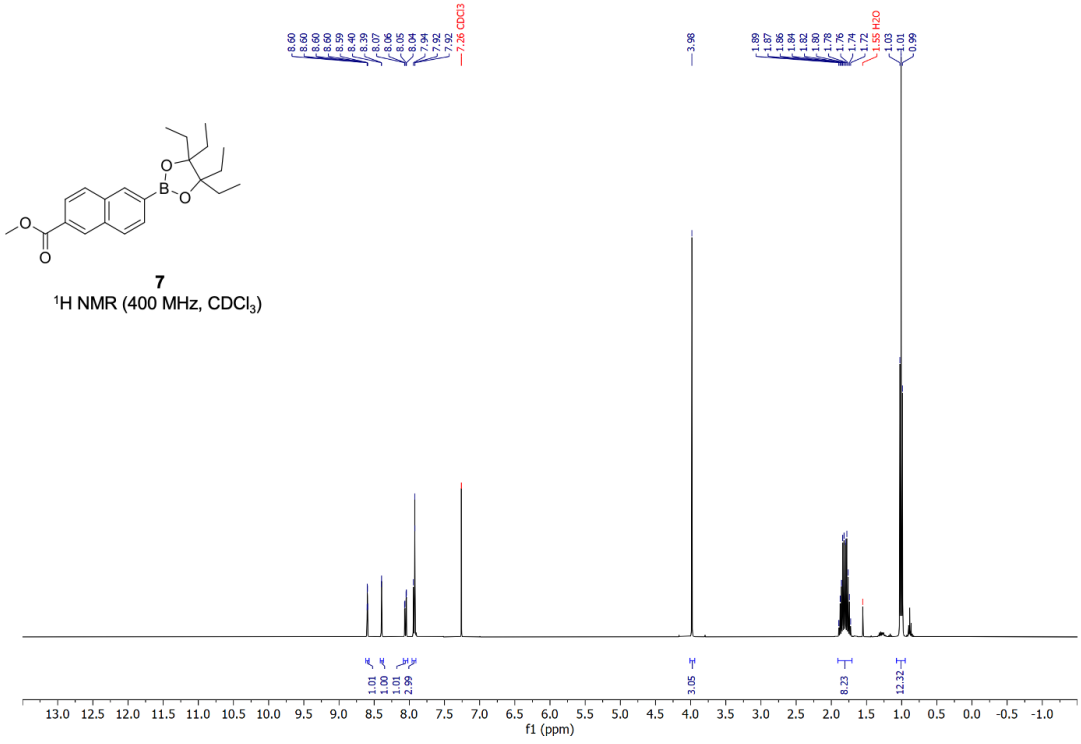
^{13}C NMR (126 MHz, $CDCl_3$)



6
^{11}B NMR (160 MHz, $CDCl_3$)

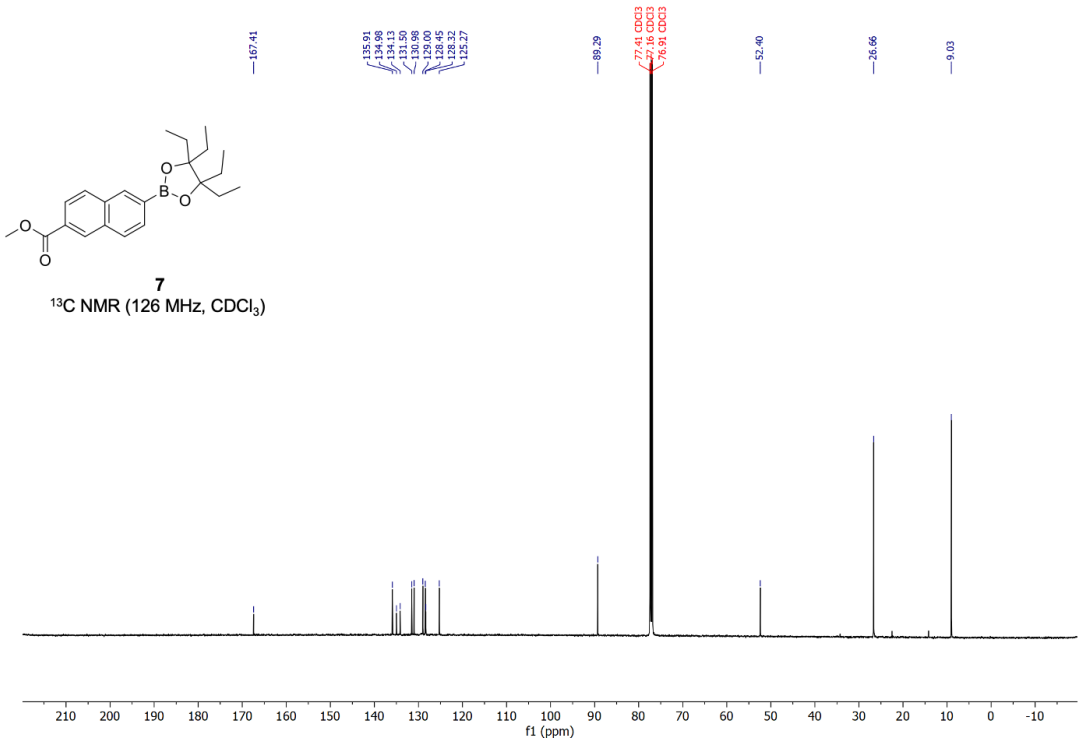


6
^{19}F NMR (471 MHz, $CDCl_3$)



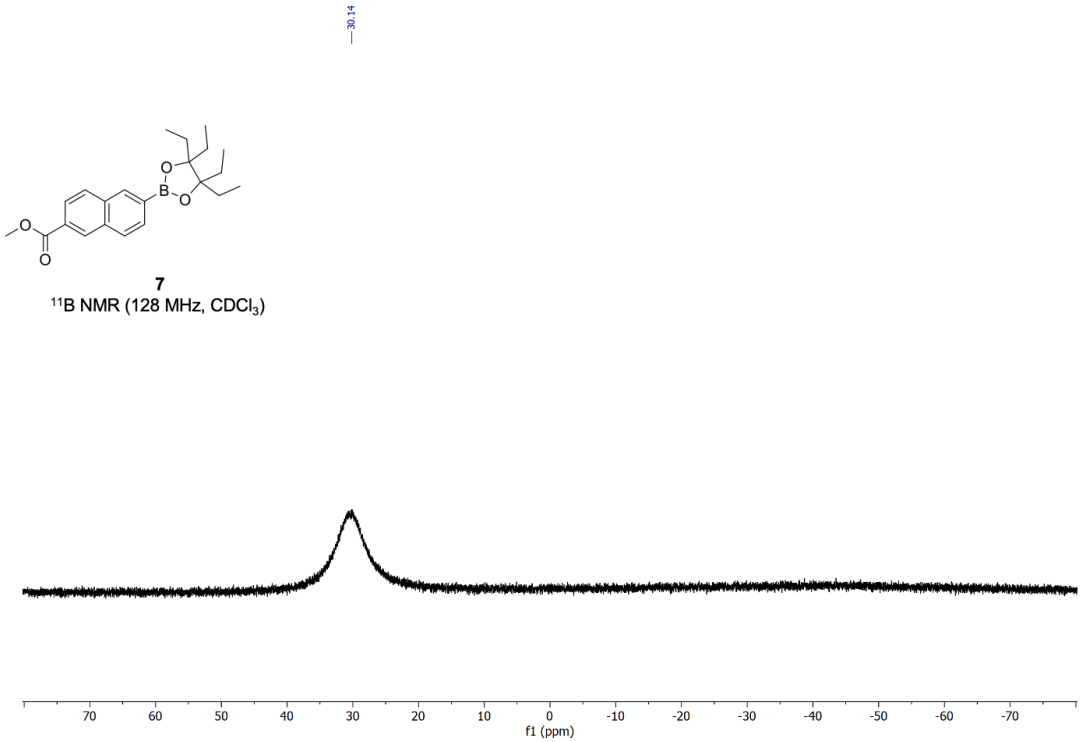
7

^{1}H NMR (400 MHz, $CDCl_3$)

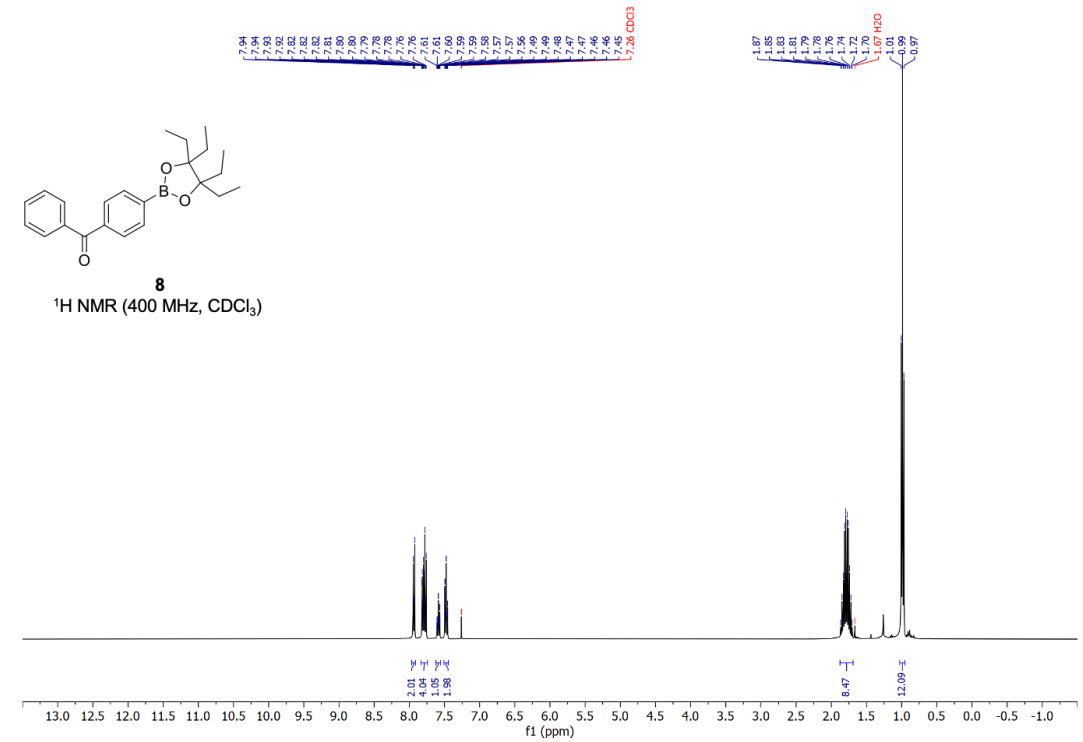


7

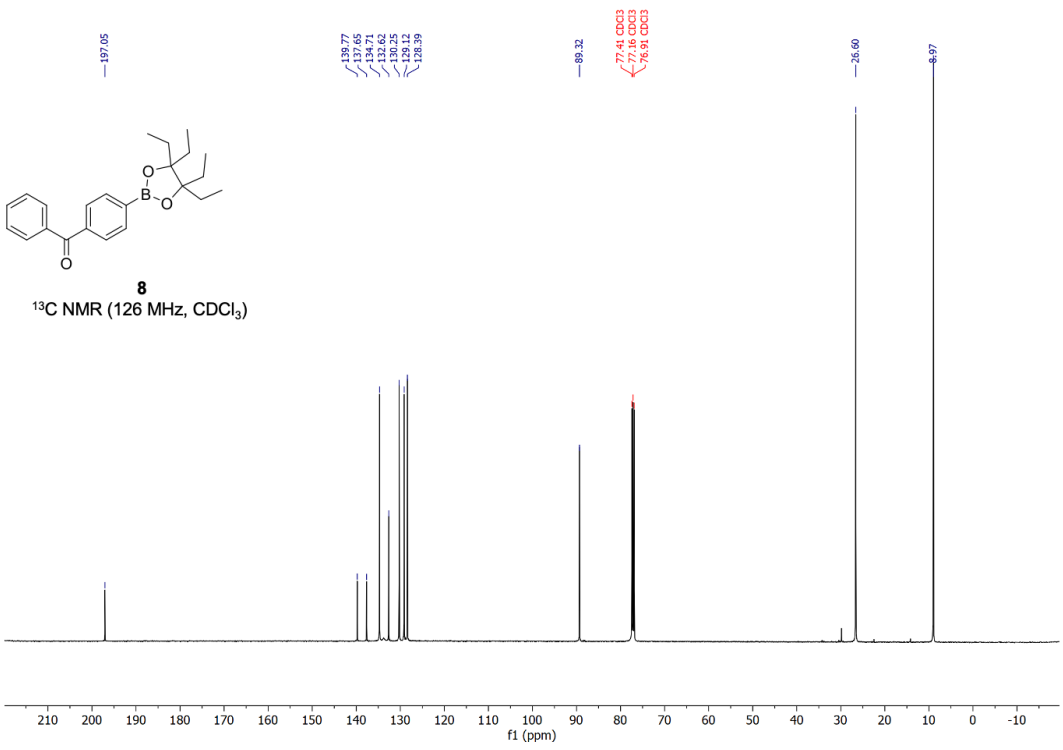
^{13}C NMR (126 MHz, $CDCl_3$)



7
^{11}B NMR (128 MHz, $CDCl_3$)

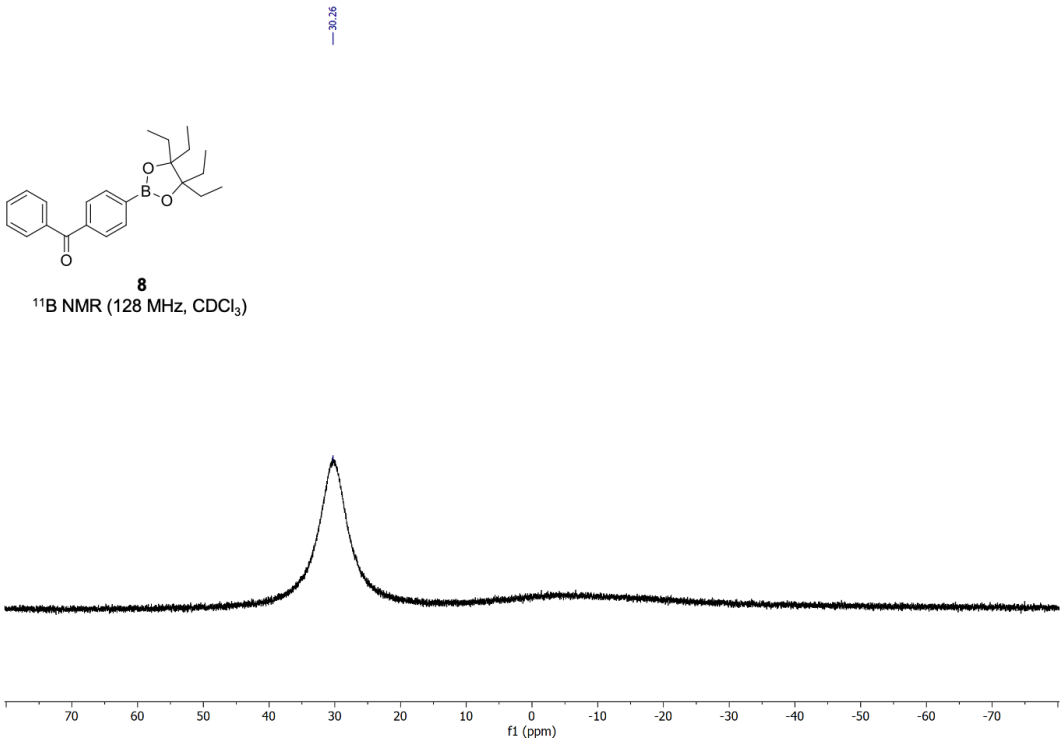


8
^{1}H NMR (400 MHz, $CDCl_3$)



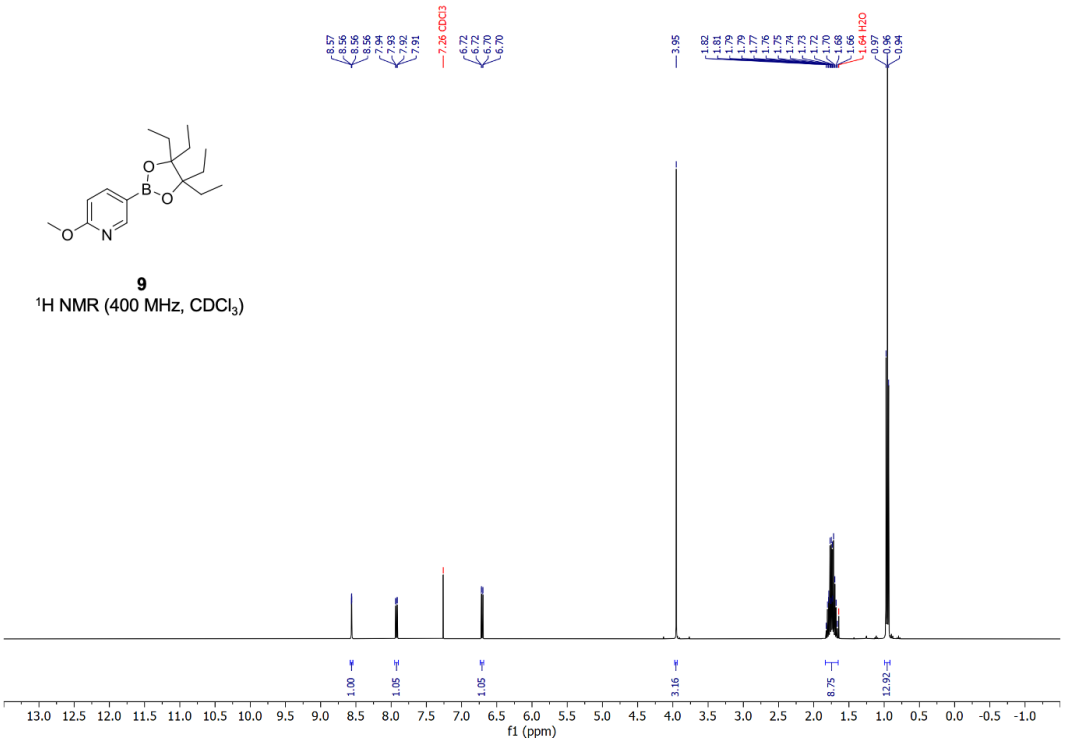
8

^{13}C NMR (126 MHz, $CDCl_3$)

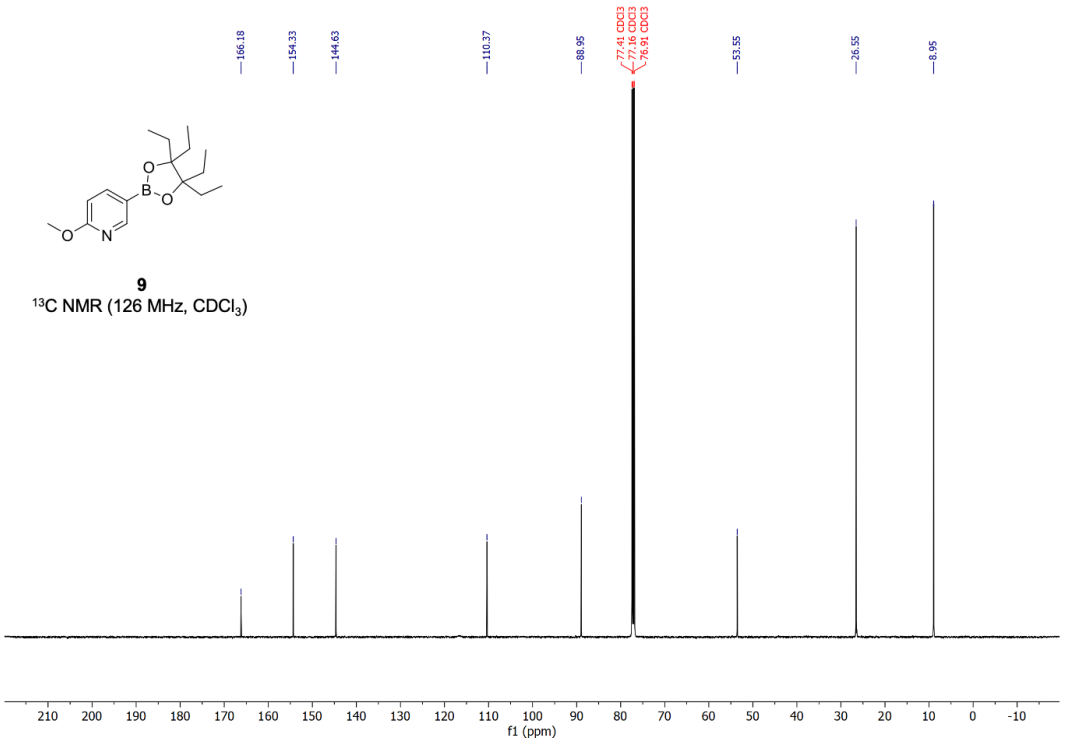


8

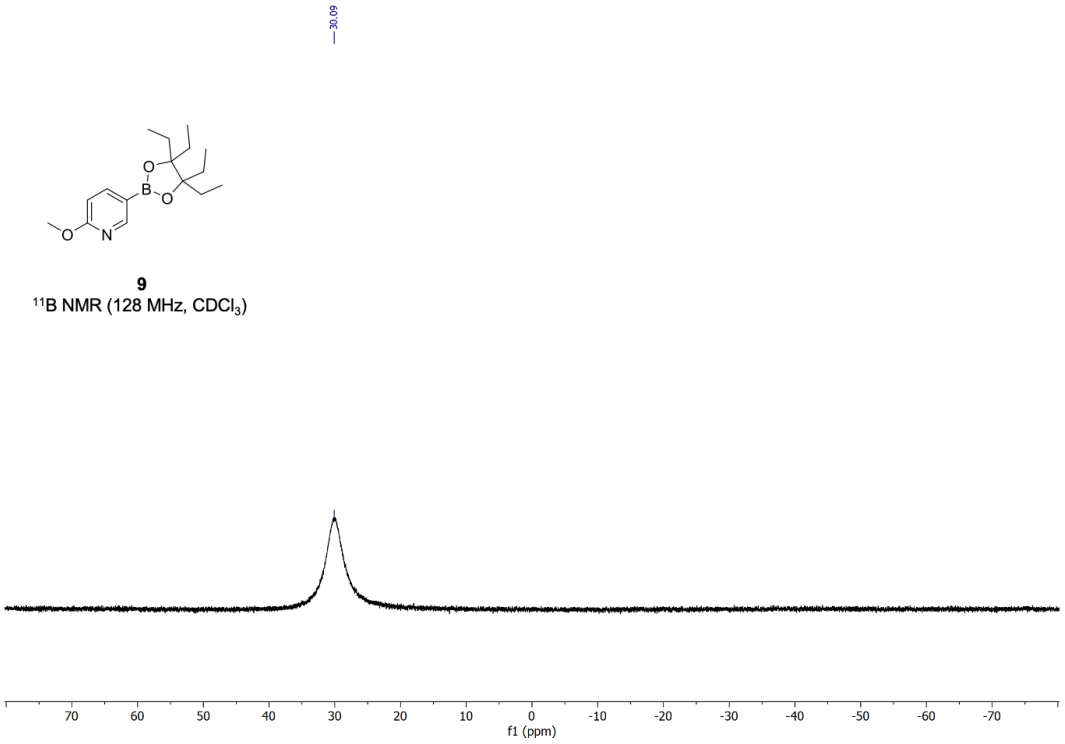
^{11}B NMR (128 MHz, $CDCl_3$)



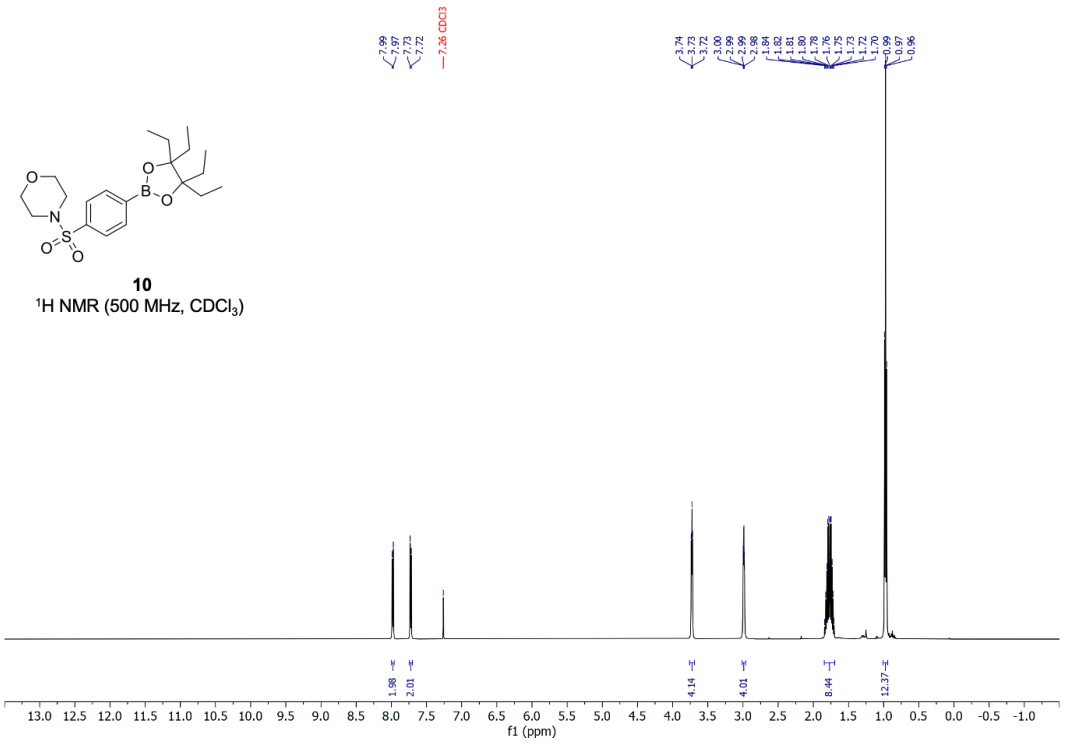
9
^{1}H NMR (400 MHz, $CDCl_3$)



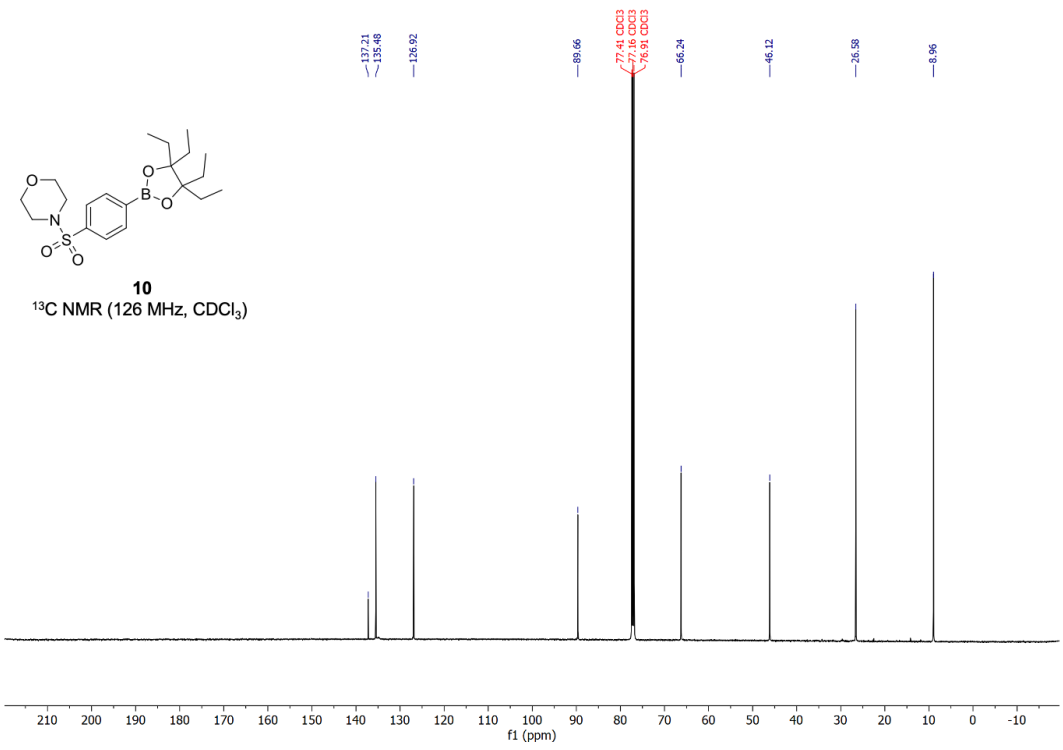
9
^{13}C NMR (126 MHz, $CDCl_3$)



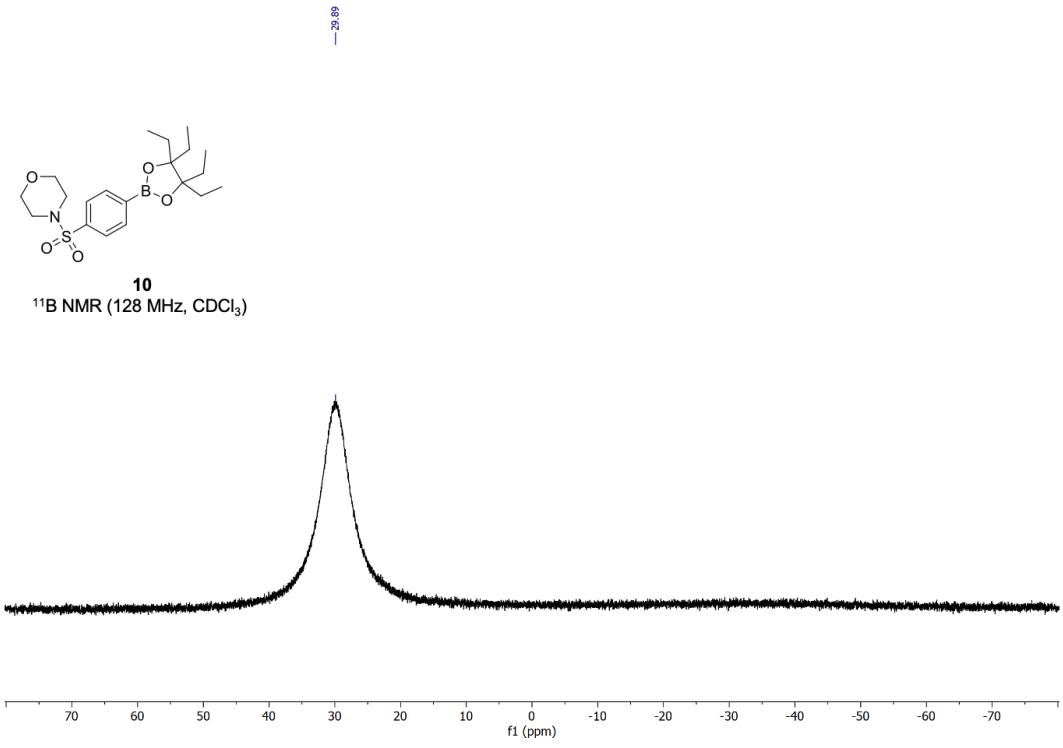
9
^{11}B NMR (128 MHz, $CDCl_3$)



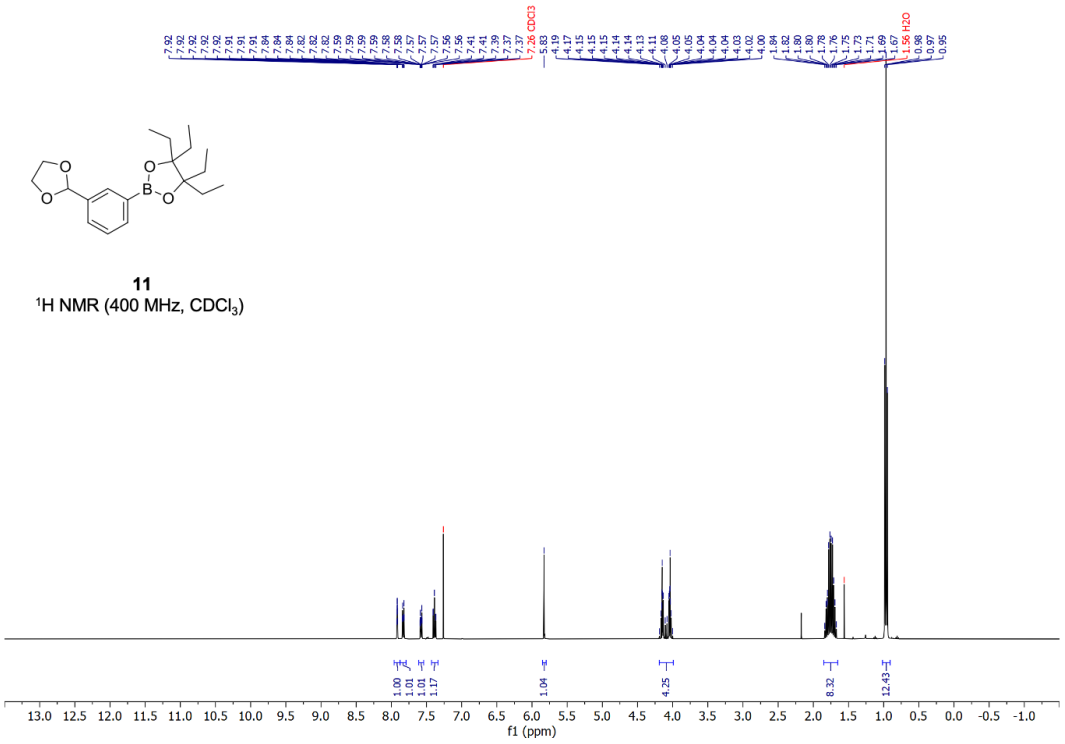
10
^{1}H NMR (500 MHz, $CDCl_3$)



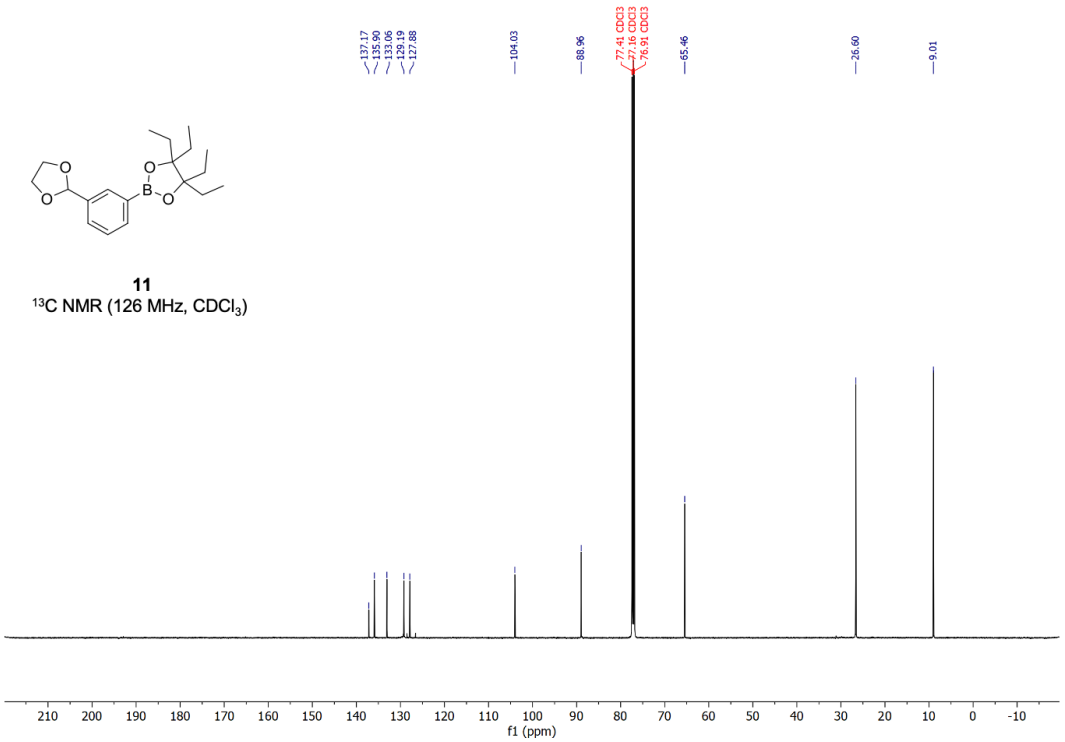
10
^{13}C NMR (126 MHz, $CDCl_3$)



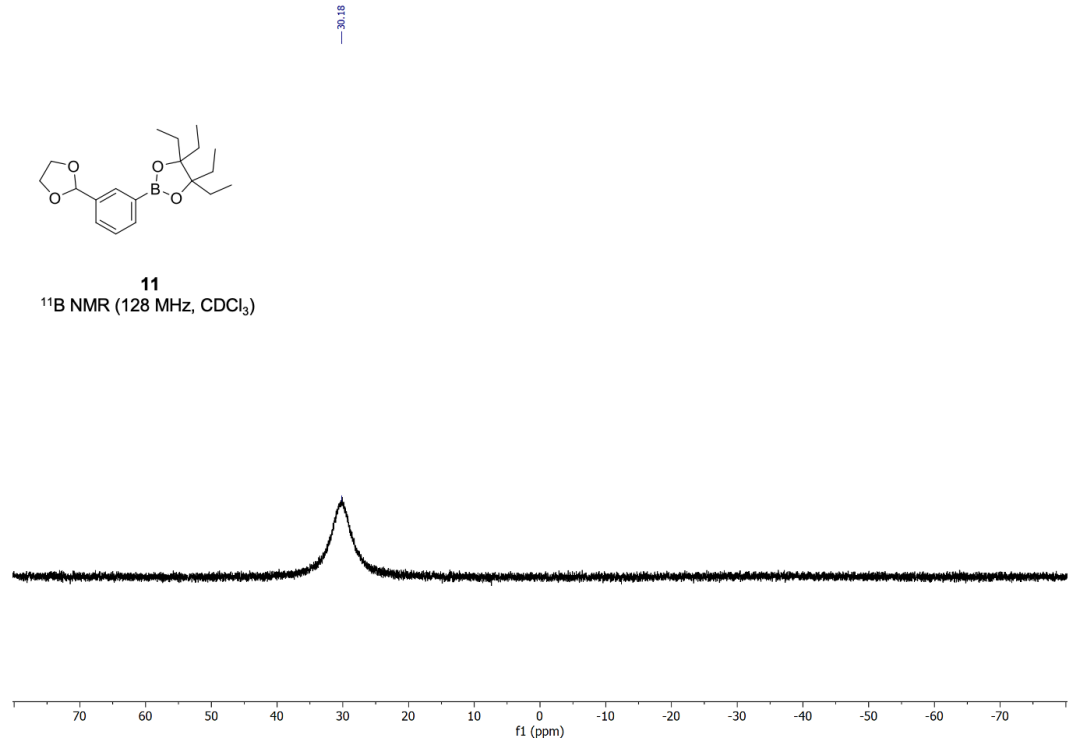
10
^{11}B NMR (128 MHz, $CDCl_3$)



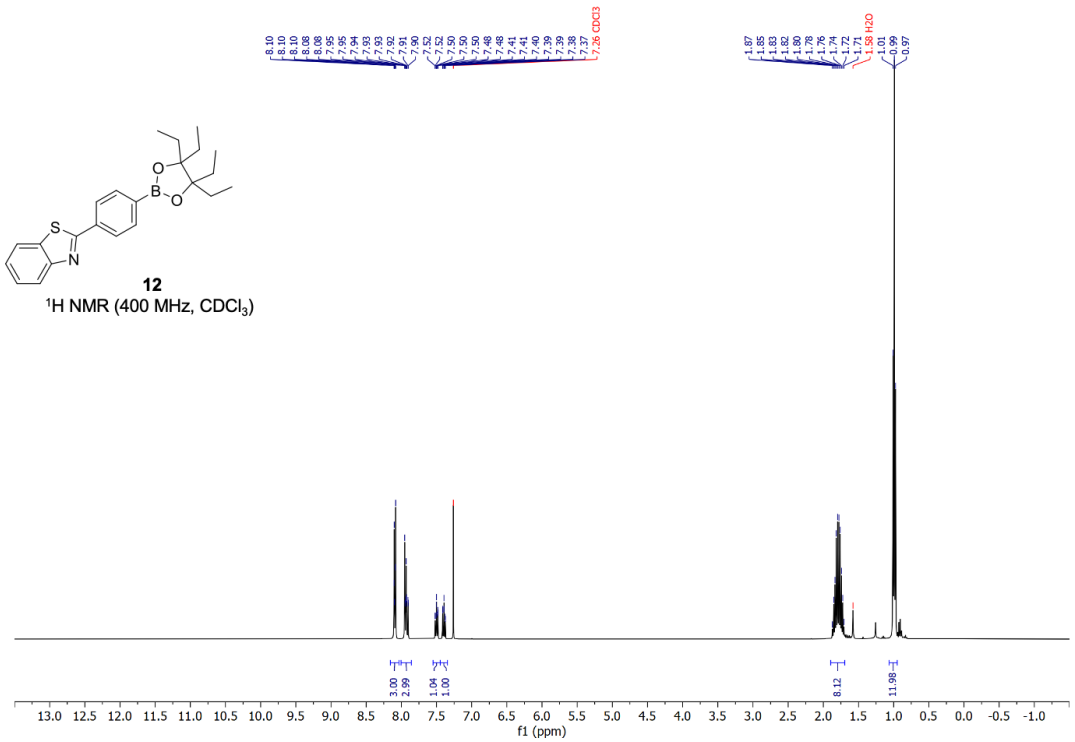
11
^{1}H NMR (400 MHz, $CDCl_3$)



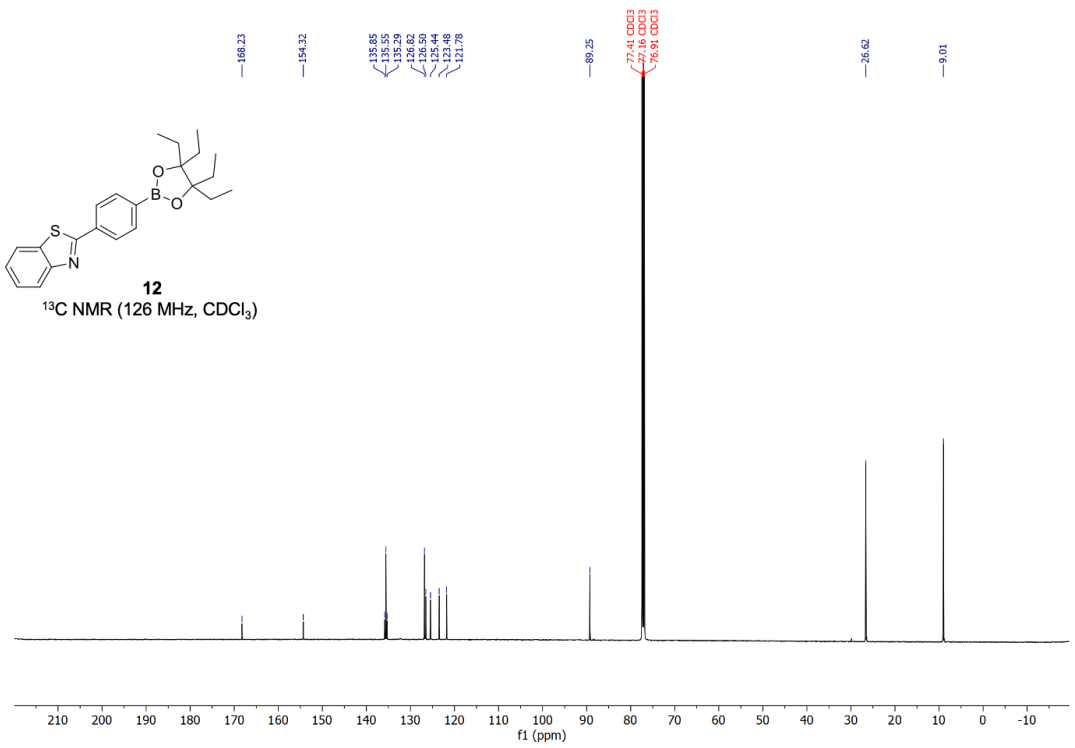
11
^{13}C NMR (126 MHz, $CDCl_3$)



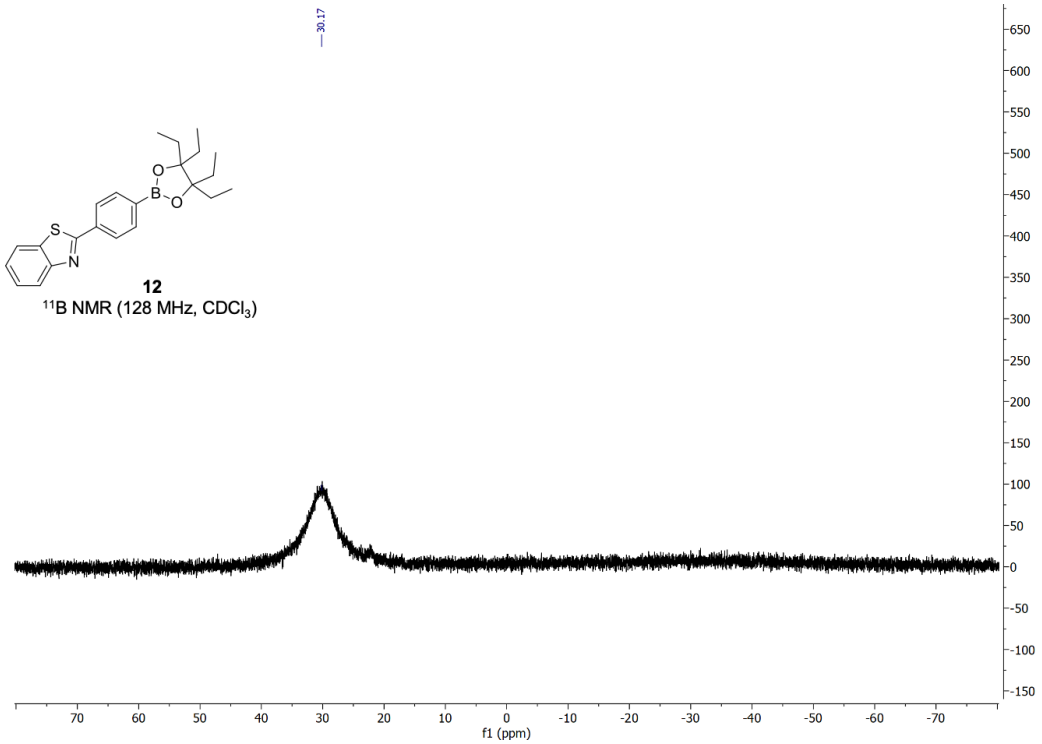
11
^{11}B NMR (128 MHz, $CDCl_3$)



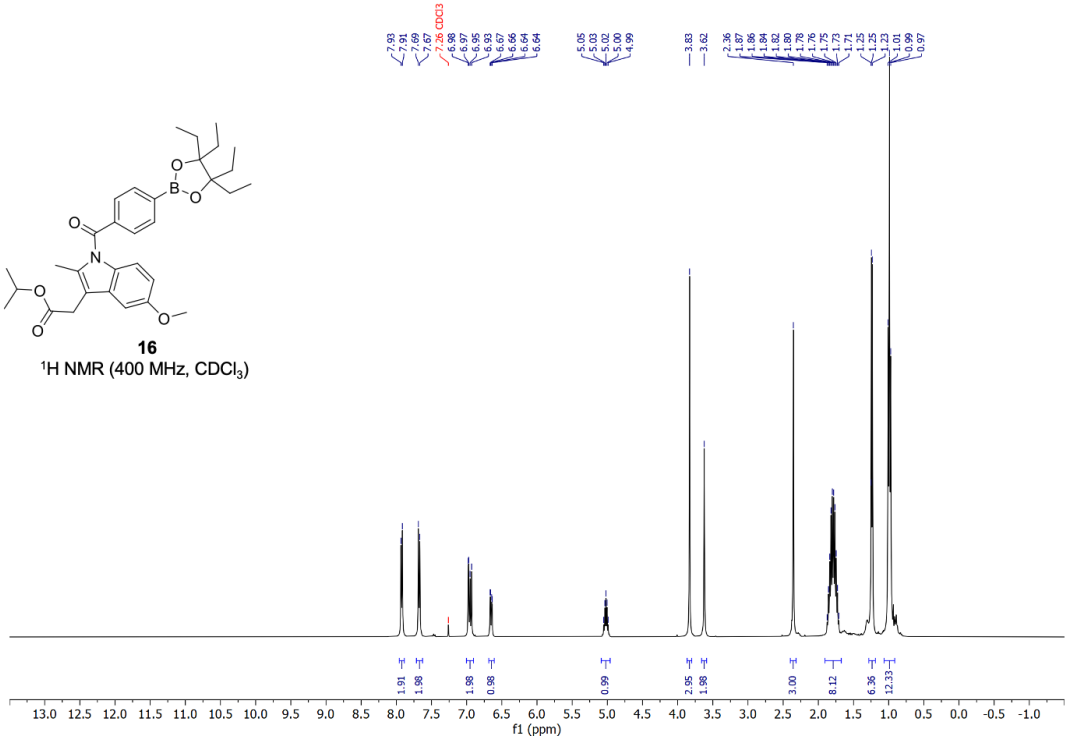
12
^{1}H NMR (400 MHz, $CDCl_3$)



12
^{13}C NMR (126 MHz, $CDCl_3$)

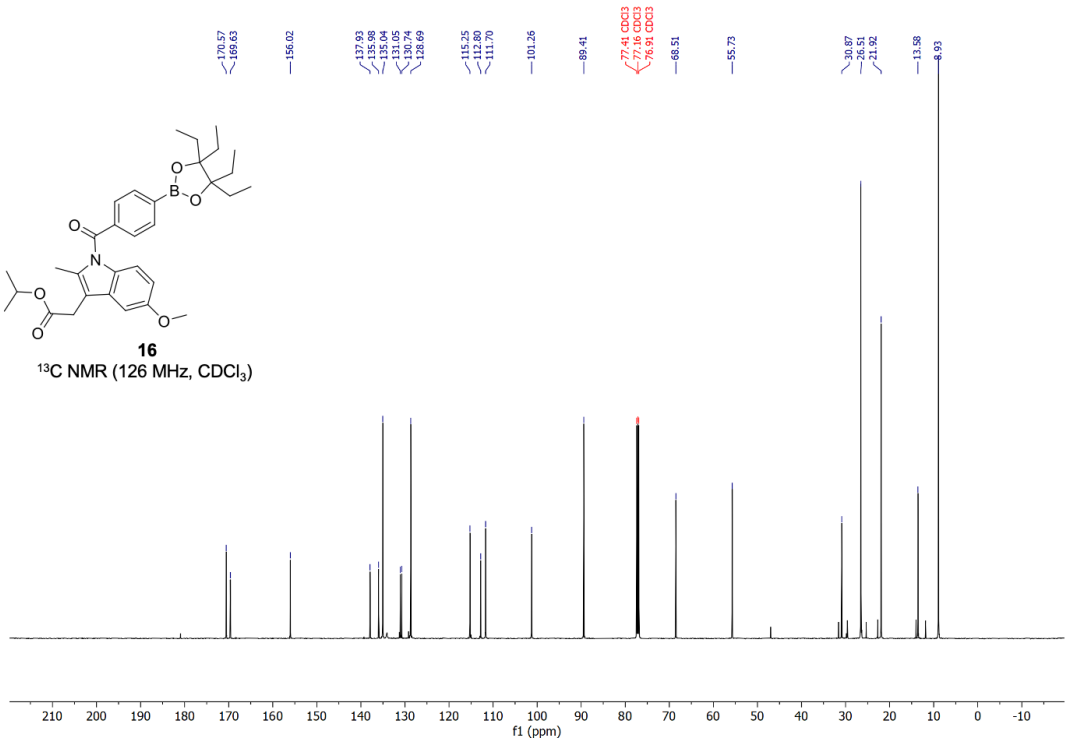


12
^{11}B NMR (128 MHz, $CDCl_3$)



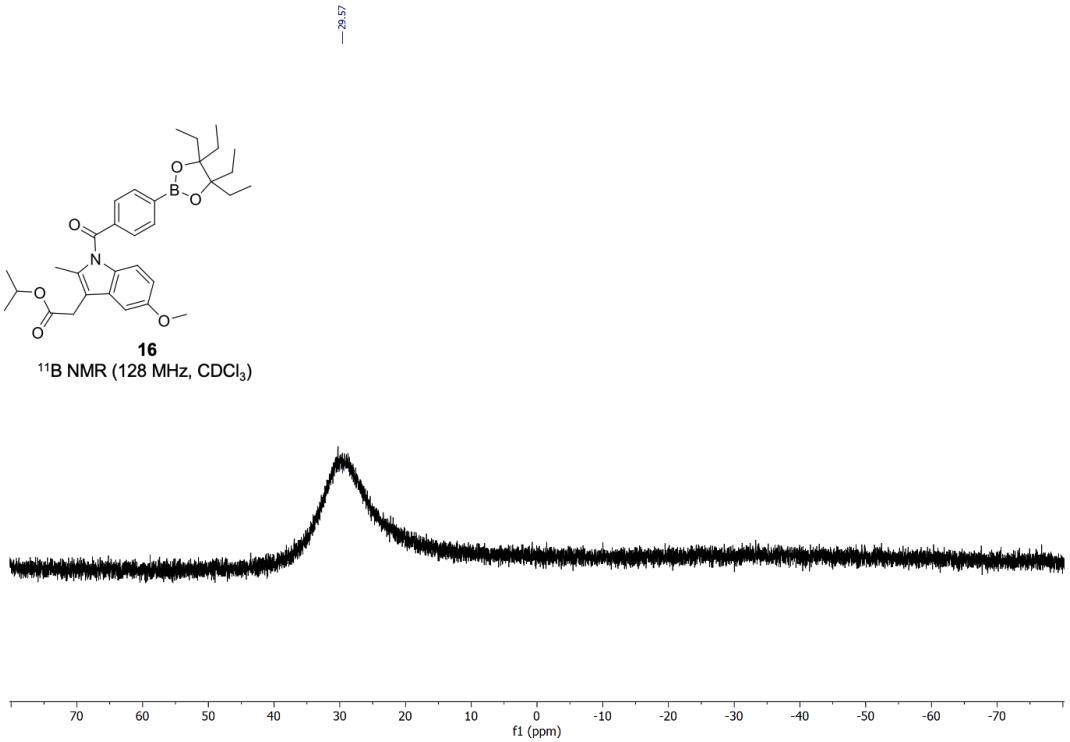
16

^{1}H NMR (400 MHz, $CDCl_3$)

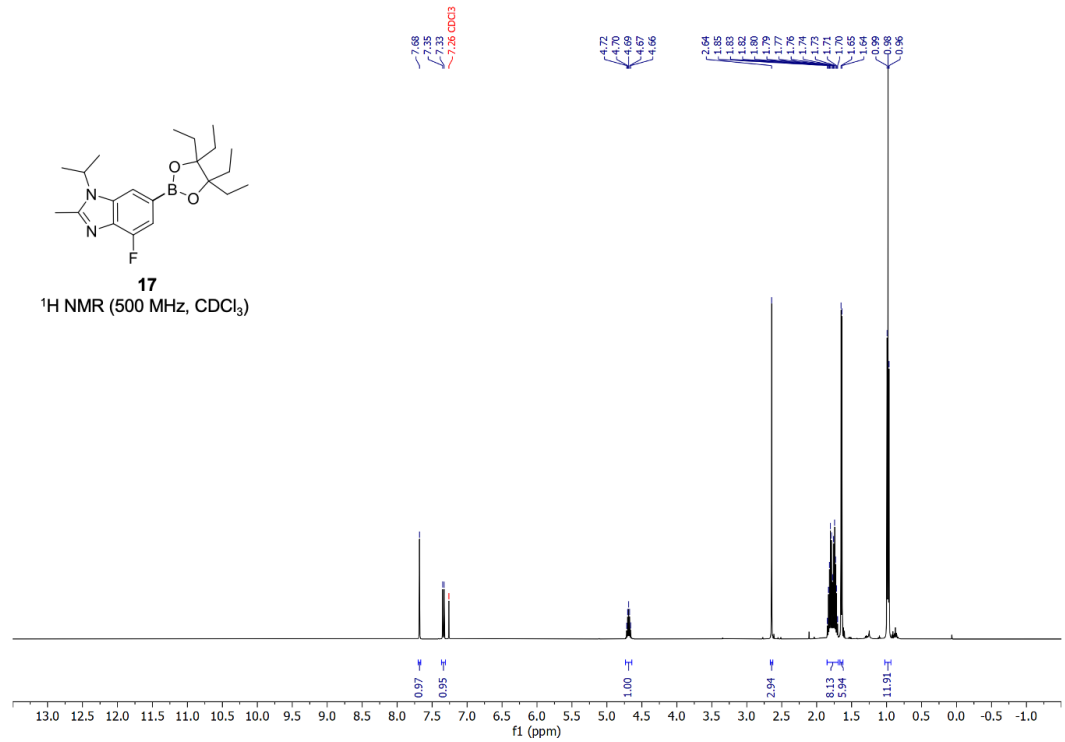


16

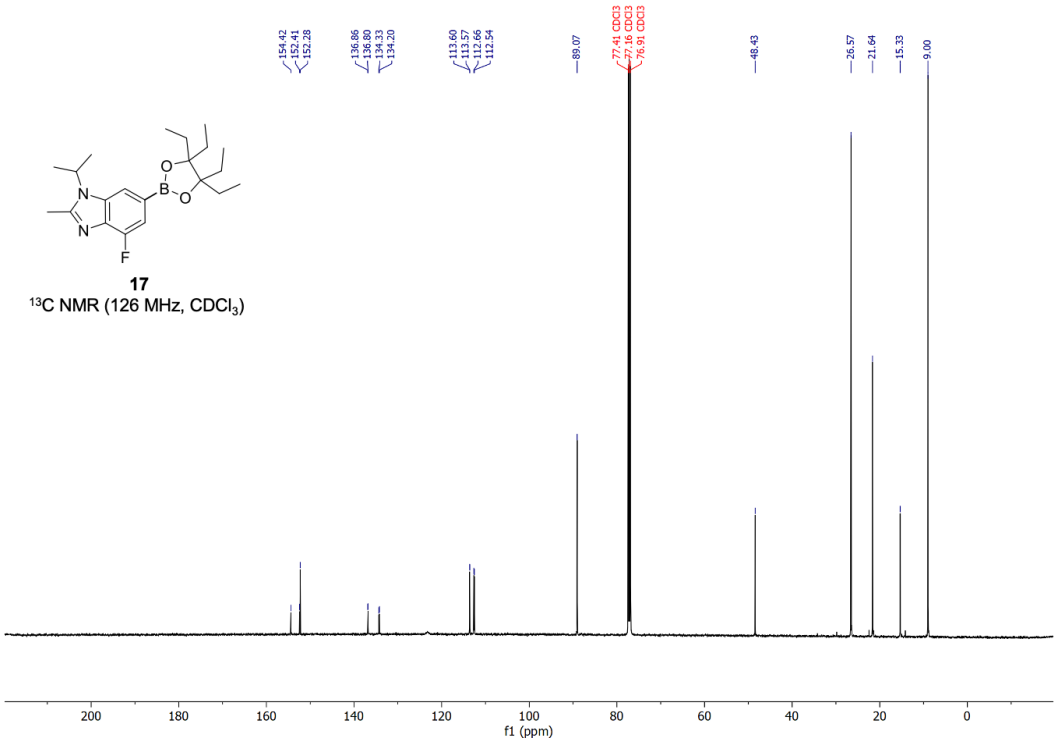
^{13}C NMR (126 MHz, $CDCl_3$)



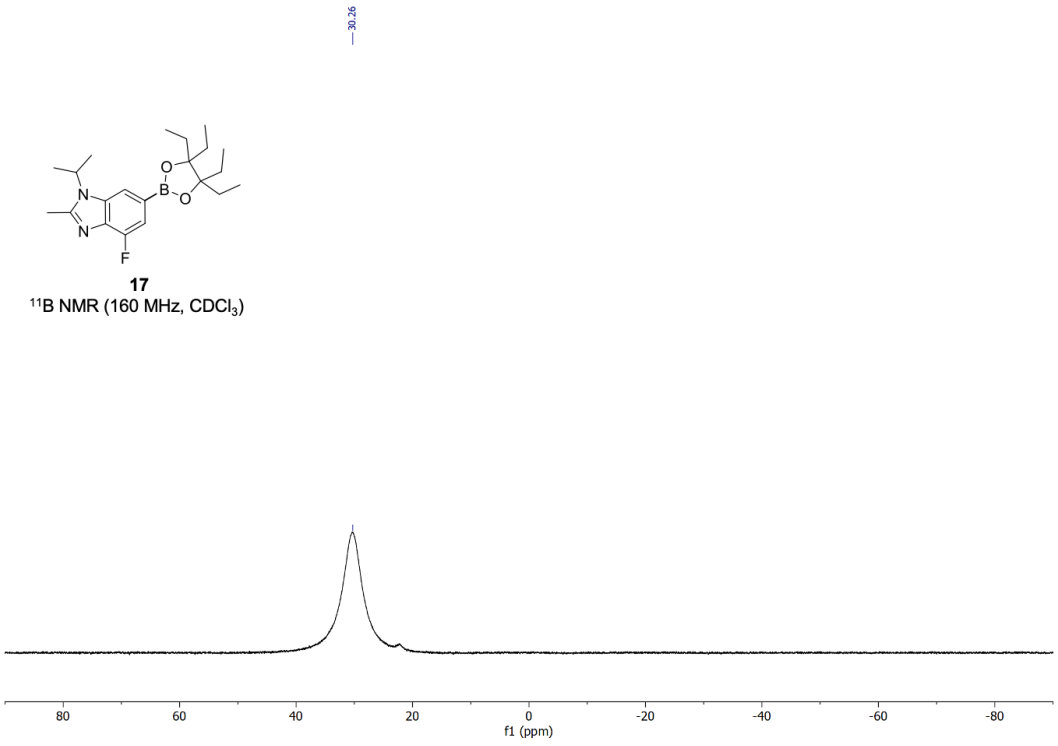
16
^{11}B NMR (128 MHz, $CDCl_3$)



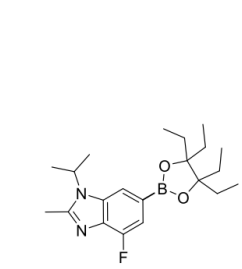
17
^{1}H NMR (500 MHz, $CDCl_3$)



17
^{13}C NMR (126 MHz, $CDCl_3$)

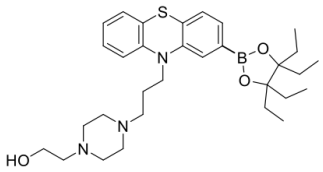


17
^{11}B NMR (160 MHz, $CDCl_3$)



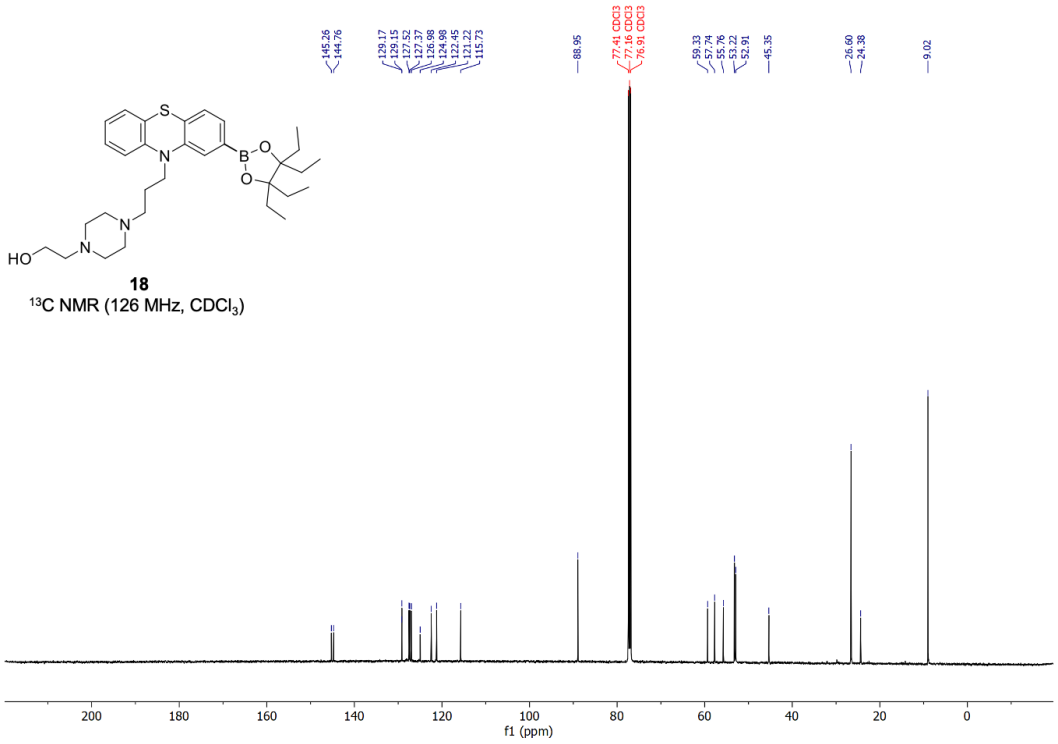
17

^{19}F NMR (471 MHz, $CDCl_3$)



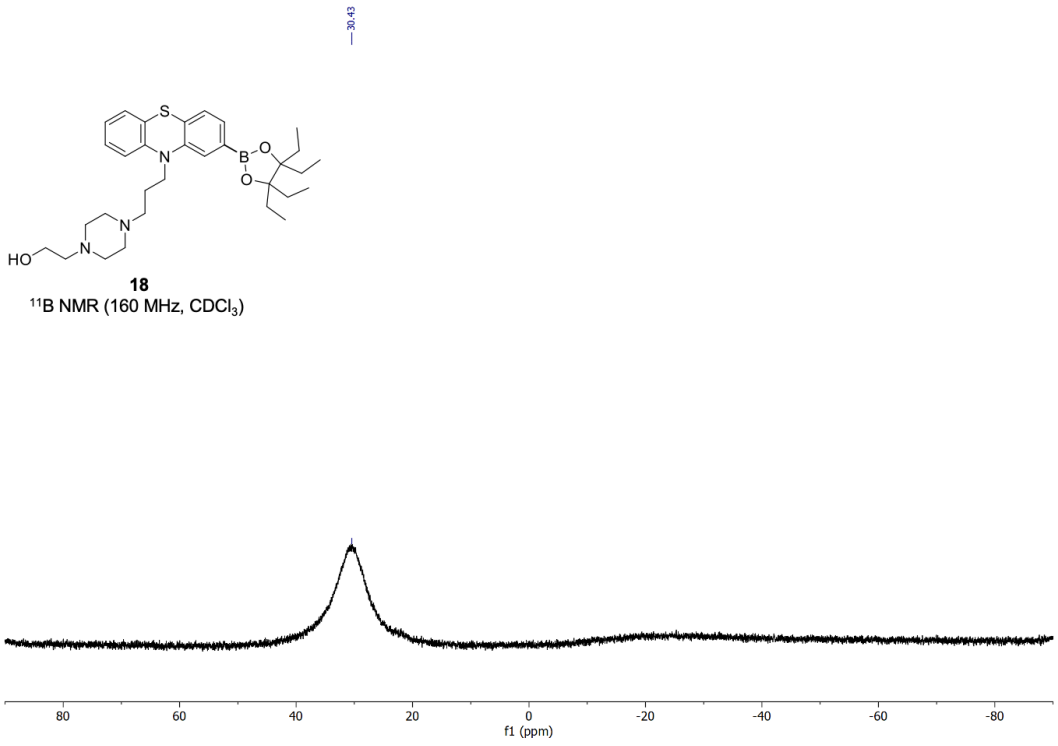
18

^{1}H NMR (500 MHz, $CDCl_3$)



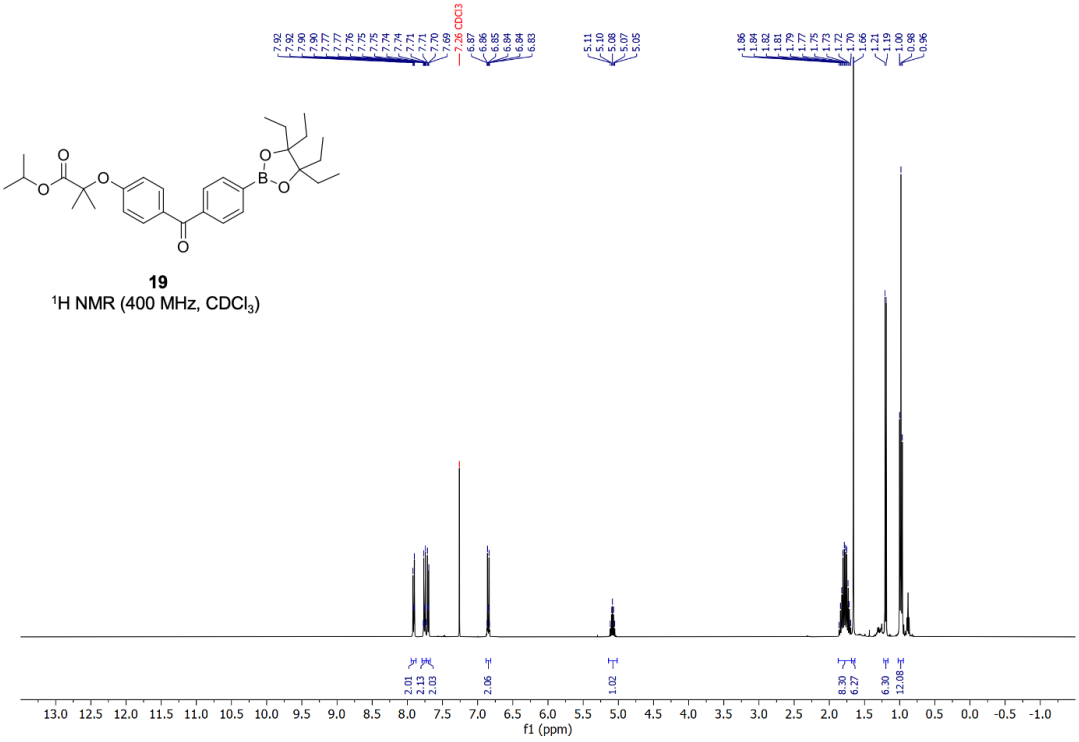
18

^{13}C NMR (126 MHz, $CDCl_3$)

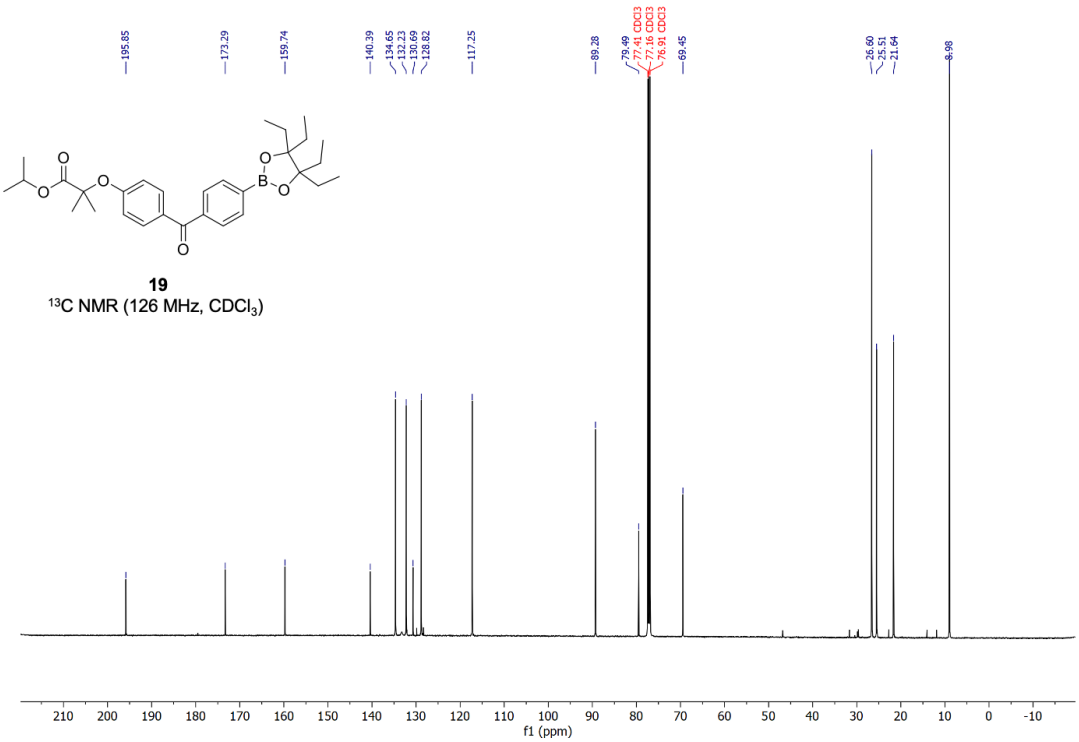


18

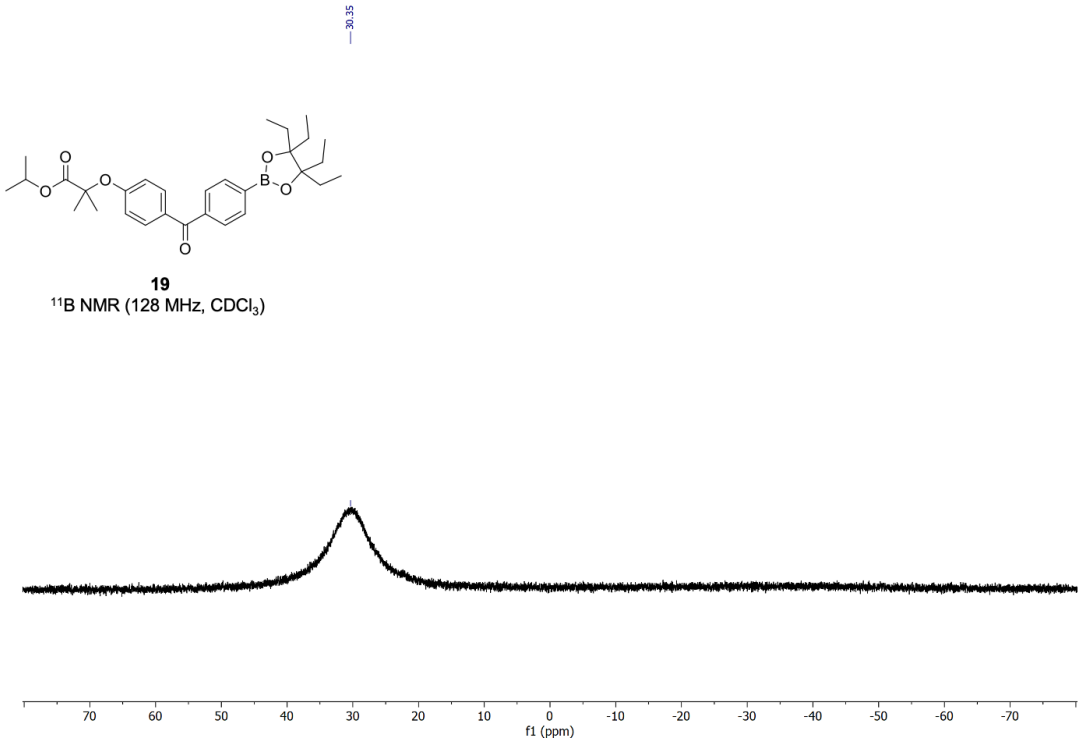
^{11}B NMR (160 MHz, $CDCl_3$)



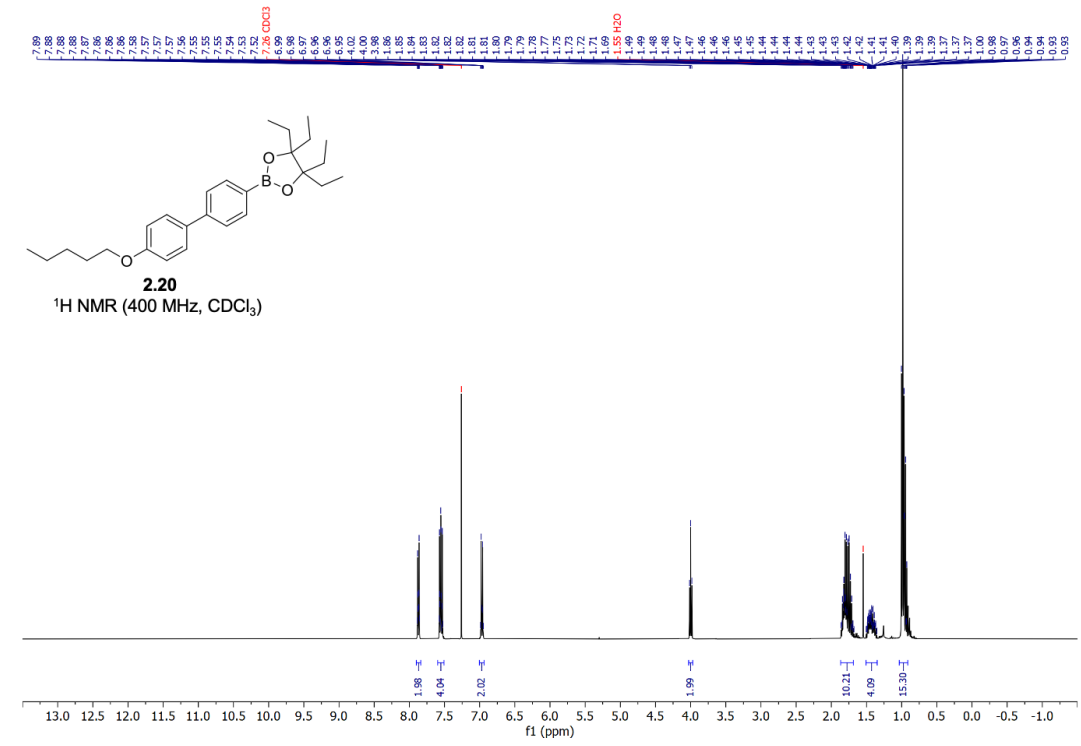
19
^{1}H NMR (400 MHz, $CDCl_3$)



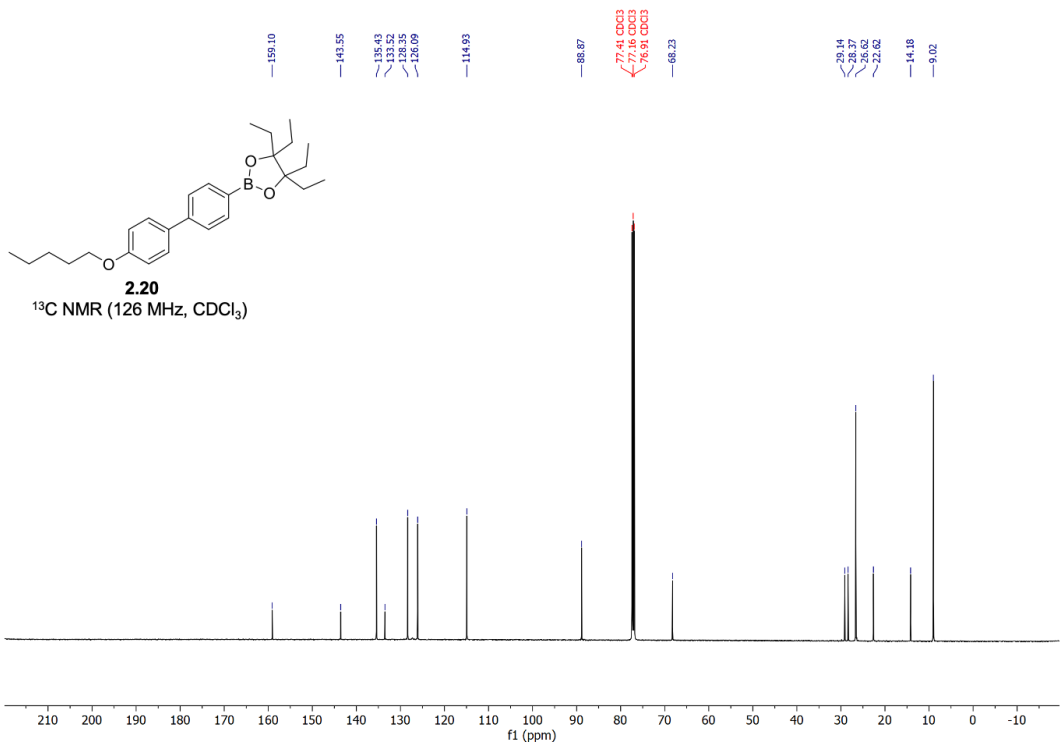
19
^{13}C NMR (126 MHz, $CDCl_3$)



19
^{11}B NMR (128 MHz, $CDCl_3$)

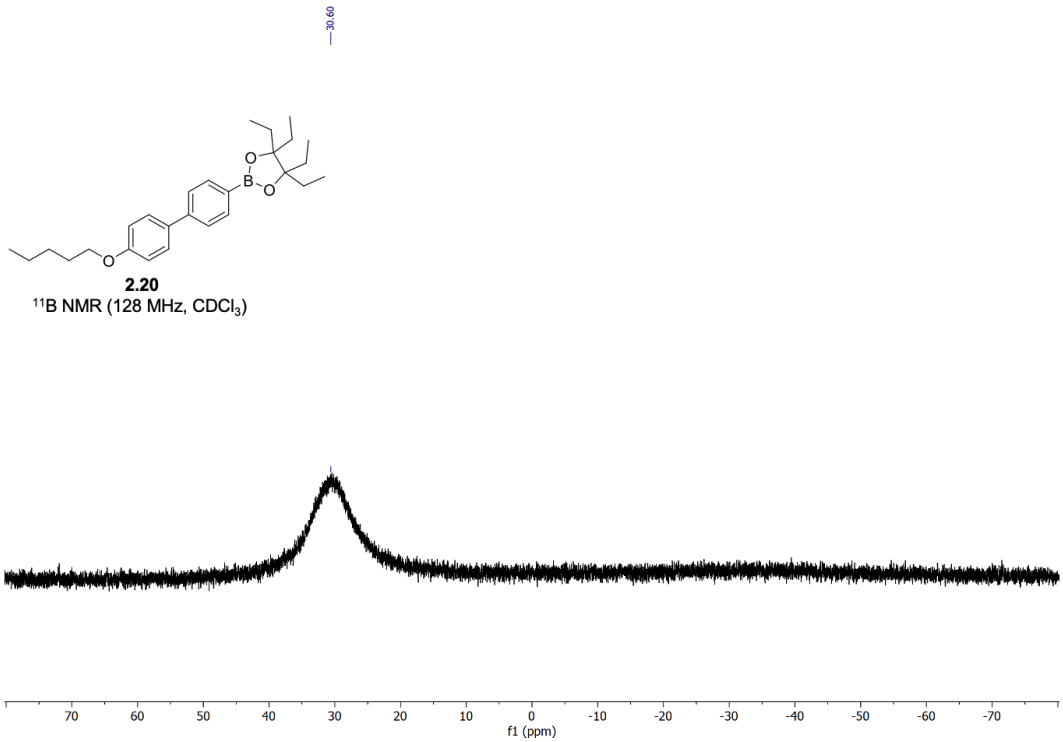


2.20
^{1}H NMR (400 MHz, $CDCl_3$)



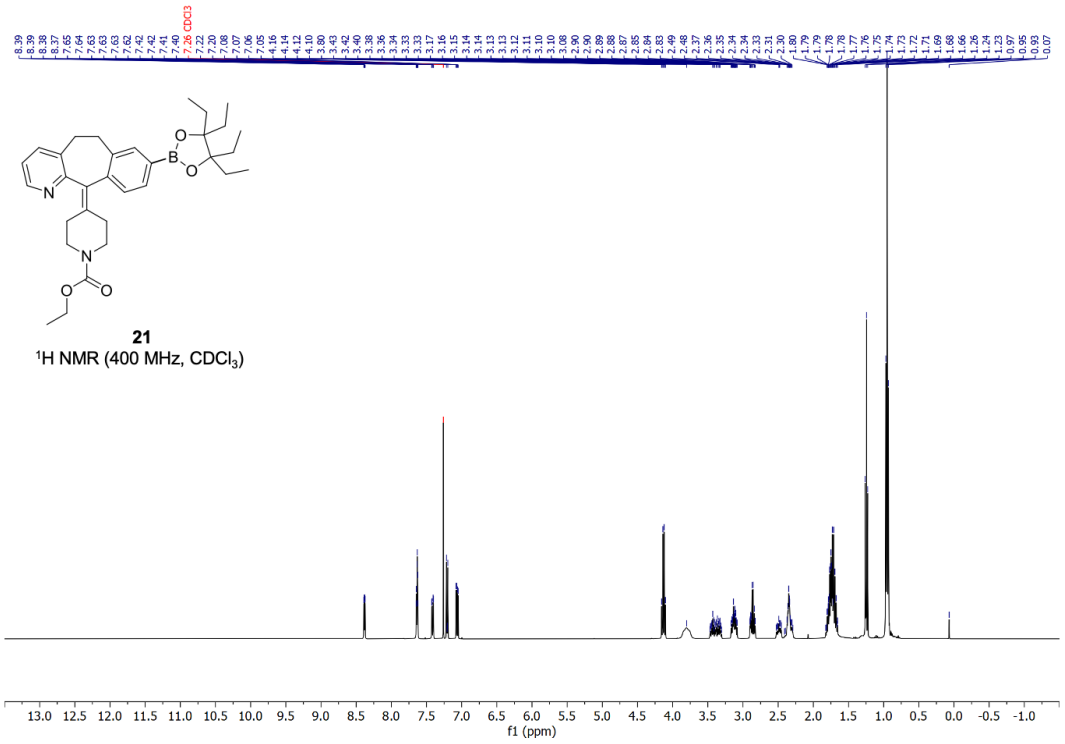
2.20

^{13}C NMR (126 MHz, $CDCl_3$)

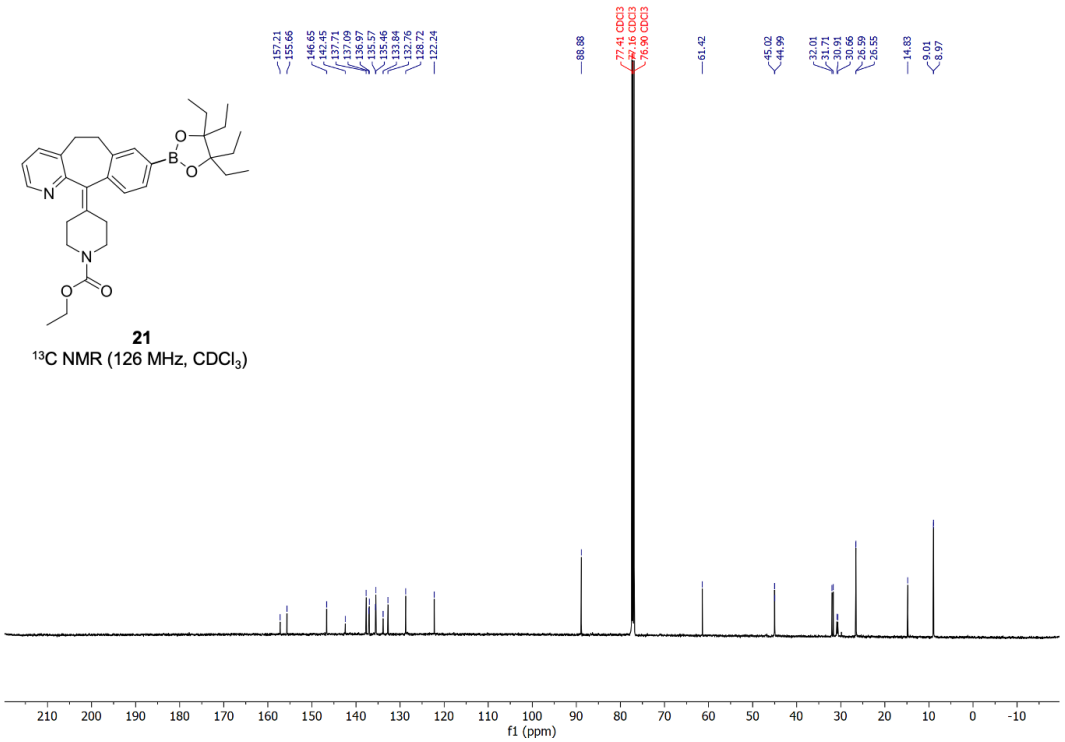


2.20

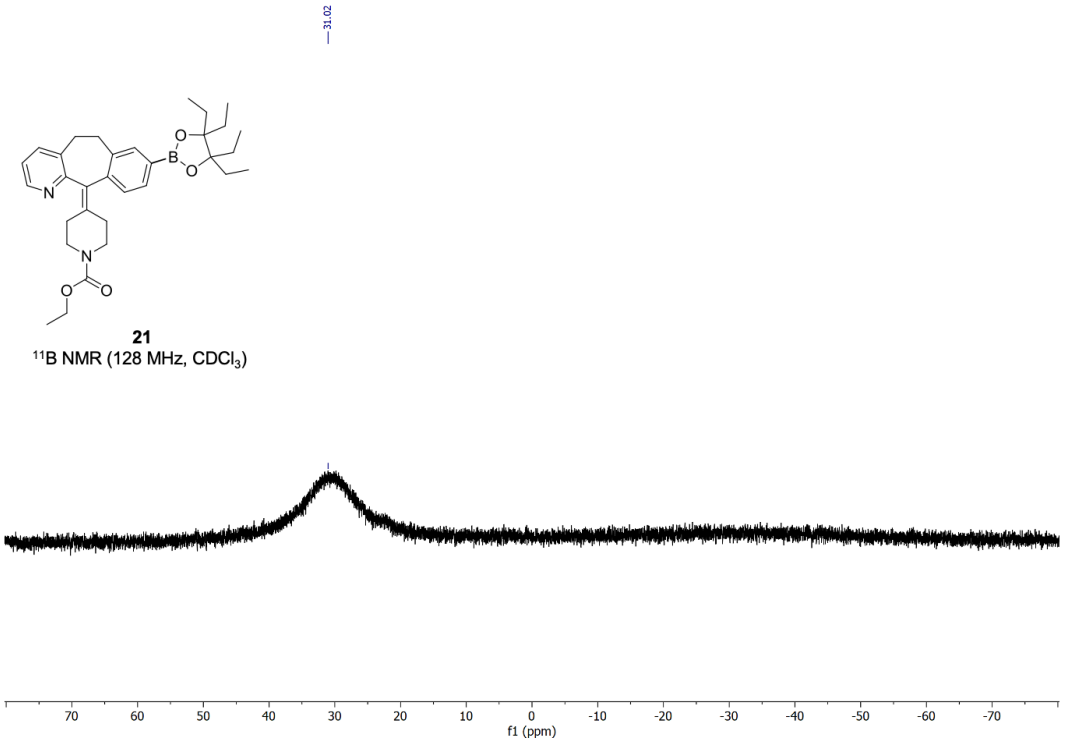
^{11}B NMR (128 MHz, $CDCl_3$)



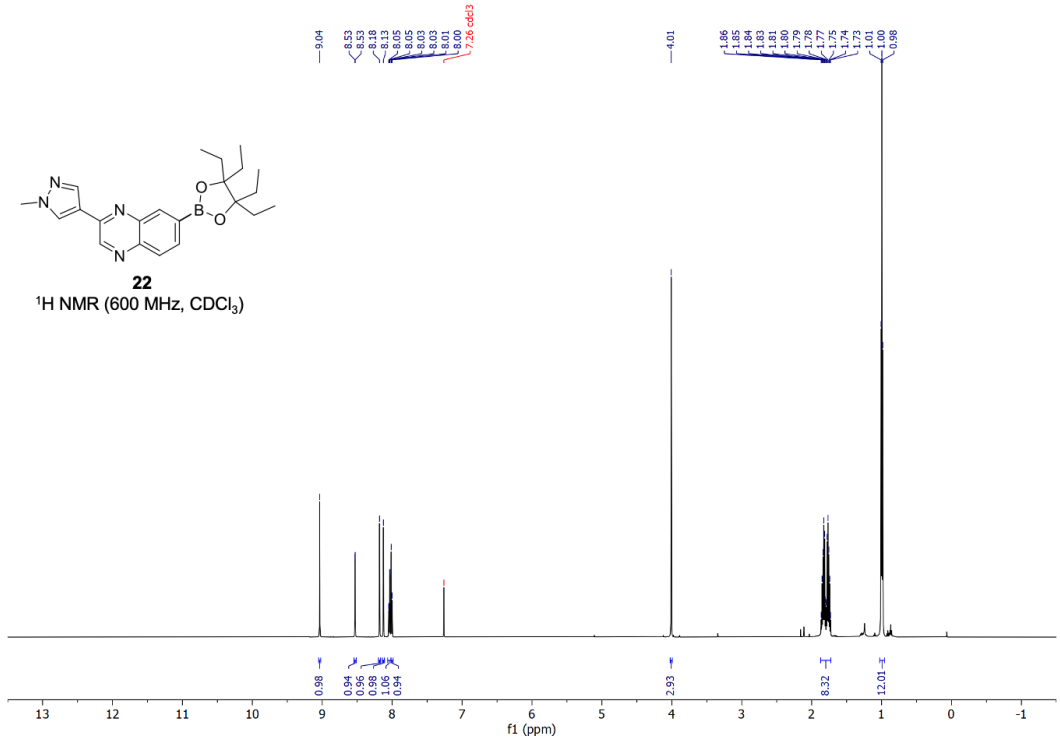
21
^{1}H NMR (400 MHz, $CDCl_3$)



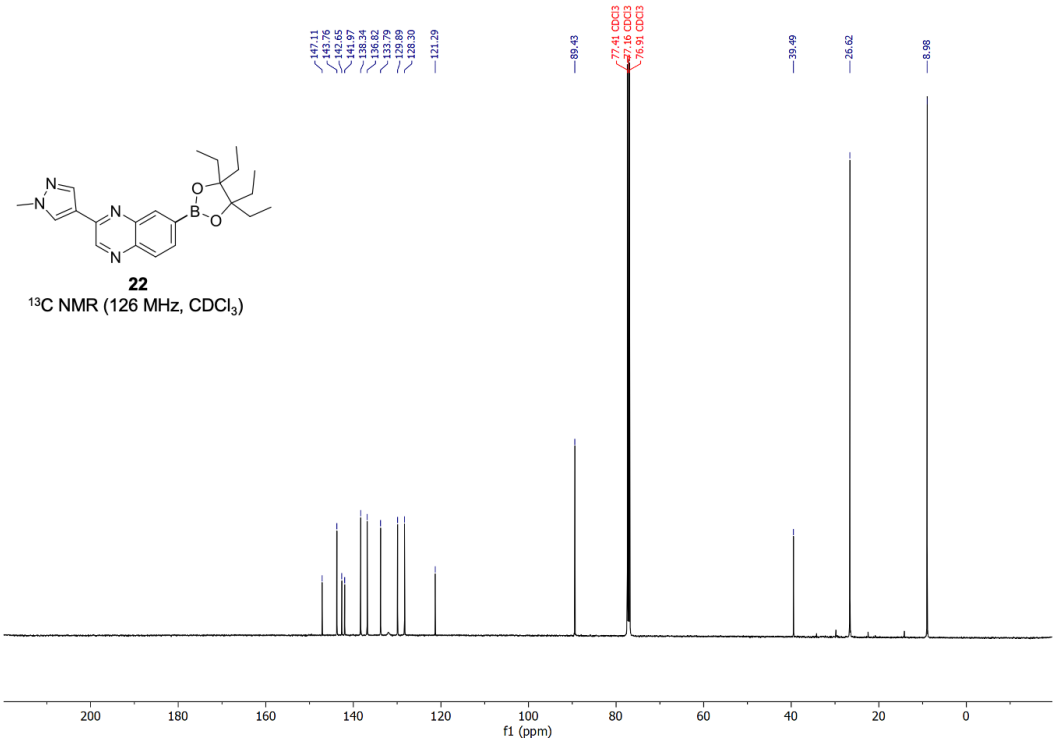
21
^{13}C NMR (126 MHz, $CDCl_3$)



21
^{11}B NMR (128 MHz, $CDCl_3$)

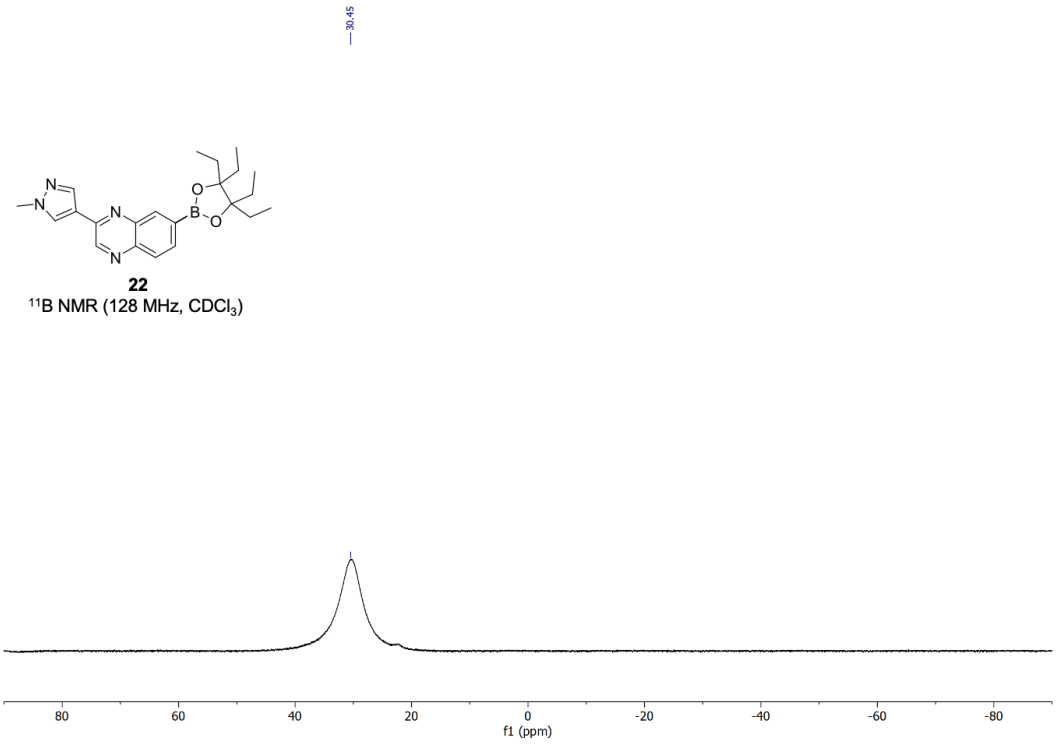


22
^{1}H NMR (600 MHz, $CDCl_3$)



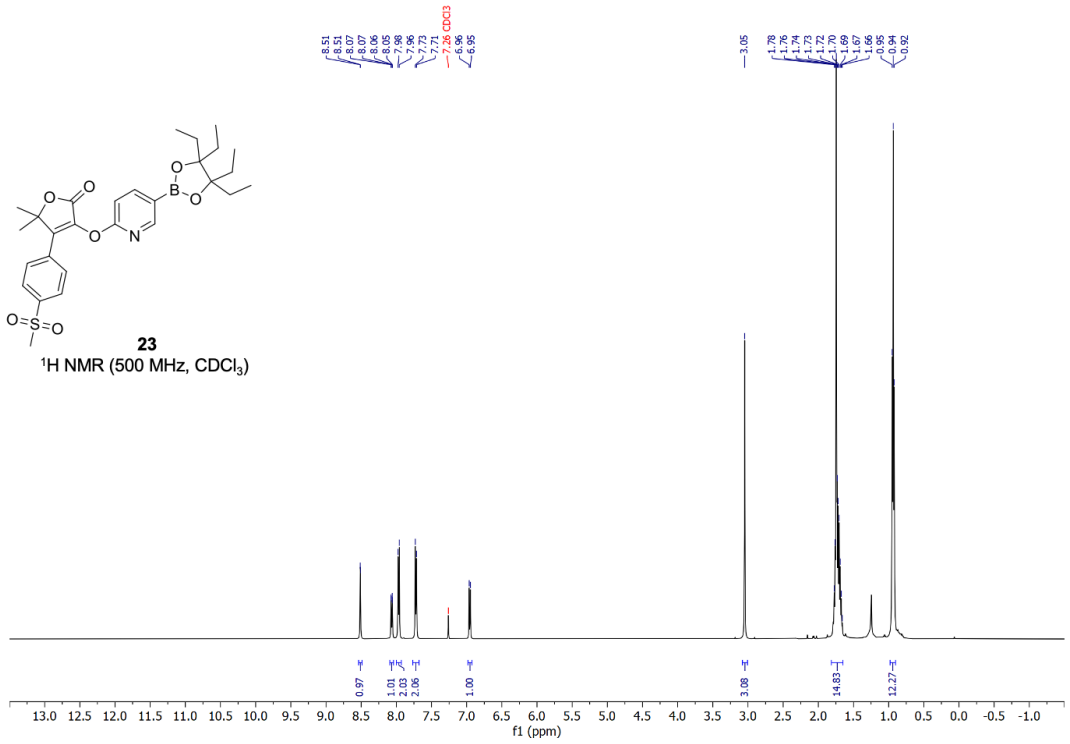
22

^{13}C NMR (126 MHz, $CDCl_3$)



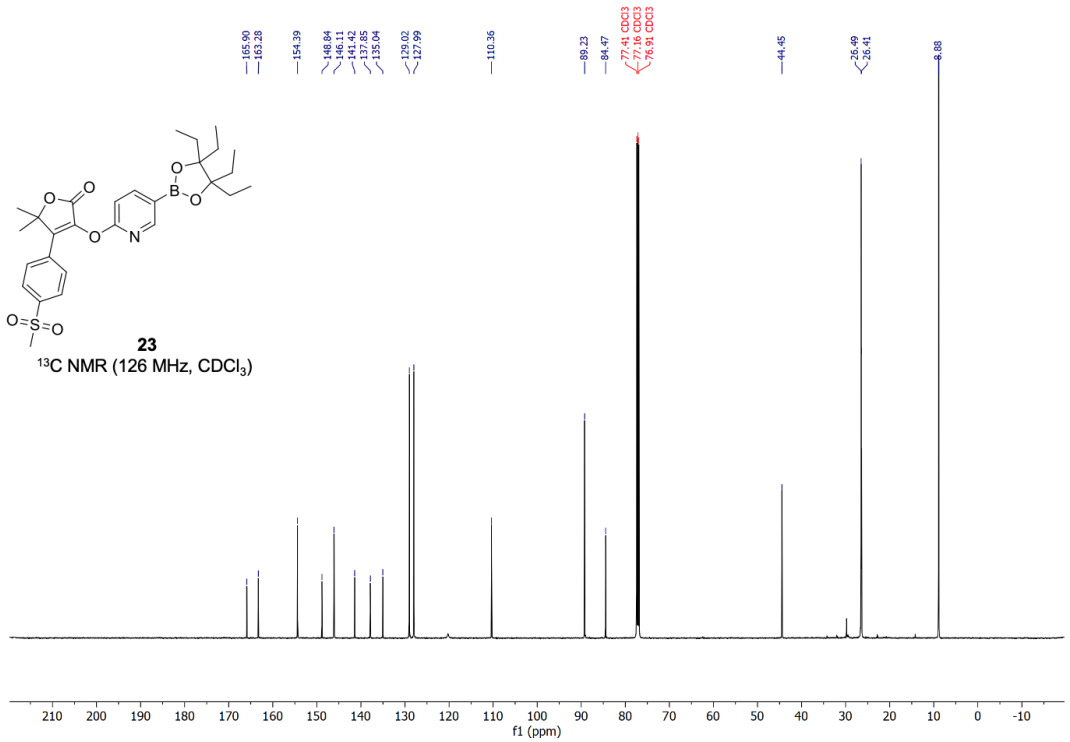
22

^{11}B NMR (128 MHz, $CDCl_3$)



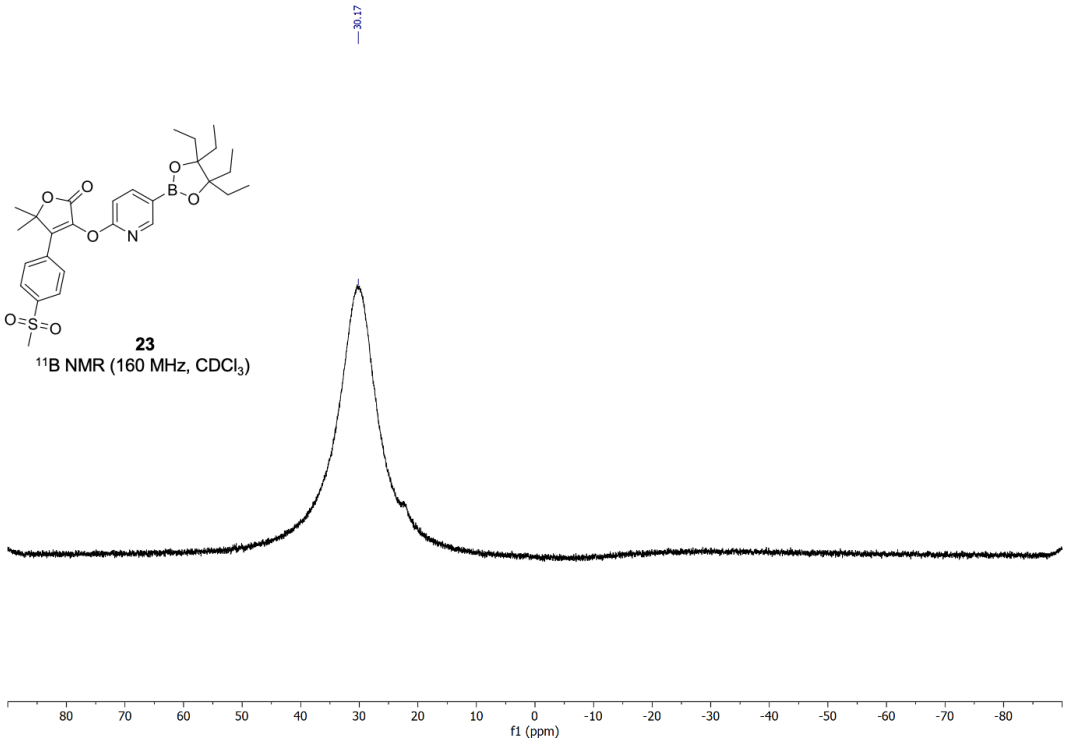
23

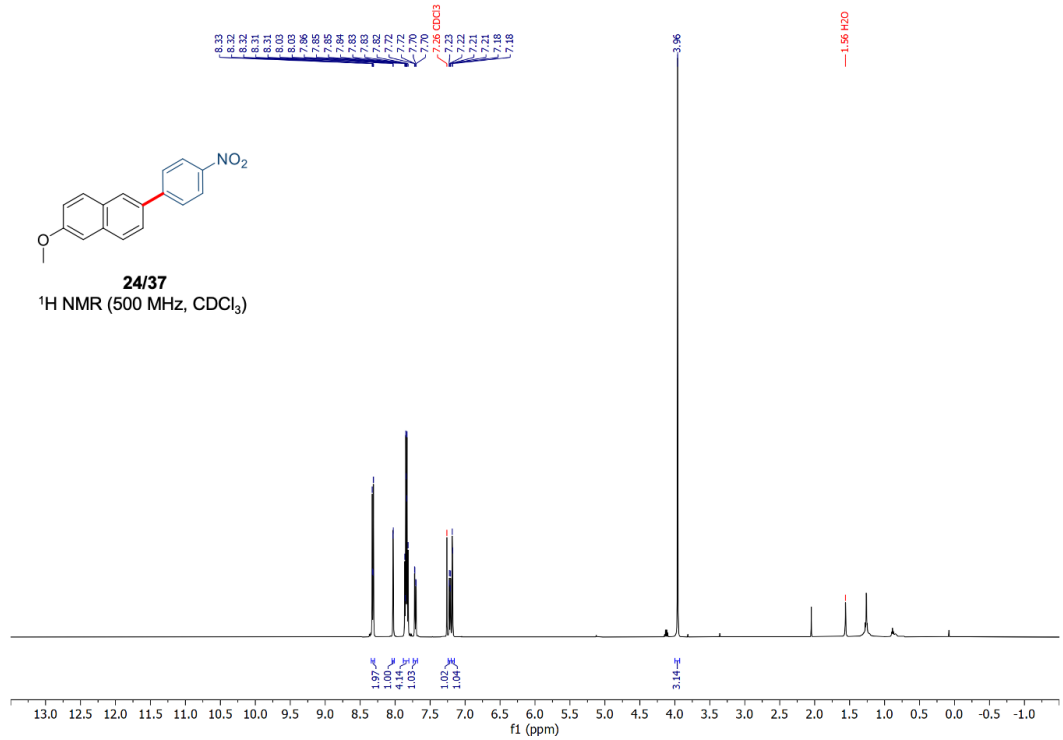
^{1}H NMR (500 MHz, $CDCl_3$)

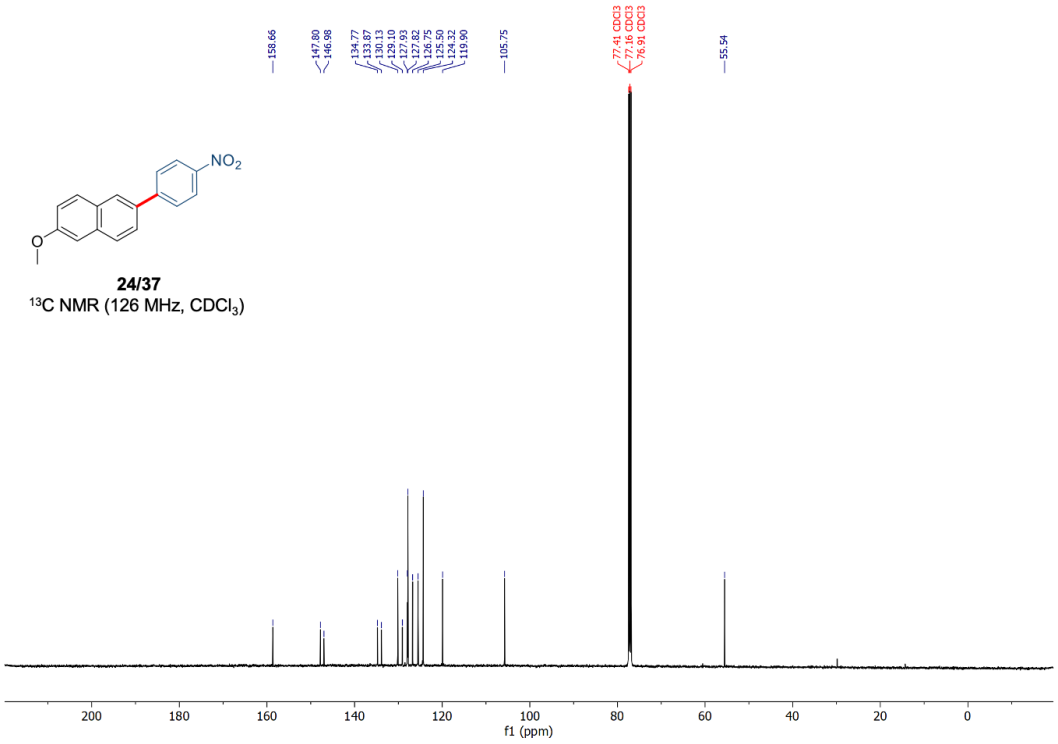


23

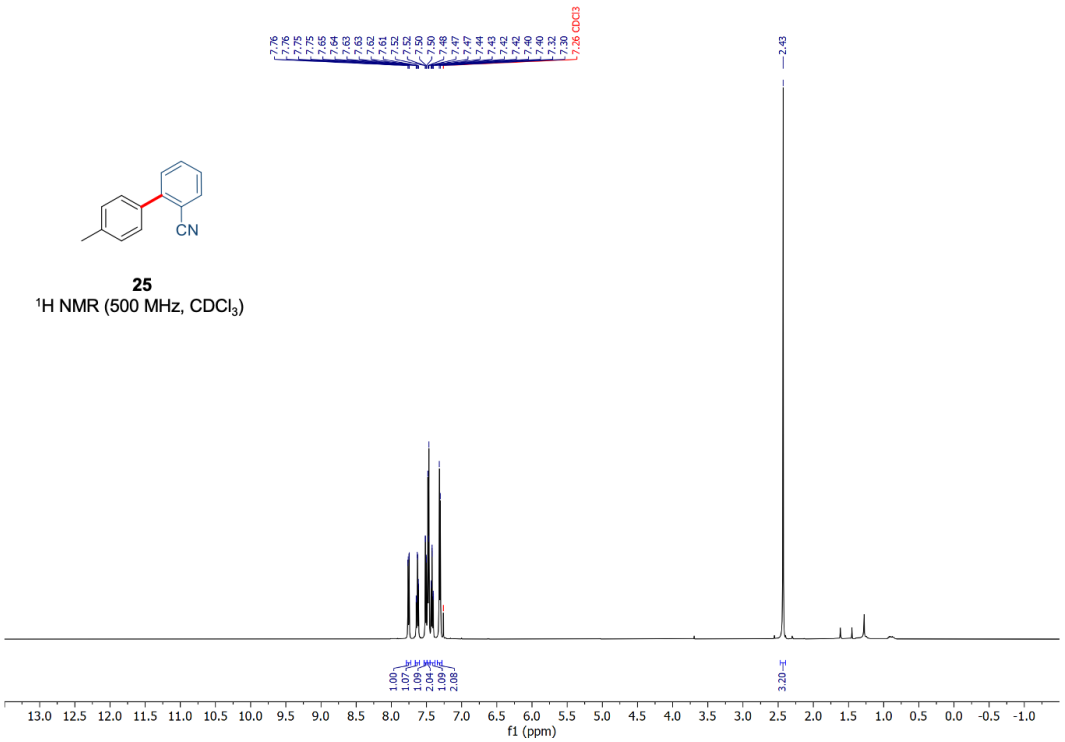
^{13}C NMR (126 MHz, $CDCl_3$)


30.17
23
^{11}B NMR (160 MHz, $CDCl_3$)
f1 (ppm)

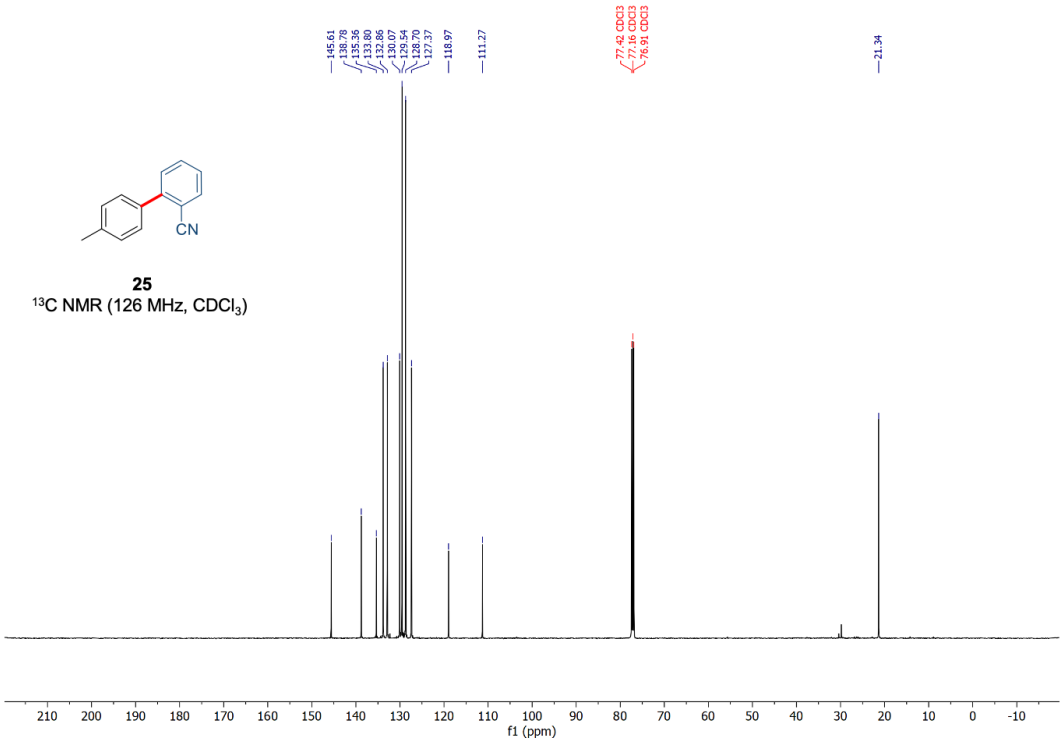

8.33
8.32
8.32
8.31
8.31
8.03
8.03
7.86
7.85
7.85
7.84
7.83
7.83
7.82
7.72
7.72
7.70
7.70
CDCl3
7.25
7.23
7.22
7.21
7.21
7.18
7.18
3.96
1.56 H2O
NO2
24/37
^{1}H NMR (500 MHz, $CDCl_3$)
1.97
1.00
4.14
1.03
1.02
1.04
3.14
f1 (ppm)



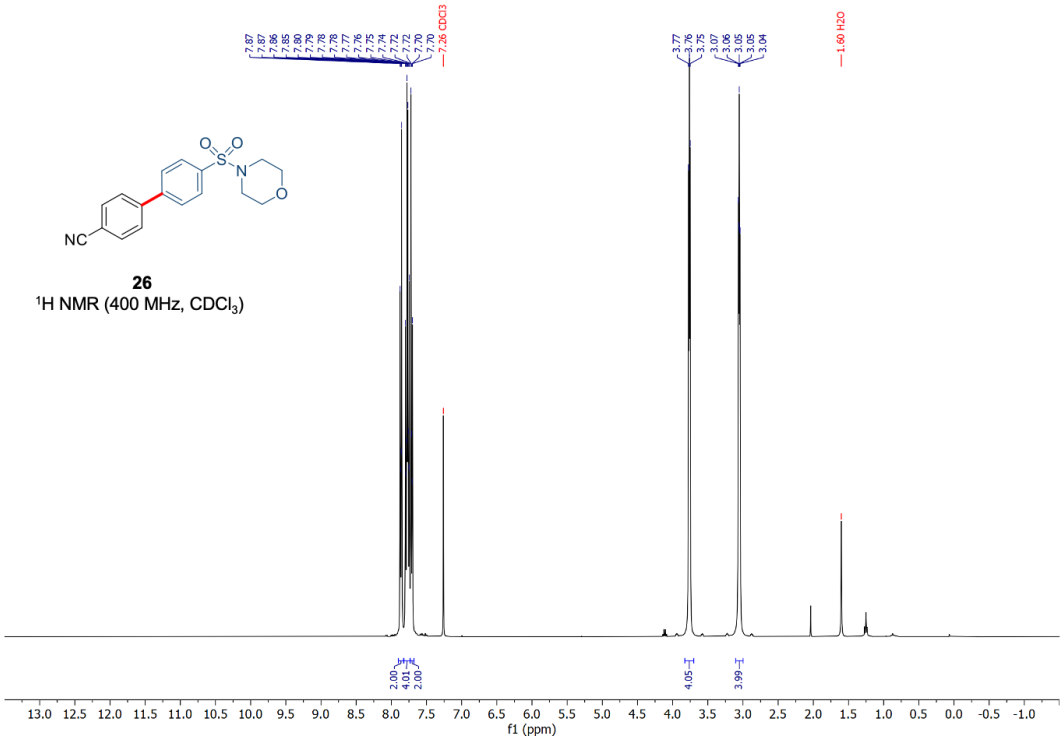
24/37
^{13}C NMR (126 MHz, $CDCl_3$)



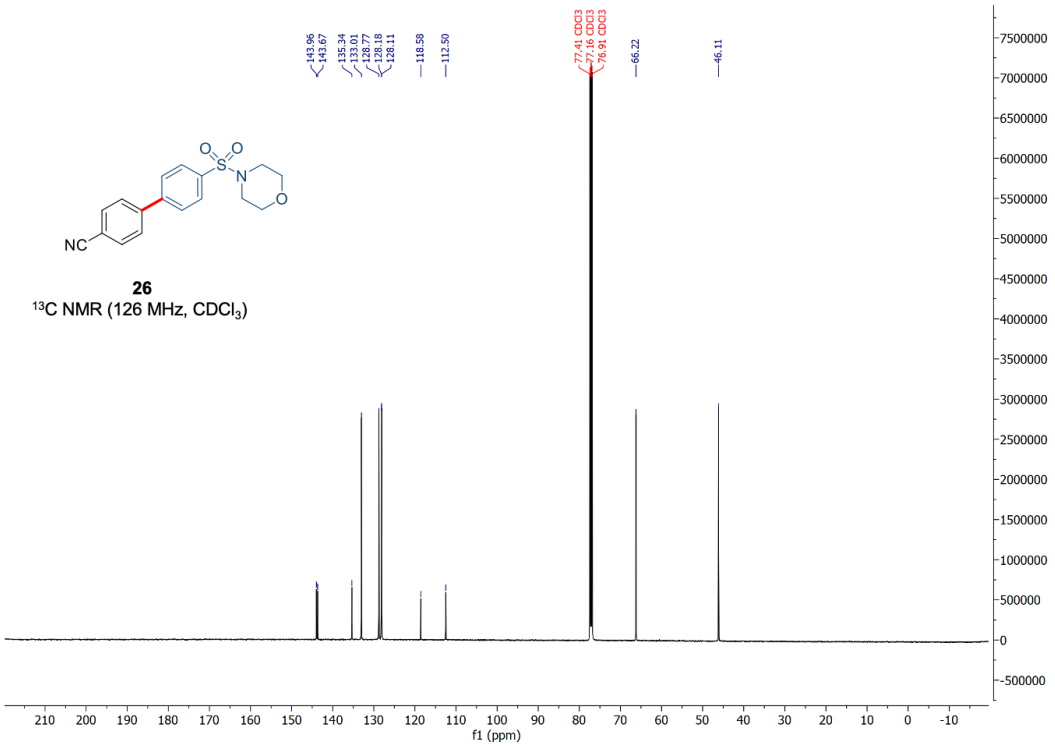
25
^{1}H NMR (500 MHz, $CDCl_3$)



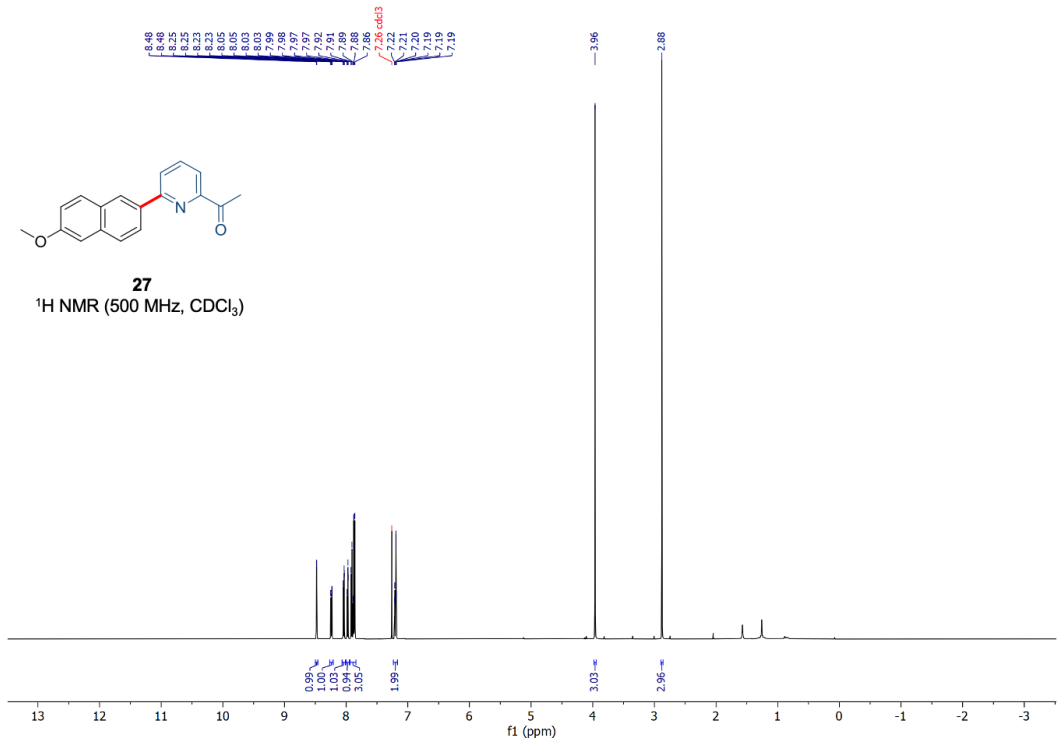
25
^{13}C NMR (126 MHz, $CDCl_3$)



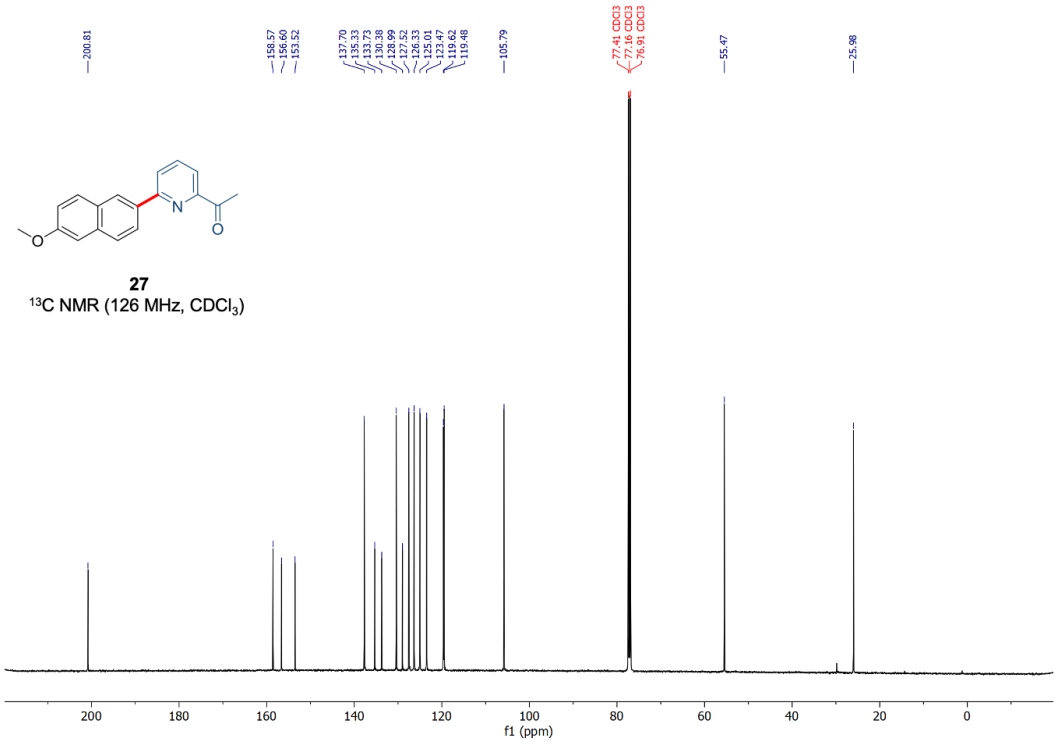
26
^{1}H NMR (400 MHz, $CDCl_3$)



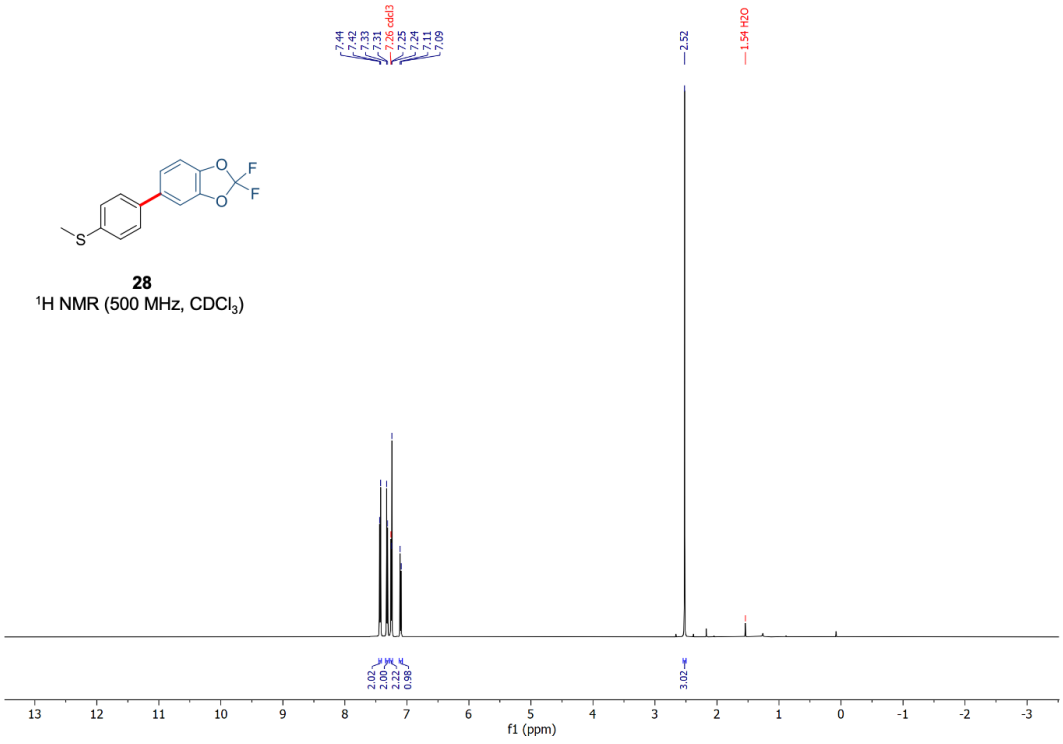
26
^{13}C NMR (126 MHz, $CDCl_3$)



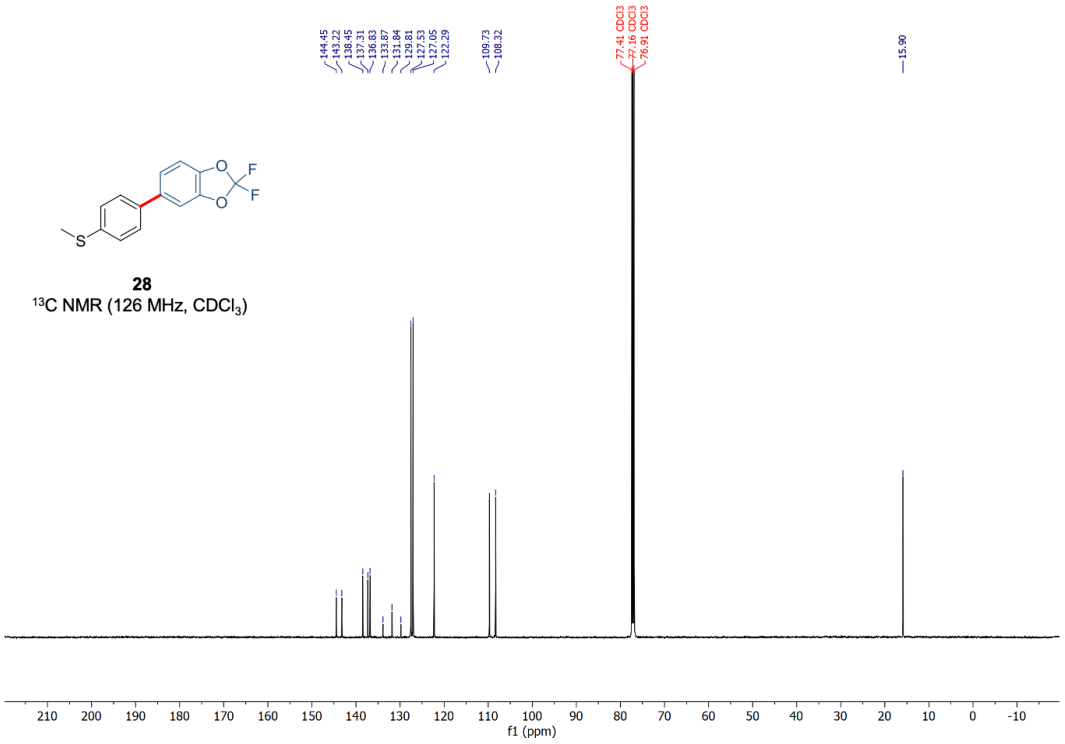
27
^{1}H NMR (500 MHz, $CDCl_3$)



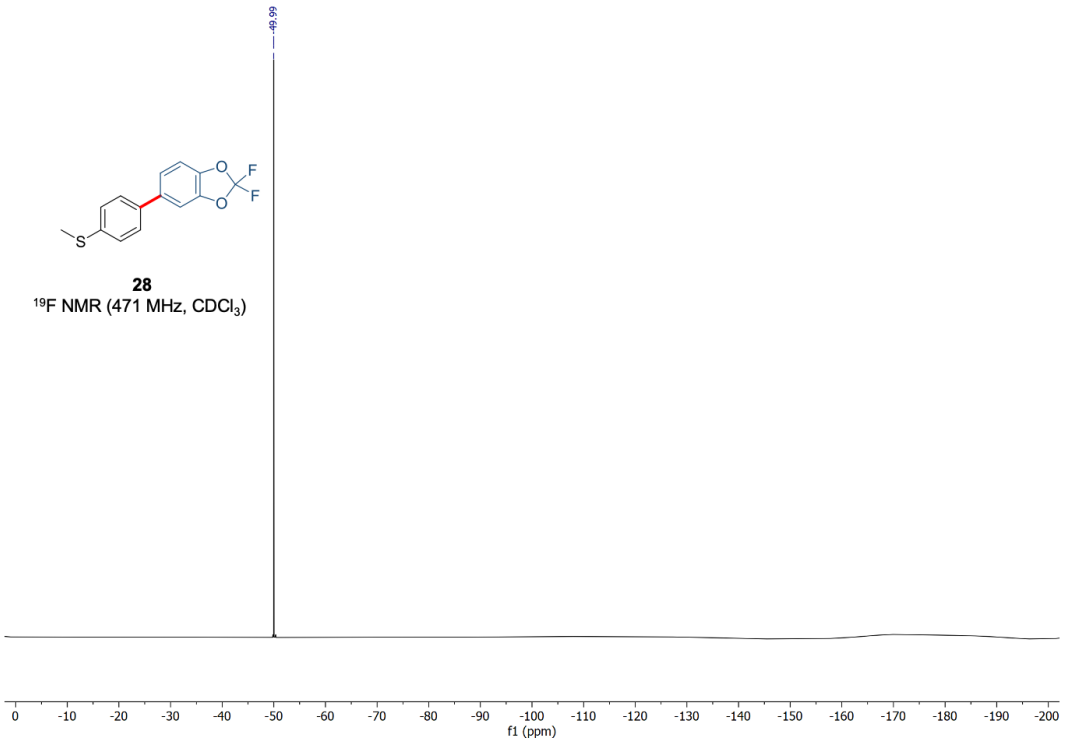
27
^{13}C NMR (126 MHz, $CDCl_3$)



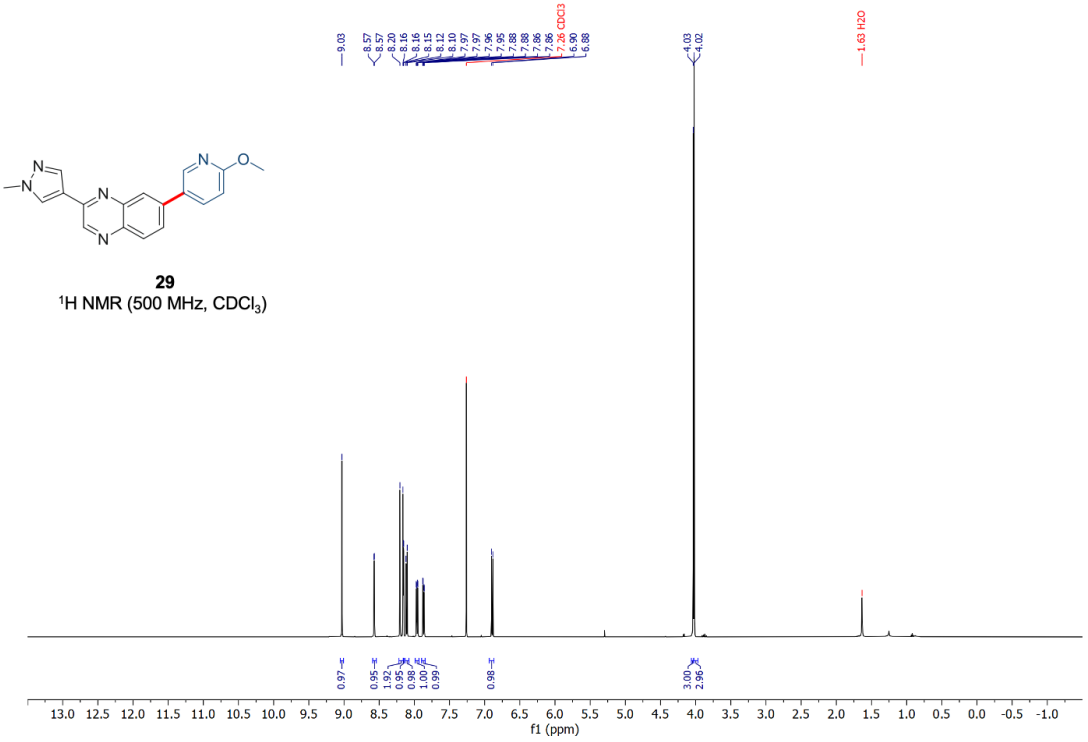
28
^{1}H NMR (500 MHz, $CDCl_3$)



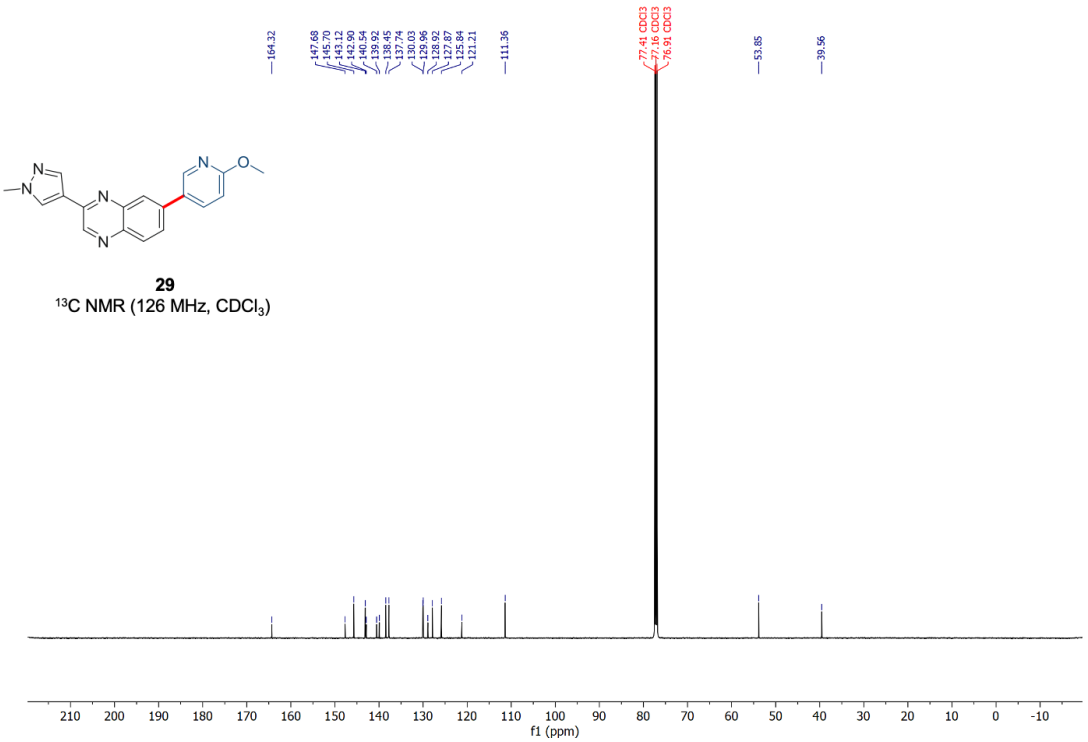
28
^{13}C NMR (126 MHz, $CDCl_3$)



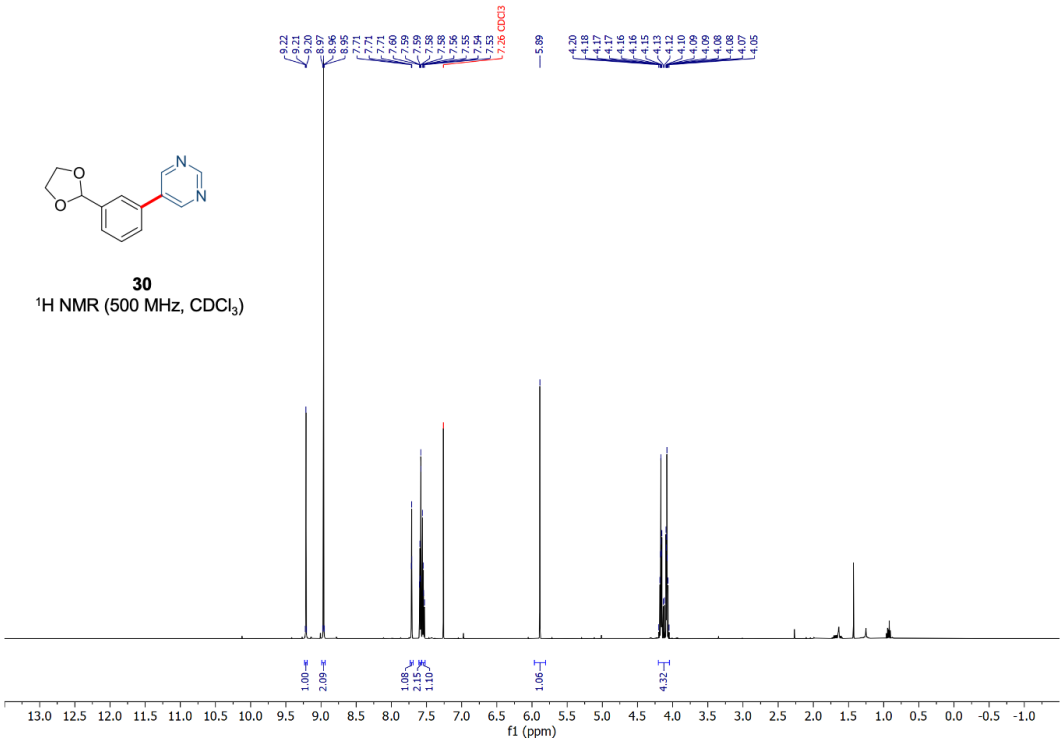
28
^{19}F NMR (471 MHz, $CDCl_3$)



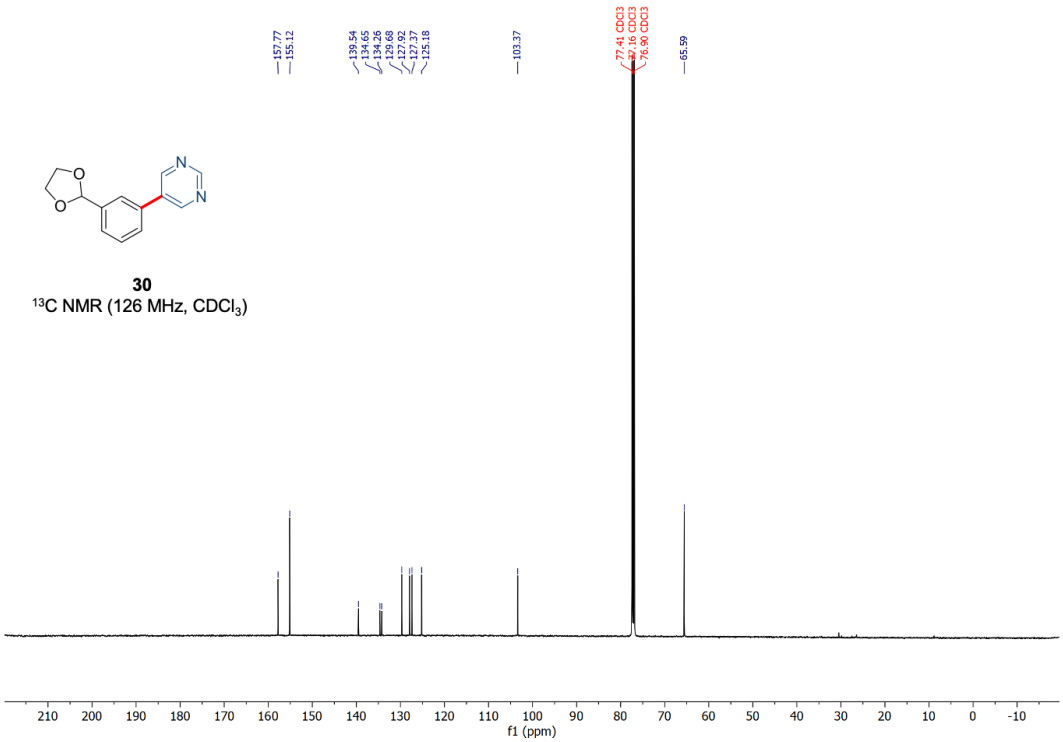
29
^{1}H NMR (500 MHz, $CDCl_3$)



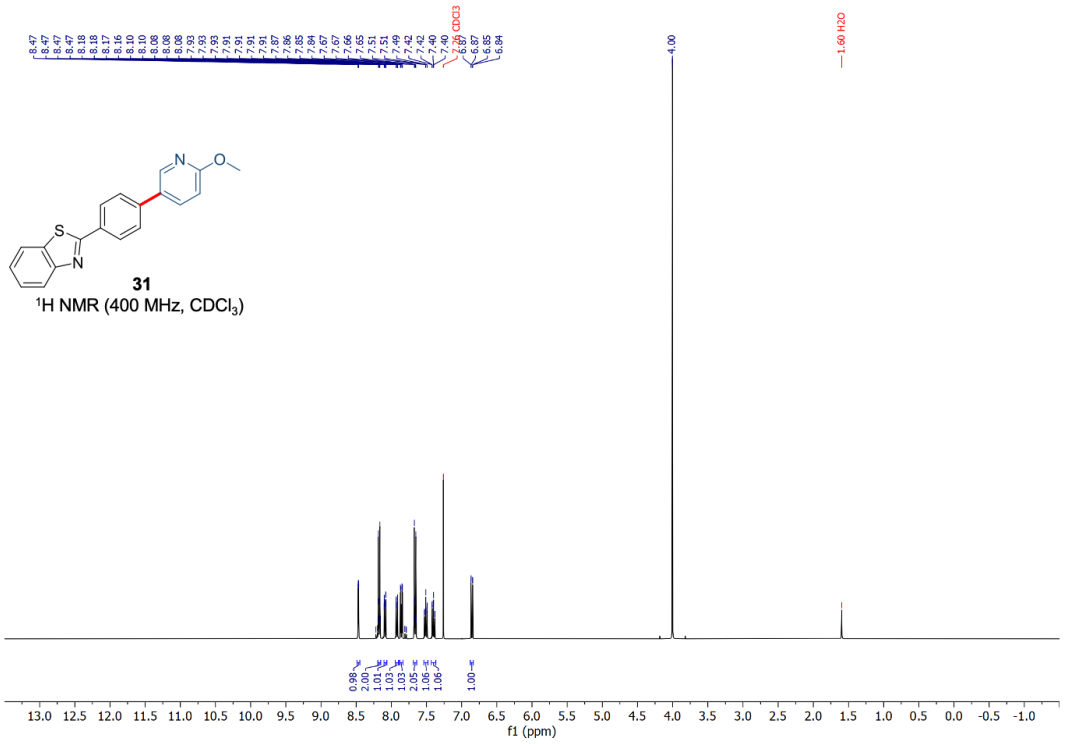
29
^{13}C NMR (126 MHz, $CDCl_3$)



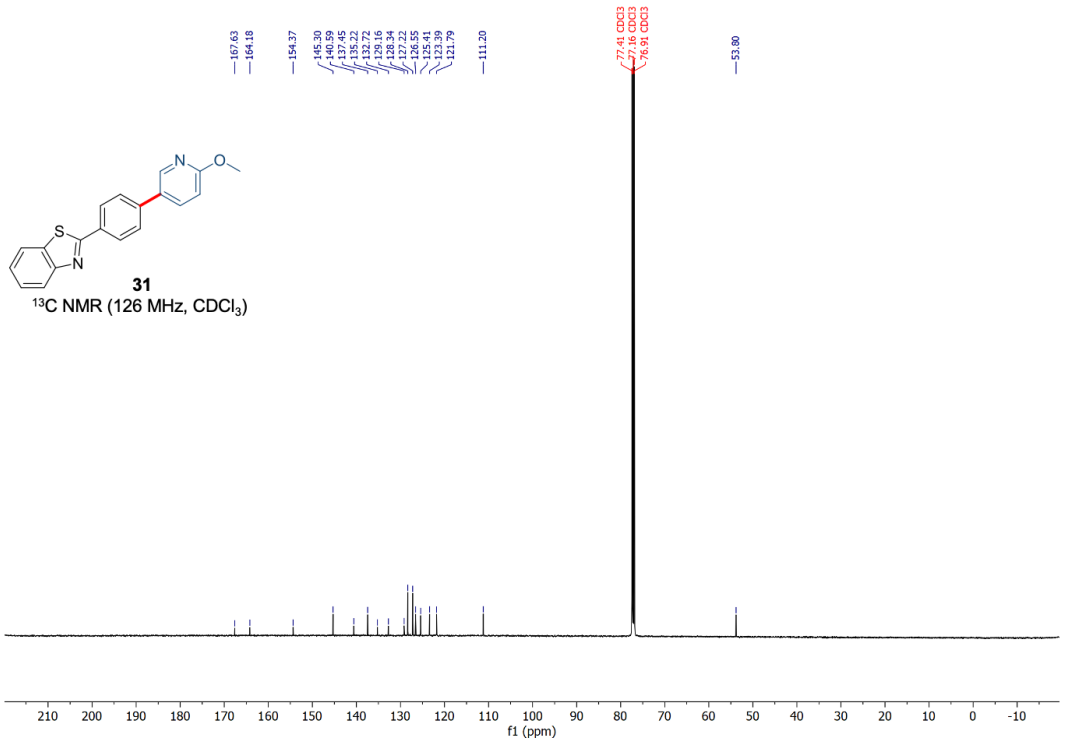
30
^{1}H NMR (500 MHz, $CDCl_3$)



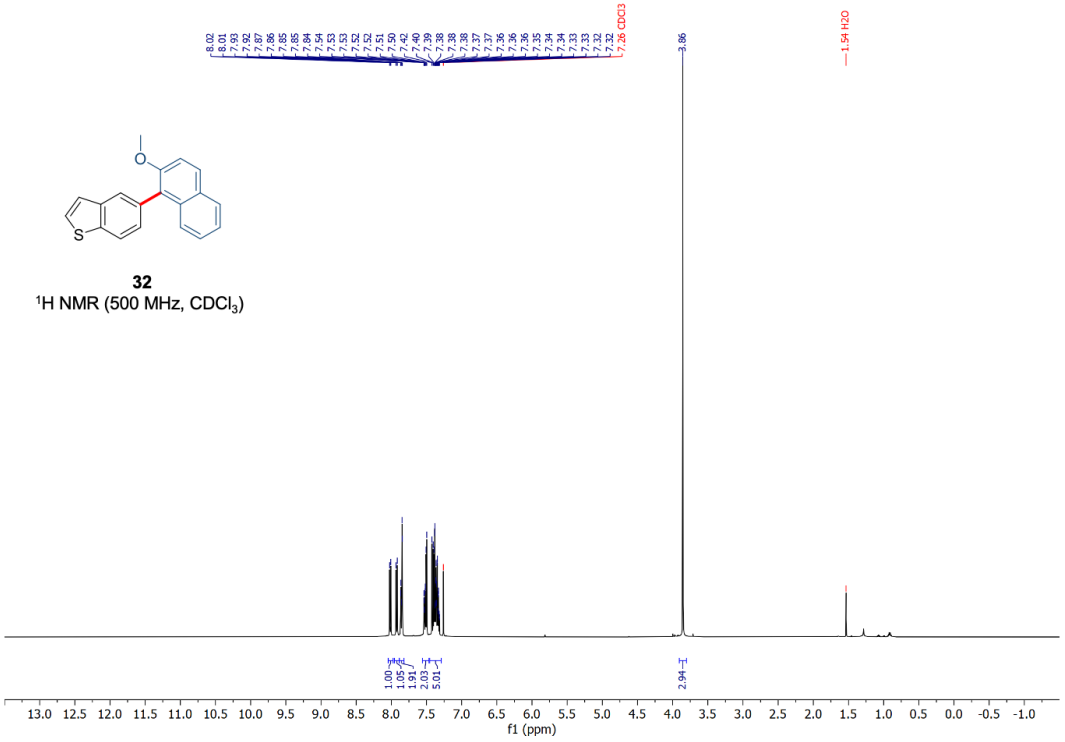
30
^{13}C NMR (126 MHz, $CDCl_3$)



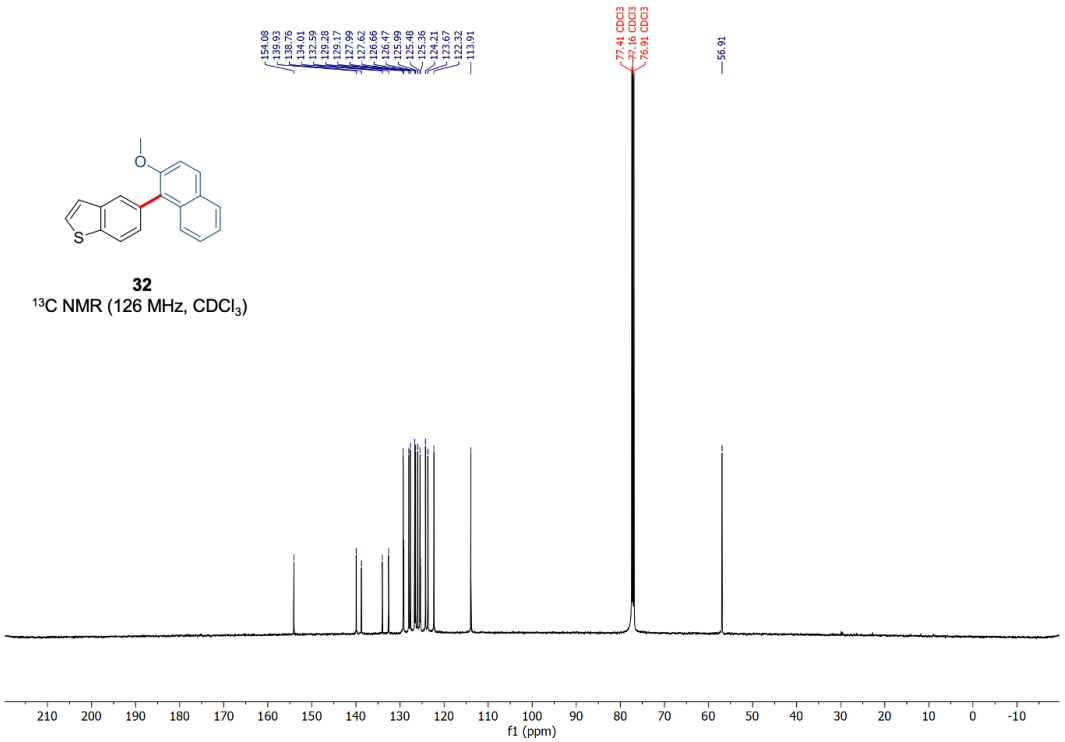
31
^{1}H NMR (400 MHz, $CDCl_3$)



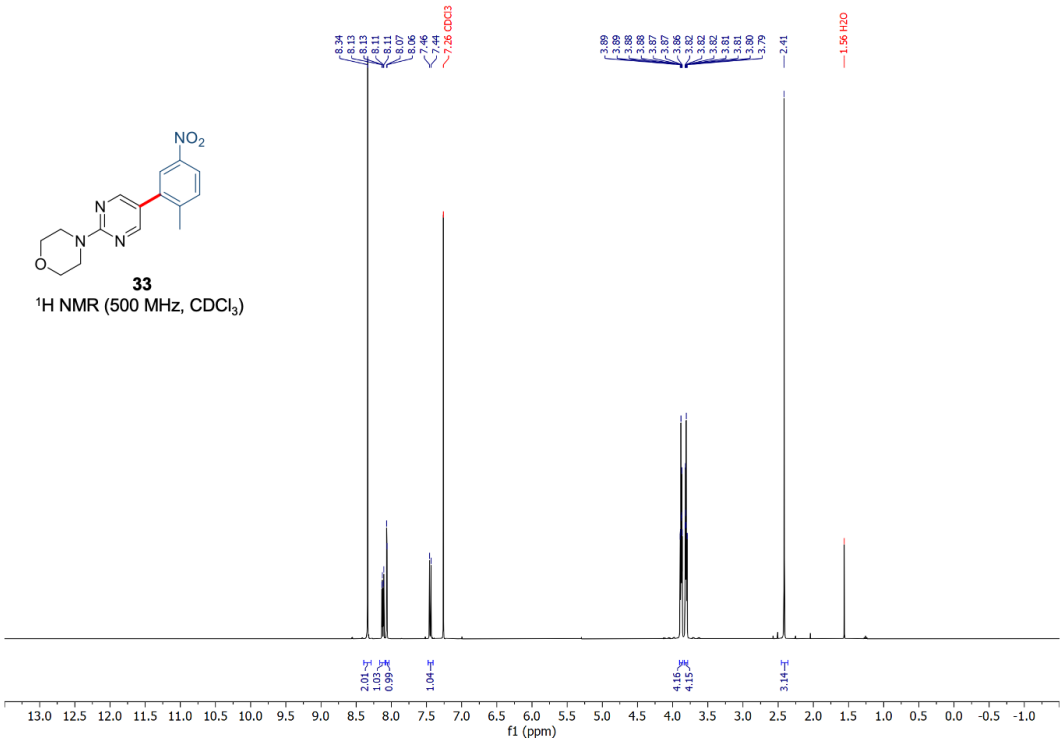
31
^{13}C NMR (126 MHz, $CDCl_3$)

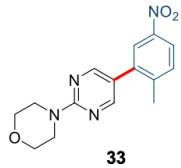


32
^{1}H NMR (500 MHz, $CDCl_3$)



32
^{13}C NMR (126 MHz, $CDCl_3$)



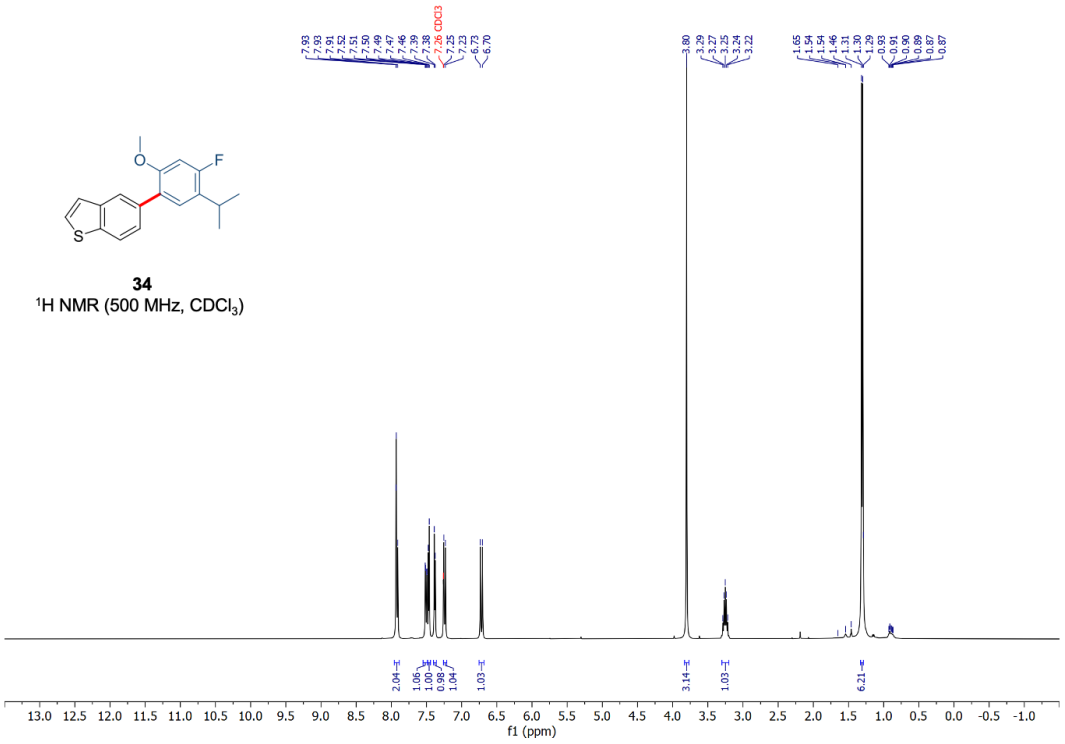


33

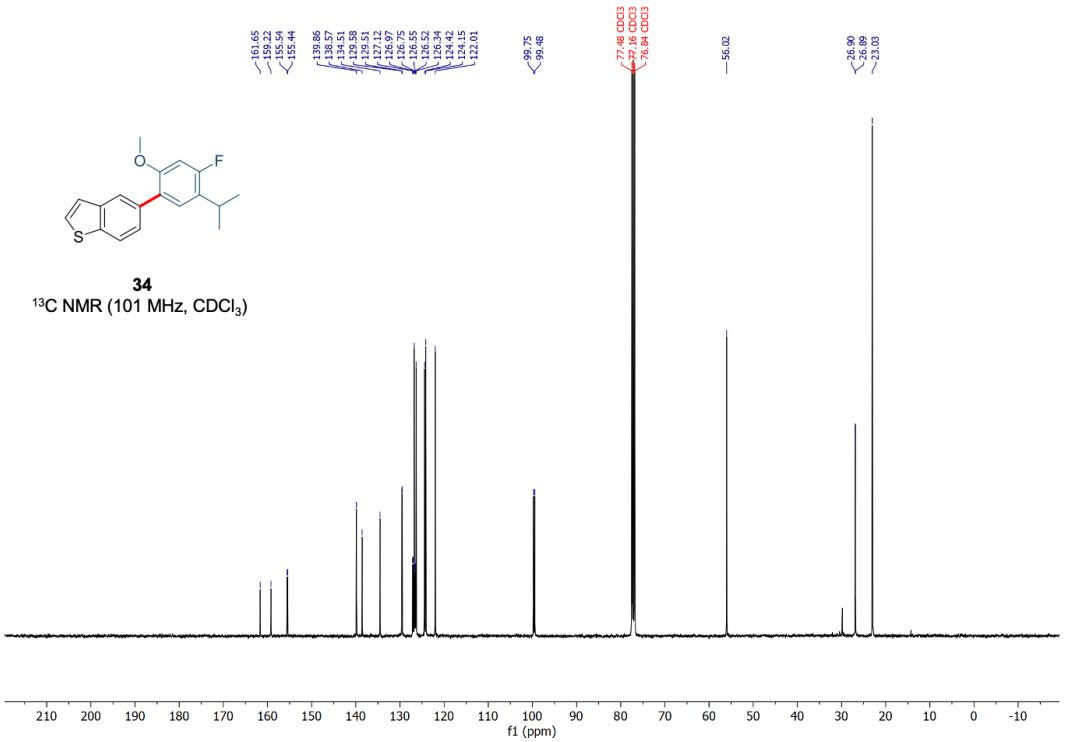
^{1}H NMR (500 MHz, $CDCl_3$)

33

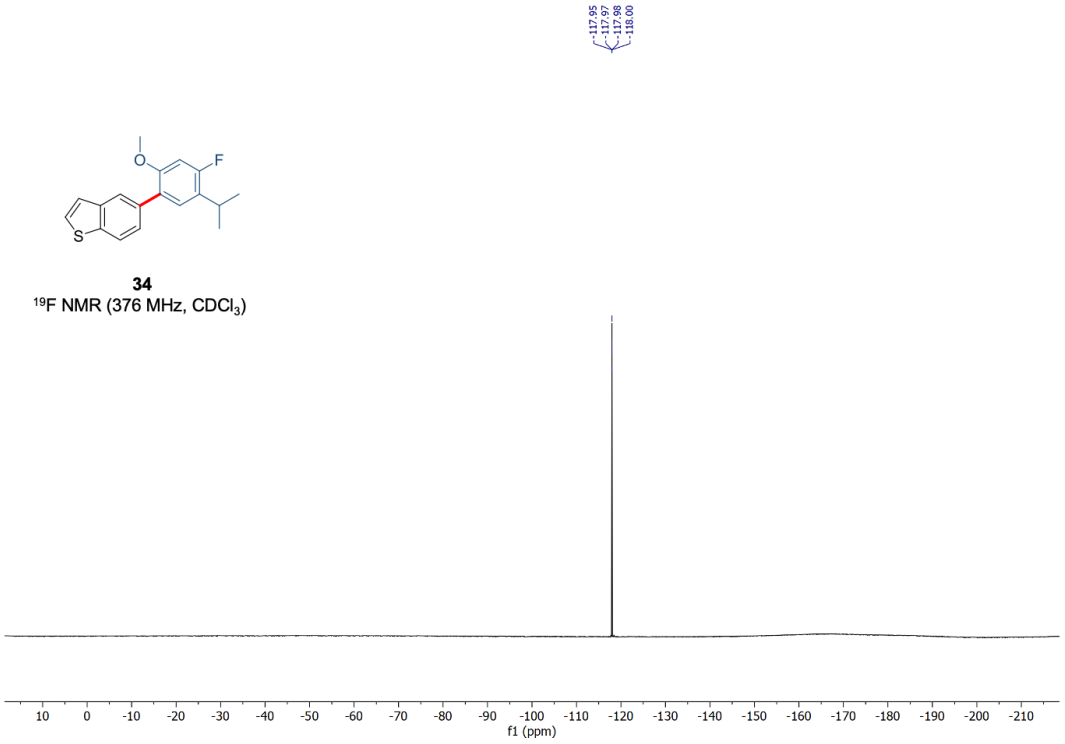
^{13}C NMR (126 MHz, $CDCl_3$)



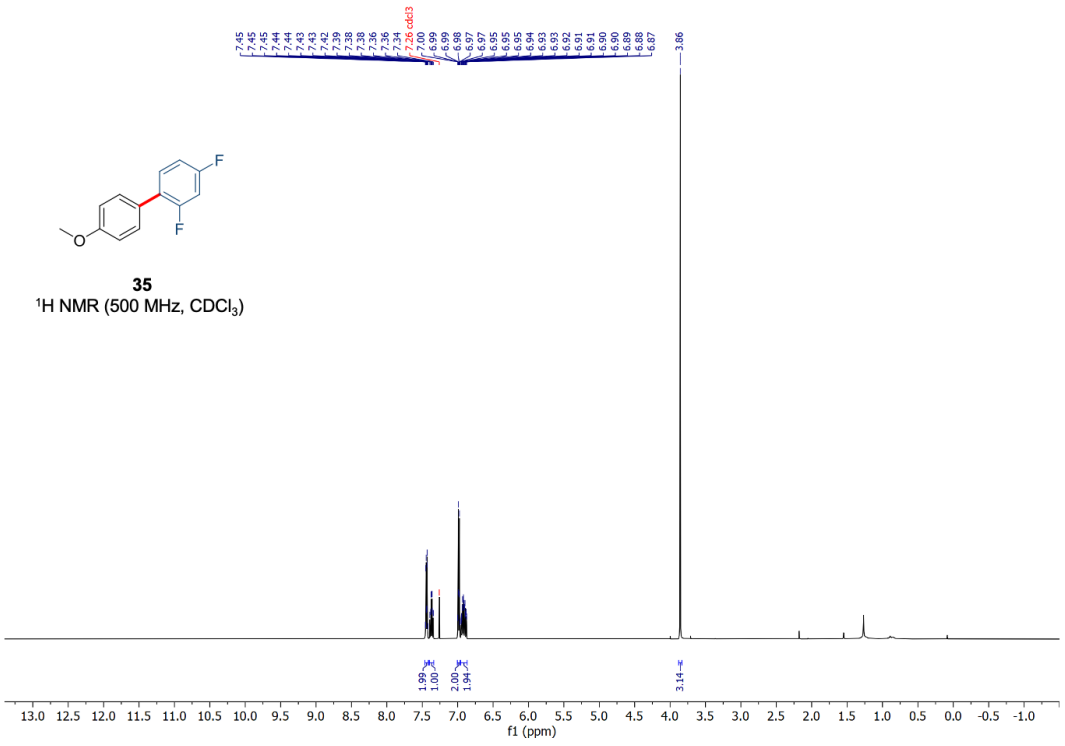
34
^{1}H NMR (500 MHz, $CDCl_3$)



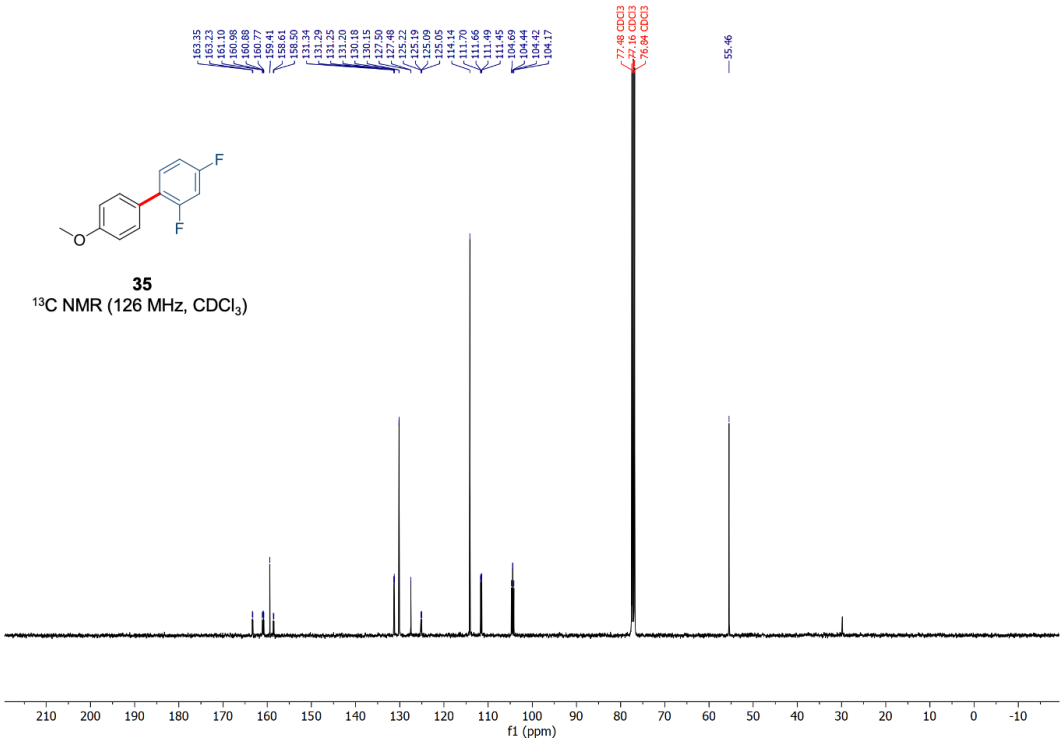
34
^{13}C NMR (101 MHz, $CDCl_3$)

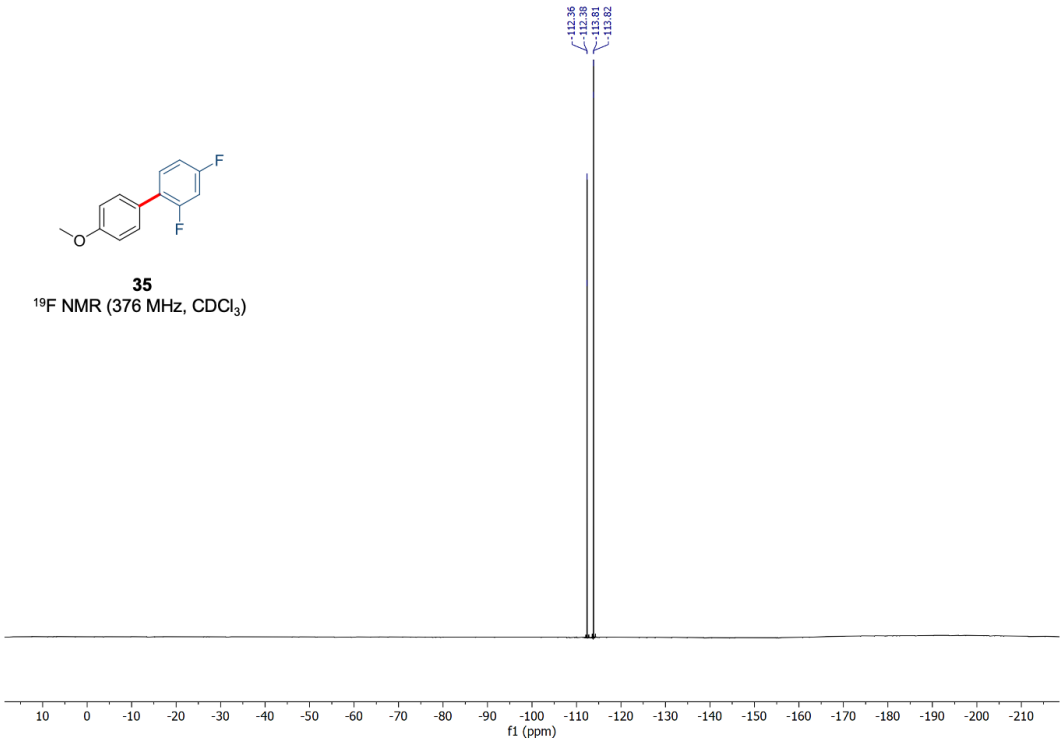


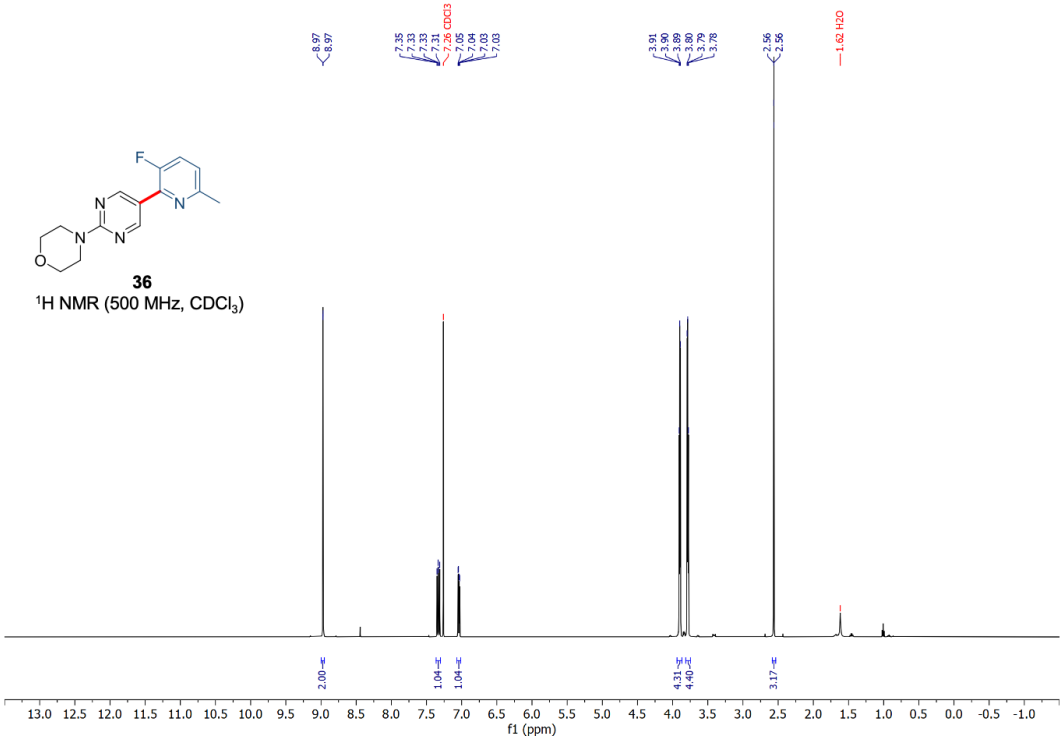
34
^{19}F NMR (376 MHz, $CDCl_3$)



35
^{1}H NMR (500 MHz, $CDCl_3$)

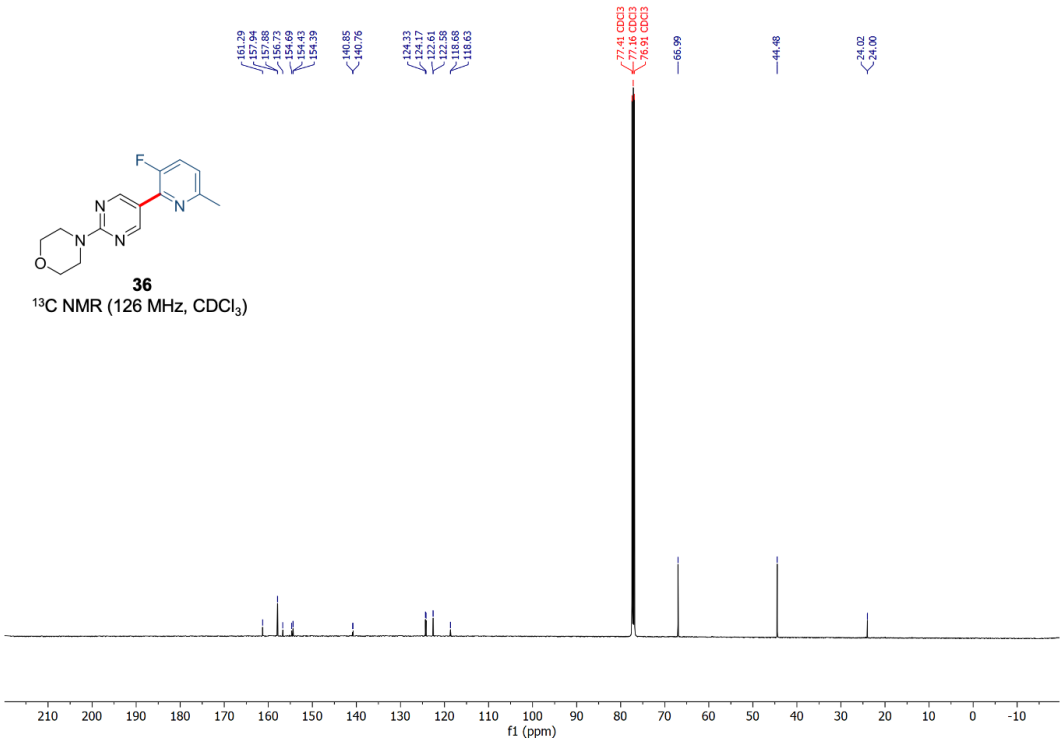

163.35
163.23
161.10
160.98
160.88
160.77
159.41
158.61
158.50
131.34
131.29
131.25
131.20
130.18
130.15
127.50
127.40
125.22
125.19
125.09
125.05
114.14
111.70
111.66
111.49
111.45
104.69
104.44
104.42
104.17
77.48 CDCl3
77.16 CDCl3
76.84 CDCl3
55.46
F
F
O
35
13C NMR (126 MHz, CDCl3)
210 200 190 180 170 160 150 140 130 120 110 100 90 80 70 60 50 40 30 20 10 0 -10
f1 (ppm)


112.36
112.38
113.81
113.82
F
F
O
35
19F NMR (376 MHz, CDCl3)
10 0 -10 -20 -30 -40 -50 -60 -70 -80 -90 -100 -110 -120 -130 -140 -150 -160 -170 -180 -190 -200 -210
f1 (ppm)



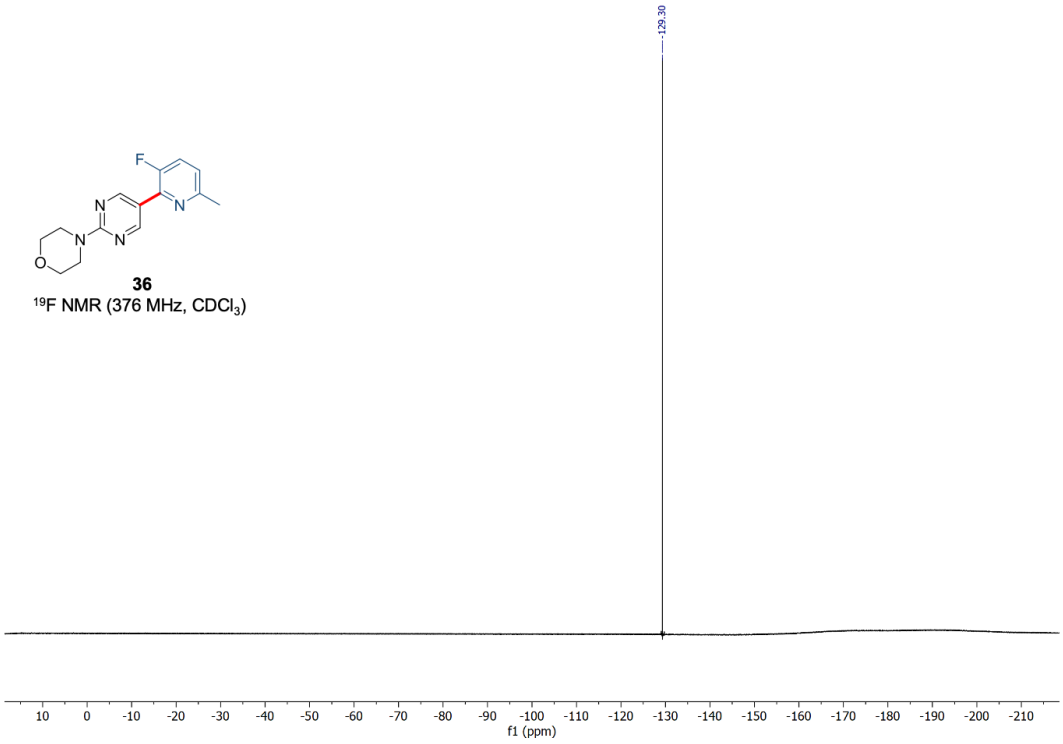
36

^{1}H NMR (500 MHz, $CDCl_3$)



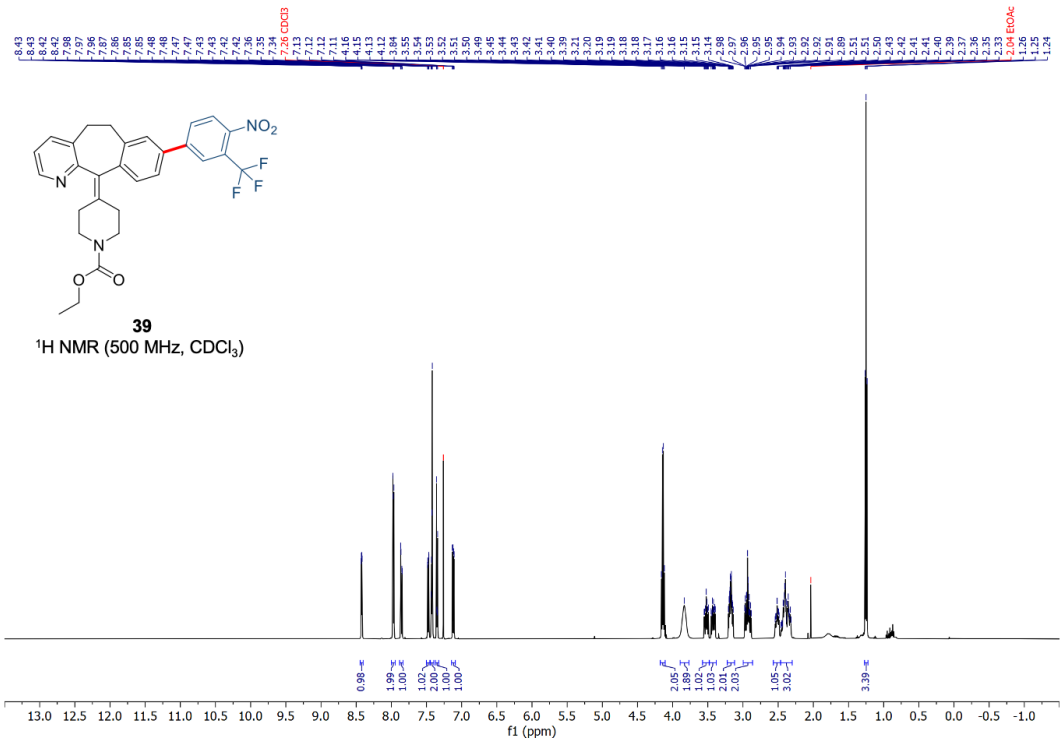
36

^{13}C NMR (126 MHz, $CDCl_3$)



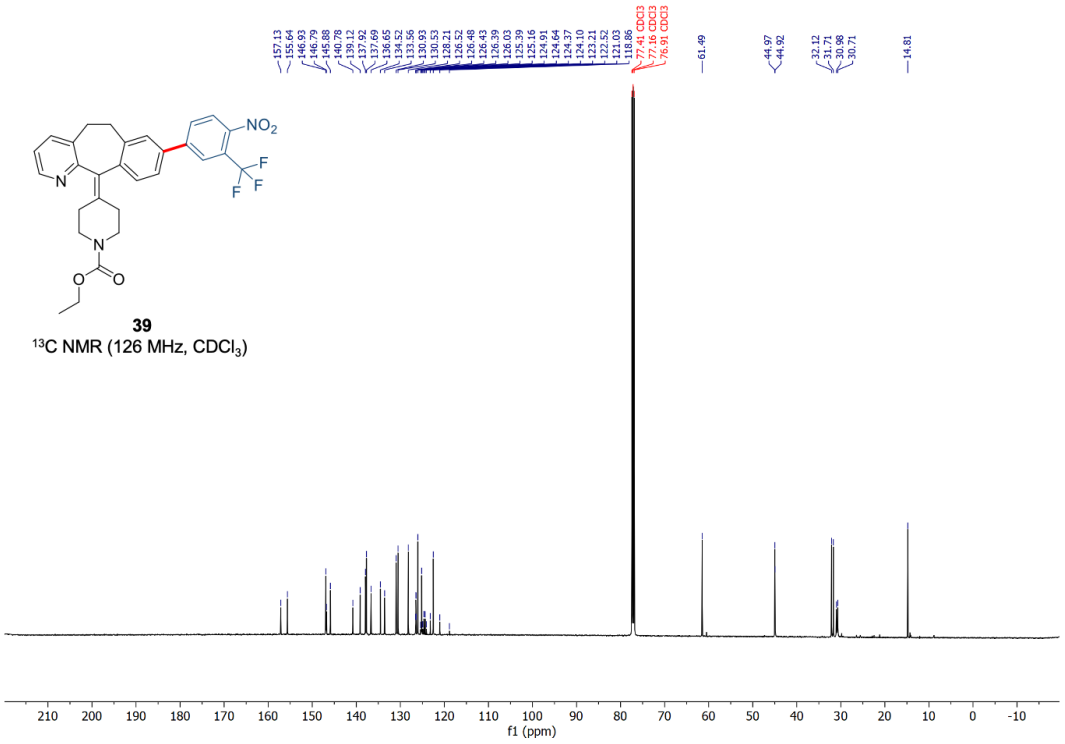
36

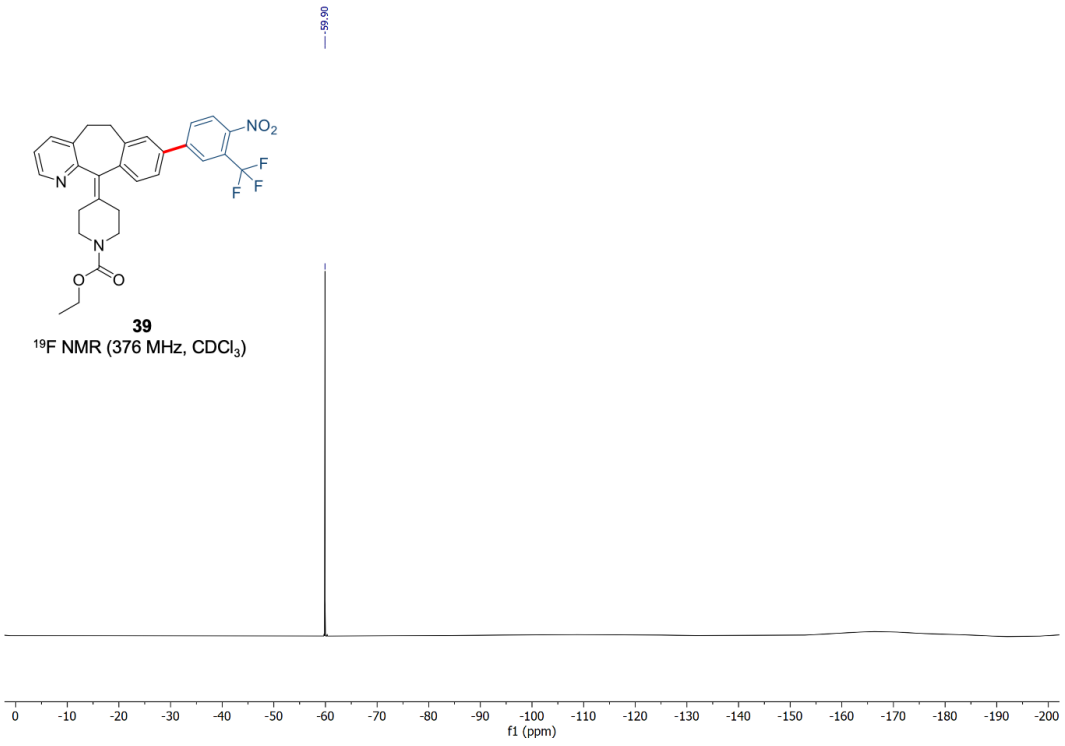
^{19}F NMR (376 MHz, $CDCl_3$)

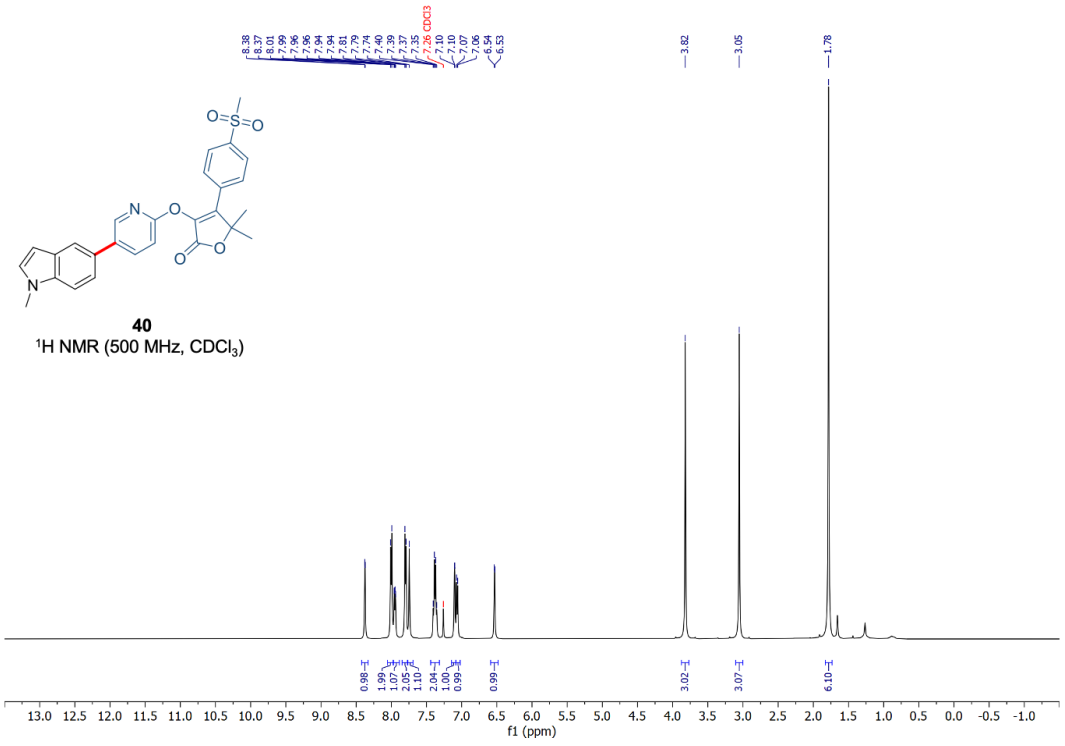


39

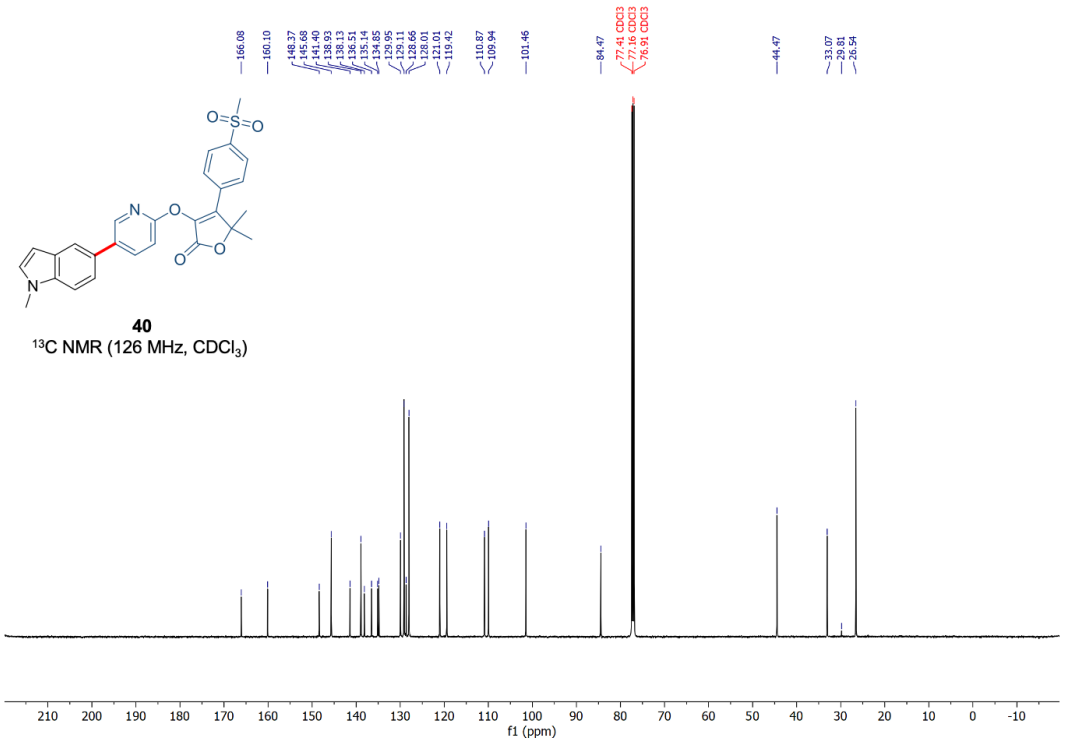
^{1}H NMR (500 MHz, $CDCl_3$)


157.13
155.64
146.93
146.79
145.88
140.78
139.72
137.92
137.69
136.65
134.52
133.56
130.93
130.53
128.21
126.52
126.48
126.43
126.39
126.03
125.39
125.16
124.91
124.64
124.37
124.10
123.21
122.52
121.03
118.88
77.41 CDCl3
77.16 CDCl3
76.91 CDCl3
61.49
44.97
44.92
32.12
31.71
30.88
30.71
14.81
NO2
F
F
F
N
N
O
O
39
13C NMR (126 MHz, CDCl3)
210 200 190 180 170 160 150 140 130 120 110 100 90 80 70 60 50 40 30 20 10 0 -10
f1 (ppm)

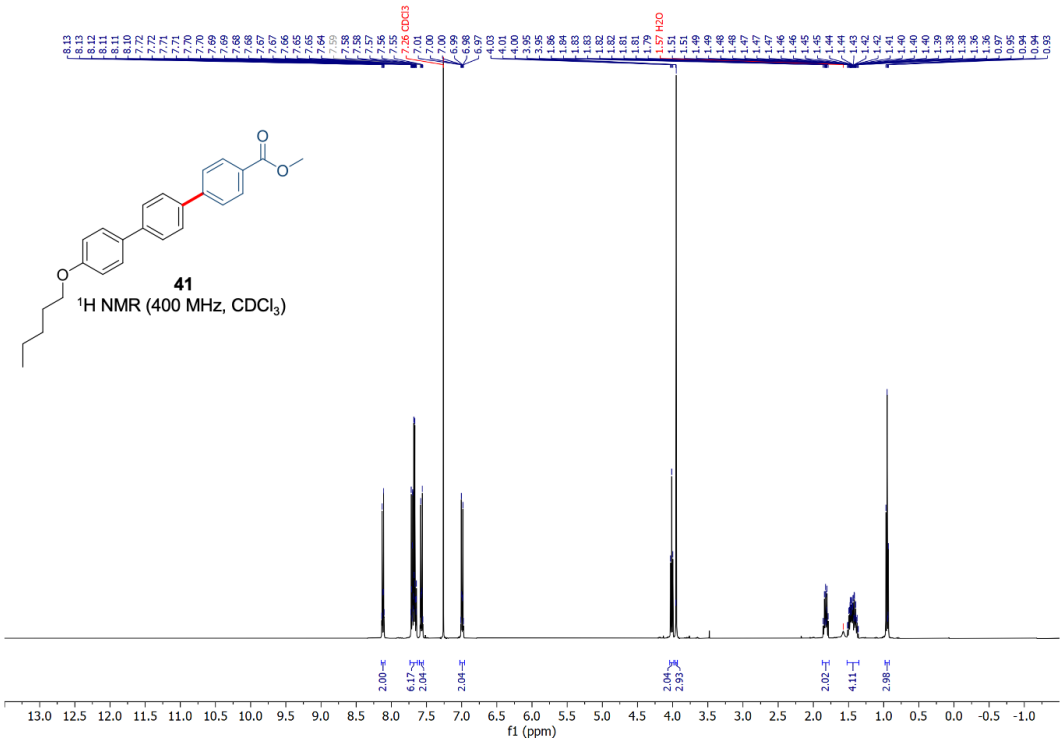

-59.90
NO2
F
F
F
N
N
O
O
39
19F NMR (376 MHz, CDCl3)
0 -10 -20 -30 -40 -50 -60 -70 -80 -90 -100 -110 -120 -130 -140 -150 -160 -170 -180 -190 -200
f1 (ppm)

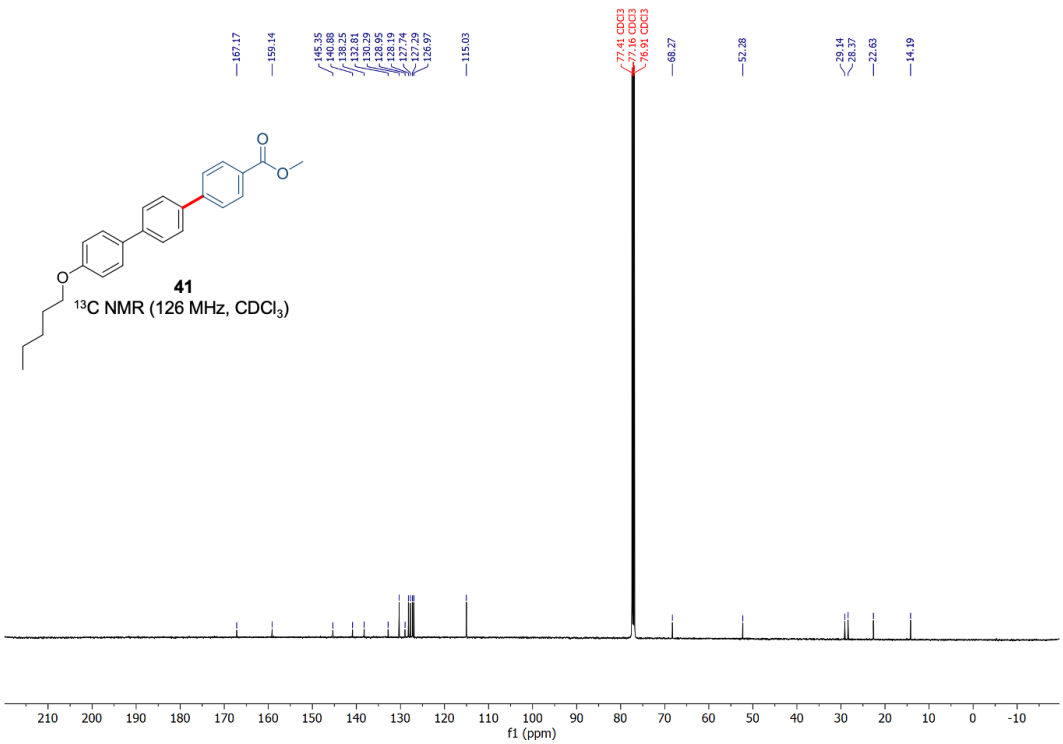


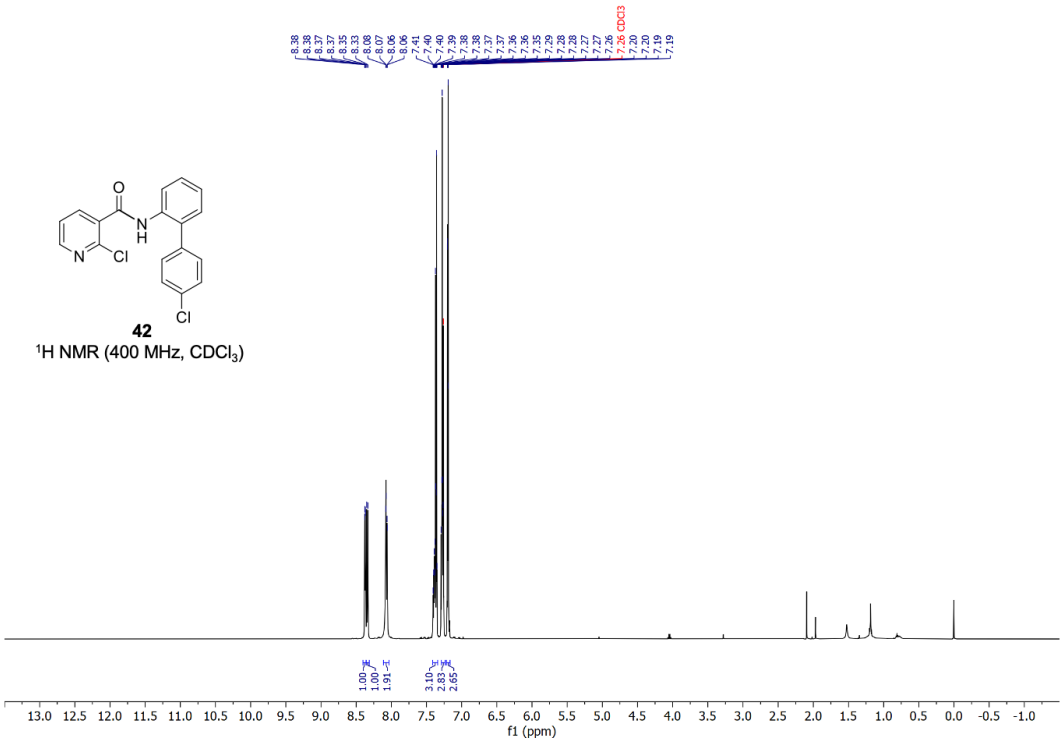
40
^{1}H NMR (500 MHz, $CDCl_3$)

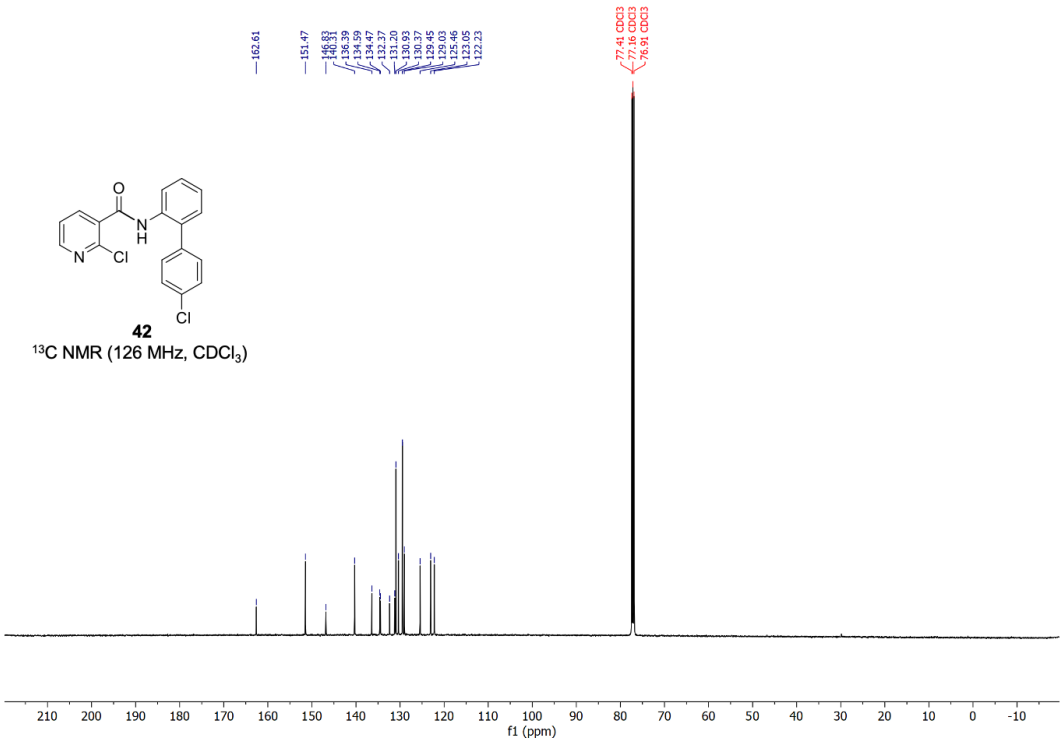


40
^{13}C NMR (126 MHz, $CDCl_3$)


41
^{1}H NMR (400 MHz, $CDCl_3$)
f1 (ppm)


41
^{13}C NMR (126 MHz, $CDCl_3$)
f1 (ppm)


42
^{1}H NMR (400 MHz, $CDCl_3$)
f1 (ppm)


42
^{13}C NMR (126 MHz, $CDCl_3$)
f1 (ppm)

Chapter 3:

A Green Chemistry Approach to the Synthesis of an Emerging Drug for the Treatment of Celiac Disease

The contents of Chapter 3 have been reproduced with permission from:

Nelson, C. B.; Yirak, J. R.; Baumann, M. E.; Freiberg, K. M.; Lipshutz, B. H. *Green Chem.* **2026**, *28*, 938–944.

Green Chem. is © The Royal Society of Chemistry 2026.

3.1 Introduction

Autoimmune disorders are lifelong illnesses that can have serious health implications for those suffering from them. These disorders are highly complex, have no cure, and, as such, are very challenging to treat. Because of this, the quality of life for patients can be severely

impacted. One such disorder in this class is celiac disease, where those afflicted cannot tolerate ingesting the protein, gluten, a common food ingredient mainly derived from grain products.[10,12] Such exposures cause the individual's immune system to generate transglutaminase 2 (TG2) autoantibodies that attack the body's own small bowel.[10,12,47] This damage can be irreversible and have serious, lasting consequences: if extensive enough, such damage to the villi of the small intestine inhibits the body's ability to absorb nutrients from food.[10] Unfortunately, celiac disease is consistent with other autoimmune diseases in that there is no cure. In fact, the only option for treating patients has been to avoid products containing gluten.[74] This can be challenging given how omnipresent this protein is in food products. Moreover, 'gluten-free' alternatives are significantly more expensive and, thus, impose a financial burden, especially on those from lower socioeconomic standings.[7] Finally, this abstention approach isn't wholly effective either: often, it is not readily evident which products contain gluten,* so accidental exposures are commonplace.[10,47] In all, it is apparent that celiac disease has a significant negative impact on quality of life, poses serious concerns for patients' long-term health, and, thus, has presented an important target for research toward novel therapeutics.

In the past couple of years, significant advancements have been made toward treating diseases where the above-mentioned TG2 enzymes play a causal or contributing role. Specifically, several peridinone compounds were found to have an inhibitory effect on TG2.[10]

*Products that one may not anticipate to have gluten include: mustards, cheeses, and broths (information obtained from https://gluten.org/2021/03/23/43-foods-where-gluten-may-be-hidden/ on 02/24/2026).

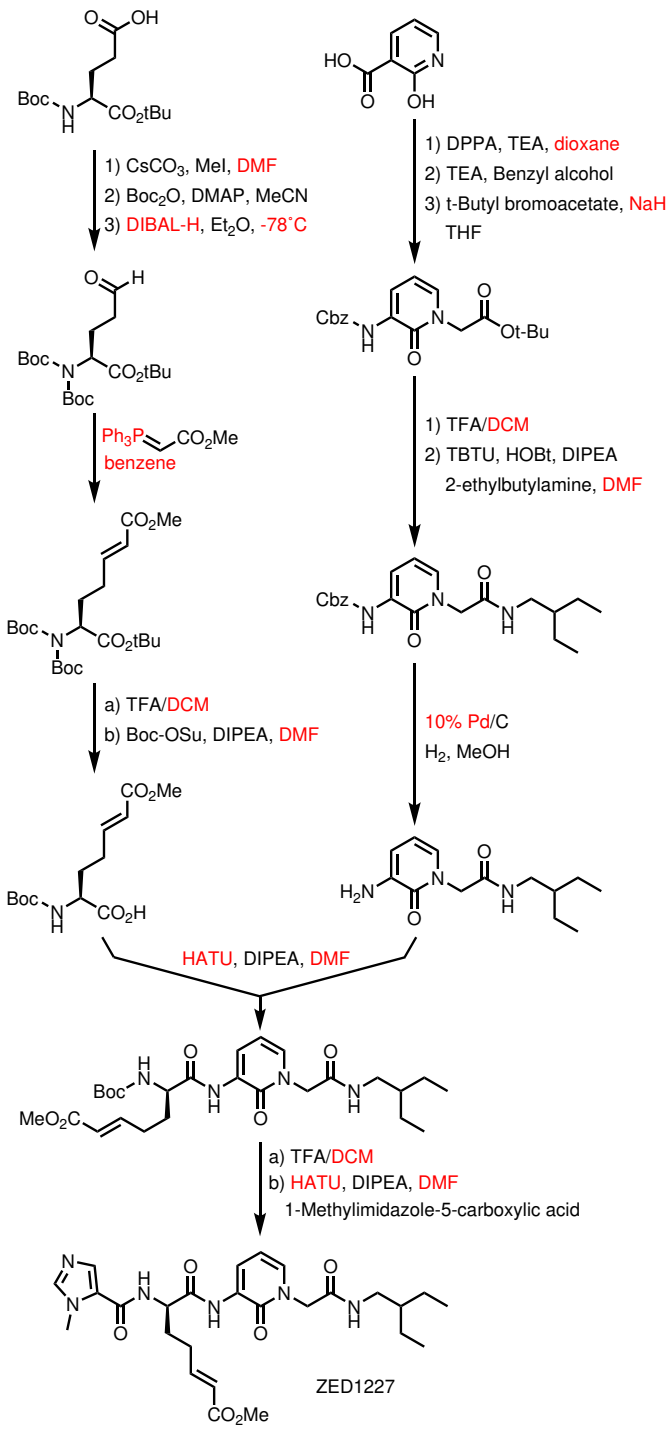


Figure 3.1: Original Literature Route.[10]

Such inhibition neutralizes, or at least attenuates, this key component in the pathogenesis of these disorders, which, beyond celiac disease, include certain cancers, fibrotic disorders, neurological disorders, and psoriasis.[51,81] Specifically for the disease at the center of this discussion, this "knocking out" of TG2 would prevent the damaging gluten-triggered autoimmune response that endangers the health of the patient.

Of the peridinones and derivatives thereof, the most prominent and close to seeing clinical application is *ZED-1227*.[10] Developed via a collaborative effort by Dr. Falk Pharma, Zedira, and Takeda, this promising API has already reached stage II clinical trials* for celiac disease, as well as nonalcoholic fatty liver disease.

*At the time of engaging in this project.[73]

Nonetheless, in drug discovery and development, the route and methods employed for medicinal chemistry studies are either undesirable or unacceptable for large-scale manufacturing of the API. As is seen by the original synthetic route of *ZED1227*[10] (Fig. 3.1), this API is no exception. The solvents utilized are hazardous and unsustainable; namely, DCM, DMF, dioxane, and benzene are used. For several amide bond formations, harsh coupling reagents HATU and HOBt/TBTU are leveraged. The route also includes undesirable reductions, including the use of DIBAL-H at cryogenic conditions and hydrogen gas with 10% palladium on carbon. Furthermore, the Wittig olefination establishing the α,β-unsaturated methyl ester gives unwanted phosphine oxide in stoichiometric amounts. All of these drawbacks demonstrated that a more efficient and sustainable synthesis must be established for this new promising therapeutic.

3.2 Results and Discussion

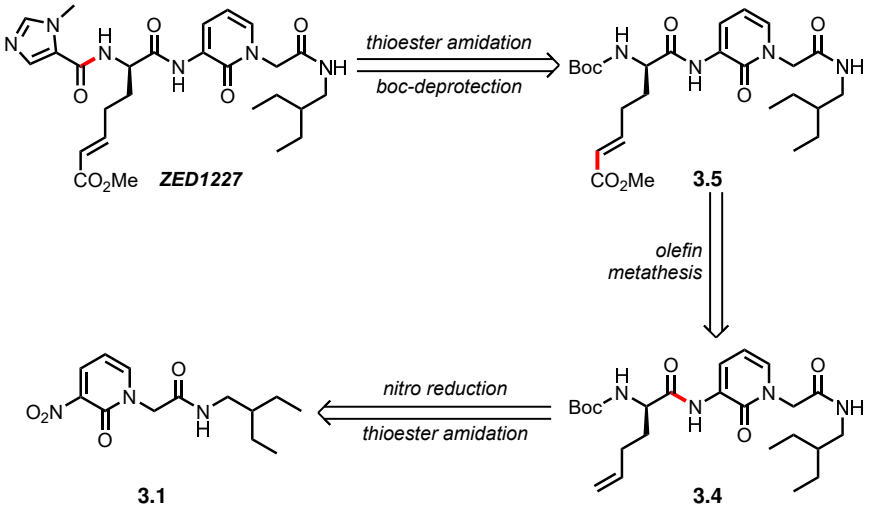


Figure 3.2: Retrosynthetic Analysis for *ZED1227*.[10]

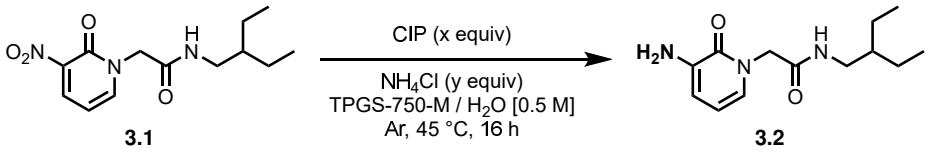
In collaboration with Takeda, my coauthors and I sought a significantly improved synthesis. After breaking down the API retrosynthetically (Fig. 3.2), we proposed a linear route that relies on fewer steps

and draws on our lab's existing sustainable methods for nitro reductions,[44] amide couplings,[27] and olefin metatheses.[84] Additionally, we anticipated that implementation of these methods would minimize the number of pots and isolations needed to reach *ZED1227*.

3.2.1 Reduction of Nitro Group on Dihydropyridinylacetamide

Prior art from our group disclosed a mild and sustainable protocol for nitro group reductions that utilizes highly economical carbonyl iron powder (CIP) under aqueous micellar conditions.[44] Though that work established a robust general method, it was, of course, pertinent to establish optimal conditions for the substrate at hand.* Table 3.1 articulates the various conditions that were tested to this end. Surprisingly, this reaction was seen to work equally well in an on-water fashion, thus, not requiring the addition of a surfactant. This assay of conditions also allowed for reducing the iron (CIP) loading. The qNMR result for the optimized reduction method (entry 7 from Table 3.1) was >99%.

Table 3.11: Nitro Group Reduction Optimization[62]



3.1 3.2

Entry[a]	CIP (x equiv)	NH_4Cl (y equiv)	Surfactant	%Yield[b]
1	5	3	TPGS-750-M	94
2	4	3	TPGS-750-M	>99
3	3	3	TPGS-750-M	93
4	2	3	TPGS-750-M	78

Continued on next page

*Conditions for preparing Compound **3.1** were provided by Takeda Pharmaceutical Company Limited. See Section 3.4 for more information.

Entry[a]	CIP (x equiv)	NH_4Cl (y equiv)	Surfactant	%Yield[b]
5	2	4	TPGS-750-M	92[c]
6	3	2	TPGS-750-M	78(72[c])
7	**3**	**3**	**none[e]**	**99[c]**
8	4	3	Savie	>99[d]
9	3	3	Coolade	>99[d]
10	2	3	SDS	70[d]
11	2	4	EtOAc[e,f]	8[d]

[a] Reactions run on a 0.25 mmol scale. [b] Isolated yield. [c] Yield determined via qNMR using 1,3,5-trimethoxybenzene as an internal standard. [d] Percent conversion determined via ratio of 1H NMR integrations for the product and starting material. [e] No surfactant utilized. [f] No H_2O utilized.

It is worth noting that before conducting investigations on a potential rate difference between the two conditions of with and without surfactant, it was observed that not only was the product amine unstable under air,* the decomposition during workup was seen to be significantly accelerated for reactions run with surfactant reactions. It was not readily obvious why this was the case, and, with the on-water reactions being simpler to handle, we proceeded with this method. I hypothesized that potentially the redox-active dihydroxyquinone moiety of TPGS-750-M played a contributing factor in facilitating the oxidation of the amine. Figure 3.3 depicts a potential pathway.† Nonetheless, further investigations are required to establish the validity of this hypothesis.

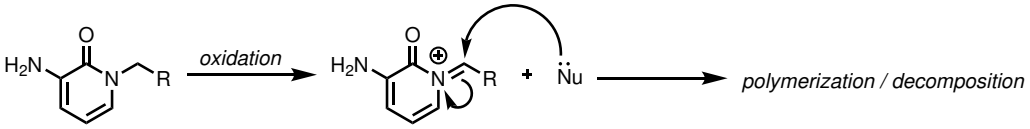


Figure 3.3: Potential pathway of decomposition for compound **3.2**.

*The amine, when exposed to air for a certain period of time, was seen to change color, and the NMR of this material was seen to contain new, unknown peaks.

†Discussions and hypothesizing with former group member and friend, Dr. David Fialho, helped to clarify this issue.

3.2.2 Use of 2-pyridyl Thioester Intermediate to Form First Amide Bond

To convert carboxylic acids to their corresponding derivatives typically requires harsh conditions. For example, carboxylic acids can be activated via conversion to the corresponding acyl chloride using toxic reagents like thionyl chloride or oxalyl chloride.* Another option is to activate the carboxylic under milder conditions with N,N'-dicyclohexylcarbodiimide (DCC); however, this coupling agent is also considered highly toxic. In the original medicinal chemistry route for *ZED1227*, Büchold *et al.* utilize HATU† for establishing a key amide bond (Fig. 3.2) in a stereoretentive manner at moderate temperatures (*e.g.*, 40 °C). Nevertheless, HATU is considered problematic as it is a serious immune sensitizer and is typically utilized in DMF.

In a significant improvement upon these more traditional methods, work from our group demonstrated that the use of benign dipyridyl dithiocarbonate (DPDTC) allows one to convert carboxylic acids to the activated 2-pyridyl thioester under neat conditions.[27] Application of an amine to this thioester in EtOAc then readily affords the corresponding amide in a highly sustainable fashion. Naturally, implementation of this green protocol was sought for establishing the amide bonds needed for this synthesis.

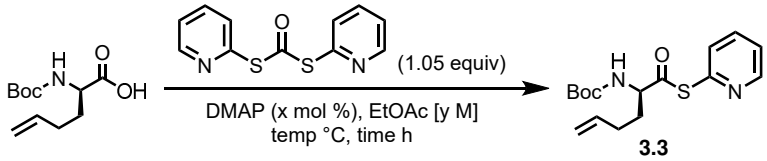
Direct implementation of the neat thioester formation method, however, was anticipated to not be amenable for the optically active non-canonical amino acid being employed. Work from our labs following the initial disclosure of the DPDTC protocol demonstrated that, to maintain the enantio-integrity of such a substrate, dilution with EtOAc, as well as a lower

*Use of oxalyl chloride produces highly toxic carbon monoxide gas. Thionyl chloride produces sulfur dioxide, which is also toxic, but less severely so.

†1-[Bis(dimethylamino)methylene]-1H-1,2,3-triazolo[5-b]pyridinium 3-oxid hexafluorophosphate.

temperature, are required for generating the thioester.[39] Of course, diminished reaction kinetics are observed under such conditions, so the introduction of a small amount of the nucleophilic catalyst, dimethylaminopyridine (DMAP), is also necessary.* With these insights from prior work in hand, we optimized the temperature, time, and DMAP loading for the non-canonical amino acid used in this synthesis (Table 3.2). Ultimately found was that 10 mol % DMAP at 35 °C in 0.5 M EtOAc provided compound **3.3** in >99% qNMR yield (Table 3.2, entry 5).

Table 3.12: Thioester Formation Optimization[62]



3.3

Entry[a]	DMAP (x equiv)	EtOAc [y M]	Temp (°C)	Time (h)	% Yield[b]
1	5	0.5	35	24	>99
2[d]	5	0.5	30	24	91
3	7.5	0.5	35	24	99
4	10	0.5	35	9	65
5	**10**	**0.5**	**35**	**16**	**>99**
6	10	0.5	35	24	94
7	10	neat	60	6	messy[c]

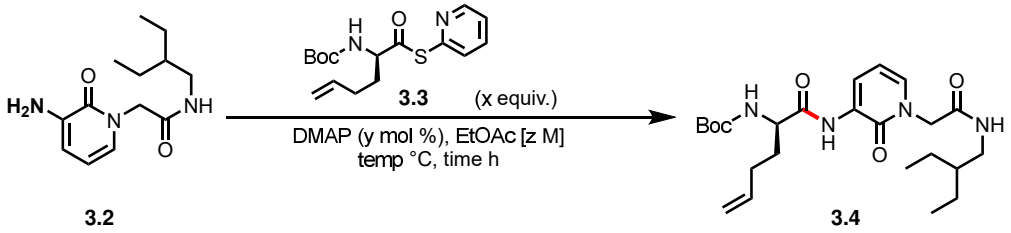
[a] Reactions run on a 0.15 mmol scale. [b] Yield determined via qNMR using 1,3,5-trimethoxybenzene as an internal standard. [c] Qualitative assessment based off TLC of crude reaction mixture.

With a method for effectively forming the thioester (compound **3.3**), conditions for coupling it with compound **3.2** to form the desired amide bond were then screened. Table 3.3 demonstrates the screening reactions done to ascertain the optimum here. Specifically, various thioester loadings, temperatures, DMAP loadings, concentrations, and reaction times were evaluated. It is noted that the previously discussed risk of epimerization was originally found

*Some substrates are still sluggish at neat conditions and necessitate the use of DMAP.

to be mostly the result of the thioester formation step.[39] The findings here support this assertion: our optimized conditions of 1 molar at 55 °C giving >99% qNMR yield of compound **3.4** with complete retention of the desired stereochemistry (>99 %ee observed via chiral HPLC).

Table 3.13: Optimization for First Amide Coupling[62]



Entry[a]	x equiv	DMAP (y mol %)	Conc. [z M]	Temp (°C)	Time (h)	%Yield[b]	%ee[c]
1	1	none	0.5	35	16	83	n.d.
2	1.1	none	0.5	35	16	89	n.d.
3	1.25	none	0.5	35	16	>99	n.d.
4	1.5	none	0.5	35	16	98	n.d.
5	**1.05**	**10**	**1**	**55**	**16**	**>99**	**>99**
6	1.1	5	0.5	35	8	91	97
7	1.1	5	1	35	8	99	98.5
8	1.1	5	2	60	8	65	>99
9	1.1	5	0.5	35	17	70	n.d.
10	1.1	5	0.5	35	17	96	>99

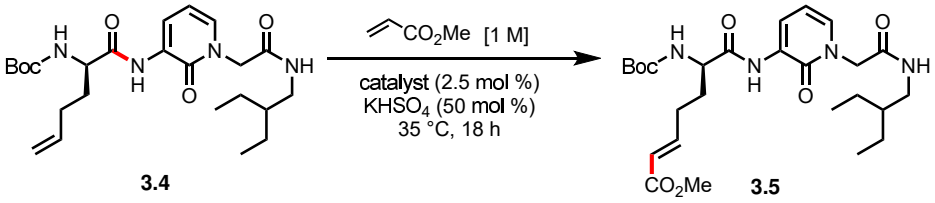
[a] Reactions run on a 0.15 mmol scale. [b] Yield determined via ^{1}H qNMR using 1,3,5-trimethoxybenzene as an internal standard. [c] Percent enantiomeric excess is determined via HPLC by (see experimental data section of Chapter 3 for more information regarding how HPLC chromatograms were obtained).

3.2.3 Installing *ZED1227*'s Unsaturated Methyl Ester

As discussed, a key behavior of *ZED1227* that contributes to its clinical efficacy is its strong inhibitory effect on the T2G enzyme. This is due in large part to the irreversible binding of the drug to the enzyme's active site as the cysteine residue of T2G's catalytic triad forms a covalent bond with the substrate. Specifically, the thiol of cysteine performs a 1,4 addition to the drug's

Michael acceptor.[10] For installing this crucial moiety, we looked to implement a Grubb's olefin metathesis under micellar conditions.[84] Initial investigations to this end, however, showed sluggish reaction times (>24 h) and non-ideal *E:Z* selectivity for a range of Grubbs II catalysts, surfactants, and cosolvents. This is perhaps due in some part to the water solubility of methyl acrylate. Such solubility would see some exclusion of the acrylate from the lipophilic micellar core and, thus, could diminish reaction kinetics and yield. Nonetheless, it was not readily obvious as to why the reaction didn't perform under these micellar conditions.

Table 3.14: Optimization for Grubbs Metathesis[62]



3.4 **3.5**

Entry[a]	Catalyst	% Conversion[b]	*E:Z*[c]
1	Grubbs II	>99	95:5
2[d]	**Hoveyda-Grubbs II**	**93**	**97:3**
3	M101	trace	n.d.
4	Neolyst M2	73	95:5

[a] Reactions run on a 0.15 mmol scale. [b] Determined by the ratio of peak integrations on HPLC for the product and starting material. [c] Determined by the ratio of peak integrations on HPLC for the *E* and *Z* isomers. [d] Run without the addition of $KHSO_4$.

The next available method that stood out was to use the methyl acrylate neat. Given its high vapor pressure, there was an anticipated ease of recovery by distillation that would make the method more attractive from the standpoint of reducing solvent waste. Initial experiments showed clear efficacy under such conditions, so various Grubbs II catalysts were then screened. Noted is that the lowest permissible concentration was seen to be 1 M for this scale of 0.15 mmol, and that higher temperatures are known to have a deleterious effect on *E:Z* selectivity.

Therefore, these variables were not modified or screened to any further extent. Ultimately, Grubbs Hoveyda II (see Table 3.4) gave the most desirable combination of conversion (93%) and selectivity (97:3 *E:Z*). It is noted that a lowering of the ruthenium loading was not pursued as, at scale, ethylene poisoning precludes process chemists from implementing anything less than 2.5 mol %.*

3.2.4 Cleavage of *N*-Boc and 2nd Amidation

The final steps needed to accomplish the synthesis involved freeing up the Boc-protected amine, and then implementing it in the final amide coupling. Cleavage of this Boc group involved a straightforward screening of HCl in various organic solvents. From this, the ammonium salt was efficiently obtained with HCl in green isopropyl alcohol. With the penultimate product in hand, we were then ready to implement the same 1-pot thioester amidation protocol that saw success in the 2nd/3rd step of this route (see Tables 3.2 and 3.3).

The efficacious implementation of this method earlier, however, was not a foreshadowing for its use in this final step. Though the *N*-methylimidazole carboxylic acid was smoothly converted to the thioester under our neat DPDTC conditions at 60 °C, it failed to adequately couple with the corresponding amine. Attempts at optimizing this amidation involved extensive assaying of a broad scope of reaction conditions. This included various bases, solvents, temperatures, orders of addition, rates of addition, and different stoichiometries of various reagents. In each case, conversion to the API was poor, and multiple side products were observed via HPLC

*A net flow of inert gas is implemented in order to purge ethylene from the reactor. Nevertheless, 2.5 mol % was seen to be the lower bound.

analysis of the crude reaction mixture. Another attempt at performing this amidation sustainably involved the use of 1-propanephosphonic anhydride (T3P) in EtOAc. This, unfortunately, was not seen to be any more effective than the methodology first tried. Ultimately, the more traditional method of using the acyl chloride with DIEA* was able to produce *ZED1227* in good yield (76% isolated).

It was not obvious, nor was it trivial to determine, why the thioester amidation was ineffectual for this substrate pair. The complex mixture of side products was challenging to parse, and so no direct insights could be readily obtained.† Nonetheless, I hypothesized a few different possible degradation pathways (Figure 3.4). First, thiols are known to readily perform conjugate addition to Michael acceptors. This, as is stated above, is the reason behind *ZED1227*'s irreversible binding to T2G. Given this fact, it is worth considering that the main byproduct of these thioester-facilitated amidations is 2-mercaptopyridine (2-MP). Though this is a relatively non-nucleophilic thiol,‡ it is conceivable that this side reaction is possible and could contribute to some degradation in yield for the desired product.

Secondly, the generation of the nucleophilic amine following *N*-Boc deprotection and deprotonation, could lead to a competing reaction where the amine also undergoes this aforementioned conjugate addition to form a pyrrolidine (see Figure 3.4).§ Our collaborators at Takeda noted that they didn't observe this side reaction when using the acyl chloride, but it is possi-

*This strategy was provided by Takeda Pharmaceutical Company Limited

†Further extensive analytical work to potentially discern these different components could not have been reasonably accomplished within the time frame of the project.

‡The poor nucleophilicity of 2MP is due to it being both a thiophenol and, as the thiol resides in the electron-poor meta position of the pyridine heterocycle.

§This potential side reaction was brought to our attention by Takeda.

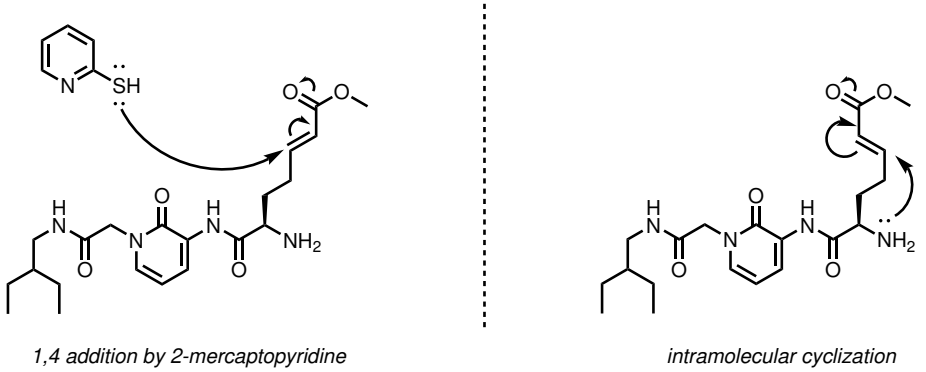


Figure 3.4: Potential Side Reactions for Final Amidation Step

ble that the kinetics for the 1-pot thioesterification/amidation were slow enough such that this cyclization became a competing reaction.

A further important observation to be made is that the acyl chloride is implemented as the HCl salt. This is by virtue of converting the carboxylic acid with thionyl or oxalyl chloride without an external base, as the basic nitrogen at the 3 position acts as such. Beyond providing a solid salt and thus simplifying handling, in solution, it prevents that nucleophilic nitrogen from causing dimerization or polymerization. For the 2-pyridyl thioester analog, it is noted that such reactivity was not observed.* Naturally, this is due to the thioester being less electrophilic than the acyl chloride. As it pertains to the mix of products witnessed in the final amidation reaction: this demonstrated lack of reactivity supports the reasoning that more elevated temperatures (relative to those used with the acyl chloride) were likely needed, but that in doing so, side reactivity would likely also increase.

*In solution at room temperature.

3.2.5 Scale Up and Sequence

Having each step optimized, I pursued the application of these conditions in a scale-up and sequence toward *ZED1227* (see Figure 3.5 for the final sequence). Run at a 9.5 mmol scale, step 1 gave compound **3.2** in 91% yield following simple filtration through Celite, extraction from the mother liquor with EtOAc, and then concentration *in vacuo*. Compound **3.3** was generated at 2 mmol under the developed optimized conditions, and the solid amine (compound **3.2**) was added to this same pot. Poor stirring was remediated with the addition of 10 v/v % of MeCN, and then the reaction was allowed to proceed to completion. The resulting amide (compound **3.4**) was recovered at 93% yield with high enantiopurity (>99 %ee) via a basic workup with EtOAc to remove residual 2-MP.

Prior experimentation had shown that 2-MP was a very potent poison for the Grubbs catalyst*. Therefore, for this scale-up and sequence, copper iodide† was included in the metathesis reaction as a prophylaxis to this poisoning (the iodide is also known to have a stabilizing effect on the catalyst).[84] Another modification to the conditions came by way of a dilution to 0.125 M of the methyl acrylate due to poor initial stirring. Nonetheless, this reaction gave the metathesis product in 92.6% yield with good selectivity (97:3 *E*:*Z*)‡ after simple filtration and washing of the filter cake with diethyl ether. Also noted is that 82% of the unreacted acrylate was recov-

*A screening reaction using pure amide (compound **3.4**) with a doping of 10 mol % of 2-MP, was seen to kill the reactivity of the Hoveyda-Grubbs catalyst in the metathesis step.

†Copper iodide is a known additive for Grubbs metatheses as it helps activate these catalysts by abstracting the phosphine from the metal center. Of course, there is no phosphine to abstract from Hoveyda-Grubbs II, but copper iodide was still included for the discussed reasons.

‡Determined by HPLC.

ered by distillation, thus attenuating some of the negative impact of this reaction dilution on the process's overall E-Factor.

The ammonium salt (compound **3.6**) was then obtained under our optimized *N*-Boc deprotection procedure using HCl in IPA, with the solvent then being decanted away from the solid product. The salt was washed with diethyl ether to give compound **3.6** as a white powder in 91% yield. Finally, this product then underwent the established final amidation protocol with the HCl salt of *N*-methylimidazole acyl chloride and Hünig's base in acetonitrile to give the final API as a white solid in 76% yield (55% overall in 6 steps).* The final compound (**3.7**) was seen to be of acceptable purity (>98% via HPLC), and was seen to have maintained total enantiopurity (>99% ee) since the original installment of the chiral center in the first amidation step.

*For the literature comparison route (Figure 3.1), the yield for just the final step was reported to be 45%.

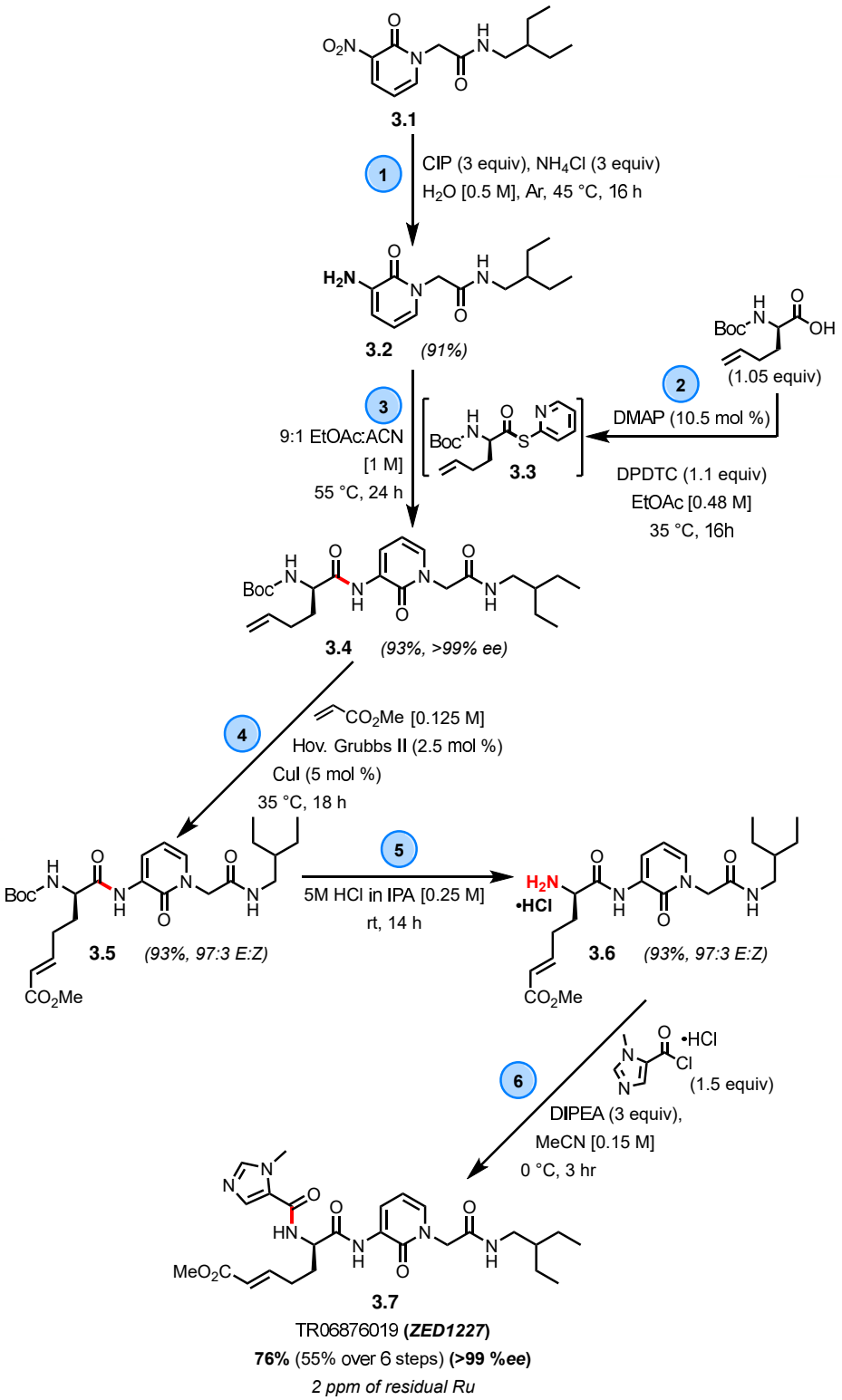


Figure 3.5: Green Synthesis of *ZED1227*

3.3 Conclusion

The original route to *ZED1227* (Figure 3.1) by Büchold and colleagues provided the material needed for structure-activity relationship (SAR) studies and provided the material needed for establishing the therapeutic efficacy of the drug.[10] Nonetheless, as discussed, such initial syntheses for medicinal chemistry studies are often inefficient and not practically scalable. In the preparation of this TG2 inhibitor, there were several issues that made their route no exception. This included the employment of toxic solvents, harsh conditions, unfavorable coupling reagents, and a high metal loading step. Moreover, their route suffers from inefficient yields and the generation of stoichiometric byproducts. These drawbacks not only set the stage for optimizing the synthesis of *ZED1227* for efficiency and safety, but also provided the opportunity to do so with a particular focus and emphasis on sustainability.

In collaboration with Takeda, retrosynthetic analysis of the drug elucidated the potential implementation of our own research group's green methodologies to establish a markedly more efficient and sustainable synthesis of this emergent celiac therapeutic. In developing the route, much of the plan established by the retrosynthesis came to fruition.[62] Our CIP nitro reduction smoothly yielded compound **3.2** in an on-water fashion. From here, I activated the non-canonical amino acid by converting it to the corresponding thioester (compound **3.3**), and then, in the same pot, coupled it with the amine obtained in the previous step. Adhering to our prior findings of preventing epimerization in such thioester amidation reactions, the chiral cen-

ter of the amino acid was observed to be entirely maintained in the resulting amide product (compound **3.4**).

Though the following olefin metathesis wasn't seen to be as ideal as hoped under micellar conditions, the implementation of a "neat" Grubbs metathesis in methyl acrylate provided the desired α,β-unsaturated ester in good yield and with good selectivity for the desired *E* isomer. Additionally, a recovery study of the methyl acrylate demonstrated the ease by which unreacted material could be recovered and, thus, recycled. Subsequently, the *N*-Boc group was trivially cleaved with HCl in green IPA to give the penultimate product as the ammonium salt.

As discussed above, the development of the efficient and direct synthesis thus far stood in contrast to the challenges encountered in the final step. With facile conditions producing the thioester from *N*-methylimidazole carboxylic acid, it was anticipated that adding this to the free-based amine* (compound **3.6**) would readily form the final amide bond. Why this was ultimately found to not be the case presents an interesting topic of potential future work. Nevertheless, the implementation of the acyl chloride in recoverable acetonitrile concluded the synthesis in a straightforward manner and yielded the drug with no observable epimerization.

In all, the synthesis makes marked improvements over the medicinal chemistry route. Beyond being fewer steps and with higher yields, solvents utilized include water, ethyl acetate, and IPA. No harsh coupling reagents are utilized, no harsh or cryogenic conditions are needed, no serious pyrophorics are implemented, a significantly more efficient metal loading is used, levels of side products are negligible, and several reagents implemented (*e.g.*, methyl acrylate)

*Free-based *in situ*.

are readily recyclable. Furthermore, each step (save the final)* provides material of sufficient purity without performing flash chromatography and, thus, obviates the need for expensive or wasteful isolation procedures. Finally, it is noted that this green synthesis retains an E-factor that is over tenfold lower than the original synthesis (see Table 3.5).[62]

Table 3.16: Optimization for Grubbs Metathesis[62]

Prior Literature[10]	**Comparison Metric**	**This Work**[62]
-78 °C	Most Extreme Temperature Employed	55 °C
DMF, benzene, DCM, dioxane, MeOH	Solvents Utilized	Water, IPA, MeCN, EtOAc
8	Total Number of Steps	6[a]
HATU, HOBt/TBTU	Amide Coupling Reagents Used	DPDTC, acyl chloride
Wittig Olefenation	Olefin Metathesis Method	Neat Grubbs Metathesis
10% Pd/C, DIBAL-H	Reducing Agents Used	CIP in/on Water
289[b,c]	E-Factor[77]	28
45% (only considering the final step)	Isolated Yield	55% (over all six steps)

[a] Includes preparation of compound **3.1**. [b] Value does not include their preparation of benzyl-1-(2-(2-ethylbutylamino)-2-oxoethyl)-2-oxo-1,2-dihydropyridin-3-ylcarbamate in order to draw a more accurate comparison with the route reported herein. [c] Readily recoverable solvents are not counted toward the overall E-factor. Moreover, due to the high dependence on scale, materials and solvents used for work up procedures are also not included. See SI for specific E-factor calculations.

3.3.1 Closing remarks

This project forged me into a better chemist in the same manner that a crucible forges new alloys. Air sensitive products, challenging workups, an epimerization-prone stereocenter, limited and expensive starting materials—all of these factors and more, contributed to an enhancement of my synthetic skills and provided a robust exercise for perseverance and endurance in the lab. Naturally, the assistance of my coauthors and collaborators made the project possible and allowed me to focus on the toughest challenges of the project. In the end, our work not only

*The final product was isolated by reverse phase flash chromatography. This was necessitated by the reaction being done on a small scale and, thus, not providing enough material for an efficient recrystallization.

provided remarkable improvements to the preparation of the drug, but it also stands as another precedent for the successful implementation of highly sustainable methods for synthesizing challenging targets.

3.3.2 Acknowledgements and Noted Contributions

This project was both made possible by and carried out in collaboration with Takeda Pharmaceutical Company Limited. Takeda scientists Dr. Joyce Leung, Dr. Erik Phipps and Dr. Mathew Campbell, specifically, made significant contributions to the project. This includes guidance during the retrosynthetic analysis, optimization of the nitro reduction step, optimization of the methyl acrylate olefin metathesis, and guidance during optimization of conditions for the last amidation step. Furthermore, they provided the conditions for synthesizing Compound **3.1**, conditions for the acyl chloride amide coupling, as well as the various HPLC methods needed for analysis of each compound. Financial support (including providing critical reagents) by Takeda Pharmaceutical Company Limited is especially acknowledged with thanks.

Thanks is given to Jordan Yirak and Max Baumann for their assistance in reaction optimization as well as for their collection of important analytical data. Early optimization work done by Kaitlyn Freiberg is acknowledged.

3.4 Experimental Data and Information.

3.4.1 General Information

NMR

^{1}H and ^{13}C NMR were recorded at 25 °C on either a Bruker Avance III HD 400 MHz, a Bruker Advance NEO 500 MHz, or on a Varian Unity Inova 500 MHz in $CDCl_3$ with residual $CHCl_3$ (^{1}H = 7.26 ppm, ^{13}C = 77.26 ppm) or residual $(CH_3)_2SO$ (^{1}H = 2.50 ppm, ^{13}C = 39.52 ppm). Chemical shifts are reported in parts per million (ppm) and coupling constants (J values) are reported in Hz. Peak splitting is reported in the following fashion: singlet (s), broad singlet (bs), doublet (d), triplet (t), quartet (q), pentet (p), and multiplet (m).

Reagents

All procured chemical reagents were utilized directly from vendors without any further purification. EtOAc, hexanes, MeOH, DCM, Et_2O, pentane, and acetonitrile were obtained from Fisher Scientific. HPLC grade solvents were purchased from Fisher Scientific and used as is. Anhydrous solvents were obtained via drying over activated 4 Å molecular sieves. Where needed, volatile solvents were degassed via freeze-pump-thaw on an argon-vacuum Schlenk manifold. Water was degassed via sparging with argon gas overnight at rt. Deuterated dimethyl sulfoxide was purchased from Sigma-Aldrich. Deuterated chloroform was purchased from Cambridge Isotope Laboratories. 4 Å molecular sieves were purchased from Fisher Scientific and were activated at 200 °C under vacuum before use. 2-Ethylbutan-1-amine hydrochloride and 3-nitro-1,2-dihydropyridin-2-one were purchased from Combi Blocks Int. and used as

received. 2-Mercaptopyridine was purchased from Combi Blocks Int. and recrystallized from EtOAc in order to remove any 2,2-dipyridyldisulfide impurity. Sodium carbonate, potassium bisulfite, and anhydrous sodium sulfate was purchased from Fisher Scientific and used as received. Chloroacetyl chloride was purchased from Sigma-Aldrich and stored at 0°C. Carbonyl iron powder (CIP), ammonium chloride, and tetrabutylammonium iodide were purchased from Sigma-Aldrich and used as received. 1-Methyl-1*H*-imidazole-5-carboxylic acid was purchased from Ambeed Inc. and used as received. (*S*)-*N*-Boc-2-(3'-Butenyl)glycine was purchased from Ambeed Inc. and gifted by Takeda Pharmaceutical Company and was stored at -20 °C. Hoveyda-Grubbs Catalyst®M720 (Hoveyda-Grubbs II) was purchased from Ambeed Inc. and was stored at -20 °C under an inert atmosphere of argon. Triphosgene was purchased from A K Scientific and used as received. 4-Dimethylaminopyridine was purchased from Acros Organics and used as received. Methyl acrylate was purchased from Sigma-Aldrich and used as received. 5.0-6.0 molar HCl in isopropanol was purchased from Oakwood Products, Inc. and was stored at 0 °C. Diisopropylethylamine was purchased from Oakwood Products, Inc. and was dried over activated 4 Å molecular sieves for 24 hours before use. *N*-Methylmorpholine was purchased from Thermo Fisher Scientific and was dried over activated 4 Å molecular sieves for 24 hours before use. TPGS-750-M was obtained from PHT International (TPGS-750-M is also available from Sigma-Aldrich catalog #733857). Thin Layer Chromatography (TLC) was performed using Silica Gel 60 F254 (Merck, 0.25mm thickness) and developed plates were visualized under a UV lamp (254 nm). Developed TLC plates were further analyzed via Ceric Ammonium Molybdate Stain, Potassium Permanganate Stain, or Bromo-Cresol Green Stain, and subsequently developed using a heat gun. Manual flash chromatography was performed utilizing Silicycle Silicaflash P60 unbonded grade silica. Automatic flash chromatography was performed utilizing a Teledyne Combi Flash and Silica Gel P60 (Teledyne). High Resolution Mass Spectrums

(HRMS) were obtained on a Waters GCT Premier GC TOF, Agilent 6230 TOF LC/MS System, or Xevo G2-XS UPLC-QTOF.

Generating a Solution of 2 wt % TPGS-750-M / H_2O

To a clean 100 mL round bottom flask charged with a PTFE coated stirbar was added 2 g of TPGS-750-M.[49] The flask was then fitted with a septum and attached to a vacuum/argon manifold via a needle through the septum. The flask was then subjected to three cycles of vacuum and then backfilling with argon. Under an atmosphere of argon, to the flask was then added 98 mL of degassed HPLC grade water. Still attached to the manifold and under an atmosphere of argon, the flask was fitted to a stir plate and vigorously stirred for 12 h. The flask was kept under a constant atmosphere of argon.

Dipyridyldithiocarbonate (DPDTC)

Dipyridyldithiocarbonate (DPDTC) was synthesized according to previously reported procedures[27] and was purified via recrystallization in EtOAc/hexanes to afford a white powder. Purity was confirmed via NMR. ***CAUTION:*** *Triphosgene has high acute toxicity. Triphosgene exists as a crystalline white solid that readily sublimates under standard atmospheric conditions and further produces phosgene gas upon exposure to moisture. It must be kept and handled in a well-ventilated fume hood.*

1-Methyl-1H-imidazole-5-carbonyl chloride hydrochloride

1-Methyl-1H-imidazole-5-carbonyl chloride hydrochloride was synthesized according to previously reported procedures[14] with no modifications. The obtained solid was confirmed pure by NMR, and kept and handled in a glovebox under an inert atmosphere of argon.

3.4.2 Synthetic Scheme

Retrosynthetic Route to *ZED1227*

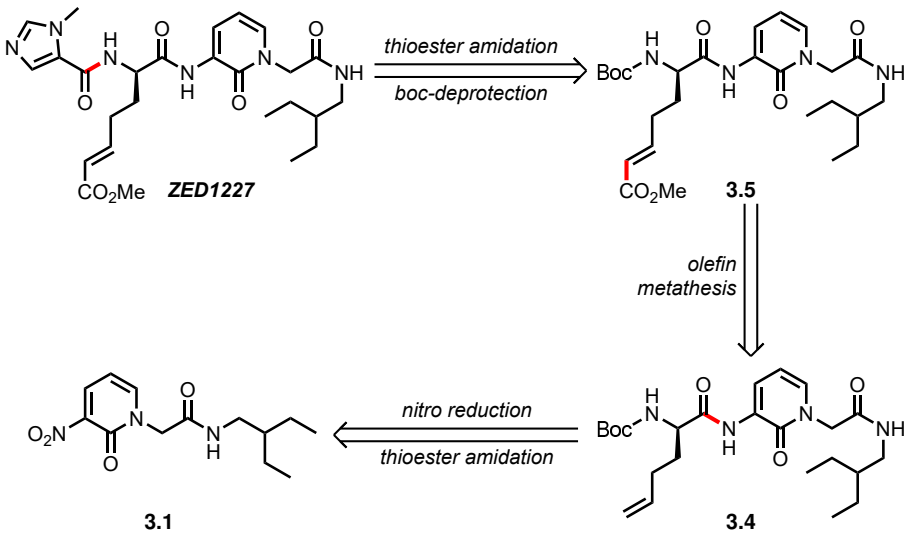


Figure 3.6: Retrosynthetic Analysis for *ZED1227*.[10]

Final Overall Route to *ZED1227*

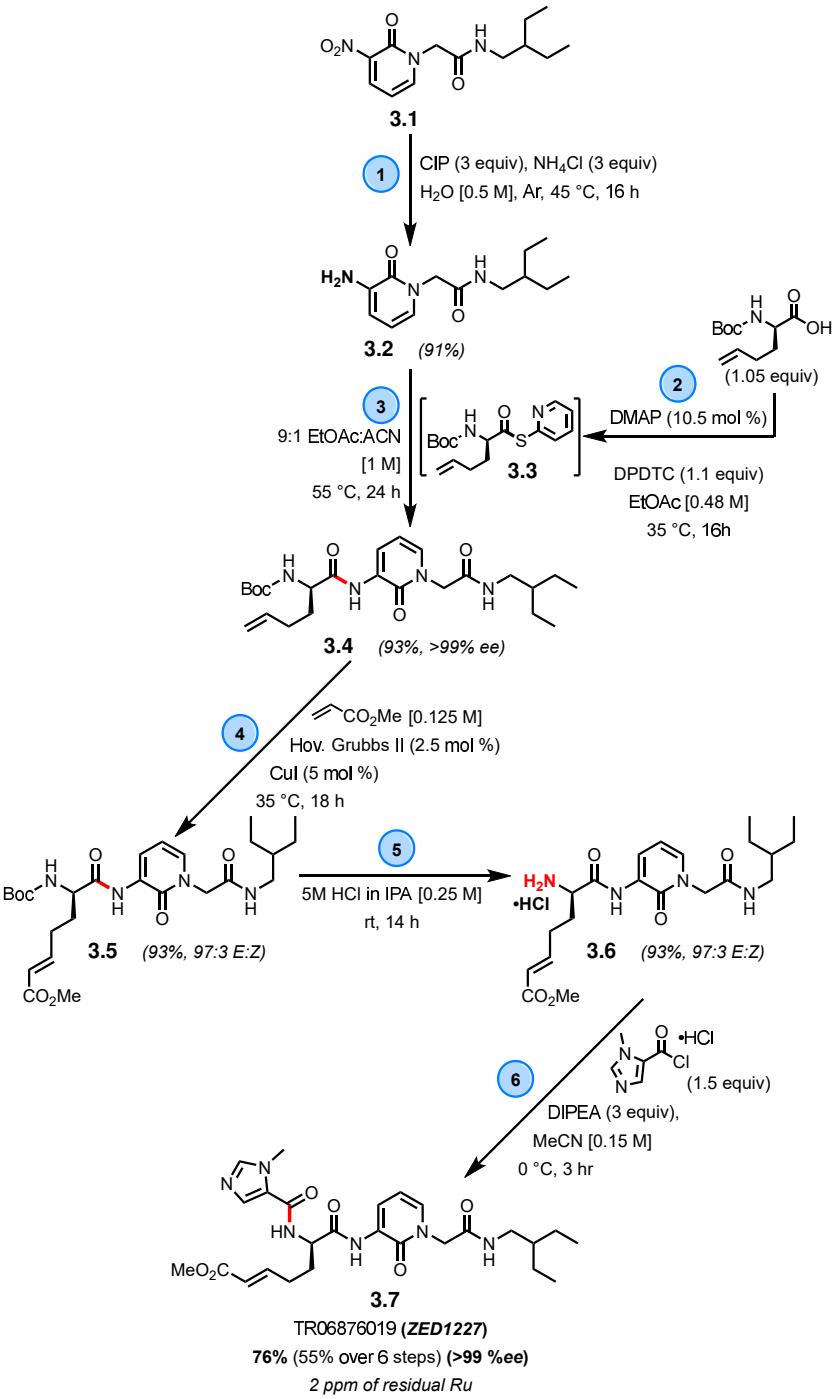
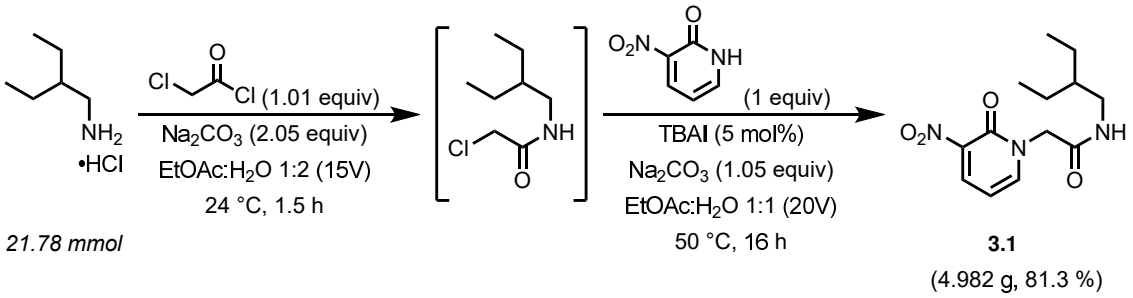


Figure 3.7: Green Synthesis of *ZED1227*

3.4.3 General Procedures:

Preparation of 3.1: *N*-(2-ethylbutyl)-2-(3-nitro-2-oxopyridin-1(2*H*)-yl)acetamide



(*NOTE: this procedure was developed by and made available to us by Takeda Pharmaceutical Company Limited.*) To a 100 mL round bottom flask charged with a PTFE coated magnetic stir bar was added 2-ethylbutan-1-amine hydrochloride (21.78 mmol, 1.00 equiv, 3.00 g) and sodium carbonate (44.65 mmol, 2.05 equiv, 4.77 g). To this, EtOAc (15 mL) and water (30 mL) were added, and the mixture was stirred at rt until homogeneous. The flask was then cooled in an ice bath to 0 °C, and then chloroacetyl chloride (22.00 mmol, 1.01 equiv, 1.75 mL) was added drop-wise via syringe. After the addition, the reaction was warmed to rt and then stirred for 1.5 h. Subsequently, the stirring was stopped, and the crude reaction mixture transferred to a 250 mL separatory funnel. Complete transfer was ensured by rinsing the flask with 30 mL of water and 3 mL of EtOAc. In the separatory funnel, the aqueous layer was observed to be white with precipitate, and the organic layer was colorless. The aqueous layer was drained, and to the separatory funnel, 30 mL of water was added, and the entire mixture was transferred to a 250 mL round-bottom flask charged with a PTFE coated magnetic stir bar. The separatory funnel was rinsed with additional EtOAc (15 mL) to ensure transfer and added to the reaction vial. To the reaction flask, tetrabutylammonium iodide (1.09 mmol, 5 mol %, 402.24 mg), sodium carbonate (22.87 mmol, 1.05 equiv, 2.42 g), and 3-nitro-1,2-dihydropyridin-2-one (21.78 mmol, 1.00 equiv, 3.05 g) were

weighed and added to the solution. The reaction flask was placed in an aluminum heating block set to 50 °C and stirred for 16 h. After completion of the reaction, the flask was cooled to rt. The precipitate produced in the reaction was filtered and then washed with EtOAc (2 x 15 mL). The filter cake was then washed with ice-cold water until the washes run clear. The obtained solid was dried on high vac overnight at 40 °C to afford 4.982 g (81.3%) of compound **3.1** as a white/light-yellow powder (R_f = 0.39; 100% EtOAc).

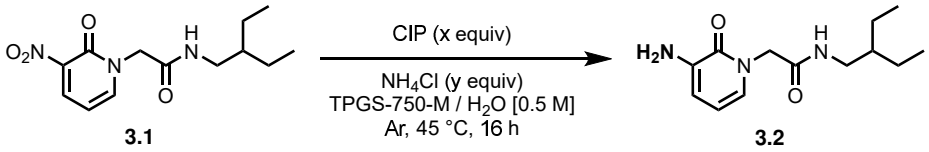
3.4.4 Optimization Data

Nitro Reduction to Afford Compound 3.2

Representative Procedure: *CIP and NH_4Cl equivalents screen.*

To a 1-dram vial charged with a PTFE coated magnetic stir bar was added *N*-(2-ethylbutyl)-2-(3-nitro-2-oxopyridin-1-(2*H*)-yl)acetamide (**3.1**) (0.25 mmol, 1 equiv, 70.32 mg), carbonyl iron powder (CIP) (0.75 mmol, 3 equiv, 41.9 mg), and NH_4Cl (0.75 mmol, 3 equiv, 40.1 mg). The vial was capped with a rubber septum, the septum secured with Teflon™ tape and attached to an argon/vacuum manifold via a needle through the septum. The vial then underwent three cycles of vacuum, and then backfilling with argon. To the vial was then added 0.5 mL of degassed 2 wt % TPGS-750-M / H_2O, after which the vial was placed on an aluminum heating block set to 45 °C and stirred for 16 h. Subsequently, the vial was allowed to cool to rt, the reaction mixture was passed through a pad of Celite, and the Celite was then rinsed with EtOAc (3 x 1 mL). The collected aqueous phase was then extracted with EtOAc (4 x 1 mL). The extracts were combined and then dried with anhydrous Na_2SO_4 before being concentrated *in vacuo*. The residue was dissolved in 0.6 mL of deuterated DMSO. 1,3,5-Trimethoxybenzene (0.5 or 1 equiv) was added, and the qNMR yield was subsequently determined via ^{1}H NMR.

Table 3.16: Nitro Group Reduction Optimization[62]



3.1 3.2

Entry[a]	CIP (x equiv)	NH_4Cl (y equiv)	Surfactant	%Yield[b]
1	5	3	TPGS-750-M	94
2	4	3	TPGS-750-M	>99
3	3	3	TPGS-750-M	93
4	2	3	TPGS-750-M	78
5	2	4	TPGS-750-M	92[c]
6	3	2	TPGS-750-M	78(72[c])
7	**3**	**3**	**none[e]**	**99[c]**
8	4	3	Savie	>99[d]
9	3	3	Coolade	>99[d]
10	2	3	SDS	70[d]
11	2	4	EtOAc[e,f]	8[d]

[a] Reactions run on a 0.25 mmol scale. [b] Yield determined via qNMR using 1,3,5-trimethoxybenzene as an internal standard.

DPDTC Thioesterification Afford Compound 3.3

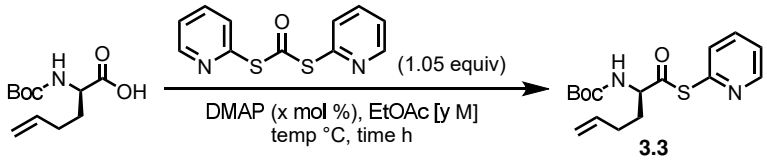
Representative Procedure: DMAP screening.

To a flame-dried 1-dram vial charged with a PTFE coated magnetic stir bar was added (*R*)-2-((t-butoxycarbonyl)amino)hex-5-enoic acid (0.150 mmol, 1 equiv, 34.4 mg), DPDTC* (0.158 mmol, 1.05 equiv, 39.1 mg), and DMAP (0.015 mmol, 10 mol %, 1.8 mg). The vial was fitted with a septum, and the septum was secured via Teflon™ tape. The vial was attached to a vacuum/argon manifold via a needle through the septum, and the vial was subjected to three cycles of vacuum, then backfilling with argon. Subsequently, anhydrous, degassed EtOAc was added to the vial *via* syringe through the septum. The vial was detached from the manifold, and the reaction was placed in an aluminum heating block set to

*Dipyridyl dithiocarbonate.

35 °C and stirred for 24 h. Subsequently, the reaction vial was removed from the heating block and allowed to cool to rt. The solvent was removed *in vacuo* and the crude residue was dissolved in 0.6 mL of deuterated DMSO. 1,3,5-Trimethoxybenzene (0.5 or 1 equiv) was added, and the qNMR yield was subsequently determined via ^{1}H NMR.

Table 3.17: Thioester Formation Optimization[62]



3.3

Entry[a]	DMAP (x mol%)	EtOAc [y M]	Temp (°C)	Time (h)	% Yield[b]
1	5	0.5	35	24	>99
2	5	0.5	30	24	91
3	7.5	0.5	35	24	99
4	10	0.5	35	9	65
5	**10**	**0.5**	**35**	**16**	**>99**
6	10	0.5	35	24	94
7	10	neat	60	6	messy[c]

[a] Reactions run on a 0.15 mmol scale. [b] Yield determined via qNMR using 1,3,5-trimethoxybenzene as an internal standard. [c] Qualitative assessment based off TLC of crude reaction mixture.

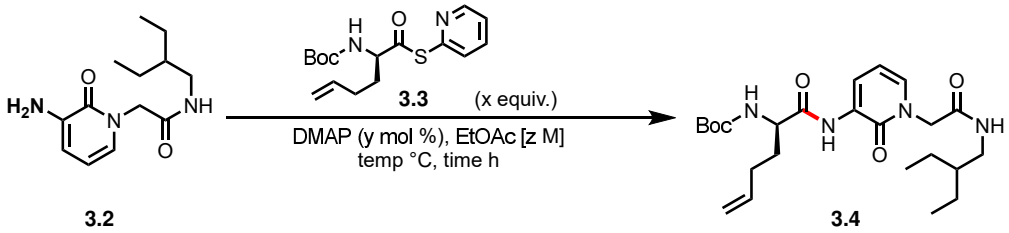
Thioester Amide Coupling to Afford Compound 3.4

Representative Procedure: *Solvent Screening*

To a flame-dried 1-dram vial charged with a PTFE-coated magnetic stir bar was added compound **3.3** (0.158 mmol, 1.05 equiv, 50.8 mg) and DMAP (0.015 mmol, 10 mol %, 1.83 mg). The vial was sealed with a rubber septum and attached to an argon/vacuum manifold via a needle through the septum and subsequently underwent three cycles of vacuum, then backfilling with argon. The vial was then removed from the manifold and brought into a glovebox under an atmosphere of argon. To the vial was then added compound **3.2** (0.15 mmol, 1 equiv, 37.7 mg). The vial was refitted with the septum,

brought out of the glovebox, and then reattached to the argon/vacuum manifold. Subsequently, anhydrous EtOAc (150 μL, 1 M) was added via a syringe through the septa. Moving rapidly so as to limit air and moisture exposure, the septa was removed, the vial was capped, and the cap was secured with Teflon™ tape. The reaction was set in an aluminum heating block set to 55 °C, and was allowed to stir at this temperature for 24 h. Conversion to compound **3.4** was confirmed via HPLC. To the vial was then added 1M NaOH (0.5 mL) and EtOAc (1 mL). The EtOAc was extracted, and the aqueous was extracted thrice more with EtOAc (1 mL aliquots). The extracts were combined, dried with anhydrous $NaSO_4$, and filtered over a cotton plug. The EtOAc was removed *in vacuo*. To the crude residue was added 1,3,5-trimethoxybenzene (0.5 or 1 equiv) as an internal standard. The crude residue was dissolved in deuterated DMSO (0.6 mL), and the qNMR yield was determined via ^{1}H NMR.

Table 3.18: Optimization for First Amide Coupling[62]



Entry[a]	x equiv	DMAP (y mol %)	Conc. [z M]	Temp (°C)	Time (h)	%Yield[b]	%ee[c]
1	1	none	0.5	35	16	83	n.d.
2	1.1	none	0.5	35	16	89	n.d.
3	1.25	none	0.5	35	16	>99	n.d.
4	1.5	none	0.5	35	16	98	n.d.
5	**1.05**	**10**	**1**	**55**	**16**	**>99**	**>99**
6	1.1	5	0.5	35	8	91	97
7	1.1	5	1	35	8	99	98.5
8	1.1	5	2	60	8	65	>99
9	1.1	5	0.5	35	17	70	n.d.

Continued on next page

Entry[a]	x equiv	DMAP (y mol %)	Conc. [z M]	Temp (°C)	Time (h)	%Yield[b]	%ee[c]
10	1.1	5	0.5	35	17	96	>99

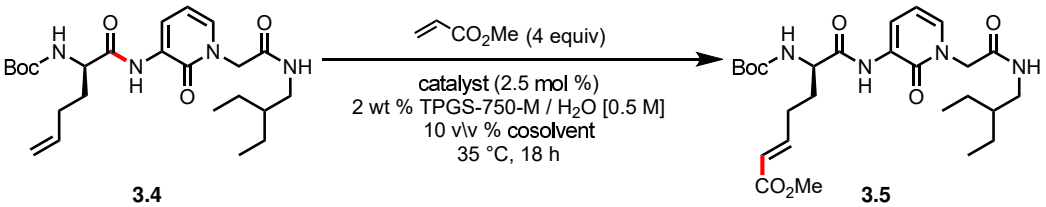
[a] Reactions run on a 0.15 mmol scale. [b] Yield determined via ^{1}H qNMR using 1,3,5-trimethoxybenzene as an internal standard. [c] Percent enantiomeric excess is determined via HPLC by (see Section 3.4.9 for more information regarding how HPLC chromatograms were obtained).

Grubbs Olefin-Metathesis to Afford Compound 3.5

Representative Procedure for Using Aqueous Surfactant: *Cosolvent Screening*

To a flame-dried 1-dram vial charged with a PTFE -oated magnetic stir bar was added compound **3.4** (0.15 mmol, 1 equiv, 69.4 mg). The vial was sealed with a rubber septum and attached to an argon/vacuum manifold via a needle through the septum and subsequently underwent three cycles of vacuum and then backfilling with argon. The vial was then removed from the manifold and brought into a glovebox under an inert atmosphere. To the vial was then added Hoveyda-Grubbs II (0.00375 mmol, 2.5 mol %, 2.3 mg). Subsequently, the vial was sealed with a rubber septum, removed from the glovebox, and the septum secured with Teflon™ tape. The vial was then reattached to the manifold, and degassed 2 wt % TPGS-750-M / H_2O (0.3 mL) was added via syringe through the septa. In the same manner, degassed THF (30 μL) was added to the crude reaction mixture. Degassed methyl acrylate (4 equiv., 54 μL) was then also added via a syringe through the septa. The vial was then placed in an aluminum heating block set to 35 °C and stirred vigorously for 24 h. The reaction mixture was allowed to cool to rt, then the crude mixture was analyzed via HPLC to determine the conversion (38%) and the ratio of *E:Z* isomers (93:7).

Table 3.19: Optimization for Grubbs Metathesis in TPGS[62]



3.4 **3.5**

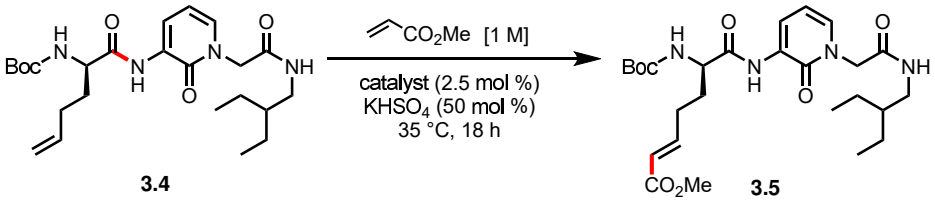
Entry[a]	Cosolvent	% Conversion[b]	*E:Z*[c]
1	none	44	96:4
2[d]	THF	38	93:7
3	toluene	49	92:8
4	MeOH	56	90:10
5	DMSO	47	92:8

[a] Reactions run on a 0.15 mmol scale. [b] Determined by the ratio of peak integrations on HPLC for the product and starting material. [c] Determined by the ratio of peak integrations on HPLC for the *E* and *Z* isomers.

Representative Procedure for Neat Method: *Catalyst Screening*

To a flame-dried 1-dram vial charged with a PTFE-coated magnetic stir bar was added compound **3.4** (0.15 mmol, 1 equiv, 69.4 mg). The vial was sealed with a rubber septum and attached to an argon/vacuum manifold via a needle through the septum and subsequently underwent three cycles of vacuum and then backfilling with argon. The vial was then removed from the manifold and brought into a glovebox under an inert atmosphere. To the vial was then added Hoveyda-Grubbs II (0.00375 mmol, 2.5 mol %, 2.3 mg). Subsequently, the vial was sealed with a rubber septum, removed from the glovebox, and the septum secured with Teflon™ tape. The vial was then reattached to the manifold, and degassed methyl acrylate (0.15 mL) was added via syringe through the septa. The vial was placed in an aluminum heating block set to 35 °C and stirred for 18 h. The reaction mixture was allowed to cool to rt, then the crude mixture was analyzed via HPLC to determine the conversion (93%) and the ratio of *E:Z* isomers (97:3).

Table 3.20: Optimization for Grubbs Metathesis[62]



3.4 3.5

Entry[a]	Catalyst	% Conversion[b]	*E:Z*[c]
1	Grubbs II	>99	95:5
2[d]	**Hoveyda-Grubbs II**	**93**	**97:3**
3	M101	trace	n.d.
4	Neolyst M2	73	95:5

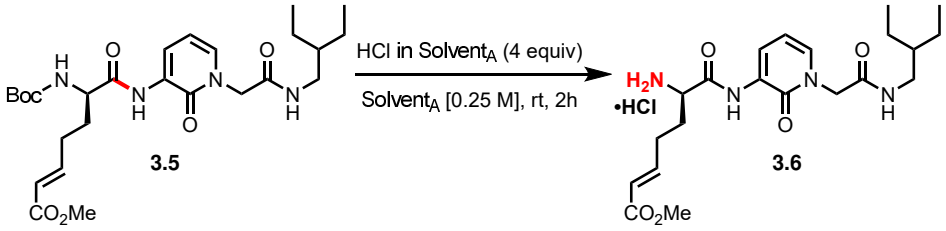
[a] Reactions run on a 0.15 mmol scale. [b] Determined by the ratio of peak integrations on HPLC for the product and starting material. [c] Determined by the ratio of peak integrations on HPLC for the *E* and *Z* isomers. [d] Run without the addition of $KHSO_4$.

N-Boc Cleavage to Yield Compound 3.6

Representative procedure: *Solvent$_A$/Solvent$_B$ Screen*

To a flame-dried 1-dram vial charged with a PTFE-coated magnetic stir bar was added compound **3.5** (0.25 mmol, 1 equiv, 130.16 mg) along with 1 mL of anhydrous MeOH. To this was then added 1 mL of a 5.0-6.0 M solution of HCl in isopropanol, the vial was capped, the cap was secured with Teflon™ tape and the reaction was stirred at rt for 2 hours. Subsequently, the solvent was removed *in vacuo*, 0.6 mL of deuterated DMSO was added, and conversion was determined via ^{1}H NMR.

Table 3.21: Solvent Optimization for *N*-Boc Deprotection[62]

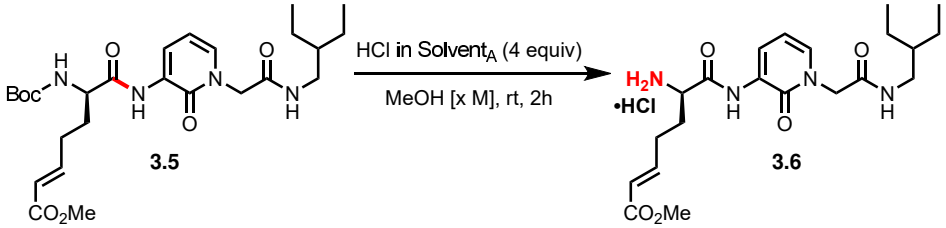


3.5 3.6

Entry[a]	5M HCl in Solvent$_A$	Solvent$_B$	% Conversion[b]
1	IPA	MeOH	100
2	IPA	1,4-dioxane	100
3	IPA	IPA	16
4	IPA	EtOAc	83
5[c]	MeOH	MeOH	31
6	IPA	EtOH	28

[a] Reactions run on a 0.25 mmol scale. [b] Determined via the ratio of peak integrations for product and starting material on ^{1}H NMR. [c] 3M HCl in MeOH.

Table 3.22: Optimization for MeOH COncentration for *N*-Boc Deprotection[62]



Entry[a]	MeOH [x M]	% Conversion[b]
1	0.1	>99
2	0.25	>99
3	0.5	96
4	0.75	97
5	1	83
5	neat	>99

[a] Reactions run on a 0.25 mmol scale. [b] Determined via the ratio of peak integrations for product and starting material on ^{1}H NMR. [c] Only 5M HCl in IPA utilized.

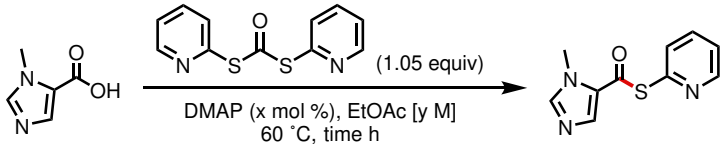
DPDTC Thioester Formation from 1-Methyl-1H-Imidazole-5-Carboxylic Acid

Representative thioester formation: *DMAP Screening*

To a flame-dried 1-dram vial charged with a PTFE coated magnetic stir bar was added 1-methyl-1*H*-imidazole-5-carboxylic acid (0.25 mmol, 1 equiv, 31.5 mg), DPDTC (0.263 mmol, 1.05 equiv, 65.2 mg), and DMAP (0.025 mmol, 10 mol %, 3.1 mg). The vial was fitted with a septum and the septum

secured via Teflon™ tape. The vial was attached to a vacuum/argon manifold via a needle through the septum, and the vial was subjected to three cycles of vacuum, then backfilling with argon. The vial was detached from the manifold and the reaction was placed in an aluminum heating block set to 60 °C and stirred for 5 h. Subsequently, the reaction vial was removed from the heating block and allowed to cool to rt. To the crude residue was added 1,3,5-trimethoxybenzene (0.5 or 1 equiv), and the crude mixture dissolved in 0.6 mL of deuterated DMSO. The qNMR yield was then determined via ^{1}H NMR.

Table 3.23: Optimization for 2nd Thioester Formation[62]



3.8

Entry[a]	DMAP (mol %)	[y M]]	Time (h)	% Yield[b]
1	0	neat	5	22
2	2.5	neat	2	71
3	5	neat	2	88
4	7.5	neat	2	91
5	10	neat	2	95
6	**10**	**neat**	**5**	**>99**
7	10	2	5	>99
8	10	neat	1	89
9	10	neat	2	95
10	10	neat	3	95
11	10	neat	4	93
12	10	neat	5	91

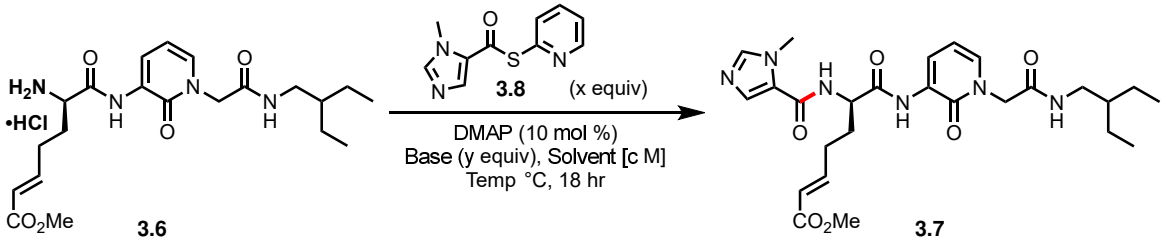
[a] Reactions run on a 0.25 mmol scale. [b] Yield determined via qNMR using 1,3,5-trimethoxybenzene as an internal standard.

Attempts at Final Amidation with 2-Pyridyl Thioester

Representative procedure for thioester amidation: *base screen*

To a flame-dried 1-dram vial charged with a PTFE coated magnetic stir bar was added DMAP* (10 mol %). The vial was taken into a glovebox under inert atmosphere, where methyl (*S*,E)-6-amino-7-((1-(2--((2-ethylbutyl)amino)-2-oxoethyl)-2-oxo-1,2-dihydropyridin-3-yl)amino)-7-oxohept-2-enoate hydrochloride (**3.6**) (0.15 mmol, 1 equiv, 63.07 mg) and *S*-(pyridin-2-yl) 1-methyl-1*H*-imidazole-5-carbothioate (**3.8**) (0.225 mmol, 1.5 equiv, 49.3 mg) were added. The vial was sealed with a rubber septum and removed from the glovebox. The septum was secured with Teflon™ tape. To the vial via a syringe through the septum was added anhydrous, degassed MeCN (0.5 M, 0.3 mL). Subsequently, *N*-methylmorpholine (33 µL, 2 equiv) was added to the vial in an identical fashion. The vial was then removed from the manifold and placed in an aluminum heating block set to 35 °C. The reaction was allowed to stir for 18 h, at which point the crude reaction mixture was analyzed via TLC and HPLC.

Table 3.24: Optimization for Final Amidation with 2-Pyridyl Thioester[62]



Entry[a]	x equiv	Base (y equiv)	Solvent [c M]	Temp (°C)	Result
1	1.5	DIPEA (1.5 equiv)	EtOAc [0.5 M]	35	N.R.[b]
2	1.5	TEA (2 equiv)	EtOAc [0.5 M]	35	poor[c]
3	1.5	NMM (2 equiv)	EtOAc [0.5 M]	35	59%[d]
4	1.5	K_2CO_3 (2 equiv)	EtOAc [0.5 M]	35	poor[b]

Continued on next page

*All reagents utilized were anhydrous

Entry[a]	x equiv	Base (y equiv)	Solvent [c M]	Temp (°C)	Result
5	1.5	$NaHCO_3$ (2 equiv)	EtOAc [0.5 M]	35	21%[d]
6	1.5	NaOAc (2 equiv)	EtOAc [0.5 M]	35	poor[b]
7	1.5	Proton Sponge™ (2 equiv)	EtOAc [0.5 M]	35	poor[c]
8	1.5	DABCO (2 equiv)	EtOAc [0.5 M]	35	poor[c]
9	1.5	2,6-Lutidine (2 equiv)	EtOAc [0.5 M]	35	poor[c]
10	1.5	pyridine (2 equiv)	EtOAc [0.5 M]	35	poor[c]
11	1.5	NMM (3 equiv)	MeCN [0.5 M]	35	poor[b]
12	2	NMM (3 equiv)	MeCN [0.5 M]	60	poor[b]
13	1.2	NMM (3 equiv)	MeCN [0.5 M]	50	poor[b]
14	1.2	NMM (3 equiv)	MeCN [0.5 M]	50	poor[b]
15	1.2	NMM (3 equiv)	MeCN [0.5 M]	50	poor[b]
16	1.2	NMM (3 equiv)	MeCN [0.5 M]	50	poor[b]
17	1.2	NMM (3 equiv)	MeCN [0.5 M]	50	poor[b]
18	1.2	NMM (1.2 equiv)	MeCN [1 M]	45	poor[b]
19	1.2	pyridine (1.2 equiv)	MeCN [1 M]	45	poor[b]
20	1.2	NMM (1.2 equiv)	MeCN [1 M]	55	poor[b]
21	1.2	NMM (1.2 equiv)	MeCN [1 M]	65	poor[b]
22	1.2	NMM (1.2 equiv)	MeCN [1 M]	75	poor[b]
23[e]	1.2	NMM (1.2 equiv)	MeCN [1 M]	65	poor[b]

[a] Reactions run on a 0.15 mmol scale. [b] Qualitative assessment based off HPLC chromatogram of the crude reaction mixture where significant starting material was present, significant side products are present, insignificant amounts of product, and combinations thereof. [c] Qualitative assessment based off TLC of the crude reaction mixture. [d] Isolated yield. [e] 20 mol % of DMAP utilized.

Attempts at Final Amidation with T3P

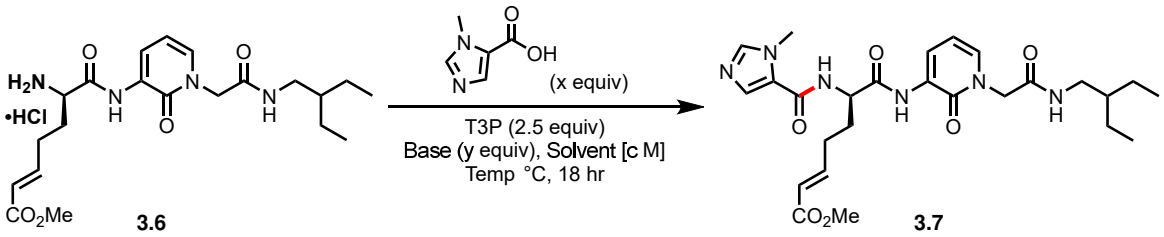
Representative procedure: *T3P base equivalents screen*

To a flame-dried 1-dram vial charged with a PTFE coated magnetic stir bar was added DMAP (10 mol %). The vial was taken into a glovebox under inert atmosphere, where methyl (*S*,E)-6-amino-7-((1-(2--((2-ethylbutyl)amino)-2-oxoethyl)-2-oxo-1,2-dihydropyridin-3-yl)amino)-7-oxohept-2-enoate hydrochloride* (**3.7**) (0.15 mmol, 1 equiv, 63.07 mg) and 1-methyl-1*H*-imidazole-5-carboxylic acid (0.18 mmol,

*All reagents utilized were anhydrous.

1.2 equiv, 22.70 mg) were added. The vial was sealed with a rubber septum and removed from the glove-box, and the septum was secured with Teflon™ tape. To the vial was added 0.3 mL of dry and degassed EtOAc via syringe, followed by DIPEA (x equiv). The reaction mixture was cooled to 0 °C in an ice bath, followed by the dropwise addition of a solution of 50 wt.% T3P in EtOAc (2.5 equiv) via syringe. The vial was removed from the ice bath and placed in an aluminum heating block set to 35 °C and stirred for 24 h. Subsequently, the vial was removed and the reaction allowed to cool to rt, after which the reaction progress was determined by HPLC.

Table 3.25: Optimization for Final Amidation with 2-Pyridyl Thioester[62]



Entry[a]	x equiv	Base (y equiv)	Solvent [c M]	Temp (°C)	Result
1	1.1	pyridine (3.5 equiv)	EtOAc [0.5 M]	35	73%[b] (70%)[c]
2	1.1	DABCO (3.5 equiv)	EtOAc [0.5 M]	35	poor[d]
3	1.1	DIPEA (3.5 equiv)	EtOAc [0.5 M]	35	47%[c]
4	1.1	TEA (3.5 equiv)	EtOAc [0.5 M]	35	26%[c]
5	1.1	NMM (3.5 equiv)	EtOAc [0.5 M]	35	17%[c]
6	1.1	$NaHCO_3$ (3.5 equiv)	EtOAc [0.5 M]	35	poor[d]
7	1.1	DBU (3.5 equiv)	EtOAc [0.5 M]	35	7%[c]
8	1.1	2,6-Lutidine (3.5 equiv)	EtOAc [0.5 M]	35	19%[c]
9	1.1	KH_2PO_4 (3.5 equiv)	EtOAc [0.5 M]	35	poor
10	1.1	pyridine (3.5 equiv)	EtOAc [0.5 M]	35	sig. SM.[d,e]
11	1.1	pyridine (2 equiv)	EtOAc [0.5 M]	35	sig. SM.[d,e]
12	1.1	pyridine (3 equiv)	EtOAc [0.5 M]	35	sig. SM.[d,e]
13	1.1	pyridine (4 equiv)	EtOAc [0.5 M]	35	sig. SM.[d,e]

Continued on next page

Entry[a]	x equiv	Base (y equiv)	Solvent [c M]	Temp (°C)	Result
14	1.1	pyridine (6 equiv)	EtOAc [0.5 M]	35	47%[c]
15	1.1	pyridine (3.5 equiv)	MeCN [0.5 M]	35	60%[c]
16	1.1	pyridine (3.5 equiv)	toluene [0.5 M]	35	sig. SM.[c]
17	1.1	pyridine (3.5 equiv)	MeCN [0.5 M]	45	47%[c]
18	1.1	pyridine (6 equiv)	MeCN [1 M]	35	56%[c]
19[f]	1.5	pyridine (4 equiv)	MeCN [1 M]	35	43%[c]

[a] Reactions run on a 0.15 mmol scale. [b] Isolated yield. [c] HPLC yield determined via external calibration plot. [d] Qualitative assessment based off of HPLC of crude reaction mixture. [e] sig. SM. = significant starting material. [f] 3 equiv. of T3P used.

3.4.5 Sequence and Scale Up

Nitro Group Reduction to Give Compound 3.2

A 50 mL round-bottom flask was charged with a PTFE coated magnetic stir bar, to which was then added *N*-(2-ethylbutyl)-2-(3-nitro-2-oxopyridin-1(2*H*)-yl)acetamide (**3.1**) (9.5 mmol, 1 equiv, 2.67 g), carbonyl iron powder (CIP) (28.5 mmol, 3 equiv, 1.59 g), and NH_4Cl (28.5 mmol, 3 equiv, 1.52 g). The flask was sealed with a rubber septum, the septum secured with Teflon™ tape, and the flask attached to a vacuum/argon manifold. The flask then underwent three cycles of vacuum, then backfilling with argon. Via syringe through the septa, degassed H_2O was added (0.5 M, 19.0 mL). The reaction was then stirred at 45 °C for 16 h at which point HPLC analysis of the crude reaction mixture showed full conversion to the product. The crude reaction mixture was brought to a pH of 8 with $NaHCO_3$, and then filtered through a pad of Celite, ensuring complete transfer with EtOAc (3 x 10 mL). The pad of Celite was washed with an additional 15 mL of EtOAc. The collected filtrate was transferred to a 250 mL separatory funnel and extracted with EtOAc (5 x 15 mL). The combined organics were washed with brine, dried over ananhydrous Na_2SO_4, and concentrated *in vacuo* to afford compound **3.2** as a tan powder* (2.173 g, 91.0%). Purity was confirmed via HPLC and NMR, then was able to be used in the subsequent step.

First Amidation to Yield Compound 3.4

To a flame-dried 6-dram vial charged with a PTFE coated magnetic stir bar was added (R)-2-((tert--butoxycarbonyl)amino)hex-5-enoic acid (2.1 mmol, 1.05 equiv, 481.5 mg), DPDTC (2.21 mmol, 1.103

*Compound **3.2** is observed to be moderately sensitive to oxidation. As such, upon drying, the solid was kept under vacuum or under an inert atmosphere of argon

equiv, 547.5 mg), and DMAP (0.21 mmol, 10.5 mol %, 25.7 mg). The vial was sealed with a rubber septum and secured with Teflon™ tape. The vial was connected to an argon/vacuum manifold and underwent three cycles of vacuum, then backfilling with argon. Dry, degassed EtOAc was added (0.48 M, 4.2 mL) *via* syringe through the septum, and the reaction was then stirred at 35 °C for 14.5 h. After this time, HPLC confirmed full conversion of the starting acid to compound **3.3**. The EtOAc was subsequently removed *in vacuo*. The vial was then was taken into a glovebox under an inert atmosphere where 2-(3-amino-2-oxopyridin-1(2*H*)-yl)-*N*-(2-ethylbutyl)acetamide (**3.2**) (2 mmol, 1 equiv, 502.6 mg) was added. The vial was refitted with a rubber septum, removed from the glovebox, and the septum was secured with Teflon™ tape. To the vial via syringe through the septum was added (1 M, 2 mL) of a 9:1 mixture of dry and degassed EtOAc:MeCN and the reaction was stirred at 60 °C for 24 h. At this time point, the crude reaction mixture was analyzed via HPLC to confirm full consumption of the starting amine. The contents of the vial were transferred to a 250 mL separatory funnel, ensuring transfer with additional EtOAc (3 x 10 mL). The organic layer was washed once with 1 M NaOH (15 mL), once with 1 M HCl (15 mL), and once again with 1 M NaOH (15 mL). The organic layer was then washed with brine, dried over anhydrous Na_2SO_4, and concentrated *in vacuo* to afford compound **3.4** as a white solid (860.8 mg, 93.0%, >99% *ee*). Purity was confirmed via HPLC and NMR, and the percent enantiomeric excess determined via chiral HPLC. The solid was then used directly in the next step.

Grubbs Olefin-Metathesis to Give Compound 3.5

To a flame-dried 2-neck 50 mL round-bottom flask charged with a PTFE-coated magnetic stir bar was added tert-butyl (R)-(1-((1-(2-((2-ethylbutyl)amino)-2-oxoethyl)-2-oxo-1,2-dihydropyridin-3-yl)amino)-1-oxohex-5-en-2-yl)carbamate (**3.4**) (1.94 mmol, 1 equiv, 897.4 mg) from the previous step. The flask was taken into a glovebox under an inert atmosphere and Hoveyda-Grubbs II (0.0485 mmol, 2.5 mol

%, 30.4 mg) was added to the flask, along with CuI (0.097 mmol, 5 mol %, 18.5 mg).* Both necks of the flask were sealed with a rubber septa and the flask was removed from the glovebox. The flask was connected to an argon/vacuum manifold via a needle through one of the septa, and degassed methyl acrylate (0.125 M, 15.5 mL) was added via syringe through the septum. The septum without an argon line was removed, and the flask was quickly fitted with an argon flushed water-jacketed condenser.† A vent needle was added at the top of the condenser to provide a constant argon flow over the reaction mixture.‡ The flask was then heated to 35 °C in an oil bath and allowed to stir for 18 h whereby the reaction was judged complete via HPLC analysis of the crude reaction mixture. Subsequently, the flask was removed from the oil bath and allowed to cool to rt. The unreacted methyl acrylate was recovered via distillation§ (12.6 mL, 82% recovery). The crude reaction residue was reconstituted in 15 mL of Et_2O and stirred vigorously for 30 min. The mixture was then passed through a glass fritted funnel, and the collected solid was triturated with Et_2O (3 x 10 mL) or until the collected solid was seen to be white/colorless. Residual Et_2O was removed *in vacuo* to afford compound **3.5** as a white solid (935.2 mg, 92.6%, 97:3 *E:Z*). Purity was confirmed via HPLC and NMR, and the ratio of *E:Z* isomers was determined via HPLC. The solid was then able to be used in the subsequent reaction step.

N-Boc Deprotection/Ammonium Salt Formation to Afford Compound 3.6

To a flame-dried 50 mL round-bottom flask charged with a PTFE coated magnetic stir bar was added methyl (R,E)-6-((tert-butoxycarbonyl)amino)-7-((1-(2-((2-ethylbutyl)amino)-2-oxoethyl)-2-oxo-1,2-dihydropyridin-3-yl)amino)-7-oxohept-2-enoate (**3.5**) (1.76 mmol, 1 equiv, 915.4mg) from the previous

*While there is no phosphine to abstract, copper iodide was included as a thiol scavenger for any trace/residual 2-mercaptopyridine remaining from the prior step.

†Included in order to reduce loss of methyl acrylate during argon flush.

‡Evolving ethylene gas during the reaction has a deleterious effect on the activity of the catalyst. An argon flush serves to remove ethylene as it's produced.

§The purity of the collected methyl acrylate was confirmed via proton NMR.

step. To this was added 5.0-6.0 M solution of HCl in isopropanol (0.25 M, 7 mL), and the reaction was stirred at rt for 14 h whereby the reaction was judged complete by proton NMR. Subsequently, the reaction mixture was transferred to a 45 mL centrifuge tube, with complete transfer being ensured by washing with Et_2O (2 x 10 mL). The crude reaction material was then centrifuged at 4,000 rpm for 10 min. The supernatant was decanted off, 10 mL of Et_2O was added, and the mixture was vortexed until homogeneous. The mixture was then centrifuged again at 4,000 rpm for 10 min, and then the supernatant was decanted off. This washing method was repeated an additional two times or until the supernatant ran clear. The solid was dried under vacuum to afford compound **3.6** as a white solid (735.0 mg, 91.5%). Purity was confirmed via NMR.

Final Amide Coupling to Afford Compound 3.7 (*ZED1227*)

To a flame-dried 2-dram vial charged with a PTFE coated stir bar was added the HCl salt of methyl (R,E)-6-amino-7-((1-(2-((2-ethylbutyl)amino)-2-oxoethyl)-2-oxo-1,2-dihydropyridin-3-yl)amino)-7-oxohept--2-enoate (**3.6**) (0.25 mmol, 1 equiv, 114.2 mg).* The solid was then azeotroped with anhydrous toluene to remove trace water, and the toluene was removed *in vacuo* at 50 °C. The vial was then brought into a glovebox under an inert atmosphere, and to the vial was added 1-methyl-1*H*-imidazole-5-carbonyl chloride hydrochloride (0.375 mmol, 1.5 equiv, 67.9 mg). The vial was then fitted with a septum, the vial brought out of the glovebox, and the septum secured with Teflon™ tape. The vial was then attached to a vacuum/argon manifold, and to the vial via syringe through the septum was added anhydrous MeCN (0.15 M, 1.7 mL). The vial was then set to stir in an ice bath at 0 °C for 15 min. To the vial via a syringe through the septum was added anhydrous DIPEA (1 mmol, 4 equiv, 172 μL) dropwise over the course of 10 min. The reaction was then allowed to stir for 3 h whereby the reaction was judged

*These conditions were developed by Takeda Pharmaceutical Company Limited.

complete via HPLC. The crude reaction mixture was then taken directly and isolated via reverse-phase flash chromatography (gradient of 0 to 30% of 0.1% formic acid in MeCN, and 0.1% formic acid, 12.5 mM NH_4COO^- in H_2O) to afford compound **3.7** (*ZED1227*) as a white solid (100.9 mg, 76.4%, >99% *ee*) and confirmed pure via NMR and HPLC (>98% pure by HPLC).

3.4.6 Calculation for Final Overall Yield of Compound 3.7 (*ZED1227*)

Table 3.26: Final Yield of Compound **3.7**[62]

Reaction	Mass of Prod (g)	Scale (mmol)	MW (g/mol)	(%) Yield
nitro reduction	2.173	9.5	251.33	*91.0106*
1st amidation	0.8608	2	462.59	*93.0414*
olefin-metathesis	0.9352	1.94	520.63	*92.5920*
N-Boc deprotection	0.7350	1.76	456.97	*91.3875*
final amidation	0.1009	0.25	528.61	*76.3511*
			Final Overall Yield:	***54.7%***

3.4.7 E-Factor[77] Calculations from Preparation of *ZED1227*

The procedure for the gram scale preparation of *ZED1227* (**3.7**) is provided in Section 3.4.5.* The E-Factor calculations for the overall reported process are provided below. Masses are normalized to 1 mmol of starting material in the first step, and each subsequent step is adjusted according to the yield of the step prior (*e.g.*, the nitro reduction has a yield of 93%, so the first amidation step is normalized to 0.93 mmol). Masses and E-Factor numbers that incorporate solvent waste are shown with a brown color.

Defining E-Factor equation.

Note: *The formulas for mass intensity and E-Factor are defined in the associated reference.*[16]

$$\text{Mass Intensity (MI)} = \frac{\text{total mass used in the process (g)}}{\text{mass of product (g)}} \tag{3.1}$$

$$\boxed{\text{E-Factor} = \text{MI} - 1} \tag{3.2}$$

Masses put into this reported process.

Table 3.27: Nitro Reduction Contributing Masses[62]

*For E-Factor calculations, pure solvents such as H_2O, Et_2O, MeCN, and EtOAc are recyclable via distillation and other purification techniques, and are, thus, not considered for the E-Factor calculation. Furthermore, it is noted that the relative volume of workup solvent is highly dependent on the scale utilized. For recent literature with representative E-Factor calculations, refer to the associated references.[27,87]

Source	Mass (g)
3.1 (Starting Material)	0.28131
CIP	0.16752
NH_4Cl	0.16014
water	2.002
TOTAL:	**0.60898 (2.6108)**

Table 3.28: First Amidation (normalized to 0.91 mmol)[62]

Source	Mass (g)
3.2 (Starting Material)	0.2887
Carboxylic Acid	0.2191
DPDTC	0.2491
DMAP	0.0117
EtOAc (1st charge)	1.7242
EtOAc (2nd charge)	0.7372
MeCN	0.0714
TOTAL:	**1.5173 (3.2415)**

Table 3.29: Olefin Metathesis Contributing Masses (normalized to 0.846 mmol)[62]

Source	Mass (g)
3.4 (Sarting Material)	0.3915
Hoveyda-Grubbs (II)	0.01326
Methyl Acrylate (amount unrecovered)	1.7987
Methyl Acrylate (recovery not cconsidered)	6.4239
CuI	0.0081
TOTAL:	**2.2115 (6.8367)**

Table 3.30: *N*-Boc Deprotection Contributing Masses (normalized to 0.784 mmol)[62]

Source	Mass (g)
3.5 (Starting Material)	0.4080
5M HCl in IPA	2.8360
TOTAL:	**3.2440**

Table 3.31: Final Amidation Contributing Masses (normalized to 0.716 mmol)[62]

Source	Mass (g)
6 (Starting Material)	0.3273
Acyl Chloride	0.1946
DIPEA	0.3700
MeCN	3.8300
TOTAL:	**0.8919 (4.7217)**

Table 3.32: Sum of Contributing Masses[62]

Source	Mass (g)
Nitro Reduction	0.6090 (2.6108)
1st Amidation	1.5173 (3.2415)
Olefin Metathesis	2.2115 (6.8367)
N-Boc-Deprotection	3.2440
2nd Amidation	0.8920 (4.7217)
TOTAL:	**8.4738 (20.6547)**

Mass Intensity and E-Factor Calculations for This Work

$$\text{Normalized overall yield in grams} = 1 \text{ mmol} * \frac{0.52861 \text{ g}}{\text{mmol}} * 54.7\% = 0.2893 \text{ g} \tag{3.3}$$

$$\text{Mass Intensity (MI)} = \frac{\text{total mass of the process normalized to 1 mmol}}{\text{total yield normalized to 1 mmol}} = \frac{8.4738 \text{ g}}{0.2893 \text{ g}} = 29.29 \text{ (71.4)} \tag{3.4}$$

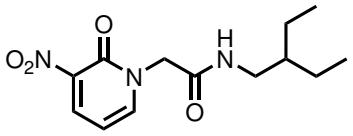
E Factor = MI - 1 = 29.29 – 1 = **28** (70) (3.5)

Note: *The E-factor for the literature comparison was calculated in an identical fashion to the calculations above. Like with the route reported in this chapter, we do not include factors resulting from work up and isolation procedures as these are highly scale dependent. Furthermore, solvents used in the literature comparison route that are considered relatively easy to recover (i.e., DCM, MeCN, etc.) are not counted toward their overall E-factor, whereas not easily separated mixtures or low vapor pressure solvents (i.e., DMF) are considered challenging to recover and are thus counted toward the overall E-Factor. Furthermore, the steps leading up to their preparation of benzyl-1-(2-(2-ethylbutylamino)-2-oxoethyl)-2-oxo-1,2-dihydropyridin-3-ylcarbamate are not counted in order to provide a more accurate comparison to this work. The E-factor calculations for the literature comparison are available in the open access ESI of the associated reference.*[62]

3.4.8 Analytical Data

Product Descriptions

***N*-(2-Ethylbutyl)-2-(3-nitro-2-oxopyridin-1(2*H*)-yl)acetamide (3.1)**



Product **3.1** was synthesized according to the procedure reported in Section 3.4.3.

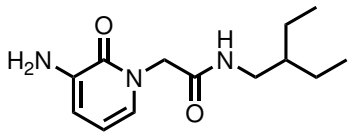
^{1}H NMR (400 MHz, DMSO): δ 8.45 (dd, J = 7.8, 2.1 Hz, 1H), 8.21 (t, J = 5.8 Hz, 1H), 8.14 (dd, J = 6.6, 2.1 Hz, 1H), 6.47 (dd, J = 7.8, 6.5 Hz, 1H), 4.71 (s, 2H), 3.05 (t, J = 5.7 Hz, 2H), 1.39 – 1.23 (m, 5H), 0.85 (t, J = 7.4 Hz, 6H).

^{13}C NMR (126 MHz, DMSO): δ 165.81, 153.71, 147.70, 139.26, 137.78, 102.93, 51.80, 41.20, 40.42, 23.10, 10.76.

R_f: 0.39 (100% EtOAc).

HRMS (ESI$^+$): *m/z* calcd for $C_{13}H_{19}N_3O_4Na$, $[M+Na]^+$: 304.1273; found: 304.1272.

2-(3-Amino-2-oxopyridin-1(2*H*)-yl)-*N*-(2-ethylbutyl)acetamide. (3.2)



Product **3.2** was synthesized according to the procedure reported in Section 3.4.5.

^{1}H NMR (400 MHz, DMSO): δ 7.97 (t, J = 5.9 Hz, 1H), 6.80 (dd, J = 6.8, 2.0 Hz, 1H), 6.43 (dd, J = 7.2, 1.9 Hz, 1H), 6.00 (t, J = 7.0 Hz, 1H), 5.01 (s, 2H), 4.49 (s, 2H), 3.02 (t, J = 5.7 Hz, 2H), 1.37 –

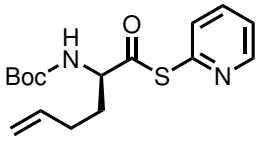
1.18 (m, 5H), 0.83 (t, J = 7.3 Hz, 6H).

^{13}C NMR (101 MHz, DMSO): δ 166.95, 157.13, 138.16, 125.80, 110.25, 105.55, 51.28, 41.05, 40.43, 23.09, 10.77.

R_f: 0.36 (100% EtOAc).

HRMS (ESI$^+$): *m/z* calcd for $C_{13}H_{19}N_3O_4Na$, $[M+Na]^+$: 304.1273; found: 304.1272.

***S*-(Pyridin-2-yl) (*S*)-2-((*t*-butoxycarbonyl)amino)hex-5-enethioate. (3.3)**



Product **3.3** was synthesized according to the optimized conditions found in Section 3.4.4 and was isolated via flash chromatography.

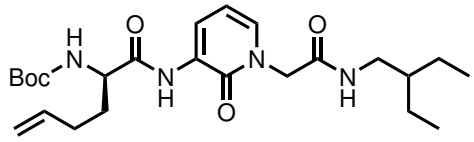
^{1}H NMR (600 MHz, $CDCl_3$): δ 8.58 (d, J = 4.9 Hz, 1H), 7.69 (td, J = 7.8, 1.9 Hz, 1H), 7.57 (m, 1H, both major and minor rotomers), 7.25 (dd, J = 7.5, 4.9 Hz, 1H), 5.73 (ddt, J = 16.9, 10.2, 6.6 Hz, 1H), 5.50 – 5.32 (m, 1H, both major and minor rotomers), 5.06 – 4.94 (m, 2H), 4.50 – 4.18 (m, 1H, both major and minor rotomers), 2.23 – 2.07 (m, 2H), 2.04 – 1.91 (m, 1H), 1.76 – 1.66 (m, 1H), 1.44 (s, 9H).

^{13}C NMR (126 MHz, $CDCl_3$): δ 199.65, 199.31, 155.29, 154.75, 151.53, 150.47, 150.33, 137.18, 136.60, 130.51, 123.57, 116.16, 81.25, 80.40, 61.83, 60.46, 31.55, 29.64, 28.37.

R_f: 0.27 (30% EtOAc/hexanes).

HRMS (ESI$^+$): *m/z* calcd for $C_{16}H_{22}N_2O_3SNa$: 345.1249, $[M+Na]^+$; found: 345.125.

_t_-Butyl(_S_)-(1-((1-(2-((2-ethylbutyl)amino)-2-oxoethyl)-2-oxo-1,2-dihydropyridin-3-yl)amino)-1-oxohex-5-en-2-yl)carbamate (3.4)



Product **3.4** was synthesized according to the procedure reported in Section 3.4.5.

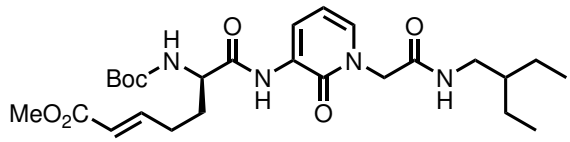
^{1}H NMR (600 MHz, DMSO): δ 9.17 (s, 1H), 8.22 (dd, J = 7.4, 2.0 Hz, 1H), 8.07 (t, J = 5.8 Hz, 1H), 7.46 (d, J = 7.7 Hz, 1H), 7.32 (dd, J = 6.9, 1.9 Hz, 1H), 6.25 (t, J = 7.1 Hz, 1H), 5.79 (ddt, J = 16.9, 10.2, 6.6 Hz, 1H), 5.04 – 4.93 (m, 2H), 4.60 (s, 2H), 4.12 – 3.99 (m, 1H), 3.08 – 2.97 (m, 2H), 2.07 (dtt, J = 21.7, 14.6, 6.8 Hz, 2H), 1.85 – 1.76 (m, 1H), 1.69 – 1.61 (m, 1H), 1.40 (s, 9H), 1.35 – 1.19 (m, 6H), 0.83 (t, J = 7.3 Hz, 6H).

^{13}C NMR (126 MHz, DMSO): δ 171.65, 166.37, 156.65, 155.60, 137.64, 133.14, 127.98, 122.04, 115.34, 104.67, 78.49, 54.83, 51.57, 41.10, 40.43, 30.29, 29.75, 28.14, 23.09, 10.77.

R_f: 0.40 (70% EtOAc/hexanes).

HRMS (ESI$^+$): *m/z* calcd for $C_{24}H_{38}N_4O_5Na$: 485.2740, $[M+Na]^+$; found: 485.2743.

Methyl (_R_,E)-6-((tert-butoxycarbonyl)amino)-7-((1-(2-((2-ethylbutyl)amino)-2-oxoethyl)-2-oxo-1,2-dihydropyridin-3-yl)amino)-7-oxohept-2-enoate (3.5)



Product **3.5** was synthesized according to the procedure reported in Section 3.4.5.

^{1}H NMR (500 MHz, DMSO): δ 9.21 (s, 1H), 8.21 (d, J = 7.2 Hz, 1H), 8.07 (t, J = 5.6 Hz, 1H), 7.47 (d, J = 7.7 Hz, 1H), 7.32 (d, J = 6.3 Hz, 1H), 6.89 (dt, J = 14.5, 6.6 Hz, 1H), 6.24 (t, J = 6.9 Hz, 1H),

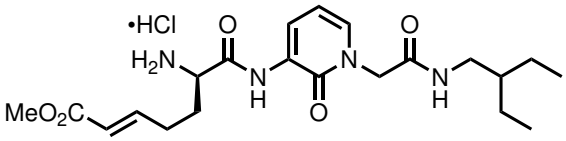
5.84 (d, *J* = 15.8 Hz, 1H), 4.59 (s, 2H), 4.09 (s, 1H), 3.63 (s, 3H), 3.07 – 2.96 (m, 2H), 2.32 – 2.20 (m, 2H), 1.94 – 1.82 (m, 1H), 1.77 – 1.65 (m, 1H), 1.39 (s, 9H), 1.27 (dp, *J* = 20.6, 6.5 Hz, 6H), 0.83 (t, *J* = 7.3 Hz, 6H).

^{13}C NMR (126 MHz, DMSO): δ 171.35, 166.34, 165.98, 156.62, 155.50, 148.55, 133.18, 127.93, 122.20, 121.02, 104.60, 78.53, 54.70, 51.53, 51.14, 41.06, 40.39, 29.39, 28.26, 28.08, 23.05, 10.73.

R_f: 0.25 (70% EtOAc/hexanes).

HRMS (ESI$^+$): *m/z* calcd for $C_{26}H_{40}N_4O_7Na$, $[M+Na]^+$: 543.2795; found: 543.2799.

Methyl-(*R*,E)-6-amino-7-((1-(2-((2-ethylbutyl)amino)-2-oxoethyl)-2-oxo-1,2-dihydropyridin-3-yl)amino)-7-oxohept-2-enoate hydrochloride (3.6)



Product **3.6** was synthesized according to the procedure reported in Section 3.4.5.

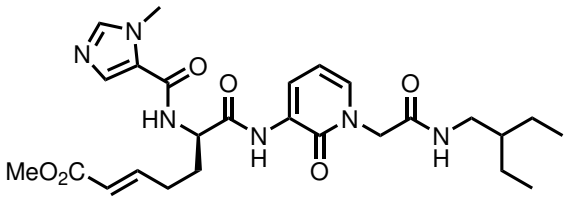
^{1}H NMR (500 MHz, DMSO): δ 10.05 (s, 1H), 8.55 (s, 3H), 8.24 – 8.15 (m, 2H), 7.41 (dd, *J* = 6.9, 1.9 Hz, 1H), 6.86 (dt, *J* = 15.7, 6.7 Hz, 1H), 6.26 (t, *J* = 7.1 Hz, 1H), 5.89 (d, *J* = 15.7 Hz, 1H), 4.62 (s, 2H), 4.29 (t, *J* = 6.5 Hz, 1H), 3.61 (s, 3H), 3.07 – 2.96 (m, 2H), 2.39 – 2.27 (m, 2H), 1.99 – 1.88 (m, 2H), 1.35 – 1.18 (m, 6H), 0.82 (t, *J* = 7.3 Hz, 6H).

^{13}C NMR (126 MHz, DMSO): δ 168.16, 166.44, 165.97, 156.75, 147.63, 134.38, 127.67, 124.79, 121.36, 104.37, 51.94, 51.62, 51.24, 41.11, 40.43, 29.65, 26.80, 23.10, 10.79.

HRMS (ESI$^+$): *m/z* calcd* for $C_{21}H_{32}N_4O_5$, $[M+Na]^+$: 443.2270; found: 443.2275.

*loss of -HCl during analysis

Methyl (*R*,E)-7-((1-(2-((2-ethylbutyl)amino)-2-oxoethyl)-2-oxo-1,2-dihydropyridin-3-yl)amino)-6-(1-methyl-1*H*-imidazole-5-carboxamido)-7-oxohept-2-enoate (*ZED1227*) (3.7)



Product **3.7** was synthesized according to the procedure reported in Section 3.4.5.

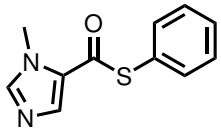
^{1}H NMR (500 MHz, DMSO): δ 9.31 (s, 1H), 8.64 (d, J = 7.9 Hz, 1H), 8.21 (dd, J = 7.4, 1.8 Hz, 1H), 8.07 (t, J = 5.8 Hz, 1H), 7.75 (d, J = 24.1 Hz, 2H), 7.33 (dd, J = 6.9, 1.9 Hz, 1H), 6.93 (dt, J = 15.7, 6.8 Hz, 1H), 6.25 (t, J = 7.1 Hz, 1H), 5.86 (dt, J = 15.7, 1.6 Hz, 1H), 4.63 – 4.54 (m, 3H), 3.79 (s, 3H), 3.62 (s, 3H), 3.01 (t, J = 5.8 Hz, 2H), 2.37 – 2.27 (m, 2H), 2.09 – 1.99 (m, 1H), 1.95 – 1.85 (m, 1H), 1.37 – 1.14 (m, 6H), 0.82 (t, J = 7.3 Hz, 6H).

^{13}C NMR (126 MHz, DMSO): δ 170.91, 166.39, 166.03, 160.28, 156.68, 148.62, 142.20, 133.29, 132.81, 128.00, 125.18, 122.48, 121.05, 104.69, 53.08, 51.59, 51.19, 41.12, 40.42, 33.50, 29.13, 28.49, 23.09, 10.76.

R_f: 0.29 (7% MeOH/DCM).

HRMS (ESI$^+$): *m/z* calcd for $C_{26}H_{36}N_6O_6Na$, $[M+Na]^+$: 551.2594; found: 551.2603.

***S*-(Pyridin-2-yl) 1-methyl-1*H*-imidazole-5-carbothioate. (3.8)**



Product **3.8** was synthesized according to the optimized conditions found in Section 3.4.4 and isolated via flash chromatography.

^{1}H NMR (400 MHz, DMSO): δ 8.64 (ddd, J = 4.8, 2.0, 1.0 Hz, 1H), 8.06 (s, 1H), 8.02 (d, J = 1.0 Hz, 1H), 7.92 (td, J = 7.7, 2.0 Hz, 1H), 7.73 (dt, J = 7.9, 1.1 Hz, 1H), 7.48 (ddd, J = 7.6, 4.8, 1.1 Hz, 1H), 3.80 (s, 3H).

^{13}C NMR (126 MHz, DMSO): δ 177.60, 150.51, 149.94, 144.95, 138.19, 137.66, 130.83, 128.40, 124.11, 33.96.

R_f: 0.21 (100% EtOAc).

HRMS (ESI$^+$): *m/z* calcd for $C_{10}H_{10}N_3OS$, $[M+H]^+$: 220.0544; found: 220.0545.

3.4.9 HPLC Traces

Determining *E:Z* Ratio

Chromatograms were obtained and analyzed on an Agilent 1260 series HPLC with a ZORBAX RRHD Eclipse Plus C18 Column, 2.1 x 100 mm, 1.8 µm, using 0.02% formic acid in MeCN, and 2.5 mM NH_4OAc / 0.02% formic acid buffered H_2O using the following gradient:*

Table 3.33: HPLC Gradient for Determining Mixture of E to Z Isomers[62]

Time (min)	Water (%)	MeCN (%)	Flow rate (mL/min)	Max Pressure (bar)
0.00	97	3	1.0	600
0.75	97	3	1.0	600
16.80	40	60	1.0	600
20.65	5	95	1.0	600
21.00	97	3	1.0	600
25.20	97	3	1.0	600

*HPLC Method provided by Takeda Pharmaceutical Company Limited.

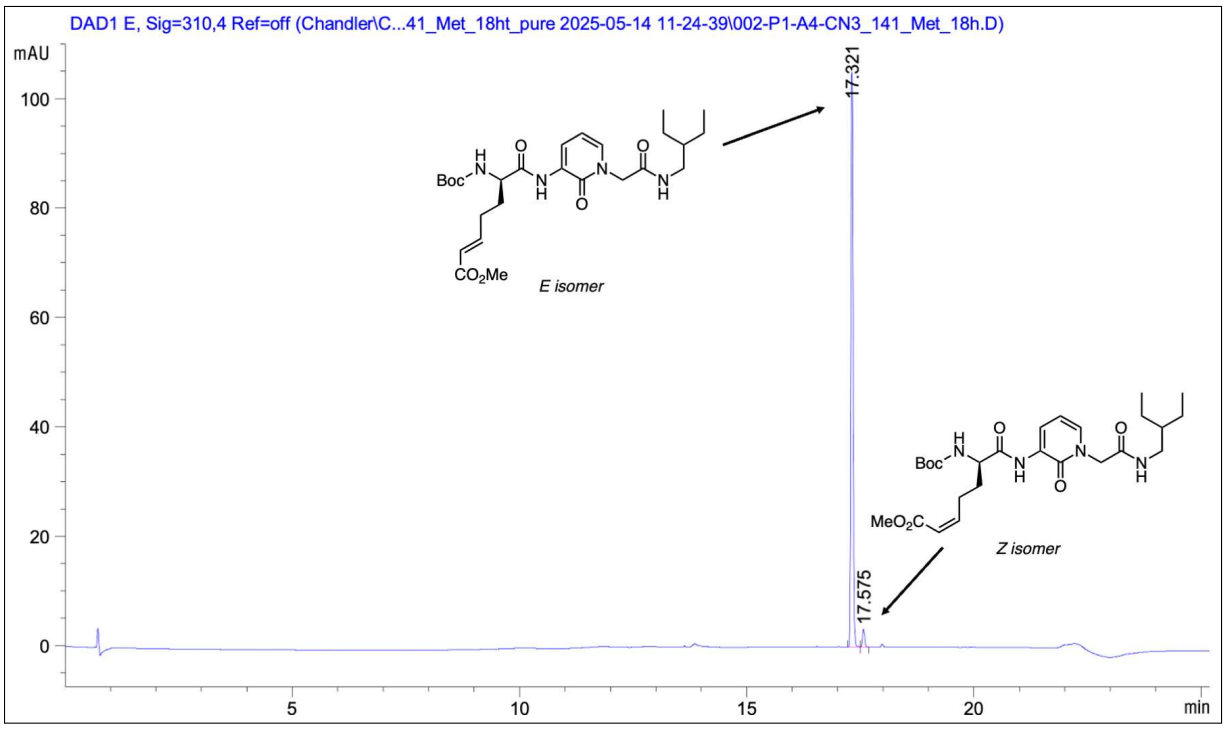


Figure 3.8: HPLC Chromatogram of Ratio of *E:Z* isomers for Compound **3.5**.

Table 3.23: HPLC Integrations for *E:Z* Isomers (ref. Fig. 3.8)

Signal 1: DAD1 E, Sig=310,4 Ref=off

Peak #	RetTime [min]	Type	Width [min]	Area [mAU*s]	Height [mAU]	Area %
1	17.321	BV	0.0499	344.50946	105.93050	96.9386
2	17.575	VB	0.0527	10.87995	3.27600	3.0614
Totals :				355.38941	109.20650	

Determining Percent Enantiomeric Excess

Chromatograms were obtained and analyzed on a Shimadzu Prominence HPLC with a ChiralPak IB Column, 250 x 4.6 mm, 5 µm. The *%ee* for both compound **3.4** and compound **3.7** were obtained monochromatically. The mobile phase for analyzing compound **3.4** was comprised of 0.02 % ethanolamine in

hexanes/EtOH/MeOH 95:3:2 (v/v/v). The mobile phase for analyzing compound **3.7** was comprised of 0.1 % ethanolamine in hexanes/EtOH/MeOH 15:3:2 (v/v/v).*

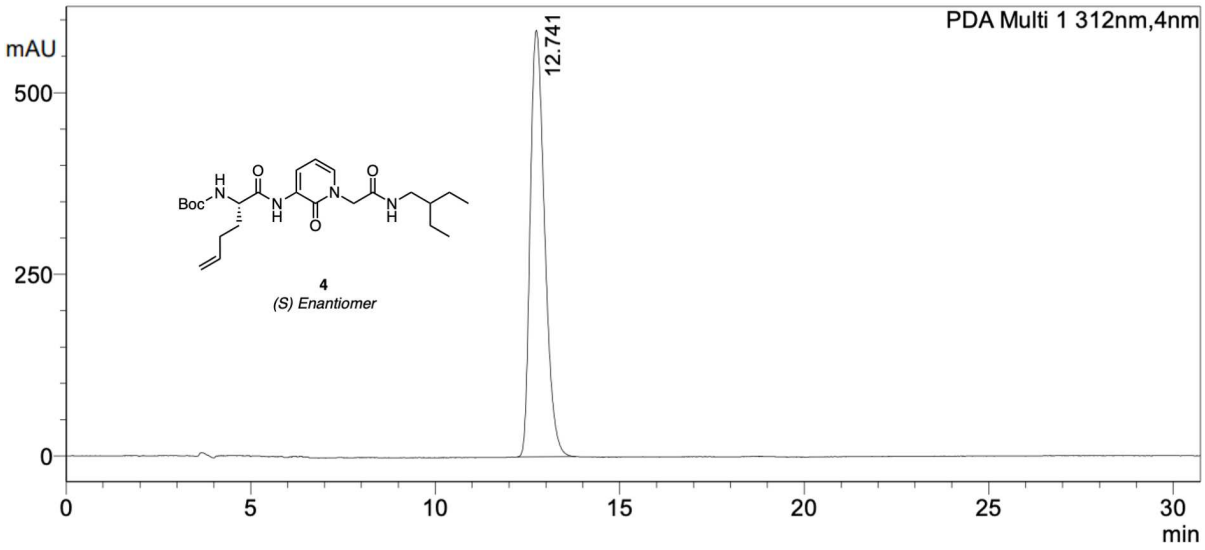


Figure 3.9: Chiral HPLC Chromatogram for Enantiomer of Compound **3.4**.

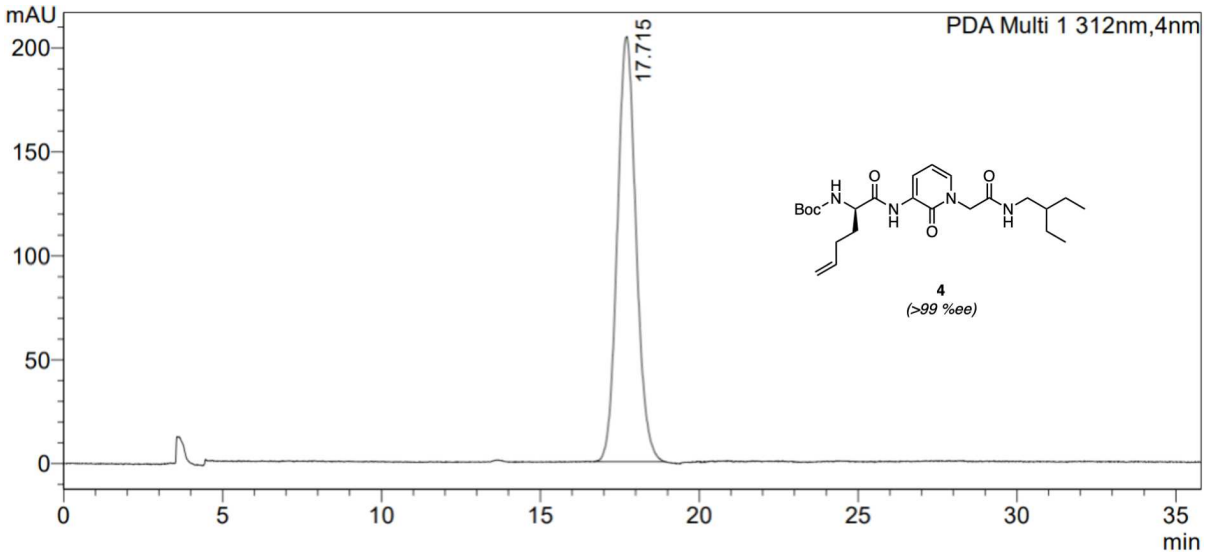


Figure 3.10: Chiral HPLC Chromatogram for Compound **3.4**.

*Method Provided by Takeda Pharmaceutical Company Limited.

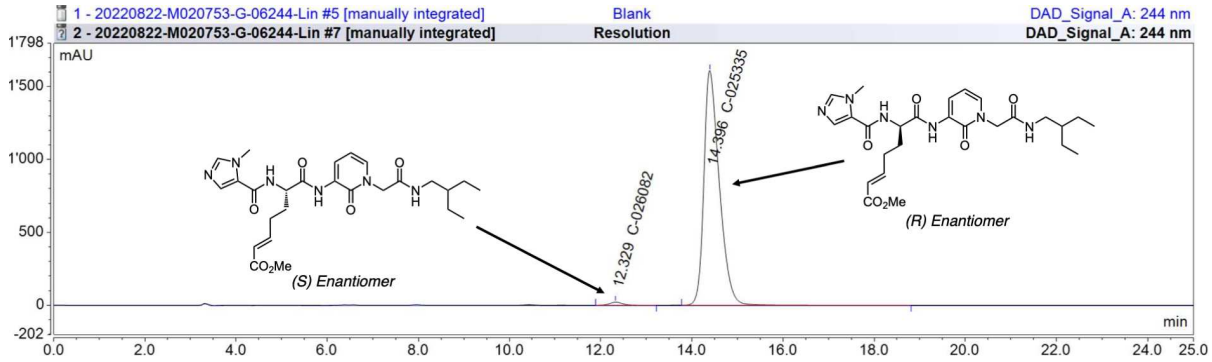


Figure 3.11: Chiral HPLC Chromatogram (provided by Takeda Pharmaceutical Company Limited) of Standard Providing Mixture of Enantiomers (Final API)
(0.1 % ethanolamine in hexanes/EtOH/MeOH 15:3:2 (v/v/v))

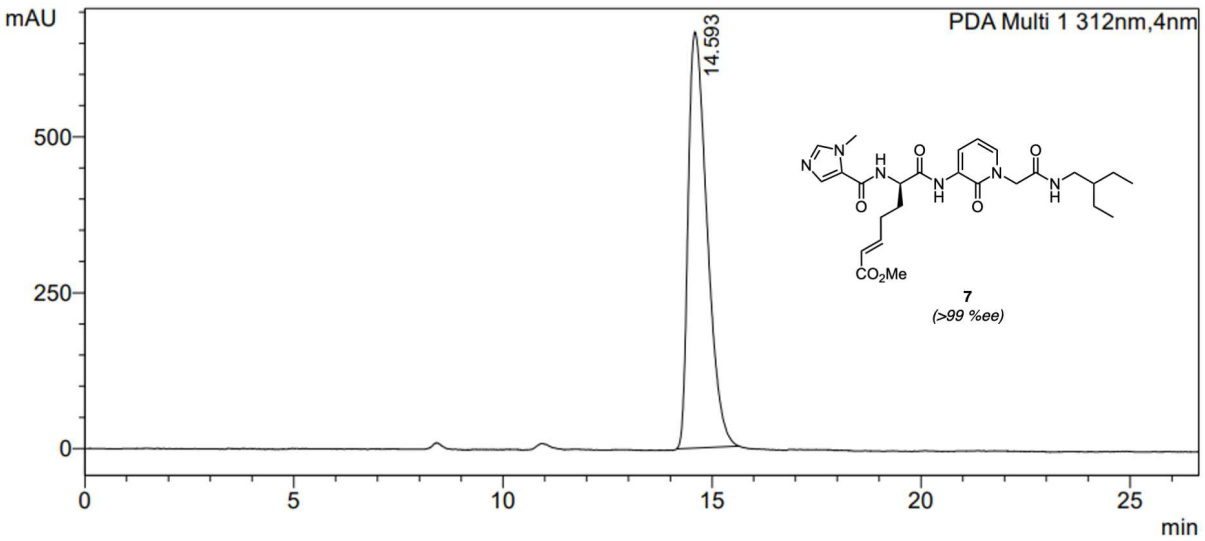


Figure 3.12: Chiral HPLC Chromatogram of Compound **3.7** (Final API)
(0.1 % ethanolamine in hexanes/EtOH/MeOH 15:3:2 (v/v/v))

HPLC Determination for Percent Purity for the Final Product (3.7)

The HPLC purity for compound ***3.7*** *was obtained using the same column and method as that utilized to determine the ratio of* E:Z *isomers for compound* ***3.5*** *(See 3.4.9).*

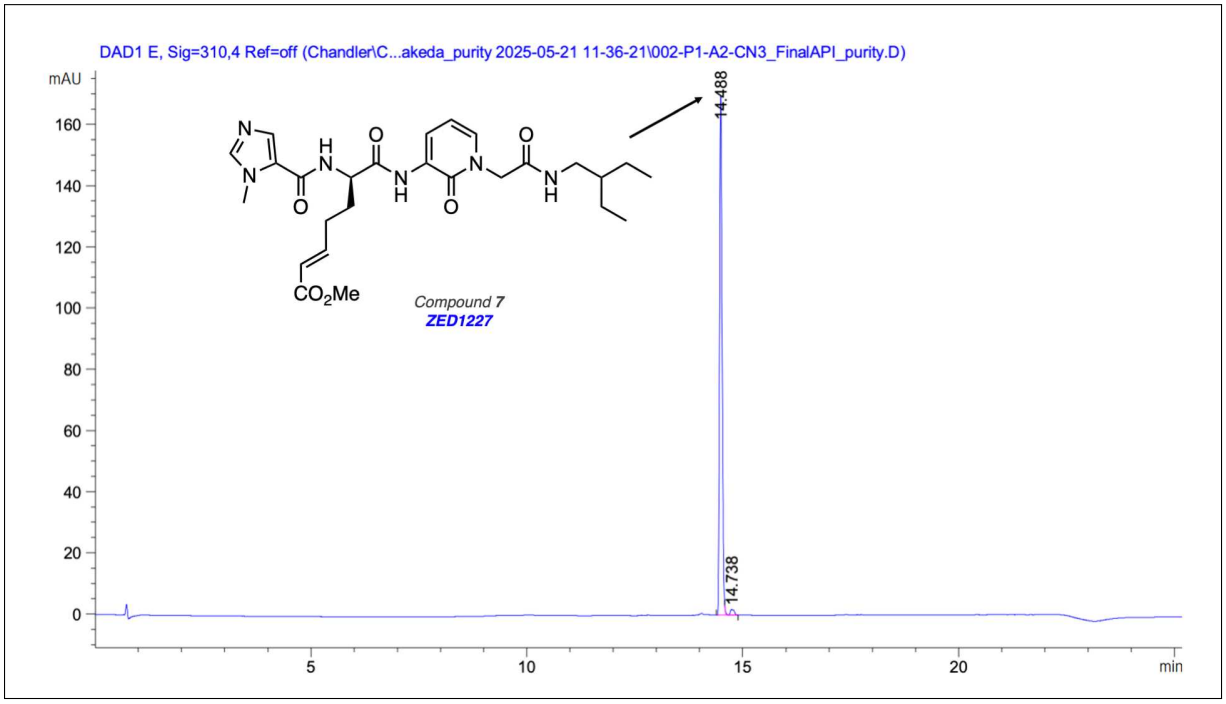


Figure 3.13: HPLC Chromatogram for Compound **3.7** (*ZED1227*).

Table 3.23: HPLC Integrations for Purity of **3.7** (*ZED1227*)

Peak #	RetTime [min]	Type	Width [min]	Area [mAU*s]	Height [mAU]	Area %
1	14.488	BV R	0.0639	697.58563	170.04660	98.2441
2	14.738	VB E	0.0893	12.46817	1.88231	1.7559
Totals :				710.05380	171.92891	

3.4.10 ICPMS Data

The final product (*ZED1227*) was analyzed via Inductively Coupled Plasma Mass Spectrometry (ICPMS) by the Nano and Pico Characterization Lab at the California NanoSystems Institute at UCLA, Dr. Chong Hyun "Paul" Chang, P.h.D.

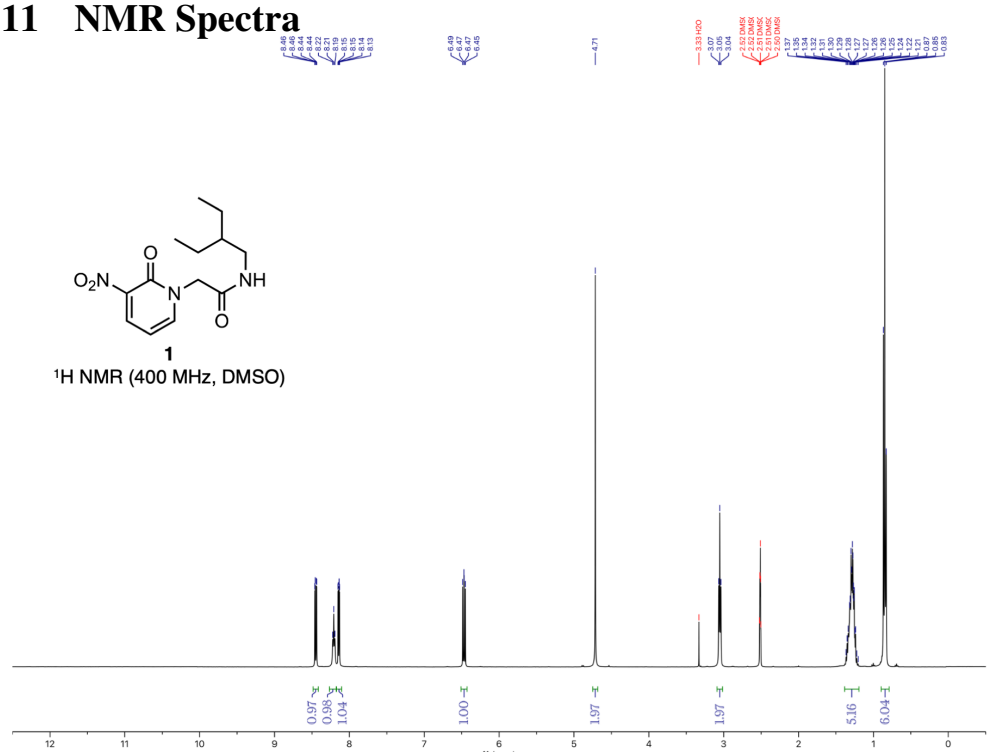
Table 3.36: ICPMS Analysis Data[61]

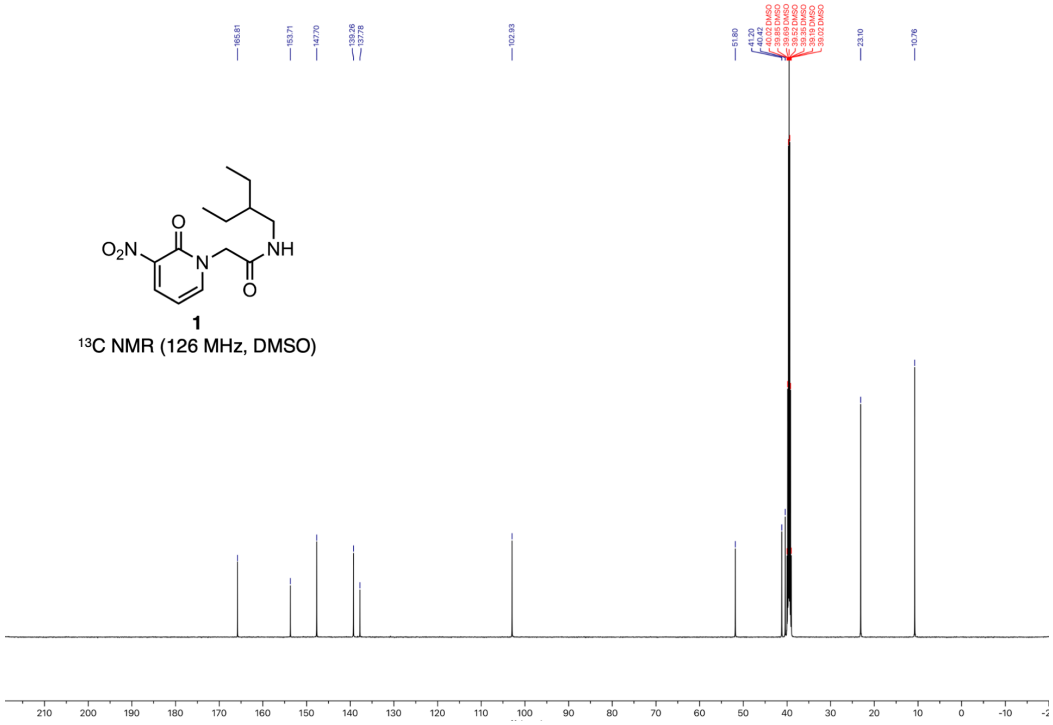
		Ruthenium [µg/g]	
Sample:	**Sample weight in analysis [mg]:**	**Average**[a]	σ[b]
Product **3.7**	4.5	*2.063*	0.050

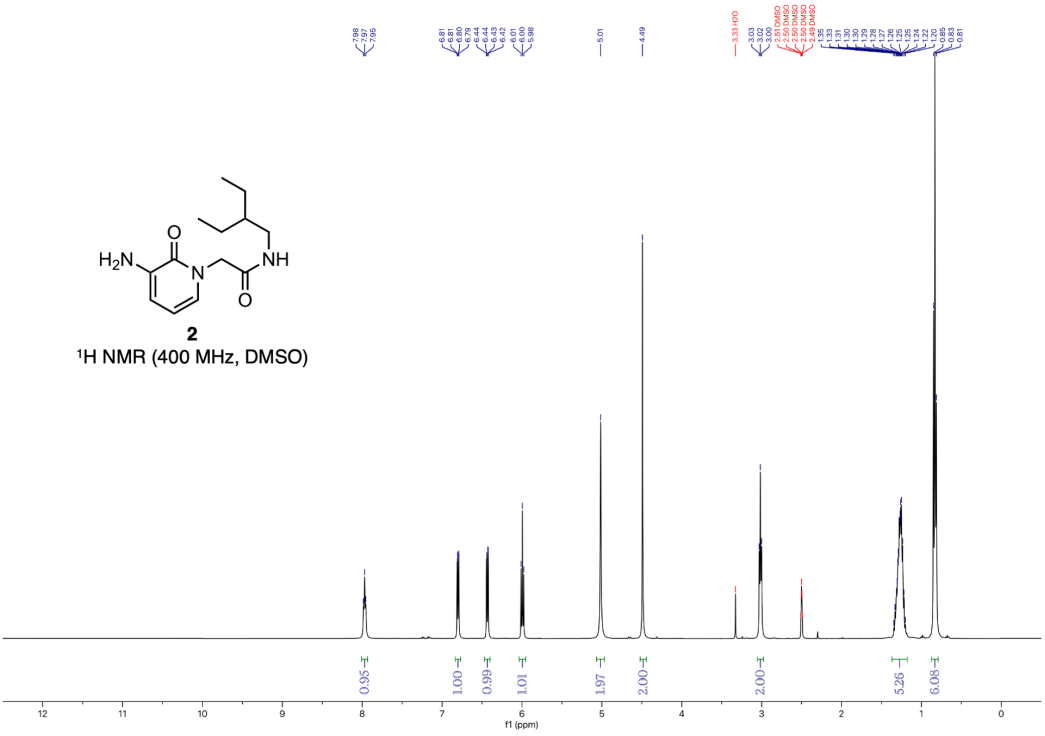
[a] Sample was done in triplicated measurements with background correction. [b] Standard deviation.

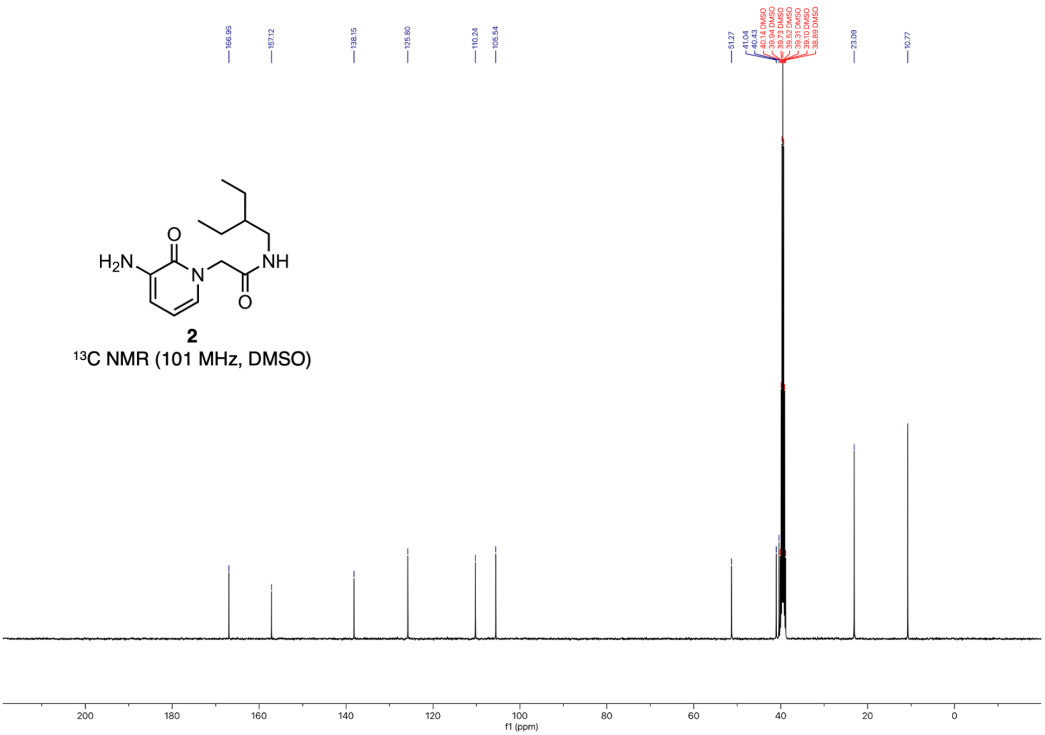
Note for the following subsection: *The compound number presented on each of the spectra is with respect to the chapter in which it presented. For example,* **10** *refers to Compound* **3.10** *presented above.*

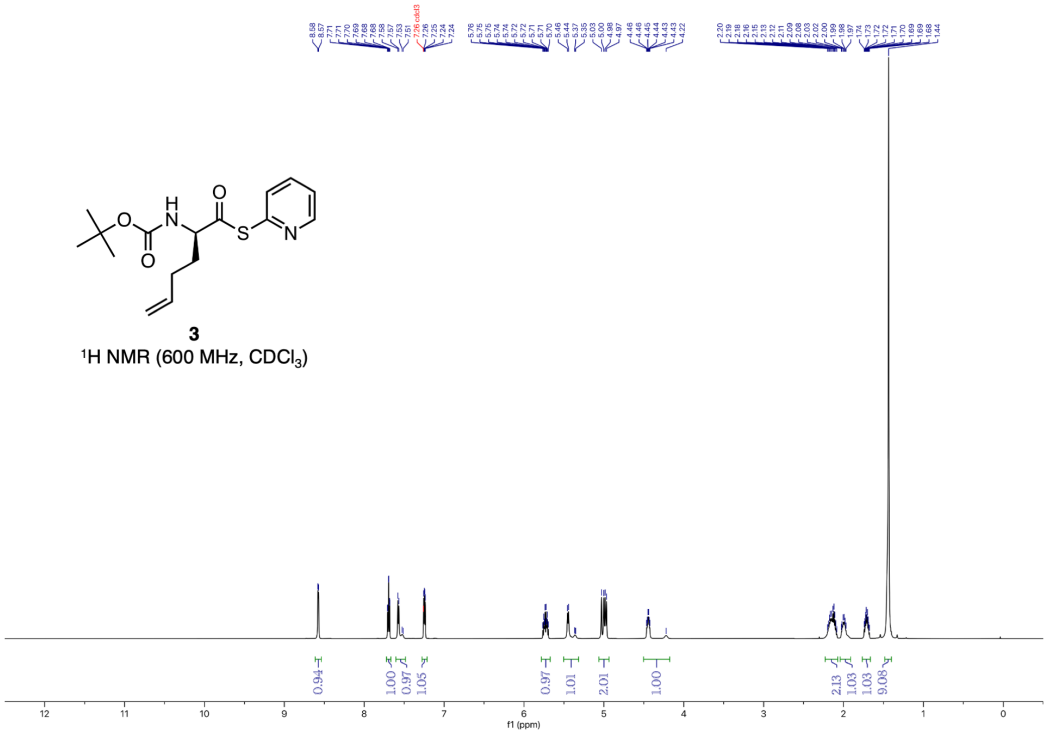
3.4.11 NMR Spectra





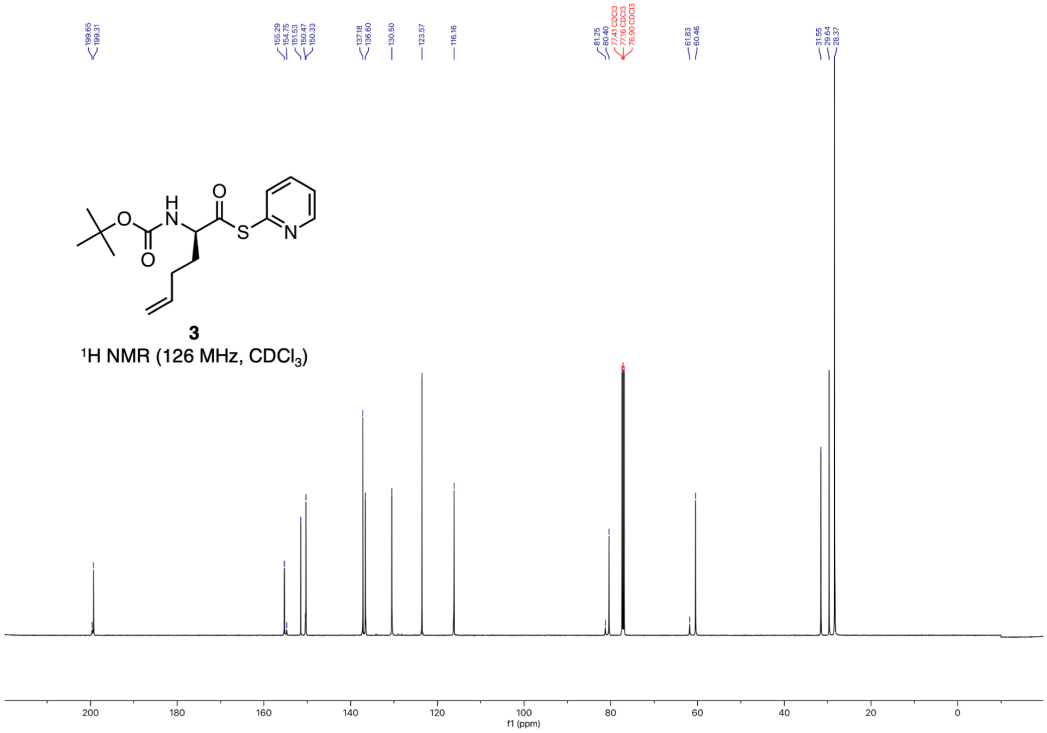

H2N
O
N
NH
O
2
1H NMR (400 MHz, DMSO)
f1 (ppm)


H2N
O
N
NH
O
2
13C NMR (101 MHz, DMSO)
f1 (ppm)



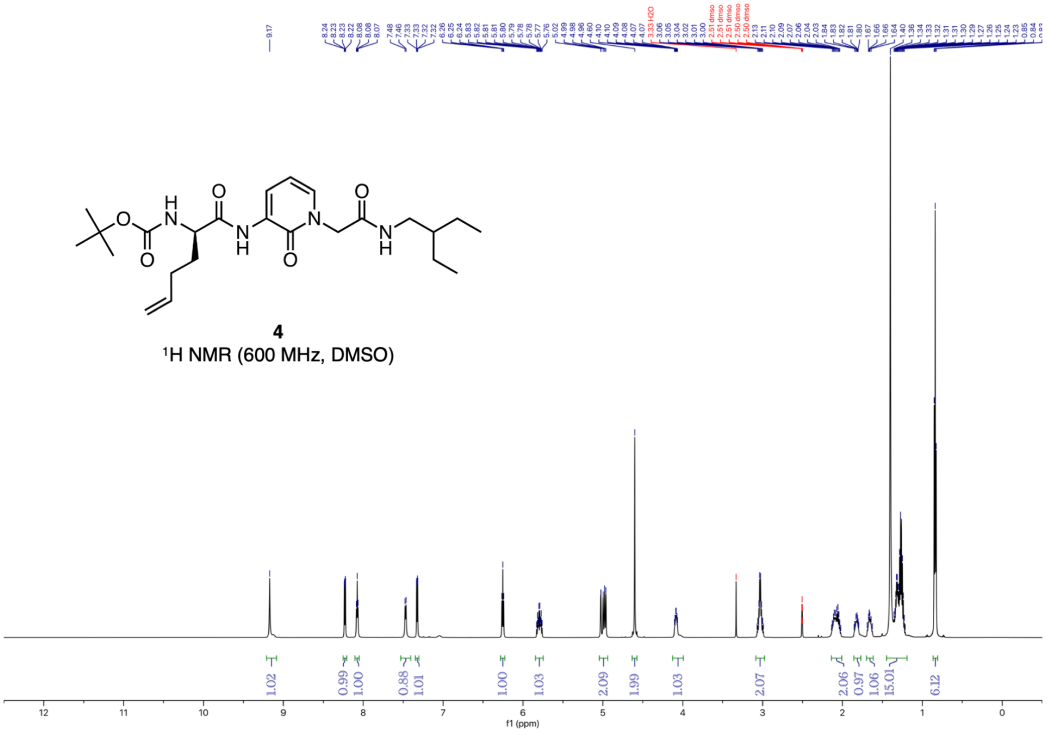
3

^{1}H NMR (600 MHz, $CDCl_3$)

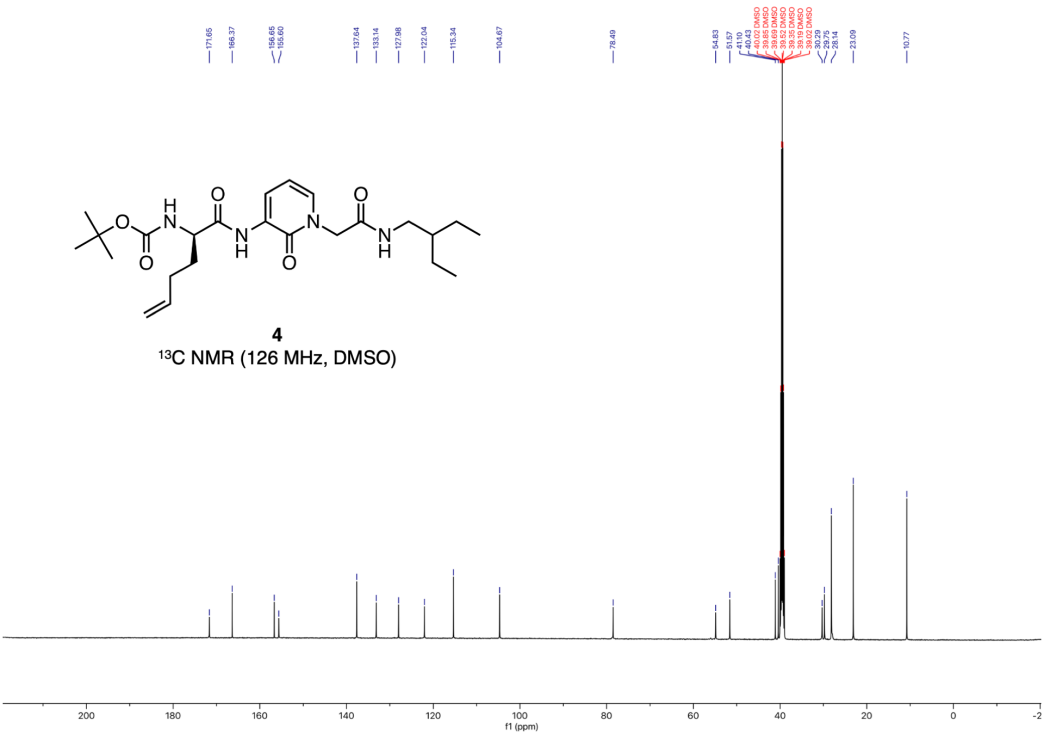


3

^{1}H NMR (126 MHz, $CDCl_3$)



4
^{1}H NMR (600 MHz, DMSO)

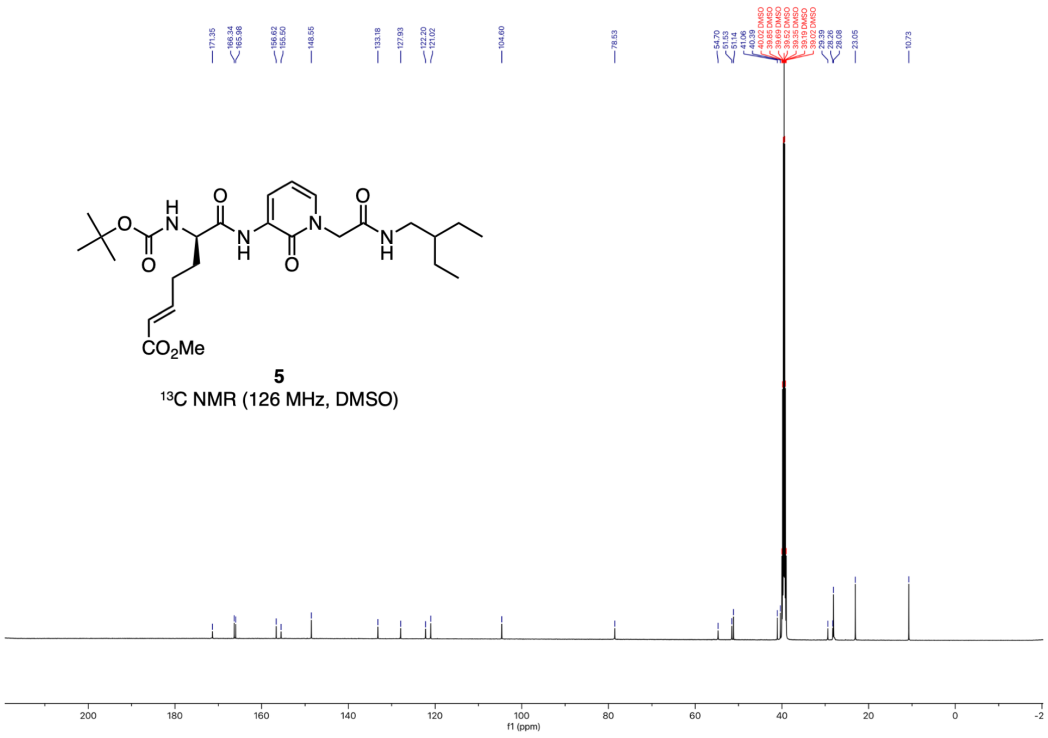


4
^{13}C NMR (126 MHz, DMSO)



5

^{1}H NMR (600 MHz, DMSO)



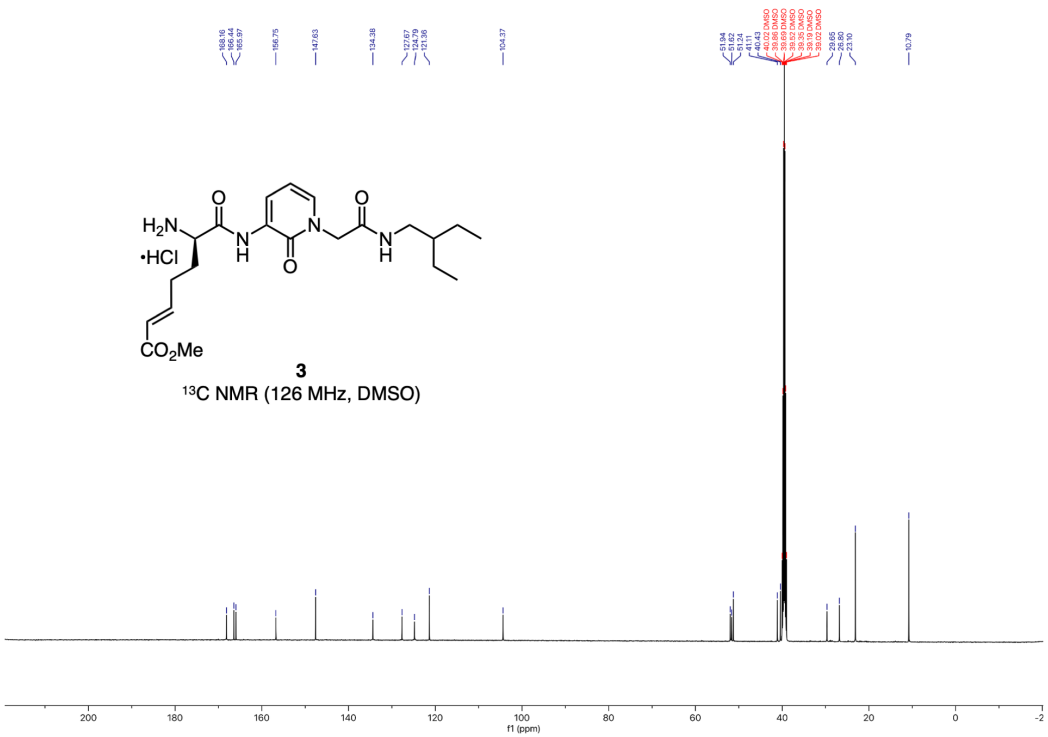
5

^{13}C NMR (126 MHz, DMSO)



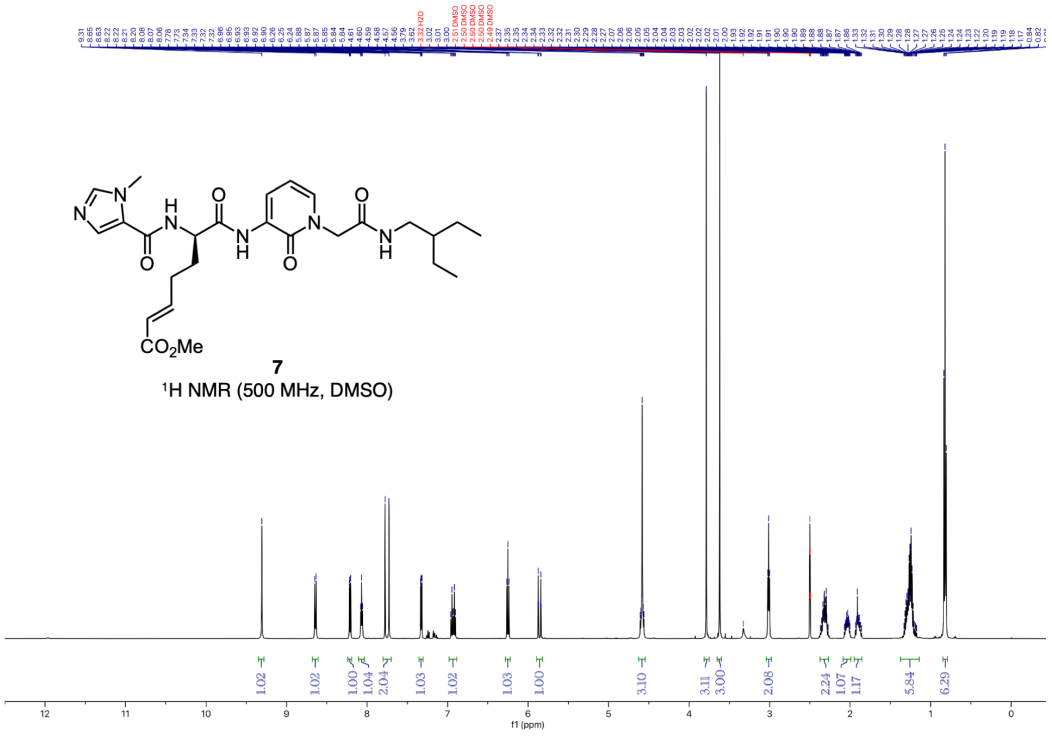
6

^{1}H NMR (500 MHz, DMSO)



3

^{13}C NMR (126 MHz, DMSO)



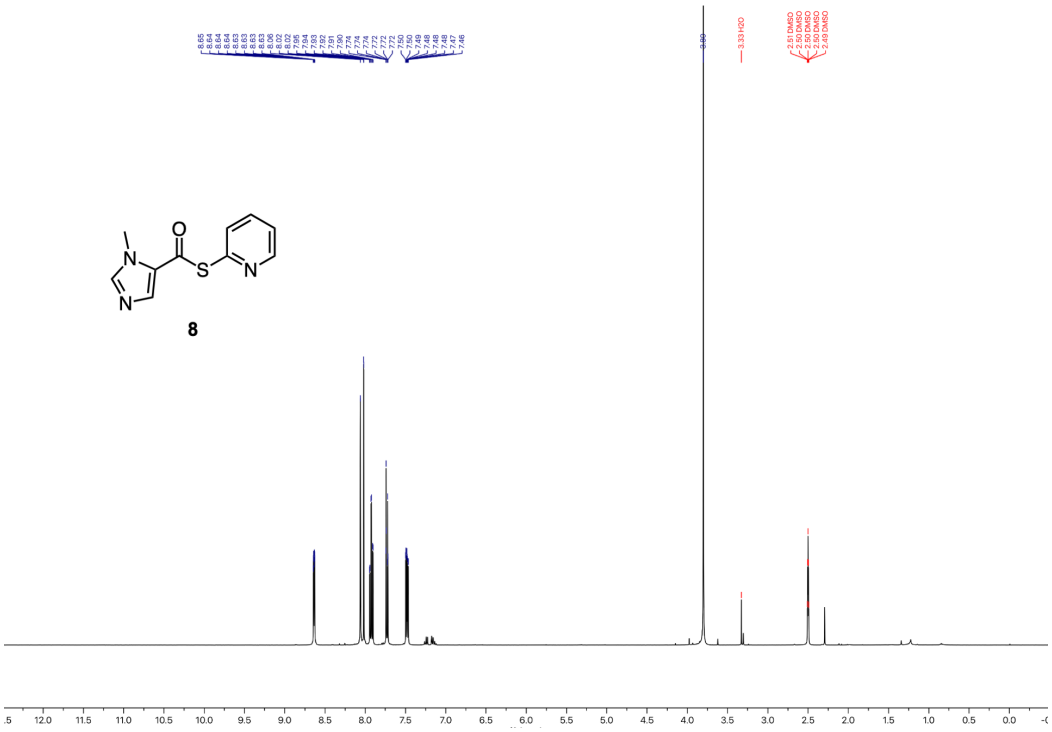
7

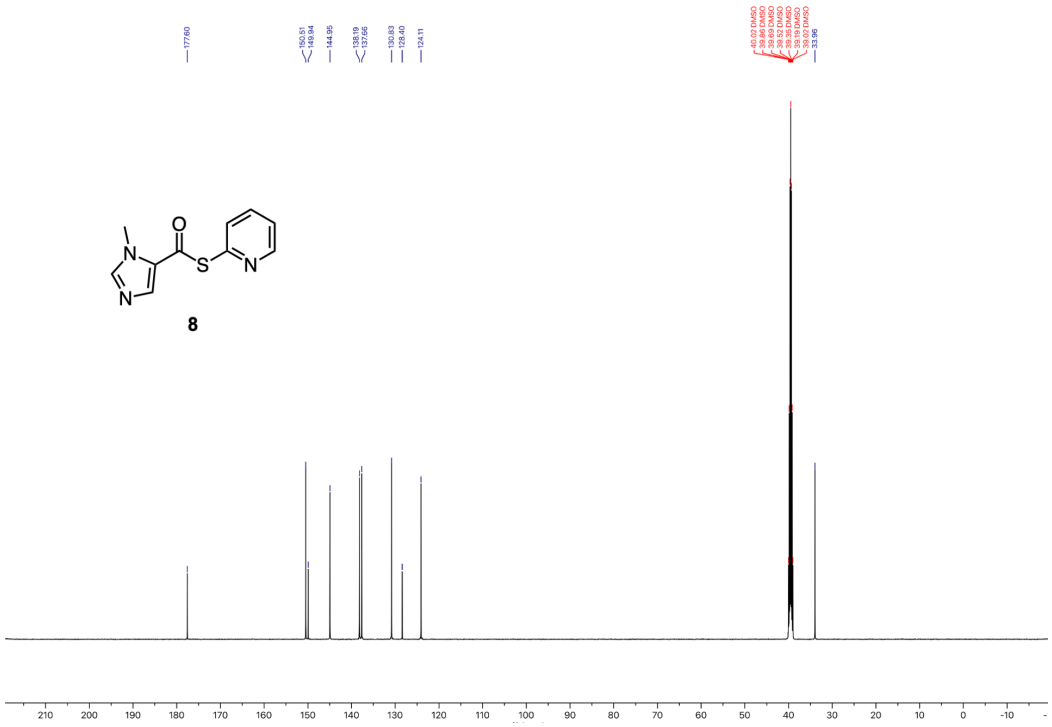
^{1}H NMR (500 MHz, DMSO)



7

^{13}C NMR (126 MHz, DMSO)


8.65
8.64
8.64
8.64
8.64
8.63
8.63
8.63
8.63
8.63
8.62
8.02
8.02
7.96
7.94
7.93
7.92
7.91
7.91
7.74
7.74
7.73
7.72
7.72
7.72
7.71
7.50
7.50
7.49
7.49
7.48
7.48
7.47
7.47
7.46
3.89
3.33 H2O
2.51 DMSO
2.50 DMSO
2.50 DMSO
2.50 DMSO
2.49 DMSO
8


177.60
150.51
149.94
144.95
138.19
137.66
130.83
128.40
124.11
40.02 DMSO
39.80 DMSO
39.59 DMSO
39.38 DMSO
39.17 DMSO
38.96 DMSO
33.96
8

Chapter 4:

Investigations Into Reactor Degassing via Ex-Situ Enzymatic Oxygen Fixation

The contents of this chapter have not been published at the time of writing this thesis. Any data and analyses presented herein should be considered preliminary.

4.1 Introduction

A significant factor pertaining to much of organic synthesis that serves to substantially increase the incurred cost, waste, and associated hazards stems from inherent incompatibilities with standard atmospheric conditions. This is especially the case for organometallic chemistry, where atmospheric oxygen can readily solubilize into the reaction media and oxidize the transition metal and/or associated phosphine ligands. This results in catalyst poisoning and, thus, a diminishing of desired reactivity. Beyond this, substrates themselves can be oxygen sensitive, as was seen with compound **3.2** from Chapter 3. To remediate this issue, chemists can fairly straightforwardly perform such reactions under atmospheres

that are inert with respect to the reaction being performed. From a life-cycle perspective, obtaining these pure gases and then using them to establish inert conditions within a reactor is, however, non-trivial, highly wasteful, and poses significant safety hazards.

Most commonly, the gases employed are nitrogen gas (N_2) and argon (Ar) gas due to their highly non-reactive nature.* In order to obtain these gases industrially in high purity, atmospheric air is first condensed into the liquid state by cooling to cryogenic temperatures.[22] The individual gases (in the liquid phase at these temperatures) are then separated from one another via fractional distillation.[22] To perform these procedures requires highly expensive specialized apparatuses for the needed thermal transfer, gas compression, and distillation processes.† Furthermore, to cool such large volumes of gas to such extreme cryogenic conditions (to temperatures of 196 °C and below) requires an immense amount of energy. This energy is largely derived from fossil fuels and, thus, contributes to the ongoing existential threat of climate change.‡

Once these purified gases are obtained, they are stored in highly pressurized (2000-2500 psi) cylinders for small-scale use, or in large Dewars where the gas is stored cryogenically as a liquid, with evaporation into the headspace of the Dewar providing the source of pressurized gas. First, such highly pressurized gas containers pose a significant and persistent safety risk. Such high pressures pose explosion risks and present a suffocation hazard should the gas be rapidly released into an enclosed area.§

*Argon is an entirely non-reactive noble gas.

†Many gas procurement companies provide this information on their websites. For this thesis, the websites of Elme Messer Gaas (https://elmemesser.lv/en/products/liquid-cryogenic-gas/production-of-air-gases/) and Applied Energy Systems Inc. (https://www.appliedenergysystems.com/the-properties-of-gas-purity-physical-gas-separation/) were utilized (visited on 03/10/2026).

‡Information on this is provided by Parker Hannifin (https://tinyurl.com/ParkerEnvironmental; website accessed on 03/10/2026).

§Information obtained from the United States Occupational Health and Safety Administration website (accessed 03/10/2026).

These hazards necessitate specific engineering controls and serve to increase the cost of handling such gases.

Dewars, having to maintain extremely cold internal temperatures, have a double-walled vacuum seal design that significantly reduces heat transfer between the contents of the tank and the outside atmosphere. This allows for the cryogenic liquid to be stored for extended periods of time. However, no such insulation is ever perfect. That is, fluctuating outside temperatures and changing usage demands cause the internal pressure of these Dewars to frequently exceed the upper threshold. Safety valves straightforwardly release some of the gas to bring the pressure back to a safe level.* However, this gas, which requires such specialized equipment and huge amounts of energy to obtain, is simply lost by being released back into the atmosphere. This greatly adds to the wastefulness and environmental impact of these processes and can present a significant inherent problem that is very challenging to mitigate.

Finally, how chemists use these gases to establish inert reaction environments is also inherently wasteful. To remove oxygen from a reaction vessel and to establish an internal atmosphere of inert gas, there are two main approaches. There is the pump-purge method, where air is removed *en vacuo*, the vessel is refilled with the inert gas, and the process is repeated until the levels of oxygen are tolerable.[78] Alternatively, vessels can be sparged. Here, there is a continuous flow of inert gas into and out of the vessel. The gas is flowed through the container until oxygen levels are sufficiently low, then the reactor is closed.[78] In both cases, large volumes of inert gas are expended to remove unwanted oxygen. As was mentioned above, intensive techniques and large amounts of power go into obtaining gas that is then simply released back into the atmosphere, thus contributing to the overall environmental egregiousness stemming from inert gas usage.

*See "Know Your Liquid Nitrogen Dewar (AKA Vertical Gas Liquid (VGL) Cylinder or Tank)" by Texas Tech's Office of Environmental Health & Safety (https://www.depts.ttu.edu/ehs/academicsafety/labsafetydocs/Liquid-Nitrogen-FAQ.pdf).

To date, unfortunately, there exist few alternatives. While there are catalyst beds that can effectively capture atmospheric oxygen, these catalyst beds, which are comprised of transition metals, have to be regenerated under reducing conditions, and have a limited capacity and lifetime. As such, these are, in their own right, not environmentally friendly. Practically, such "scrubbers" are usually implemented for removing trace levels of oxygen for obtaining highly inert conditions (*e.g.*, gloveboxes storing air-sensitive catalysts*).[56]

Given all of these drawbacks of procuring purified argon and nitrogen gas, it is clear that new technologies are needed to establish oxygen-free environments in a much more sustainable way. In exploring such options, I specifically sought a method that would address or circumvent the intense energy demands for establishing such inert environments. Moreover, I sought to implement a method that enables the oxygen-sensitive chemistry presented in Chapters 2 and 3.

4.2 Results and Discussion

Electrochemical biosensors are incredibly useful devices that can rapidly detect biological analytes of interest. While invaluable, a significant shortcoming of such devices, however, is that interference by atmospheric oxygen can render such measurements inaccurate. While fairly simple to address in a laboratory with inert gas flow systems, this drawback has precluded direct measurement in the field, which is more desirable for rapid acquisition of the needed data. In 2012, however, Campbell and colleagues reported a clever solution to this problem as it pertains to nitrate biosensors that rely on cyclic voltammetry.[68] In their disclosure, they articulated how oxygen can be consumed in an aqueous solution

*Glovebox manufacturers' websites offer supporting information on this. For example: MBraun (https://www.mbraun.com/us/applications/laboratory-chemistry.html)

via the enzymatic oxidation of glucose. After incorporation of catalase to remove unwanted hydrogen peroxide byproduct, and with optimization of the buffer concentration and glucose loading, Campbell and colleagues reported a system that can maintain an oxygen-free environment* in a solution that is, remarkably, open to air.† Upon reading this, I considered the potential application of this method toward our group's organometallic methodologies given our use of aqueous micellar systems, and demonstrated compatibility of our surfactant technology with enzymatic catalysis.[79]

It was apparent from the start, however, that this was not going to be as simple as just adapting Campbell's (and Benesch's) method to our aqueous surfactant system. For one, the oxidase and catalase enzymes are pH sensitive[68] and would not be functional under the basic conditions needed for cross-coupling reactions like Suzuki-Miyaura couplings or Buchwald-Hartwig aminations. Furthermore, it is desirable in the production of pharmaceutical agents to minimize the number of reagents or components present in the reaction media. In this manner, process chemists inherently limit the number of impurities needed to be purged from the desired product and, thus, make pure material easier to obtain. With this in mind, I hypothesized that there may be an *ex situ* means of enzymatically reaching oxygen-free reaction environments.

Though the reaction media would not contain the enzyme itself and, therefore, could not be open to air, I reasoned that, in a closed system, the enzyme could act as an oxygen sink for the reaction media. For this, I proposed a dual-chamber system (Figure 4.1) where the two solutions would be physically separated but share the same atmosphere. As oxygen is fixated in the oxidation of glucose to gluconic acid, a gradient between aerobic and anaerobic solutions would cause diffusion of oxygen out of the

*Of course, how long an oxygen-free environment can be maintained under open air is dependent on the concentration of glucose and enzymes used.

†It is important to note that this phenomenon of using oxidase and catalse to maintain an oxygen free solution under open air was first presented by Ruth E. Benesch and Reinhold Benesch in 1953.[5] The work of Campbell *et al.* is largely an adaptation of their work in the application of maintaining oxygen free nitrate sensors.

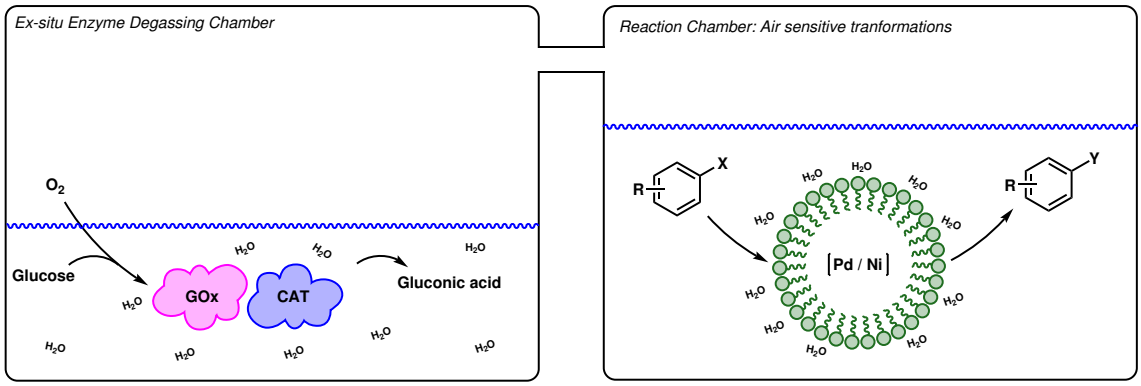


Figure 4.1: Proposed Dual-Chamber System for *Ex situ* Enzyme Degassing

reaction media and into the enzyme solution.* This effectively would lead to the desired degassing of the reaction media.

An early qualitative experiment using our borylation method (see Chapter 2) for loratadine in aqueous 2 wt % TPGS yielded promising results. Here, the deoxygenation was allowed to take place for 24 h, at which point the catalyst solution was added to initiate the borylation. The final result of full conversion to the product (as determined by TLC and ^{1}H NMR) initially indicated that the media was sufficiently degassed, as there was not any appreciable catalyst poisoning or degradation associated with the overall conversion. However, as is the case with any experiment, the data is only as good as the control. When the reaction was rerun in an identical fashion, but without being connected to the *ex situ* enzyme solution, the same result of full conversion was obtained. Beyond being surprising that this specific reaction was unaffected by being run in non-degassed conditions,† it indicated that the enzyme was not properly isolated as a dependent variable. While the borylations are known to be oxygen sensitive, specific reaction and substrate dependence on oxygen sensitivity showed that this was an indirect and

*Discussion is provided as to why this reasoning was found to be erroneous (*vide infra*).
†Our borylation of loratidine proved remarkably robust.

unreliable means of moving forward. This prompted me to turn my focus to measuring the effectiveness of the enzyme by attempting to measure the oxygen levels directly.

Oximeters, especially those that are sensitive enough to measure at the ppm level, are costly and are generally not accessible in an academic context. Given this limitation, my approach toward ascertaining the level of oxygen present involved the same cyclic voltammetry method used by Campbell and colleagues.[68] I first prepared three solutions of 2 wt% TPGS-750-M: one solution was traditionally prepared via sparging with argon, one solution was degassed via my *ex situ* enzyme set-up (Figure 4.1), and the third solution was not treated with any degassing procedure in order to serve as a control. The result of performing cyclic voltammetry (CV) on these three solutions provided an encouraging data point: the argon-sparged solution showed no oxygen interference, the enzyme-degassed solution showed minimal interference, and the control showed the presence of oxygen. Noted, however, is that this was qualitative and not able to be precisely controlled to yield a quantitative result for the levels present in each case. Furthermore, it is crucial to note that the procedure for obtaining these voltammograms was seen to contain experimental error that was challenging, if not impossible, to remove. For one, the degassed solutions required the use of argon in handling and transferring the solutions to the instrument. As such, there was no adequate way to control for any oxygen diffusion out of the solutions by exposing them to inert gas during handling. Similarly, a nitrogen flush is necessary in running cyclic voltammetry in this instrument to remove atmospheric oxygen interference. Again, here, there was no means by which to control for oxygen diffusion out of the system that would occur from having a continually flushed headspace. Indeed, the control of non-sparged solution showed the presence of oxygen despite the overhead nitrogen flush, but, again, diffusion of oxygen was a variable that could not be accounted for in any case. Perhaps the enzyme was only partially effective, but appeared completely effective as inert

gas flow removed the remaining detectable levels of oxygen. The control, perhaps, could have shown a greater oxygen interference. Having the CV incorporated into the enclosed dual-chamber system in order to run measurements directly would be more ideal, but as the instrument was borrowed from another research group and was incompatible with such a setup, this was not pursuable. Ultimately, the results could not be used quantitatively and would only serve as qualitative supporting information for other quantitative results. Moreover, it became evident that the project, even if eventually viable, was veering away from my skill set as a synthetic organic chemist, and becoming a more relevant problem in an engineering context.

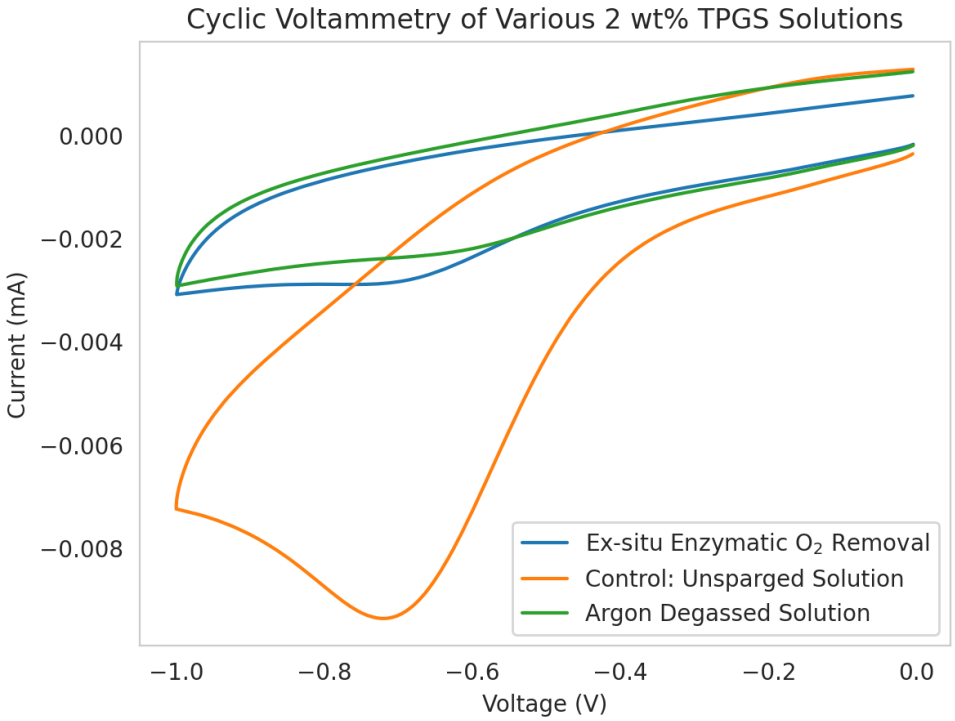


Figure 4.2: Cyclic Voltammetry Measurements (with PGE at $50mV^{-1}s$) for Various 2 wt% TPGS Solutions

(NOTE: See discussion regarding potential experimental error for this data.)

In another attempt to assess the oxygen level, our collaborators at NECi Superior Enzymes* leveraged their own oximeter, which is capable of measuring oxygen to the ppb level. In this, they were able to obtain measurements for our dual-chamber setup. The findings here are not as we had hoped: no appreciable change in oxygen was observed. Our collaborators did try a singular pump-purge of the headspace that yielded a trend showing a decrease in oxygen in the solution over time. However, this does not at all provide any support for the enzyme functioning as hoped. By removing the headspace and backfilling with nitrogen, there was a gradient established between the oxygen present in the water and the lack of oxygen present in the atmosphere. This, of course, subsequently drove diffusion of the dissolved oxygen into the atmosphere of the apparatus. In turn, the oximeter read a decrease in dissolved oxygen over time. Even if the enzyme did fixate some of this oxygen, there was no readily available means to ascertain what percentage of oxygen loss was due to fixation and what percentage was due to simple diffusion. Oximeter measurements for the atmosphere in addition to the oxygen levels in the water were not requested from NECi. This is because, if it turned out that in this scenario the enzyme had made some contribution, the need for a pump purge cycle to initiate this ran contrary to the entire motivation for the project.

The inability of the ex-situ enzyme solution to degas the reaction media can be rationalized in a straightforward manner. First, oxygen comprises about 20% of a standard atmosphere.[18] Therefore, if all of the oxygen were removed from our closed dual-chamber system, there would be a pressure decrease from 1 atm to 0.8 atm: effectively establishing a vacuum within our system. Just by taking the simple Boltzmann definition of entropy being correlated to the natural log of the microstates in the system, that removal of gas would be fairly entropically disfavored. Additionally, diffusion into the

*NECi Superior Enzymes' website: https://nitrate.com/

enzyme solution would diminish with decreasing pressure. Without a means of gas replacement,* it became clear that this ex-situ method was simply not going to be viable, at least not on the time frame that would be relevant to synthetic work.

4.3 Conclusion

The goal of this project was to address, within the context of organic chemistry, the environmental impact resulting from inert gas usage. Given the large amounts of energy and resources required to procure these purified gases, the inherently wasteful means by which they are stored and used, and with the safety concerns surrounding their usage, I sought a different means by which to remove oxygen from our reaction vessels. Inspiration was drawn from the work of Campbell et al.,[68] and the primary work of Ruth E. Benesch and Reinhold Benesch.[5] Specifically, I sought to use the oxidase/catalase dual enzyme system as an *ex situ* oxygen sink in a dual-chamber setup. In this fashion, oxygen removal could potentially be achieved without concerns regarding orthogonality of the organic transformations with the enzymes themselves.

The initial qualitative assessment of running a borylation reaction in this manner revealed that this was an indirect and potentially misleading means of determining efficacy, as oxygen sensitivity varies from reaction to reaction, and not measuring the dependent variable directly could lead to incorrect conclusions. I then attempted the cyclic voltammetry techniques utilized in the literature.[68] The issues with accuracy in these measurements for the ex-situ case, where we tried to determine the dissolved oxygen levels in the reaction media, became apparent in running the experiment. Specifically, the use

*An inert gas inlet could be provided, but this would defeat the purpose of using the enzyme system in the first place.

of inert gases used for transferring the solutions and those used in the running of the CV would cause oxygen diffusion that could not be accounted for. Without a better CV setup being available to us, we reached out to our collaborators at NECi Superior Enzymes* who have an oximeter that is sensitive to the ppb level. Unfortunately, this experiment confirmed that the enzyme system was showing no appreciable effect on the level of oxygen in the system.

There are several implementations that may be able to overcome the barriers faced. First, a pump system that would be able to uptake the air in the headspace and bubble it through the enzyme solution may provide a much more effective means of delivering the oxygen to the oxidase/catalase system. Secondly, there must be a means of compensating for the volume of air lost. Perhaps some sort of piston pressurization apparatus could be implemented. Nonetheless, these solutions highlight again that answers to these issues were engineering-based and not in line with my focus area of organic synthesis.

I believe it is important to point out that this enzyme deoxygenation system is quite analogous to an air-free glovebox system. Gloveboxes similarly involve two-chambers:† the main chamber for handling air-sensitive materials and reactions and the second chamber containing a copper-based catalyst bed‡ for removing trace oxygen. A circulator continuously moves air from the main chamber, pushes it through the catalyst bed, and returns the purified air to the main chamber. I believe the two-chamber enzyme system could function in much the same way for efficiently maintaining inert systems. Here, the enzyme system would act as the catalyst bed for removing oxygen. What is important to note from this comparison is that glovebox catalyst beds are not effective in bringing a system down from atmospheric levels of oxygen to levels below 4 ppm. Normally, the system is purged with inert gas to reach a level

*NECi Superior Enzymes' website: https://nitrate.com/

†Not counting the antechambers used for moving into and out of the glovebox.

‡These beds can also contain materials for removing other undesirable atmospheric impurities (*e.g.*, zeolite can be included to absorb trace moisture).[56]

of 20 ppm oxygen, at which point the catalyst bed can bring the oxygen to trace levels. Thinking of the enzyme system as the catalyst bed in this case, it would make sense that it also would not be applicable to establishing inert conditions from a standard atmosphere. Rather, its application would be in maintaining an already highly inert system.

Much of air-sensitive chemistry relies on positive pressures of inert gases as well as continual inert gas flow. This maintains air-free environments during solid and liquid transfer procedures. The enzyme cannot, or is not yet in a position to, provide such inert gas flows. It is also important to note that nitrogen (N_2) is highly abundant, comprising 78% of the earth's atmosphere.[18] With streamlined industrial fractional distillation processes, nitrogen gas is actually rather economical and facile to obtain. The environmental impact of these practices may therefore be best addressed by implementing sustainable energy sources for fractional distillations and by investing more into inert gas recovery systems.

4.3.1 Closing Remarks

In all, while the project was interesting and seemed initially promising, adherence to proper control experiments and careful analysis of the results allowed me to properly characterize the system, demonstrate that it was not performing as effectively as hoped, and allowed me to articulate why this was potentially the case. Solutions to problems encountered were postulated, but were not pursued further given that they are beyond the scope of topics presented in this thesis.

4.3.2 Acknowledgements and Noted Contributions

Acknowledgement is given to Monica Lopez Lemus and Jordan Yirak for their assistance in running experiments, including prepping samples for the CV experiment. Assistance by Kaden Wheeler, a

graduate student in Professor Leor Sepunaru's Lab, in obtaining CV data is acknowledged with thanks. Furthermore, thanks is given to NECi Superior Enzymes for providing the Oxybo enzyme gels and buffer solutions needed for this project, as well as for providing relevant data from their oximeter for the *ex situ* enzyme system.

4.4 Experimental Data and Information.

4.4.1 General Information

NMR

^{1}H and ^{13}C NMR were recorded at 25 °C on either a Bruker Avance III HD 400 MHz, a Bruker Advance NEO 500 MHz, or on a Varian Unity Inova 500 MHz in $CDCl_3$ with residual $CHCl_3$ (^{1}H = 7.26 ppm, ^{13}C = 77.26 ppm). Chemical shifts are reported in parts per million (ppm) and coupling constants (J values) are reported in Hz. Peak splitting is reported in the following fashion: singlet (s), broad singlet (bs), doublet (d), triplet (t), quartet (q), pentet (p), and multiplet (m).

Reagents

Unless mentioned otherwise, all chemical reagents were utilized directly from vendors without any further purification. EtOAc and hexanes were obtained from Fischer Scientific and no special considerations were taken to ensure these solvents were anhydrous. When needed, EtOAc and water were degassed by sparging the solvent with a stream of argon gas. Deuterated chloroform was purchased from Cambridge Isotope Laboratories and kept over activated 4 Å molecular sieves in order to maintain dryness. $Pd(OAc)_2$ was purchased from Johnson Matthey. XPhos was obtained from Combi Blocks Int. *Tetrakis*(dimethylamino)diboron and 3,4-diethylhexane-3,4-diol were purchased from Ambeed Inc. Potassium 2-ethylhexanoate (2-KEH) was purchased from Ambeed Inc. and was kept and handled in a glovebox under an atmosphere of argon. Potassium phosphate tribasic was purchased from Sigma Aldrich. TPGS-750-M[49] was obtained from PHT International (TPGS-750-M is also available from

Sigma-Aldrich catalog #733857). All other chemical reagents, including aryl/heteroaryl halides and organic and inorganic bases, were purchased from Combi Blocks Int., Ambeed Inc., Fischer Scientific, Enamine, PHT International, Fluorochem, Alfa Aesar, Acros Organics, and Chem Scene. Thin Layer Chromatography (TLC) was performed using Silica Gel 60 F254 (Merck, 0.25mm thickness), and developed plates were visualized under a UV lamp (254 nm). Further analysis was performed via cerium molybdate stain or potassium permanganate stain and subsequently developed using a heat gun.

Generating a Solution of Non-degassed 2 wt % TPGS-750-M / H_2O

To a clean 100 mL round bottom flask charged with a PTFE coated stir bar was added 2 g of TPGS-750-M.[49] To the flask was then added 98 mL of degassed HPLC grade water. The flask was fitted to a stir plate and vigorously stirred for 12 h. The flask, when not being used, was sealed with a rubber septum to prevent evaporation.

Generating a Solution of Degassed 2 wt % TPGS-750-M / H_2O

To a clean 100 mL round bottom flask charged with a PTFE coated stir bar was added 2 g of TPGS-750-M.[49] The flask was then fitted with a septum and attached to a vacuum/argon manifold via a needle through the septum. The flask was then subjected to three cycles of vacuum and then backfilling with argon. Under an atmosphere of argon, to the flask was then added 98 mL of degassed HPLC grade water. Still attached to the manifold and under an atmosphere of argon, the flask was fitted to a stir plate and vigorously stirred for 12 h. The flask was kept under a constant atmosphere of argon.

4.4.2 General Procedures and Results

Dual Chamber Enzymatic Oxygen Removal Set Up

In a 2-dram vial charged with a PTFE-coated stir bar was added two Oxybot© gels (NECi's proprietary dual oxidase/catalase enzyme system on a solid support gel).* To the vial was added 2 mL of NECi's sugar and phosphate buffer solution* (with the sugar loading being in large excess of what can be anticipated for oxygen levels stemming from the headspace and aqueous solutions). The vial is sealed with a septum and connected via cannula† to a sealed non-degassed 100 mL flask containing 100 mL of 2 wt% of TPGS-750-M as well as a PTFE-coated stir bar. The dual-chamber setup was then fixed to a stirplate and set to vigorous stirring for a minimum of 24 hr before the solution was used or analyzed.

Borylation Test Reactions

The borylation of loratidine was performed on a 0.25 mmol scale according to the procedures found in Section 2.4 using 2.5 M of non-degassed 2 wt% TPGS-750-M / H_2O, and with no degassing of the headspace. The control reaction was allowed to proceed as is. For the *ex-situ* enzyme test, no catalyst was added, and the sealed, non-degassed reaction vial was connected to the *ex-situ* enzyme system described above. Stirring of the two-chamber system was allowed to proceed for 24 h. The XPhos catalyst solution was then added to the vial, the vial was disconnected from the two-chamber apparatus, and the reaction was allowed to proceed according to the above-mentioned general procedure. Both reactions were stopped after 4 h, and full conversion was confirmed by TLC and crude proton NMR.

*Formulation of these gels, the ratio and amount of enzymes present in the gel, the glucose concentration, the phosphate buffer concentration, etc. are all proprietary to NECi Superior Enzymes. For more information, they can be contacted on their website (https://nitrate.com/).

†Different inner diameters of cannula were tried with no observable effect on the efficacy of oxygen fixation.

References

(1) Achilli, C.; Ciana, A.; Fagnoni, M.; Balduini, C.; Minetti, G. *Open Chemistry* **2013**, *11*, 137–139.

(2) Alder, C. M.; Hayler, J. D.; Henderson, R. K.; Redman, A. M.; Shukla, L.; Shuster, L. E.; Sneddon, H. F. *Green Chem.* **2016**, *18*, 3879–3890.

(3) Anastas, P. T.; Warner, J. C., *Green Chemistry: Theory and Practice*; Oxford University Press: Oxford, New York, 2000.

(4) Badone, D.; Baroni, M.; Cardamone, R.; Ielmini, A.; Guzzi, U. *J. Org. Chem.* **1997**, *62*, 7170–7173.

(5) Benesch, R. E.; Benesch, R. *Science* **1953**, *118*, 447–448.

(6) Billingsley, K.; Buchwald, S. L. *J. Am. Chem. Soc.* **2007**, *129*, 3358–3366.

(7) Bozorg, S. R.; Lee, A. R.; Mårild, K.; Murray, J. A. *Gastroenterology* **2024**, *167*, 172–182.

(8) Britton, J.; Jamison, T. F. *European Journal of Organic Chemistry* **2017**, *2017*, 6566–6574.

(9) Brown, D. G.; Boström, J. *J. Med. Chem.* **2016**, *59*, 4443–4458.

(10) Büchold, C.; Hils, M.; Gerlach, U.; Weber, J.; Pelzer, C.; Heil, A.; Aeschlimann, D.; Pasternack, R. *Cells* **2022**, *11*, 1667.

(11) Cai, M.; Luo, C.; Xu, C.; Huang, B. *Synthesis* **2022**, *54*, 1339–1346.

(12) Choung, R. S.; Unalp-Arida, A.; Ruhl, C. E.; Brantner, T. L.; Everhart, J. E.; Murray, J. A. *Mayo Clinic Proceedings* **2017**, *92*, 30–38.

(13) Chow, W. K.; Yuen, O. Y.; Choy, P. Y.; So, C. M.; Lau, C. P.; Wong, W. T.; Kwong, F. Y. *RSC Adv.* **2013**, *3*, 12518–12539.

(14) Collman, J. P.; Yan, Y.-L.; Lei, J.; Dinolfo, P. H. *Org. Lett.* **2006**, *8*, 923–926.

(15) Compagno, N.; Lucchetti, N.; Palmisano, A.; Profeta, R.; Scarso, A. *J. Org. Chem.* **2024**, *89*, 12452–12461.

(16) Constable, D. J. C.; Curzons, A. D.; Cunningham, V. L. *Green Chem.* **2002**, *4*, 521–527.

(17) Coombs, J. R.; Green, R. A.; Roberts, F.; Simmons, E. M.; Stevens, J. M.; Wisniewski, S. R. *Organometallics* **2019**, *38*, 157–166.

(18) *Allen's Astrophysical Quantities*; Cox, A. N., Ed.; Springer: New York, NY, 2002.

(19) Cox, P. A.; Reid, M.; Leach, A. G.; Campbell, A. D.; King, E. J.; Lloyd-Jones, G. C. *J. Am. Chem. Soc.* **2017**, *139*, 13156–13165.

(20) D'Amico, F.; Papucci, C.; Franchi, D.; Reginato, G.; Taddei, M.; Mordini, A.; Zani, L.; Dessì, A.; Calamante, M. *J. Org. Chem.* **2024**, *89*, 6991–7003.

(21) Dhangar, G.; Serrano, J. L.; Schulzke, C.; Gunturu, K. C.; Kapdi, A. R. *ACS Omega* **2017**, *2*, 3144–3156.
(22) Emsley, J., *Nature's Building Blocks*; Oxford University Press: 2001.
(23) Epp, J. B.; Schmitzer, P. R.; Crouse, G. D. *Pest Management Science* **2018**, *74*, 9–16.
(24) FDA Q3D (R1) Elemental Impurities Guidance for Industry, https://www.fda.gov, 2022.
(25) Filonchyk, M.; Peterson, M. P.; Zhang, L.; Hurynovich, V.; He, Y. *Science of The Total Environment* **2024**, *935*, 173359.
(26) Foote, E. *American Journal of Art and Science* **1856**, *XXII*, 382–383.
(27) Freiberg, K. M.; Ghiglietti, E.; Scurria, M.; Lipshutz, B. H. *Green Chem.* **2023**, *25*, 9941–9947.
(28) Gallego, G. M.; Sarpong, R. *Chem. Sci.* **2012**, *3*, 1338–1342.
(29) Gurung, S. R.; Mitchell, C.; Huang, J.; Jonas, M.; Strawser, J. D.; Daia, E.; Hardy, A.; O'Brien, E.; Hicks, F.; Papageorgiou, C. D. *Org. Process Res. Dev.* **2017**, *21*, 65–74.
(30) Gusoff, C. Officials Outraged after Chemical Drums Found Buried in Long Island Park - CBS New York, https://www.cbsnews.com/newyork/news/chemical-drums-found-buried-in-brthpage-long-island-park/, 2024.
(31) Hartwig, J. F. *Acc. Chem. Res.* **2012**, *45*, 864–873.
(32) Hatcher, W.; Vanaparthi, S.; Young, M.; Romero, E. Contrary to Popular Belief, B2pin2 Is Not Air Stable, 2025.
(33) Hayes, H. L. D.; Wei, R.; Assante, M.; Geogheghan, K. J.; Jin, N.; Tomasi, S.; Noonan, G.; Leach, A. G.; Lloyd-Jones, G. C. *J. Am. Chem. Soc.* **2021**, *143*, 14814–14826.
(34) Iino, H.; Hanna, J.-i. *Polym J* **2017**, *49*, 23–30.
(35) Ishiyama, T.; Murata, M.; Miyaura, N. *J. Org. Chem.* **1995**, *60*, 7508–7510.
(36) Iyer, K. S.; Nelson, C.; Lipshutz, B. H. *Green Chem.* **2023**, *25*, 2663–2671.
(37) St-Jean, F.; Remarchuk, T.; Angelaud, R.; Carrera, D. E.; Beaudry, D.; Malhotra, S.; McClory, A.; Kumar, A.; Ohlenbusch, G.; Schuster, A. M.; Gosselin, F. *Org. Process Res. Dev.* **2019**, *23*, 783–793.
(38) Jones, L. H. *Nature Chem* **2015**, *7*, 952–960.
(39) Kincaid, J. R. A.; Caravez, J. C.; Iyer, K. S.; Kavthe, R. D.; Fleck, N.; Aue, D. H.; Lipshutz, B. H. *Commun Chem* **2022**, *5*, 1–7.
(40) Kincaid, J. R. A.; Wong, M. J.; Akporji, N.; Gallou, F.; Fialho, D. M.; Lipshutz, B. H. *J. Am. Chem. Soc.* **2023**, *145*, 4266–4278.
(41) Klumphu, P.; Lipshutz, B. H. *J. Org. Chem.* **2014**, *79*, 888–900.
(42) Knapp, D. M.; Gillis, E. P.; Burke, M. D. *J. Am. Chem. Soc.* **2009**, *131*, 6961–6963.
(43) Larsen, M. A.; Hartwig, J. F. *J. Am. Chem. Soc.* **2014**, *136*, 4287–4299.

(44) Lee, N. R.; Bikovtseva, A. A.; Cortes-Clerget, M.; Gallou, F.; Lipshutz, B. H. *Org. Lett.* **2017**, *19*, 6518–6521.
(45) Liang, M.; Liu, C.; Ju, W.; Han, S.; Zhang, J.; Zhao, Y. *Org. Lett.* **2024**, *26*, 4224–4228.
(46) Lichtenberg, F. R. *Economics & Human Biology* **2022**, *46*, 101124.
(47) Lindfors, K.; Ciacci, C.; Kurppa, K.; Lundin, K. E. A.; Makharia, G. K.; Mearin, M. L.; Murray, J. A.; Verdu, E. F.; Kaukinen, K. *Nat Rev Dis Primers* **2019**, *5*, 3.
(48) Lipshutz, B. H.; Abela, A. R. *Org. Lett.* **2008**, *10*, 5329–5332.
(49) Lipshutz, B. H.; Ghorai, S.; Abela, A. R.; Moser, R.; Nishikata, T.; Duplais, C.; Krasovskiy, A.; Gaston, R. D.; Gadwood, R. C. *J. Org. Chem.* **2011**, *76*, 4379–4391.
(50) Lipshutz, B. H.; Moser, R.; Voigtritter, K. R. *Isr J Chem* **2010**, *50*, 691–695.
(51) Lorand, L.; Iismaa, S. E. *The FASEB Journal* **2019**, *33*, 3–12.
(52) Macho, J. M.; Blue, R. M.; Lee, H.-W.; MacMillan, J. B. *Org. Lett.* **2022**, *24*, 3161–3166.
(53) Mailyan, A. K.; Mata, G.; Miles, D. H.; Sharif, E. U.; Leleti, M. R.; Powers, J. P.; Jeffrey, J. L. *Org. Process Res. Dev.* **2022**, *26*, 2915–2925.
(54) Matteson, D. S. In *The Metal-Carbon Bond: Vol. 4 (1987)*, Hartley, F. R., Ed.; John Wiley & Sons, Inc.: Chichester, UK, 1987, pp 307–409.
(55) Merritt, J. M.; Borkar, I., et al. *Org. Process Res. Dev.* **2022**, *26*, 773–784.
(56) Miller, A. RISE Catalysis Center Glovebox Manual, 2012.
(57) Miyaura, N.; Yamada, K.; Suzuki, A. *Tetrahedron Lett.* **1979**, *20*, 3437–3440.
(58) Molander, G. A.; Cavalcanti, L. N.; García-García, C. *J Org Chem* **2013**, *78*, 6427–6439.
(59) Molander, G. A.; Trice, S. L. J.; Kennedy, S. M.; Dreher, S. D.; Tudge, M. T. *J. Am. Chem. Soc.* **2012**, *134*, 11667–11673.
(60) Munteanu, C.; Spiller, T. E.; Qiu, J.; DelMonte, A. J.; Wisniewski, S. R.; Simmons, E. M.; Frantz, D. E. *J. Org. Chem.* **2020**, *85*, 10334–10349.
(61) Nelson, C. B.; L'Heureux, S. J.; Wong, M. J.; Kuhn, S. L.; Ghiglietti, E.; Lipshutz, B. H. *Green Chem.* **2024**, *26*, 10115–10122.
(62) Nelson, C. B.; Yirak, J. R.; Baumann, M. E.; Freiberg, K. M.; Lipshutz, B. H. *Green Chem.* **2026**, *28*, 938–944.
(63) Newby, J. A.; Huck, L.; Blaylock, D. W.; Witt, P. M.; Ley, S. V.; Browne, D. L. *Chemistry – A European Journal* **2014**, *20*, 263–271.
(64) Oka, N.; Yamada, T.; Sajiki, H.; Akai, S.; Ikawa, T. *Org. Lett.* **2022**, *24*, 3510–3514.
(65) Old, D. W.; Wolfe, J. P.; Buchwald, S. L. *J. Am. Chem. Soc.* **1998**, *120*, 9722–9723.
(66) Organic Solvents | NIOSH | CDC, 2024.

(67) Patil, A.; Ferritto, M. S. In *Polymers for Personal Care and Cosmetics*; ACS Symposium Series, Vol. 1148; Am. Chem. Soc.: 2013; Chapter 1; https://doi.org/10.1021/bk-2013-1148.ch001, pp 3–11.
(68) Plumeré, N.; Henig, J.; Campbell, W. H. *Anal. Chem.* **2012**, *84*, 2141–2146.
(69) Rare Earth Elements—Critical Resources for High Technology | USGS Fact Sheet 087-02, https://pubs.usgs.gov/fs/2002/fs087-02/.
(70) RSC. Palladium - Element Information, Properties and Uses | Periodic Table, periodic-table.rsc.org/element/46/palladium.
(71) Sabatino, D. *J. Med. Chem.* **2020**, *63*, 14184–14196.
(72) Schlosser, P. M.; Bale, A. S.; Gibbons, C. F.; Wilkins, A.; Cooper, G. S. *Environ Health Perspect* **2015**, *123*, 114–119.
(73) Schuppan, D.; Mäki, M., et al. *New England Journal of Medicine* **2021**, *385*, 35–45.
(74) See, J.; Murray, J. A. *Nutrition in Clinical Practice* **2006**, *21*, 1–15.
(75) Sheldon, R. A. *Chem. Ind.* **1992**, 903–906.
(76) Sheldon, R. A. *Chem. Commun.* **2008**, 3352–3365.
(77) Sheldon, R. A. *Green Chem.* **2007**, *9*, 1273–1283.
(78) Shriver, D. F.; Drezdzon, M. A., *The Manipulation of Air-Sensitive Compounds*; J. Wiley and Sons: New York: 1986.
(79) Singhania, V.; Cortes-Clerget, M.; Dussart-Gautheret, J.; Akkachairin, B.; Yu, J.; Akporji, N.; Gallou, F.; Lipshutz, B. H. *Chem. Sci.* **2022**, *13*, 1440–1445.
(80) Singhania, V.; Nelson, C. B.; Reamey, M.; Morin, E.; Kavthe, R. D.; Lipshutz, B. H. *Org. Lett.* **2023**, *25*, 4308–4312.
(81) Szondy, Z.; Korponay-Szabó, I.; Király, R.; Sarang, Z.; Tsay, G. J. *Biomedicine (Taipei)* **2017**, *7*, 15.
(82) Thomas, A. A.; Zahrt, A. F.; Delaney, C. P.; Denmark, S. E. *J Am Chem Soc* **2018**, *140*, 4401–4416.
(83) Torborg, C.; Beller, M. *Adv. Synth. Catal.* **2009**, *351*, 3027–3043.
(84) Voigtritter, K.; Ghorai, S.; Lipshutz, B. H. *J. Org. Chem.* **2011**, *76*, 4697–4702.
(85) Wan, T.; Capaldo, L.; Djossou, J.; Staffa, A.; de Zwart, F. J.; de Bruin, B.; Noël, T. *Nat Commun* **2024**, *15*, 4028.
(86) Whitaker, L.; Harb, H. Y.; Pulis, A. P. *Chem. Commun.* **2017**, *53*, 9364–9367.
(87) Wong, M. J.; Oftadeh, E.; Saunders, J. M.; Wood, A. B.; Lipshutz, B. H. *ACS Catal.* **2024**, *14*, 1545–1552.

(88) Xiong, L.; Shen, Y.-Q.; Jiang, L.-N.; Zhu, X.-L.; Yang, W.-C.; Huang, W.; Yang, G.-F. In *Discovery and Synthesis of Crop Protection Products*; ACS Symposium Series, Vol. 1204; American Chemical Society: 2015; Chapter 13, pp 175–194.

(89) Xu, L.; Dong, Z.; Zhang, Q.; Deng, N.; Li, S.-Y.; Xu, H.-J. *J. Org. Chem.* **2022**, *87*, 14879–14888.

(90) Zhang, X.; Jia, F.; Guo, X.; Liu, G. *Org. Lett.* **2024**, *26*, 10419–10423.